MAGNETOHYDRODYNAMIC SURFACE WAVES IN THE SOLAR ATMOSPHERE

Alan J. Miles

A Thesis Submitted for the Degree of PhD
at the
University of St Andrews

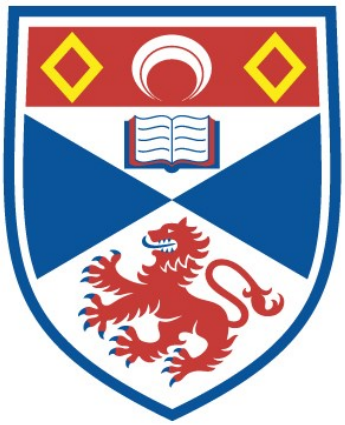

1991

Magnetohydrodynamic Surface Waves in The Solar Atmosphere

Alan J. Miles

A thesis submitted for the degree of Doctor of Philosophy
at the University of St. Andrews

ProQuest LLC.
789 East Eisenhower Parkway
P.O. Box 1346
Ann Arbor, MI 48106 – 1346

Dedication

I dedicated this thesis to the many friends I have acquired during my years (1983-91) at this fine university of St. Andrews. Thanks for the memories, I won't let the sun go down on them.

Copyright

In submitting this thesis to the university of St. Andrews I understand that I am giving permission for it to be made available for use in accordance with the regulations of the University Library for the time being in force, subject to any copyright vested in the work not affected thereby. I also understand that the title and abstract will be published and that a copy of the work may be made and supplied to any **bona fide** library worker.

Postgraduate Career

I was admitted to the Faculty of Science of the University of St. Andrews under Ordinance General No 12 on 1/10/87 and as a candidate for the degree of Ph.D. on 1/10/88.

Signed .. Date 17th May 1991

Declaration

I hereby certify that this thesis has been composed by myself, that it is a record of my own work, and that it has not been accepted in partial or complete fulfilment of any other degree or professional qualification.

Signed ..... Date 17th May 1991

Certificate

I hereby certify that the candidate has fulfilled the conditions of the Resolution and Regulations appropriate to the Degree of Ph.D.

Signature of Supervisor ..... Date 17 May 1991

Acknowledgements

It is my great pleasure to acknowledge the support and guidance of my supervisor Dr. Bernard Roberts without whose map of the kingdom of waves that exists on the sun, I could never have found such a safe and interesting route to the completion of this work. It is also with much gratitude that I acknowledge Drs. Hania Allen, John Ball, Alan Hood, David Evans, Peter De Bruyne and Andrew de Ville for their generosity,expertise and friendship. Finally these acknowledgements would not be complete without my sincere thanks to my colleague Miss Rekha Jain for laughing at my witticisms and for taking my work to a higher plane.

Contents

Abstract

In this thesis the nature of magnetoacoustic surface waves at a single magnetic interface is examined for the case of parallel propagation. Above the interface is an isothermal medium permeated by a horizontal magnetic field. The lower region is a field-free medium of different density to the magnetic atmosphere. We consider both the incompressible and compressible situations and the effect of including gravity. In each case a transcendental dispersion relation is solved numerically for a range of parameters and the resulting dispersion curves plotted.

In the first chapter we provide a general introduction to the work, reviewing previous work in this area and considering applications of surface waves. In the second chapter we consider the existence of surface waves for the case when the media are incompressible either side of the interface. We consider the cases of both uniform and non-uniform distributions of densities and the effect of including gravity. We show that the f-mode exists in a restricted band of horizontal wavenumber.

In the subsequent chapters we consider the effect of compressibility on surface waves. The media either side of the interface are taken to be isothermal. In the absence of gravity the interface may support one or two surface modes determined by the relative temperatures and magnetism of the two media. This case is studied in Chapter 3 where phase-speeds and penetration depths of the waves and the associated pressure perturbations are investigated for a variety of field strengths and sound speeds.

In Chapters 4 and 5 we consider the effect of gravity on the compressible modes described in Chapter 3. In Chapter 4 an exact dispersion relation is obtained for the case of a constant Alfvén speed, whilst in Chapter 5 the case of a uniform magnetic field is considered. In the absence of the magnetic field the transcendental dispersion relation may be reduced to a polynomial. This polynomial possesses two acceptable solutions, only one of which may exist at any given circumstance depending on the densities either side of the interface. If the gas density within the field exceeds that in the field-free medium, then the f-mode may propagate; otherwise, a magnetic surface-

gravity mode propagates. As in the incompressible case, the f-mode exists in a restricted band of horizontal wavenumber. An analytical form for the wave speed of the f-mode is obtained for small values of the Alfvén speed. It is shown that the f-mode is related to the fast magnetoacoustic surface wave, merging into that mode at short wavelengths.

Chapter 1 : Magnetohydrodynamic Surface Waves

1.1 Motivation

The solar atmosphere is an inhomogeneous medium richly structured in both its magnetic and plasma properties. Recent reviews include Edwin and Roberts (1986,1987), Hollweg (1985), Roberts (1986,1990a,b,c) and Thomas (1985). Examples of magnetic structuring in the solar atmosphere are provided by surfaces of discontinuity across which the plasma and magnetic properties vary rapidly. Magnetohydrodynamic surface waves can exist on discontinuities in the magnetic field, plasma density, pressure or temperature. A theoretical understanding of magnetoacoustic surface waves under conditions appropriate to the solar atmosphere is of intrinsic and current interest. In this thesis we consider the behaviour of magnetohydrodynamic surface waves and their relevance to solar phenomena.

By the term surface wave we mean a wave that propagates on a sharp (discontinuous) interface. The case of a smoothly varying interface will not be considered in this thesis, but for completeness shall be discussed briefly in Section 1.3; see also Lee and Roberts (1986), Hollweg (1990a,b,1991), and Goossens (1991).

Surface waves are a two-dimensional phenomenon and so their propagation characteristics are influenced by the geometry of the surface. Throughout this thesis we will be concerned with a plane surface, the single magnetic interface. Provided we consider wavelengths that are smaller than the thickness of the magnetic structure concerned, we may legitimately approximate the structure by a single interface. Although the single magnetic interface is the most elementary of field structures, its detailed study provides a valuable insight into the general nature of surface wave propagation. The single magnetic interface is a reasonable representation of the field structure in several solar features, the lower boundary of the penumbral magnetic field of a sunspot being a particularly important one. The characteristic property of a surface wave is that its propagation is directional (anisotropic), being guided by the interface. The energy of the surface wave is confined to within roughly a wavelength of the

surface. Its speed is generally intermediate between the basic bulk speeds of the media either side of the interface, though the presence of stratification may distort this property.

Surface waves can occur in a variety of circumstances including both astrophysical and laboratory situations. The solar wind contains surfaces in the form of discontinuities, the properties of which have been discussed by several authors (e.g., Behannon, 1978; Hollweg, 1982). There are two large scale discontinuities inside the Earth's magnetosphere, namely at the plasmapause and on the inner plasma sheet boundary. Surface waves on the plasmapause have been investigated by, for example, Southwood (1974) and Chen and Hasegawa (1974). Waves on the plasma sheet have been considered by Nenovski (1978,1985) and Maltsev and Lyatsky (1984). Magnetospheric applications are reviewed in Southwood and Hughes (1983).

The study of surface waves continues to be of interest for laboratory applications (e.g., Amagishi, 1986), especially with regard to stability considerations (e.g.,Gratton *et al.*, 1988; Gonzalez and Gratton, 1990). Magnetoacoustic surface waves can be generated along plasma columns (see the review by Moisan, Shivarova and Trivelpiece, 1982). The study of surface waves under laboratory conditions has suggested a mechanism for the heating of the plasma (Grossmann and Tataronis, 1973; Hasegawa and Chen, 1974,1976; Appert *et al*, 1986).

There are as yet no unequivocal observations of magnetohydrodynamic surface waves in the solar atmosphere, though a number of phenomena are strong candidates for exhibiting such a mode. Solar applications are discussed in Edwin and Roberts (1987). For example, rapid variations in the magnetic field arise on the edges of a sunspot or an intense tube. In the solar atmosphere an interest in surface waves also arises in studies of coronal heating (see the discussion in Section 1.3) (Ionson, 1978, 1985; Wentzel, 1979; Rae and Roberts, 1981; Hollweg, 1985,1987a,c; Lee and Roberts, 1986), in oscillations in sunspot penumbrae (Nye and Thomas, 1976b,Small and Roberts, 1984), and in helioseismology (Deubner and Gough, 1984; Christensen-Dalsgaard *et al.*,1985; Leibacher *et al.*,1985).

Certainly a sunspot configuration regarded as a single flux tube is capable of supporting surface waves (Roberts 1980, 1981a,b,c; Edwin and Roberts, 1983; Cally, 1985, 1986; Abdelatif, 1988; Evans and Roberts,1990a), and such waves would be guided along the lower penumbral magnetic field as the field of the sunspot fans out. That is, a surface wave generated below the observable layers of the spot would result in a visible, outwardly propagating, wave in the penumbral layers. The running penumbral wave observed emanating from sunspots may be such a surface wave (Small and Roberts, 1984); see the discussion in Section 1.2.

Running penumbral waves were first observed by Giovanelli (1972) and Zirin and Stein (1972), and their properties have been reviewed by Giovanelli (1974) and Moore (1981a). They have been modelled as magnetoacoustic-gravity modes by Nye and Thomas (1974, 1976b), who interpreted the running penumbral wave as a mode trapped by the increasing sound speed into the convection zone and the increasing Alfvén speed into the penumbral atmosphere. Small and Roberts (1984), on the other hand, modelled the running penumbral mode as a fast magnetoacoustic surface wave, its existence depending only upon the presence of a discontinuity (or rapid variation) in the field with no trapping (i.e. wave reflection or refraction) being required. We view the modes discussed by Nye and Thomas as p-modes influenced by the presence of a penumbral field; such modes would be absent in the case of zero gravity, whereas the surface mode considered in Small and Roberts (1984) exists even in the absence of gravity. Thus the two discussions - though closely related - are distinct in that different modes are examined.

Surface waves may propagate on magnetic structures that are more complicated than the single interface which we consider in this thesis. Thus, a magnetic flux tube or slab supports surface waves. The surface waves in this context are waves that are confined to the edges of the flux tube or slab. Body waves in photospheric tubes also have some of the features of surface waves, since they are confined to the edge of the tube and its interior, decaying laterally from its sides into the environment of the tube (Roberts, 1981a,b). The specific topic of waves in magnetic flux tubes has been

reviewed in Roberts (1980,1981c,1984,1985,1986,1990a,b,c), Spruit (1981b), Spruit and Roberts (1983), Hollweg (1985), Thomas (1985) and Ryutova (1990).

Another possible example of a surface wave phenomenon is the f-mode. This is a buoyancy driven mode lying just below the acoustic p-mode ridges of the sun's global oscillations. The "f" denotes the fundamental of the mode, a nomenclature introduced by Cowling (1941). The mode's frequency ω is essentially independent of the solar stratification, having the dispersion relation (in the absence of a magnetic field) $\omega^2 = gk_x$ for horizontal wavenumber k_x and local gravitational acceleration g. The f-mode is an important oscillation of the sun, of use in determining the structure and dynamics of the solar interior. Together with p-modes, the f-mode with periods around 5 minutes has been observed with great accuracy (see, for example, Duvall *et al.*, 1988; Libbrecht and Kaufman, 1988; Libbrecht *et al.*, 1990). The f-mode has been observed both at high k_x (Libbrecht and Kaufman, 1988; Tarbell *et al.*, 1988; Libbrecht, Woodard and Kaufman, 1990) and at low k_x (Rabaey, Hill and Barry, 1988).

The chromosphere is dominated by magnetic field and therefore magnetism will have an influence on the nature of p- and f-modes. It is thus important to consider the effect of a magnetic field on these oscillations (see Campbell and Roberts, 1989; Evans and Roberts, 1990b). In this thesis we also examine the influence of a horizontal magnetic field on the f-mode. Oscillations in this region of the solar atmosphere will tend to distort the overlying canopy field. Motions in the f-mode must therefore disturb the overlying magnetic canopy. In moving the magnetic field the oscillations do work against it and therefore the amplitude of the oscillation tends to be reduced. In bending the magnetic field lines, the oscillations gain extra elasticity from the magnetic field which therefore tends to speed up the wave. The result is an f-mode which departs slightly from the deep water wave result of $\omega^2 = gk_x$, lying more and more above this ω,k_x parabola for larger and larger k_x. This is the conclusion reached in theoretical calculations carried out in this thesis and by Campbell and Roberts (1989) and Evans and Roberts (1990b). However, the available observational evidence (Libbrecht *et al.*,

1990) suggests quite the opposite, giving a reduction in the ω,k_x curve. An explanation for this behaviour has yet to be found.

There is thus a widespread interest in the behaviour of surface waves and their possible application to observations of waves in the solar atmosphere. Given the variety of applications of surface waves and their natural intrinsic interest, we examine in some detail the nature of magnetoacoustic surface modes on a field-free interface. In order to bring out clearly the various characteristics of surface waves, we begin our investigations by ignoring the effect of gravity and concentrating on waves that propagate parallel to the applied magnetic field. Gravity is, however, important in applications to the penumbral magnetic field, as is clear from the analyses of Small and Roberts (1984) and Nye and Thomas (1974, 1976b). The nature of the propagation of magnetoacoustic surface modes in a gravitationally stratified atmosphere is severely complicated and therefore a theory of such modes in a non-gravitational medium is a useful preliminary study to a fuller understanding of the more complicated problem. Therefore, to begin with, we feel it important to focus attention on the intrinsic properties of magnetoacoustic surface waves in an unstratified medium, deferring the complications of gravity to the later chapters.

The simplest theoretical case is one in which we have a single magnetic interface in an incompressible medium and thus the only restoring force is provided by the magnetic tension and magnetic pressure. The interface supports a magnetohydrodynamic surface wave which propagates with a speed which is intermediate between the two Alfvén speeds on either side of the interface. In an incompressible medium, a single magnetic interface supports a magnetohydrodynamic surface wave which propagates with a speed c_k, given by (Kruskal and Schwarzschild, 1954; see also Dungey and Loughhead, 1954; Chandrasekhar 1961; see also Chapter 2)

$$c_k^2 = \frac{\rho_0 v_A^2 + \rho_e v_{Ae}^2}{(\rho_0 + \rho_e)}, \tag{1.1}$$

where ρ_0 and v_A are the density and Alfvén speed on one side of the interface and ρ_e and v_{Ae} are their respective values on the other side. This speed lies between the two Alfvén speeds, v_A and v_{Ae}. The speed c_k arises also in descriptions of waves in flux tubes (see, for example, the reviews by Spruit, 1981a,b, 1983; Spruit and Roberts, 1983; Thomas, 1985; Roberts, 1986). For the special case of an interface one side of which is field-free, of interest to this thesis, Equation (1.1) with (say) $v_{Ae} = 0$ reduces to

$$c_k^2 = \frac{\rho_0 v_A^2}{(\rho_0 + \rho_e)}. \tag{1.2}$$

The assumptions of incompressibility and zero gravity that permit the result (1.2) are too drastic to allow it to be of more than a rough guide to the actual behaviour of surface waves in the solar atmosphere, which of course is far from incompressible and is also stratified. The allowance of compressibility - but with gravity still ignored - modifies (1.2) to the result (Wentzel, 1979; Roberts, 1980; Roberts, 1981a,c) that a surface wave propagates according to (see Chapter 3)

$$\frac{\omega^2}{k_x^2} = \frac{\rho_0}{(\rho_0 + \rho_e \frac{m_0}{m_e})} v_A^2, \tag{1.3}$$

where m_0 and m_e, both positive, are functions of ω^2 and k_x^2. In the incompressible limit $\frac{m_0}{m_e}$ approaches unity and we recover the relation (1.2). Generally, however, the dispersion relation (1.3) is transcendental and may admit two modes (Roberts, 1981a), both of which have speeds that are sub-Alfvénic.

With the addition of this second restoring force - compressibility - and in the absence of gravity, a magnetic interface supports two surface waves (Roberts, 1981a; Miles and Roberts, 1989; Jain and Roberts, 1991), depending on the relative temperatures of the media either side of the interface. These are referred to as the fast and slow magnetoacoustic surface waves according to their respective speeds. Their counterparts arise when gravity is included. Depending upon the relative temperatures of the two sides of the interface, the slow wave only may be permissible (Roberts,

1981a; see also Wentzel, 1979). Surface waves in a compressible medium are always magnetoacoustic in nature, the motions possessing some compression; in this respect the common description "Alfvén surface wave", referring as it does to the Alfvén wave, is incorrect.

How does stratification modify the above results? The presence of gravity modifies the equilibrium state of the medium and so the behaviour of a surface wave is changed in two ways: first, because the wave samples a non-uniform medium, and secondly because additional forces - buoyancy forces - arise to modify the propagation of the wave. These two effects seriously complicate any description of the waves. The inclusion of gravity not only introduces a preferred direction additional to that determined by the magnetic field, but also imposes length and time scales in the system. The length scales introduced by the gravitational field are defined by the equilibrium density and pressure profiles, while the imposed time scales arise from the acoustic cutoff frequency and the buoyancy (Brunt-Väisälä) frequency. The combined presence of these two forces, gravity and magnetism, makes any description of the wave motions in the solar atmosphere necessarily complicated. However, when the medium is both *incompressible* and *uniform* in density, we have the result (e.g. Chandrasekhar 1961) that (see Chapter 2)

$$\frac{\omega^2}{k_x^2} = \frac{\rho_0}{(\rho_0 + \rho_e)} v_A^2 - \frac{g}{k_x} \frac{(\rho_0 - \rho_e)}{(\rho_0 + \rho_e)}, \qquad (1.4)$$

revealing that in the presence of gravity the surface mode is rendered dispersive and is also subject to instability (the Rayleigh-Taylor instability) at long wavelengths if a dense fluid rests on top of a light fluid (i.e. if $\rho_0 > \rho_e$). Equation (1.4) is a familiar result, often used in astrophysical applications. But we should remember the restrictions under which it is derived, namely an incompressible fluid, uniform (unstratified) in density (though stratified in pressure). Neither of these assumptions is likely to be met under solar conditions.

The inclusion of a gravitational field also permits the f-mode to propagate, although only for a limited range of horizontal wavenumber. Like the fast magnetoacoustic surface wave, its existence depends upon the relative temperatures of the media either side of the interface; both the f-mode and the fast magnetoacoustic surface wave can propagate only when the field-free region is warmer than the magnetic atmosphere.

However, in general, any disturbance in the solar atmosphere is subject to the three restoring forces of buoyancy, compressibility and magnetism. Consequently, the nature of the propagation of magnetoacoustic-gravity surface waves is even more complicated, a reflection of the highly anisotropic character of a magnetically structured and stratified atmosphere. A theoretical understanding of magnetoacoustic surface waves in a gravitationally stratified atmosphere permeated by a magnetic field is therefore of natural interest. We shall refer to such waves as magnetoacoustic-gravity surface waves. The study of magnetoacoustic surface waves in a gravitationally stratified medium may be investigated for a variety of models. For example, one might consider an isothermal atmosphere permeated by a horizontal magnetic field that decreases exponentially with height such that the Alfvén speed is constant (see Chapter 4). Such an equilibrium profile is amenable to an analytical investigation yielding a relatively simple, though transcendental, dispersion relation. However, the assumption of a constant Alfvén velocity is reasonable only if we are interested in a small region close to the surface of the sun, it is not a good global approximation for the sun's atmosphere.

So what replaces the result (1.4) when a stratified compressible gas is considered? We show, in fact, that for the case of two isothermal gases in contact at a magnetic non-magnetic interface, with constant Alfvén speed within the magnetic region, the dispersion relation (1.4) is replaced by the highly transcendental form

$$\frac{\omega^2}{k_x^2} = \frac{\rho_0}{\left(\rho_0 + \rho_e \dfrac{(M_e + 1/2H_e)\, m_0^2}{(M_0 - 1/2H_B)\, m_e^2}\right)} v_A^2 - g \frac{\left\{ \dfrac{\rho_0 c_0^2}{(k_x^2 c_0^2 - \omega^2)} - \dfrac{\rho_e c_e^2}{(k_x^2 c_e^2 - \omega^2)} \right\}}{\rho_0 \dfrac{(M_0 - 1/2H_B)}{m_0^2} + \rho_e \dfrac{(M_e + 1/2H_e)}{m_e^2}}, \tag{1.5}$$

where M_0, M_e are functions of ω^2 and k_x and H_B, H_e are constants. The derivation of this relation and an unfolding of its properties provides the topic of our investigation in Chapter 4.

An alternative, and perhaps more realistic, model for solar applications, is the case of an isothermal atmosphere permeated by a *uniform* horizontal magnetic field. In this case the Alfvén speed increases exponentially with height, and this leads to an ordinary differential equation with non-constant coefficients, a solution of which may be given in terms of hypergeometric functions. We examine this case in Chapter 5.

In the remainder of this opening chapter we shall discuss the various studies that have been carried out on magnetohydrodynamic surface waves. We consider their applications to solar heating in Section 1.3 and consider the effect of nonlinearity in Section 1.4. In the last section of this chapter we derive the basic magnetohydrodynamic equations that we shall use throughout the thesis. These equations describe linear, perturbations of a plasma which we consider to be perfectly conducting, stratified by gravity and permeated by a magnetic field. S. I. units are used throughout.

Let us first consider the phenomenon of the running penumbral wave which was one of the main instigators for the study of magnetohydrodynamic surface waves carried out in this thesis.

1.2 Running Penumbral Waves

A possibly important application of magnetoacoustic-gravity surface wave theory is to the running penumbral wave phenomenon. Running penumbral waves are commonly observed by line of sight velocity measurements and are present in most sizable spots with regular stable structures. The waves consist of circular wavefronts originating at the umbra-penumbral boundary, though the connection between umbral oscillations and running penumbral waves is uncertain (Moore 1981a,b). Several authors have reported such a connection (Giovanelli, 1972; Lites, White and Packman, 1982; Lites 1988). The waves propagate radially outwards with horizontal phase-speeds in the chromosphere of between 8-25kms^{-1}, horizontal wavelengths in the range 2300-3800km and amplitudes of approximately 1kms^{-1}.

However, the situation is not as clear cut as this. Simultaneous observations of running penumbral waves have been made in the chromosphere (in Hα and Ca II) and in the photosphere (in Fe I) (Musman *et al.*,1976; Lites, 1988). Observations in the photosphere, however, have been more intermittent. The observed periods of the running penumbral waves vary considerably. Lites (1988) observed periods as high as 1400s (frequencies as low as 0.7mHz), while Thomas, Cram and Nye (1984) found periods of only 200-300s. Additionally, Lites (1988) reports different frequencies and periods at different levels in the penumbral atmosphere. In the upper photosphere he reports frequencies of around 3.5mHz (periods of about 285s) and around 2mHz (periods of about 500s), while in the penumbral chromosphere only the 3.5mHz frequency is detected. Lites also reports that motions in the photosphere are predominantly aligned with the field but the alignment of the motions in the penumbral chromosphere remain uncertain.

As we shall see from our investigations, depending on the ordering of the sound speeds in our model two surface waves may propagate at a given instant. These are the fast and slow magnetoacoustic surface waves. The penetration depth (i.e. the distance from the interface at which the amplitude is reduced by an exponential factor e) for the fast surface wave is greater than that for the slow mode. Also the motions

associated with the slow surface wave are predominantly field aligned. If we identify the 2mHz frequencies with the slow magnetoacoustic surface wave and the 3.5mHz with the fast, then we can explain Lites's observations. Since the slow surface wave penetrates less than the fast wave we would expect not to be able to detect the slow surface wave in the upper penumbral atmosphere, since this is further away from the interface. Additionally, since the chromospheric oscillations observed will originate from nearer the centre of the spot than the photospheric ones, we would expect a reduction in strength of the slow surface wave compared to the fast in the centre of the spot.

The photospheric penumbral waves have horizontal phase-speeds at least twice those of the chromospheric penumbral waves, typically 40-90 kms^{-1}. Thomas (1981) suggested that this difference between the horizontal phase-speeds of the chromospheric and photospheric penumbral waves could be explained by the Evershed flow. At photospheric levels the Evershed flow consists of a radial horizontal outflow from the sunspot to the surroundings, while at chromospheric levels the direction is reversed and material flows into the sunspot umbra. Radial outflows of up to $6kms^{-1}$ are found in the photosphere, inflows of up to $20kms^{-1}$ in the chromosphere. Also, recently Alissandrakis *et al.* (1988) have shown that at transition zone temperatures (10^5 K), the flow has the same characteristics as the inward chromospheric flow but higher flow velocity. Thus with such a flow present, the actual horizontal phase-speeds for the running penumbral waves in photosphere would be in the range 35-$85kms^{-1}$, say, while those in the chromospheric region would lie in the range 20-$40kms^{-1}$.

Observations suggest that running penumbral waves originate near the umbra-penumbral boundary; Musman (1967), Savage (1969) and Moore (1973) have suggested overstable convection in the umbra as a possible source of the excitation of the waves. Galloway (1978), however, conjectured that the waves are generated in the penumbra itself through overstable convection in magnetic flux ropes. Zhugzhda and Dzhalilov (1984) have suggested that the running penumbral waves can be explained by the transformation of 5-minute waves (p-modes) from the convective zone under the

influence of an almost horizontal magnetic field. Evans and Roberts (1990a) have argued that fast body waves (tube waves), as they propagate upwards leak energy and transform into fast surface waves, which in turn manifest themselves as running penumbral waves. They have also suggested that slow surface waves, driven by granular buffeting or overstable convection, produce penumbral waves but with longer periods. Although the slow surface wave has small phase-speeds it is possible to generate periods as large as those detected by Lites (1988) with wavelengths of around 1000km. Thus it is possible that the slow surface wave may be generated by granules impacting upon the sides of the spot. The shorter periods observed in the 200-300s range could indicate some connection between the running penumbral waves and the three minute oscillations observed in the umbra of a spot.

Running penumbral waves have been modelled as magneto-atmospheric modes (i.e.magnetoacoustic-gravity modes) by Nye and Thomas (1974,1976b). They interpreted the running penumbral wave as a vertically trapped mode, the trapping being caused due to the increasing sound speed into the convection zone and the increasing Alfvén speed into the penumbral atmosphere. They showed that due to the slow propagation speed of the penumbral wave most of the wave's energy resides in the penumbral photosphere, although the amplitude of the wave is much greater in the chromosphere. This increase in amplitude of the wave in the chromosphere is due to the fact that the density is much lower there than in the photosphere. By contrast, Small and Roberts (1984) modelled the running penumbral wave phenomenon as a fast magnetoacoustic-gravity surface wave; its existence depending purely upon the rapid variation in the penumbral field with no trapping (i.e. wave reflection or refraction) being invoked. Following the work of Small and Roberts, we shall also model the running penumbral wave as a fast magnetoacoustic-gravity surface mode.

1.3 Heating by Surface Waves

Wave theories of coronal heating face the dual problem of identifying a wave mode which is simultaneously able to propagate the required energy flux into the corona and to dissipate that energy there. The corona is a highly structured nonuniform medium, the structuring including thin discontinuities. Surface waves appear to be excellent candidates since they are supported by nonuniformities and therefore thrive in the inhomogeneous environment which characterises the corona. Hollweg (1981a) suggested that magnetohydrodynamic surface waves could in principle satisfy the two criteria stated above. Hollweg (1981b) pointed out that their propagation is similar to that of Alfvén waves, which are capable of carrying enough energy into the corona, but unlike Alfvén waves, which are difficult to dissipate, surface waves are compressional and therefore capable of heating the plasma through dissipation (by viscosity and heat conduction).

Gordon and Hollweg (1983) considered the damping of magnetohydrodynamic surface waves in the solar corona by collisional dissipation. They excluded coronal holes from their analysis and confined their attention to dense coronal regions where collisions are more frequent. They made the assumption that the magnetic pressure dominates the thermal pressure so that the wave dynamics could be approximately evaluated by assuming the plasma to be cold. This is not an unreasonable assumption for the corona which is dominated by magnetic fields and therefore is a low beta plasma. Their main conclusion was that surface waves could dissipate in a reasonable distance in the solar corona only if their periods were shorter than a few tens of seconds and the magnitude of the magnetic field was comparable to that of the quiet corona ($\leq$ 10G). Thus the collisional damping of surface waves may serve to heat the quiet coronal regions, if the wave periods are short enough. However, the large magnetic field strengths which are presumed to exist in coronal active regions (say about 100G) suggests that collisional dissipation of surface waves is too weak to heat these regions.

There are several mechanisms for increasing surface wave damping. The most popular of these is "resonant absorption" (see, for example, Ionson, 1978). Other

possible mechanisms include leakage of surface waves (Cadez and Okretic, 1989) and nonlinear steepening of surface waves (Ruderman, 1985). We shall consider briefly each of these mechanisms.

1.3.1 Resonant Absorption

In the analysis pursued in this thesis, the interface (taken to be at z=0) is assumed to be strictly a sharp discontinuity separating two media with different properties. In reality the spatial inhomogenities are smooth rather than discontinuous, in which case resonance absorption occurs. Although an incompressible medium gives a poor description of the solar corona, to convey the essence of resonance absorption it is convenient to consider the simple example of a surface wave supported by a discontinuity in an incompressible plasma. Since the Alfvén speed is much larger than the sound speed, a better approximation is the low beta assumption (since in the corona the fluid pressure is negligible compared with the magnetic field pressure).

In the simple case of an incompressible atmosphere with no gravitational stratification (see Chapter 2), the amplitude of the velocity perturbation satisfies the following second order ordinary differential equation (see, for example, Uberoi, 1972; Roberts, 1981a)

$$\frac{d}{dz}\left\{\varepsilon(z)\frac{dv_z}{dz}\right\} - k_x^2\,\varepsilon(z)v_z = 0, \tag{1.6}$$

where

$$\varepsilon(z) = \rho_0(z)(\omega^2 - k_x^2 v_A^2(z)). \tag{1.7}$$

Here ω is the frequency of the perturbation and k_x is its wavenumber in the direction of the field; the motion $(v_x,0,v_z)$ is assumed to be in the xz-plane.

If $\varepsilon(z)$ is a discontinuous function consisting of a step function, the singularity in the governing ordinary differential Equation (1.6) is removable since the Alfvén speed is considered to be a constant on either side of the interface z=0 (see Chapter 2).

Then using the normal mode approach a dispersion relation is derived, the roots of which yield a discrete set of normal modes.

If, however, the discontinuity at z=0 is replaced by a continuous profile, then the governing differential Equation (1.6) contains a singularity at the zero of $\varepsilon(z)$. That is, there must be a location, $z=z_1$ say, at which $\varepsilon(z_1)=0$. In an ideal system this singularity is fundamental to the differential equation and cannot be removed. Near this singular point the amplitude of the perturbed velocity behaves like (Barston, 1964)

$$v_z \sim \log_e | z - z_1| \pm i\pi H(z - z_1), \tag{1.8}$$

where H(z) is the Heaviside unit step function.

In the case where the function $\varepsilon(z)$ possesses a continuous profile there are no discrete normal modes and only singular modes occur (Barston, 1964). By Equation (1.8) v_z cannot be continuous over the entire domain $(-\infty,\infty)$ and so the only solution obtained by the normal mode approach is the trivial solution $v_z = 0$. There is no dispersion relation and no free oscillations of the system at a single frequency, instead a continuous spectrum of modes arises.

The existence of such a critical point z_1 at which $\frac{\omega}{k_x} = v_A(z_1)$, i.e. where the wave phase-speed is equal to the local Alfvén speed, leads to the decay of a surface disturbance propagating along the interface. It is within this context that Grossmann and Tataronis (1973), Hasegawa and Chen (1974) and Rae and Roberts (1981) considered the heating of a plasma by resonant absorption. Resonant absorption is the phenomenon whereby a plasma at a singular (or resonant) point can absorb energy from the external forcing field. That is, when the frequency of an incident wave matches the local Alfvén frequency, the local mode receives energy from the incident wave and its amplitude grows; correspondingly, the incident mode loses energy and decays in amplitude. The point at which resonance occurs is defined as the spatial resonance point and the region about the spatial resonance is defined as the resonant absorption layer.

Ionson (1978) applied this analysis to explain the heating of "coronal rain" loops which are often seen over sunspot umbrae. They are termed coronal rain loops since observations of these loops indicate the existence of Hα condensations which appear to originate at the apex of the loops and flow downwards along the legs. Since there is a difference in density and possibly magnetic field strength between adjacent loops,the Alfvén speeds inside and outside the loops are different. Then, by turbulent photospheric motion or the 300s 5-10kms^{-1} chromospheric oscillations, shaking the footpoints of the loop may excite both surface and body modes. The surface wave travels along the boundary of the loop's magnetic field lines. At a point where the phase-speed of the surface wave matches the local Alfvén speed of a body mode, the surface wave will resonate with the body wave (Ionson, 1978). The body mode absorbs energy from the surface wave and its amplitude grows considerably. The body mode dissipates in a thin layer (the resonant absorption layer) around the loop via Joule and viscous heating. Thus, surface waves heat the loop through Joule and viscous dissipation.

According to Ionson (1978), the intense heat in the thin sheath at the edges of the loop will drive upward convection in a layer next to the heated sheath. The plasma rises in the convection layer and, being continuously replaced, extracts heat from the sheath. The upward flowing hot convection layer cools near the top of the loop via radiation. The plasma becomes Rayleigh-Taylor unstable and falls into the cool interior of the loop. Upon entering the loop's interior the plasma condenses into clumps, loses buoyancy and falls downwards along the loop's field lines. Ionson offers this process as an explanation for coronal rain loops.

Ionson's predictions agree qualitatively with observed hot loops having cool cores, but the heated sheath ($\simeq$ 1km) and the convection layer (3-30km) have yet to be observed. We note that Ionson's analysis is only valid for loops with cool cores, although in general loops have hot cores. The above analysis cannot be applied to loops with hot cores since it is difficult to justify how the interior could attain a higher

temperature than the layer heated by the surface waves. Confirmation of heating by surface waves still requires both theoretical and observational investigations.

Although he starts with a strictly non-dissipative, ideal system, Ionson obtains a non-zero value for the damping rate. Lee (1980), Rae and Roberts (1981) and Lee and Roberts (1986) have suggested that the wave decay rate should be interpreted as a redistribution of wave energy in space or a mode-conversion rate. They suggest that in applications and dissipation of surface waves in the solar corona the decay rate cannot in general be interpreted as a coronal heating rate. They argue that since the decaying surface disturbance associated with a continuous interface is not a normal mode of the system, the decay rate cannot be considered to be a dissipation rate. This is not unreasonable since the governing equations are those of ideal magnetohydrodynamics, and so are a conservative system. The unattenuated surface wave about a discontinuous interface is replaced at a continuous thin interface by a "collective surface disturbance" which decays with the associated energy density flowing into local oscillations within the interface. They consider the decay rate as the time-scale for build up, from an initial state, of the continuous spectrum of oscillations and that motions undergo a conversion from transverse to longitudinal oscillations within the resonance layer. That is, they interpret the decay rate as a mode conversion of the collective surface disturbance into local oscillations. The conversion arises mathematically from the singular point in the differential equation. However, Lee and Roberts note that for resistive dissipation and sufficiently small wavenumber compared with the width of the interface this ideal mode conversion rate could be considered as a plasma heating rate. Also, in the presence of some dissipative agents, Hollweg (1987a,c) has interpreted the mode conversion rate as a plasma heating rate.

In the case of a compressional plasma, in addition to the Alfvén resonance point we have the cusp resonance where the phase speed matches the magnetoacoustic cusp speed:

$$\frac{\omega}{k_x} = \frac{c_S v_A}{(c_S^2 + v_A^2)^{1/2}} . \qquad (1.9)$$

In a low beta plasma such as the corona the cusp resonance is usually not of interest because it is excited only for slowly propagating waves which carry little energy. However, the cusp resonance could be important in regions where the plasma beta is not so small such as photospheric magnetic flux tubes.

1.3.2 Leaky Waves

Cadez and Okretic (1989) have discussed the possibility of magnetohydrodynamic surface wave energy dissipation by "leakage". They consider two boundaries (interfaces) where surface waves propagating along one boundary are influenced by the presence of an additional parallel boundary. They show that with such a configuration, magnetohydrodynamic surface waves at the first boundary induce body-wave generation at the second.

They consider the following basic equilibrium state

$$\rho_0(x),\, T_0(x),\, B_0(x) = \begin{cases} \rho_{01},\ T_{01},\ B_{01}, & x \le 0, \\ \rho_{02},\ T_{02},\ B_{02}, & 0 < x \le a, \\ \rho_{03},\ T_{03},\ B_{03}, & x > a, \end{cases} \tag{1.10}$$

representing a single component, perfectly conducting, compressible static fluid having discontinuities in density $\rho_0(x)$, temperature $T_0(x)$ and magnetic field strength $B_0(x)$ at two parallel planes, x=0 and x=a. The magnetic field $\underline{B}_0 = (0,0,B_0)$ is parallel to the boundaries in each region. The quantities ρ_{0i}, T_{0i} and B_{0i} (i=1,2,3) are constants.

They impose that there is continuous total pressure perturbation at the interfaces x=0 and x=a, and that the perturbed velocity remains finite as $|x| \to \infty$. (These are the same conditions that we have imposed in our investigations.) Their solutions in the three regions are

$$\begin{aligned} v_1(x) &= d_1 e^{k_1 x}, && x \le 0 \quad \text{region I}, \\ v_2(x) &= d_2 e^{k_2 x} + d_3 e^{-k_2 x}, && 0 < x \le a \quad \text{region II}, \\ v_3(x) &= d_4 e^{-k_3 x}, && x > a \quad \text{region III}, \end{aligned} \tag{1.11}$$

where d_1, d_2, d_3 and d_4 are constants, $k_i = (m_{0i}^2 + k_y^2)^{1/2}$ (i=1,2,3), and where

$$m_{0i}^2 = \frac{(k_i^2 v_{Ai}^2 - \omega^2)(k_i^2 c_i^2 - \omega^2)}{(c_i^2 + v_{Ai}^2)(k_i^2 c_{Ti}^2 - \omega^2)}. \qquad (1.12)$$

Here c_i, v_{Ai} and c_{Ti} are the sound, Alfvén and cusp speeds, respectively, where the cusp speed is defined by

$$c_{Ti} = \frac{c_i v_{Ai}}{(c_i^2 + v_{Ai}^2)^{1/2}}. \qquad (1.13)$$

If k_i is purely real then only surface waves propagate (see Chapter 3). However, Cadez and Okretic considered the case when k_2 and k_3 are real but k_1 is imaginary. This is possible only if $m_{01}^2 + k_y^2 < 0$, which is the condition for a body mode to propagate (Roberts, 1981a); the solution for $v_1(x)$ in $x \leq 0$ with k_1 imaginary is now oscillatory rather than evanescent. In this case Cadez and Okretic state that a surface wave propagating along the interface at x=a will be partially converted to a body wave spreading through region I ($x \leq 0$) with a constant amplitude in space. The surface wave at x=a will therefore lose energy and its amplitude will decrease in time. This is the effect that they refer to as leakage. They propose this as a mechanism for surface wave energy dissipation in a structured medium.

Cadez and Okretic derive a dispersion relation which is not dissimilar to that we obtain in Chapter 3. The two dispersion relations differ only in an exponential term which can be neglected except for the imaginary part which is important in the case of surface wave leakage. This extra term couples the two interfaces and is proportional to $\exp(-2k_2a)$. In the limit of $a \to \infty$ this extra term is negligible and we recover the dispersion relation for magnetoacoustic surface waves at a single interface, which with one side field-free is the same as the dispersion relation we consider in Chapter 3.

We consider now a third mechanism for accelerating surface wave damping, by the nonlinear steepening of the surface waves.

1.4 Nonlinear Surface Waves

The nonlinear nature of surface waves in both the compressible and incompressible cases has been extensively investigated by Ruderman (1985,1986,1988,1989,1991). Gravitational effects have yet to be considered in any detail; see, however, Ruderman (1987) where gravity is taken into account in a study of nonlinear internal waves in a fluid of infinite depth. Consider firstly the case of an incompressible fluid. Although in the corona, and generally in an astrophysical context, compressibility should be considered, the simpler case of an incompressible fluid should provide a valuable insight and some reasonable estimation of timescales, etc.. The nonlinear effect on surface wave propagation at a single magnetic interface in an incompressible fluid have been considered by Ruderman (1985) and Hollweg (1987b).

Since surface wave propagation in a non-gravitational medium is non-dispersive (i.e. ω/k_x is a constant), we do not expect the formation of solitons when we consider nonlinear effects. The introduction of nonlinearity in wave propagation will generate soliton solutions only when the nonlinearity is balanced by the dispersion. However, Ruderman (1985) shows that a perturbation, initially in the form of a sinusoidal wave, will steepen and overturn or break at the point where infinite gradients arise. The consequence of this is that surface waves could dissipate in a medium with arbitrarily small viscosity and heat conduction.

Ruderman (1985), using a multiple scale analysis and a moving coordinate system, shows that the propagation of a low-amplitude nonlinear surface wave disturbance of the form $z=\eta(x,t)$ in an incompressible fluid, in the absence of any dissipative processes, is described by the nonlinear integrodifferential equation

$$\alpha\left(\frac{\partial\eta}{\partial t}+c_k\frac{\partial\eta}{\partial X}\right)+\frac{\partial}{\partial X}\left\{\mathcal{H}\left(\eta\frac{\partial\eta}{\partial X}\right)-\eta\,\mathcal{H}\left(\frac{\partial\eta}{\partial X}\right)\right\}-\frac{\partial\eta}{\partial X}\,\mathcal{H}\left(\frac{\partial\eta}{\partial X}\right)=0, \qquad (1.14)$$

where the coordinate $X = x - c_k t$ moves with the linear surface wave phase-speed c_k defined by Equation (1.1). The parameter α is given by

$$\alpha = \frac{c_k}{(v_{Ao}^2 - v_{Ae}^2)} \frac{(\rho_0 + \rho_e)^2}{\rho_0 \rho_e}. \tag{1.15}$$

Depending on the ordering of the Alfvén speeds either side of the interface, we observe that this parameter can be positive or negative. $\mathcal{H}(\eta)$ denotes the Hilbert transform of the displaced interface defined by

$$\mathcal{H}(\eta(x,t)) = \frac{1}{\pi} \int_{-\infty}^{\infty} \frac{\eta(s,t)}{s - X} \, ds, \tag{1.16}$$

a Cauchy principal value integral.

Clearly, the more realistic conditions of compressibility and atmospheric stratification due to gravity may severely change Equation (1.14). The effect of compressibility has been considered by Ruderman (1988), where once again using a multiscale expansion he derives the equation governing time evolution of nonlinear small amplitude magnetoacoustic surface waves. The governing nonlinear integrodifferential equation is similar to Equation (1.14) except that the parameter α is now considerably more complicated and the incompressible phase-speed c_k is replaced by either the fast or slow magnetoacoustic phase-speeds. These speeds are discussed in detail in Chapter 3. A numerical solution of the evolution equation again shows that a sinusoidal disturbance of amplitude η_0 and wavelength λ defined by

$$\eta(x) = \eta_0 \sin\left(\frac{2\pi x}{\lambda}\right), \tag{1.17}$$

radiated by a source from x=0 at t=0, overturns (i.e. $\partial\eta/\partial X \to \infty$) in a time $t = t_c$. This critical time t_c is given by (Ruderman, 1985; Hollweg, 1987b)

$$t_c = \frac{\lambda^2 |\alpha| T_c}{4\pi^2 \eta_0}, \tag{1.18}$$

where estimates from the numerical integration of the evolution equation give $T_c \approx 0.55$ at the point where $\partial\eta/\partial X \to \infty$.

Ruderman (1986) extended his investigations to include the effect of viscosity on nonlinear surface waves for the incompressible case. The equation he derives differs from Equation (1.14) in the ideal case by an additional term describing the dissipation. It turns out that, provided the viscosity is weak, the damping distance of nonlinear surface waves in an inviscid fluid does not depend on the magnitude of the viscosity. This results he states, is analogous to nonlinear sound wave damping after overturning and shock formation when viscosity controls the shock structure thickness but does not affect the damping rate.

We may illustrate this timescale for the penumbra of a sunspot. Taking $v_{A0} = c_0 = 10\text{kms}^{-1}$ and $v_{Ae} = 0$ (i.e. one side of the interface is field-free) with $\rho_0 \approx \rho_e$, then $c_k \approx 7\text{kms}^{-1}$. Then, with an amplitude $\eta_0 = 10\text{km}$ and a wavelength $\lambda = 10^3\text{km}$, we obtain a turn over time of $t_c = 700\text{s}$. That is, a surface wave propagating along the penumbral magnetic field with a speed c_k would travel approximately 5000km before it would eventually overturn and break at the outermost part of the penumbra.

Ruderman (1989) applied his theory to nonlinear surface wave propagation on the heliospheric current sheet. He models the current sheet as a tangential discontinuity and the plasma is taken to be cold. He states that if the viscosity is small the steepening is very strong and consequently there are large gradients in the plasma. As a result a large increase in dissipation takes place. Ruderman states that this damping rate can be several orders of magnitude larger than that in the linear case and concludes that the nonlinear dissipation of surface waves leads to the heating of the current sheet.

Hollweg (1987b), in an alternative approach, looked for the solution in the form of the sum of sinusoidal waves plus a small term proportional to the square of the amplitude. This additional term grows with time; thus, due to this secular behaviour, Hollweg's expansion is for short times only. Hollweg finds the same sharpening as Ruderman for propagating surface waves but also describes "wave crest sharpening" of standing surface waves. Crest sharpening occurs on the leading edge of the surface wave if $v_{A0} > v_{Ae}$ and on the trailing edge if $v_{A0} < v_{Ae}$. Ruderman (1985) obtains the same result for steepening of nonlinear surface waves. Wave breaking occurs at the

leading or trailing edge of the surface wave depending on the sign of α i.e. on the ordering of the Alfvén speeds. For both the standing and propagating cases Hollweg (1987b) determines the same breaking or sharpening time for the surface wave, given by Equation (1.18).

1.5 Magnetohydrodynamic Equations

1.5.1 Electromagnetic Equations

The behaviour of a continuous plasma is governed by Maxwell's Equations, which for a plasma having a current density $\underline{J}$, charge density ρ_{charge}, a magnetic field $\underline{H}$ with magnetic induction $\underline{B}$ and an electric field $\underline{E}$ with electrical displacement $\underline{D}$ are

$$\underline{\nabla} \times \underline{H} = \underline{J} + \frac{\partial \underline{D}}{\partial t}, \tag{1.19}$$

$$\underline{\nabla} \cdot \underline{B} = 0, \tag{1.20}$$

$$\underline{\nabla} \times \underline{E} = -\frac{\partial \underline{B}}{\partial t}, \tag{1.21}$$

and

$$\underline{\nabla} \cdot \underline{D} = \rho_{charge}. \tag{1.22}$$

For a linear isotropic medium we have the following relationships connecting the electrical displacement with the electric field, and the magnetic induction with the magnetic field:

$$\underline{D} = \varepsilon \underline{E}, \qquad \underline{B} = \mu \underline{H}, \tag{1.23}$$

where, for solar purposes, ε and μ are generally approximated by their vacuum values ε_0 ($\approx 8.854 \times 10^{-12}$ Fm^{-1}) and μ_0 ($= 4\pi \times 10^{-7}$ Hm^{-1}), the permittivity and magnetic permeability of free space, respectively; ε_0 and μ_0 are related to the speed of light c in a vacuum by

$$c = (\mu_0 \varepsilon_0)^{-1/2} \approx 2.998 \times 10^8 \text{ ms}^{-1}. \tag{1.24}$$

The relations given by Equation (1.23) may be used to eliminate the magnetic field $\underline{H}$ and the electric displacement $\underline{D}$ in Maxwell's Equations.

Plasma moving with a non-relativistic velocity $\underline{v}$ in the presence of a magnetic field is subject to an electric field $\underline{v} \times \underline{B}$ in addition to an electric field $\underline{E}$ which may act on the plasma at rest. Ohm's Law states that

$$\underline{J} = \sigma(\underline{E} + \underline{v} \times \underline{B}), \tag{1.25}$$

so that the current density $\underline{J}$ is proportional to the total electric field $\underline{E} + \underline{v} \times \underline{B}$. The constant of proportionality σ is termed the electrical conductivity. It is measured in mho m^{-1}.

It is convenient to eliminate the electric field $\underline{E}$ and the current density $\underline{J}$ between Equations (1.21) and (1.25), whilst ensuring that Equation (1.20) is obeyed. The result is

$$\frac{\partial \underline{B}}{\partial t} = \underline{\nabla} \times (\underline{v} \times \underline{B}) + \eta \nabla^2 \underline{B}, \tag{1.26}$$

where $\eta = (\mu\sigma)^{-1}$ is the magnetic diffusivity. This is the induction equation and may be used to determine the magnetic induction $\underline{B}$ (commonly, in the solar context, referred to as the magnetic field) when the velocity of the plasma is known. The induction equation indicates that changes in the magnetic field in time are the result of transport of the field with the plasma, together with diffusion of the field through the plasma.

In order of magnitude, the ratio of these two terms in the induction equation defines the magnetic Reynolds number (c.f. the viscous Reynolds number in fluid mechanics)

$$R_m = \frac{v_0 l_0}{\eta}, \tag{1.27}$$

where v_0 and l_0 are typical plasma velocity and length scales. Except in regions of high current density, such as in filaments or sheets, most areas of the sun are such that $R_m \gg 1$ (for example, $R_m \approx 10^6$-10^8 for typical coronal structures, since l_0 is large) and

so the diffusion term in Equation (1.26) is negligible. Therefore the plasma acts as though it were a perfect conductor ($\sigma \rightarrow \infty$). In this case the induction Equation (1.26) reduces to

$$\frac{\partial \underline{B}}{\partial t} = \underline{\nabla} \times (\underline{v} \times \underline{B}), \tag{1.28}$$

indicating that the magnetic field is effectively "frozen" to the plasma. Ohm's Law, given by Equation (1.25), in the perfectly conducting limit reduces to

$$\underline{E} + \underline{v} \times \underline{B} = \underline{0}, \tag{1.29}$$

and the current density is determined from Ampère's Law,

$$\mu_0 \underline{J} = \underline{\nabla} \times \underline{B}. \tag{1.30}$$

1.5.2 Plasma Equations

The plasma motion is governed by the equations of mass continuity, motion and energy. The equation of mass continuity is

$$\frac{D\rho}{Dt} + \rho \, (\underline{\nabla}.\underline{v}) = 0, \tag{1.31}$$

where

$$\frac{D}{Dt} \equiv \frac{\partial}{\partial t} + \underline{v}.\underline{\nabla} \tag{1.32}$$

is the convective or total derivative for time variations following the motion. Ignoring the effect of viscosity, the equation of motion for a plasma subject to the force of gravity, a pressure gradient $\underline{\nabla} p$, and a Lorentz force $\underline{J} \times \underline{B}$ across the magnetic field may be written as

$$\rho \frac{D\underline{v}}{Dt} = - \underline{\nabla} p + \underline{J} \times \underline{B} + \rho \underline{g}, \tag{1.33}$$

where g (= 274 ms^{-2}) is the solar gravitational acceleration and p the gas pressure.

Considering only adiabatic perturbations gives the energy equation

$$\frac{Dp}{Dt} = \frac{\gamma p}{\rho}\frac{D\rho}{Dt}, \tag{1.34}$$

where γ is the ratio of specific heats. The gas pressure p is determined by the equation of state of the gas. We shall consider an ideal gas for which the equation of state is

$$p = \frac{k_B}{m}\rho T, \tag{1.35}$$

where k_B (= 1.481×10^{-23} $Jdeg^{-1}$) is Boltzmann's constant, m the mean particle mass and T the temperature of the gas.

Then in general any disturbance in the solar atmosphere is subject to the three restoring forces of buoyancy, compressibility and magnetism. Motions are therefore expected to be anisotropic, reflecting the preferred directions from the inclusion of gravity and a magnetic field. We therefore expect wave motions, driven by these three restoring forces, that are distinct from a pure sound wave, characterised by the speed c_S defined by

$$c_S = \left(\frac{\gamma p_0}{\rho_0}\right)^{1/2}, \tag{1.36}$$

where p_0 and ρ_0 are the equilibrium values of pressure and density of the gas and γ the ratio of specific heat, and an Alfvén wave with speed v_A defined by

$$v_A = \left(\frac{B_0^2}{\mu_0 \rho_0}\right)^{1/2}, \tag{1.37}$$

where B_0 is the equilibrium magnetic field strength. In fact, two magnetoacoustic modes arise from combinations of the two characteristic speeds c_S and v_A:

$$c_f^2 = c_S^2 + v_A^2 \quad \text{and} \quad c_T^{-2} = c_S^{-2} + v_A^{-2}, \tag{1.38}$$

where c_f is referred to as the fast magnetoacoustic speed and c_T ($< c_f$) is the slow magnetoacoustic speed. The fast speed is both supersonic and super-Alfvénic, while the slow speed c_T is both subsonic and sub-Alfvénic. The speed c_T is also referred to as the cusp or tube speed (Roberts, 1981a).

The presence of gravity also means that there is a natural length-scale in the system; this is the density scale-height H, defined by

$$H = -\frac{\rho_0}{d\rho_0/dz}. \tag{1.39}$$

There is also a length-scale defined by pressure variations. This is the pressure scale height Λ, defined by

$$\Lambda = -\frac{p_0}{dp_0/dz}. \tag{1.40}$$

Associated with an imposed length-scale, we may introduce an imposed timescale, namely the time taken for a sound wave to travel the distance H and back again, i.e. $2H/c_S$. We can therefore construct a frequency defined by

$$\omega_a = \frac{c_S}{2H}. \tag{1.41}$$

This is the acoustic cut-off frequency of an isothermal atmosphere.

In addition to the acoustic cut-off frequency we can construct on dimensional grounds, and through the use of gravity, the frequencies g/c_S and $(g/H)^{1/2}$. In fact, the difference between the squares of both these terms arises, namely

$$\omega_g^2 = \frac{g}{H} - \left(\frac{g}{c_S}\right)^2; \tag{1.42}$$

ω_g is the buoyancy (or Brunt-Väisälä) frequency of the atmosphere.

We note that for an isothermal atmosphere in the absence of a magnetic field the density scale height and the pressure scale-heights are both constants and in fact equal ($H = \Lambda = H_0$, a constant). Then

$$\omega_a^2 = \frac{\gamma g}{4H_0}, \qquad \omega_g^2 = \frac{g}{H_0}\left(\frac{\gamma - 1}{\gamma}\right). \tag{1.43}$$

Thus with $\gamma = 5/3$ we note that ω_a^2 exceeds ω_g^2 by $1/60\ (g/H_0)$.

Chapter 2 : Magnetohydrodynamic Surface Waves in an Incompressible Medium

2.1 Introduction

An incompressible flow is one in which we have fluid motion without a change in density. Thus, provided density variations during a flow are negligible, the flow will be effectively incompressible. The term hydrodynamic is often used to describe the science of incompressible fluids in motion. Liquids are assumed to flow incompressibly. However, even for liquids, abrupt changes in velocity may produce compression or rarefaction. Usually a liquid flows under the action of gravity to occupy the lower portion of some open space. A gas, in contrast, flows compressibly to occupy any closed space to which it is confined, regardless of the initial volumes of gas and space. This property distinguishes a gas from a liquid.

In general, gases are not incompressible in nature. However, as with liquids, the slow flow of a gas is closely approximated by assuming it to be incompressible. Therefore such a neglect of plasma motion without change in density is only valid when the typical plasma speeds are much smaller than any other environmental speeds in which the plasma resides. At relatively low speeds the changes in temperature of a fluid, caused say by the motion of a body in the fluid, are almost negligible. Thus, for an incompressible flow one does not need to consider the thermodynamics of the flow, which would usually be done through an energy equation. Therefore, for an incompressible flow one does not need to consider an energy equation.

In this chapter we determine the fundamental magnetohydrodynamic equations that describe linear, incompressible perturbations of a plasma which we consider to be perfectly conducting, stratified by gravity and permeated by a magnetic field. Having derived these governing equations, we consider the problem of a fluid containing a sharp discontinuity at z=0, say. Firstly, we consider the problem when gravity is neglected and the density distribution is uniform either side of the interface at z=0. Secondly, we include the effect of gravitational stratification and determine the modes

that exist in the case of both uniform and non-uniform density distributions. We also discuss the case when the magnetic field is absent.

2.2 Governing Equations

For an incompressible plasma the density changes of a moving plasma element are negligible, i.e. $D\rho/Dt = 0$. Thus the continuity Equation (1.31) reduces to

$$\underline{\nabla} \cdot \underline{v} = 0 \tag{2.1}$$

and the energy Equation (1.34) may then be written as

$$\frac{1}{\gamma}\frac{Dp}{Dt} = 0, \tag{2.2}$$

which is satisfied if $\gamma \to \infty$. Thus, mathematically we may obtain the incompressible limit from the equations for a gas by considering $\gamma \to \infty$.

The governing magnetohydrodynamic equations for a perfectly conducting plasma which is assumed to be incompressible are thus

$$\frac{\partial \underline{B}}{\partial t} = \underline{\nabla} \times (\underline{v} \times \underline{B}), \tag{2.3}$$

$$\rho \frac{D\underline{v}}{Dt} = -\underline{\nabla} p + \underline{J} \times \underline{B} + \rho \underline{g}, \tag{2.4}$$

$$\frac{D\rho}{Dt} = 0, \tag{2.5}$$

$$\underline{\nabla} \cdot \underline{v} = 0. \tag{2.6}$$

Equations (2.3) and (2.4) were given previously in Chapter 1 but for convenience are quoted again here. It should be noted that Equation (2.5) does not necessarily require that ρ is a constant at all points in the plasma. However, from the definition of $D\rho/Dt$, in the incompressible case the density ρ is a constant along each pathline of the flow.

Consider a non-uniform (structured in z) horizontal equilibrium magnetic field $\underline{B}_0 = B_0(z)\hat{\underline{x}}$. Then, since the magnetic field is straight there are no tension effects and the only contribution from the Lorentz force is the magnetic pressure. Then, with $\underline{v}=0$,

the horizontal component of the momentum Equation (2.4) implies that the pressure is a function of z only and the equilibrium is one of magnetohydrostatic balance determined by the vertical component of Equation (2.4), that is

$$\frac{d}{dz}\left(p_0(z) + \frac{B_0^2(z)}{2\mu_0}\right) = -\rho_0(z)g, \tag{2.7}$$

demonstrating that the magnetic pressure may provide support against gravity $-g\hat{\underline{z}}$. Here $p_0(z)$, $\rho_0(z)$ and $B_0(z)$ are the equilibrium pressure, density and magnetic field (assumed horizontal). In the disturbed state the pressure, density, magnetic field and velocity are denoted by $p_0 + p$, $\rho_0 + \rho$, $\underline{B}_0 + \underline{B}$ and $\underline{v}$, respectively. We now consider the plasma to be perturbed slightly from the magnetohydrostatic equilibrium (2.7). We consider only small departures from the equilibrium, so that $|p/p_0|$, $|\rho/\rho_0|$, $\underline{B}/|\underline{B}_0|$ and $|\underline{v}|$ are small quantities. Then the perturbed form of Equations (2.3)-(2.6) are

$$\frac{\partial \underline{B}}{\partial t} = (\underline{B}_0 \cdot \underline{\nabla})\,\underline{v} - (\underline{v} \cdot \underline{\nabla})\,\underline{B}_0, \tag{2.8}$$

$$\rho_0 \frac{\partial \underline{v}}{\partial t} = -\underline{\nabla} p_T + \frac{1}{\mu_0}(\underline{B}_0 \cdot \underline{\nabla})\,\underline{B} + \frac{1}{\mu_0}(\underline{B} \cdot \underline{\nabla})\,\underline{B}_0 + \rho g, \tag{2.9}$$

$$\frac{\partial \rho}{\partial t} + (\underline{v} \cdot \underline{\nabla})\rho_0 = 0, \tag{2.10}$$

$$\underline{\nabla} \cdot \underline{v} = 0, \tag{2.11}$$

where p_T is the perturbed total (gas plus magnetic) pressure defined by

$$p_T = p + \frac{\underline{B}_0 \cdot \underline{B}}{\mu_0}. \tag{2.12}$$

We can now use these equations for the perturbations to derive a second order differential equation for the velocity $\underline{v}$. If we differentiate Equation (2.9) with respect to time t and use Equation (2.8) we obtain the partial differential equation

$$\rho_0 \frac{\partial^2 \underline{v}}{\partial t^2} = -\underline{\nabla} \frac{\partial p_T}{\partial t} + \frac{1}{\mu_0}(\underline{B}_0 \cdot \underline{\nabla}) \frac{\partial \underline{B}}{\partial t} + \frac{1}{\mu_0}\left(\frac{\partial \underline{B}}{\partial t} \cdot \underline{\nabla}\right)\underline{B}_0 + g\frac{\partial \rho}{\partial t}. \qquad (2.13)$$

With a structured horizontal equilibrium magnetic field $\underline{B}_0 = B_0(z)\hat{\underline{x}}$ and the z-axis pointing upwards, so that $\underline{g} = -g\hat{\underline{z}}$, then Equation (2.13) may be written as

$$\frac{\partial^2 \underline{v}}{\partial t^2} = -\frac{1}{\rho_0}\underline{\nabla}\frac{\partial p_T}{\partial t} + v_A^2 \frac{\partial^2 \underline{v}}{\partial x^2} - \frac{g}{\rho_0}\frac{\partial \rho}{\partial t}\hat{\underline{z}}. \qquad (2.14)$$

Since there is no stratification in the x-direction,we may Fourier decompose the total pressure perturbation as

$$p_T(x,z,t) = p_T(z)e^{i(\omega t - k_x x)}, \qquad (2.15)$$

and consider two-dimensional, linear disturbances of the form

$$\underline{v}(x,z,t) = (v_x(z), 0, v_z(z))e^{i(\omega t - k_x x)}, \qquad (2.16)$$

for frequency ω and horizontal wavenumber k_x.

Then, in Fourier space, the partial differential equation (2.14) yields the first order ordinary differential equation

$$i\left(\frac{dp_T}{dz} + g\frac{k_x^2}{\omega^2}p_T\right) = \frac{\rho_0}{\omega}\left(\omega^2 - k_x^2 v_A^2 + \frac{g}{\rho_0}\frac{d\rho_0}{dz}\right)v_z + \frac{g\rho_0}{\omega}\left(1 - \frac{k_x^2 v_A^2}{\omega^2}\right)\frac{dv_z}{dz}, \qquad (2.17)$$

while for the total pressure perturbation we obtain

$$p_T = -\frac{i\rho_0}{\omega}\left(\frac{\omega^2 - k_x^2 v_A^2}{k_x^2}\right)\frac{dv_z}{dz}. \qquad (2.18)$$

Eliminating p_T between Equations (2.17) and (2.18) yields the following second order ordinary differential equation for v_z (the z-component of the amplitude of the disturbance $\underline{v}$) (see, for example, Uberoi, 1972; Roberts, 1981a)

$$\frac{d}{dz}\left\{\rho_0(z)(\omega^2 - k_x^2 v_A^2(z))\frac{dv_z}{dz}\right\} - \left\{\rho_0(z)k_x^2(\omega^2 - k_x^2 v_A^2(z)) + k_x^2 g\frac{d\rho_0}{dz}\right\} v_z = 0. \quad (2.19)$$

We shall refer to this as the governing differential equation.

2.3 The Dispersion Relation in The Absence of Gravity

To motivate our study, consider a magnetic interface between two uniform and incompressible fluids having an equilibrium state in which the pressure $p_0(z)$, density $\rho_0(z)$ and magnetic field $B_0(z)$ are given by

$$p_0(z),\ \rho_0(z),\ B_0(z) = \begin{cases} p_0, & \rho_0, & B_0, & z > 0, \\ p_e, & \rho_e, & 0, & z < 0, \end{cases} \quad (2.20)$$

where p_0,ρ_0,B_0,p_e and ρ_e are constants. We shall adopt the notation throughout that quantities above (in $z>0$) the interface are denoted by a subscript '0',quantities below (in $z<0$) by a subscript 'e'. See Figure 2.1. However, above the interface where quantities have a magnetic as well as a non-magnetic version, the magnetic version will be denoted by a subscript 'B',the non-magnetic version by the subscript '0'.

The two sides of the interface are related by the requirement of total pressure balance. Pressure balance at the interface $z = 0$ dictates that the total (magnetic plus gas) pressure in $z>0$ equals that in the field-free region $z<0$:

$$p_0 + \frac{B_0^2}{2\mu_0} = p_e. \quad (2.21)$$

Either side of the interface ($z=0$) is a uniform medium so the governing differential Equation (2.19), in the non-gravity case, yields

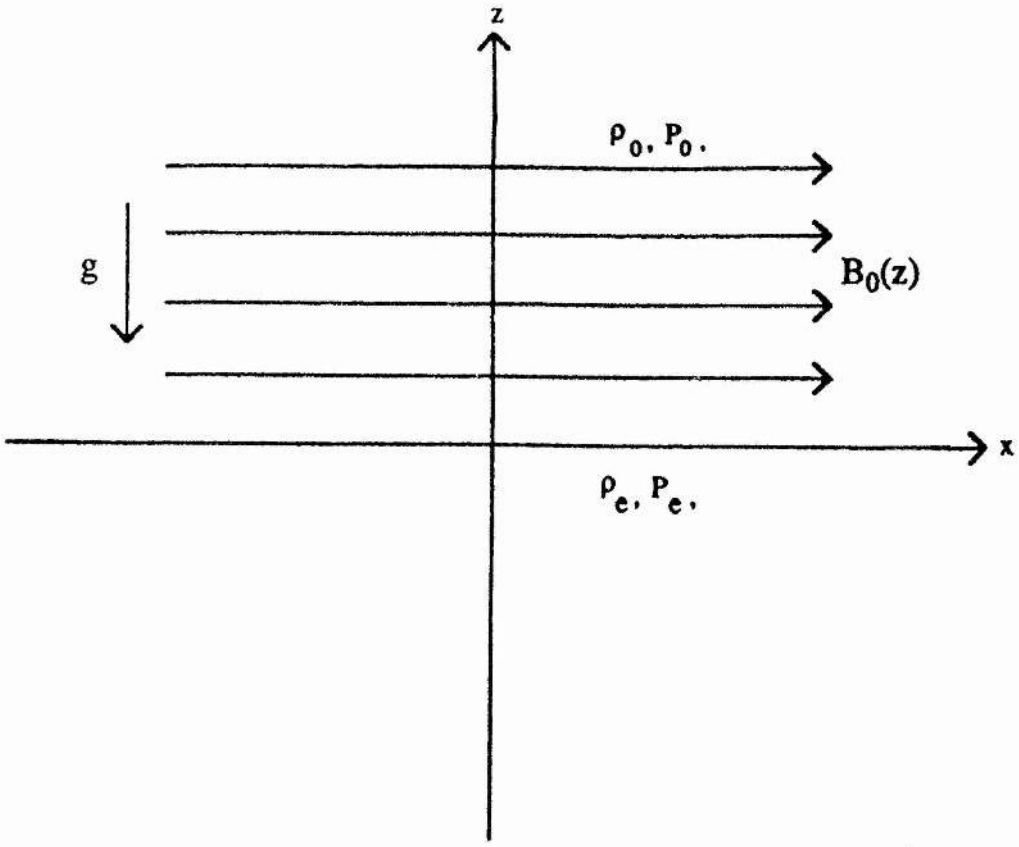

FIGURE 2.1 The equilibrium model of a single magnetic interface at z = 0.

$$\rho_0(\omega^2 - k_x^2 v_A^2)\left(\frac{d^2 v_z}{dz^2} - k_x^2 v_z\right) = 0, \qquad z > 0, \tag{2.22}$$

$$\frac{d^2 v_z}{dz^2} - k_x^2 v_z = 0, \qquad z < 0. \tag{2.23}$$

Thus assuming $\omega^2 \neq k_x^2 v_A^2$, the solutions for $v_z(z)$ in the two regions are

$$v_z(z) = \begin{cases} d_1 e^{-k_x z}, & z > 0, \\ d_2 e^{k_x z}, & z < 0, \end{cases} \tag{2.24}$$

where d_1 and d_2 are arbitrary constants and where in writing the solutions (2.24) we have assumed that the horizontal wavenumber $k_x > 0$ and chosen the solutions which satisfy the condition that $v_z \to 0$ as $|z| \to \infty$.

To determine the dispersion relation relating ω and k_x we match the two solutions given by Equation (2.24) across the interface z=0. We impose the condition that the normal component of velocity, v_z, be continuous at z=0; this gives $d_1 = d_2$. With v_z continuous, it follows from Equation (2.19) (with g=0) that the quantity

$$\rho_0(z)(\omega^2 - k_x^2 v_A^2(z))\frac{dv_z}{dz} \tag{2.25}$$

must also be continuous at z=0. The expression in (2.25) is in fact proportional to the total pressure perturbation p_T, so the condition that it be continuous across the interface is equivalent to there being no unbalanced pressure force at z=0.

Continuity of the two quantities v_z and p_T yields the dispersion relation

$$\frac{\omega^2}{k_x^2} = \frac{\rho_0}{(\rho_0 + \rho_e)} v_A^2. \tag{2.26}$$

This is the well-known result (see Kruskal and Schwarzschild 1954; Chandrasekhar 1961, Sect. 97; see also Dungey and Loughhead, 1954) that describes a hydromagnetic surface wave propagating at a speed $c_k \left(=\left(\frac{\rho_0}{\rho_0 + \rho_e}\right)^{1/2} v_A\right)$ that is intermediate between the Alfvén speeds of the two media, with one of those speeds here taken to be

zero. However, the assumptions of incompressibility and zero gravity that permit the result (2.26) are too drastic to allow it to be of more than a rough guide to the actual behaviour of surface waves in the solar atmosphere, which of course is far from incompressible and is also stratified. We shall consider the effect of compressibility in later chapters, but consider now how stratification modifies the above result.

2.4 Dispersion Relations in The Presence of Gravity

(i) Uniform Density Distribution

The presence of gravity modifies the equilibrium state of a medium and so the behaviour of a surface wave is changed in two ways: first, because the wave samples a non-uniform medium, and secondly because additional forces - buoyancy forces - arise to modify the propagation of the wave. These two effects seriously complicate any description of the waves.

As in the non-gravity case we again assume a constant Alfvén speed and a uniform density profile. Then, under these assumptions of a constant Alfvén speed and a uniform density distribution, the magnetic field is uniform also and the equilibrium given by Equation (2.7) reduces to one of hydrostatic balance. Once again we have the same equations either side of the interface as Equations (2.22) and (2.23). Consequently we have the same solutions for the vertical velocity v_z, which again is assumed to be continuous across the interface z=0. However, with the inclusion of gravity, integration of Equation (2.19) about a small neighbourhood of the interface gives the second matching condition that

$$\rho_0(z)(\omega^2 - k_x^2 v_A^2(z))\frac{dv_z}{dz} - gk_x^2\rho_0(z)v_z(z) \qquad (2.27)$$

must be continuous at z=0. The expression in (2.27) is related to the total pressure perturbation p_T; in fact, it equals $k_x^2(i\omega p_T - g\rho_0(z)v_z(z))$. Then, applying these two conditions to match the two solutions for v_z (given by Equation (2.24)) at z=0 yields the dispersion relation (e.g. Chandrasekhar, 1961, Sect. 97)

$$\frac{\omega^2}{k_x^2} = \frac{\rho_0}{(\rho_0 + \rho_e)} v_A^2 - \frac{g}{k_x} \frac{(\rho_0 - \rho_e)}{(\rho_0 + \rho_e)}, \qquad (2.28)$$

revealing that in the presence of gravity the surface mode is rendered dispersive and is also subject to instability (i.e. $\omega^2<0$) at long wavelengths if a dense fluid rests on top of a light fluid (i.e. if $\rho_0 > \rho_e$). This is the familiar Rayleigh-Taylor instability (Chandrasekhar, 1961, Sect. 97). The effect, then, of including a magnetic field is to stabilize the interface against short wavelength oscillations.

Equation (2.28) is a familiar result, widely used in astrophysical applications. But we should remember the restrictions under which it is derived, namely an incompressible fluid, uniform (unstratified) in density (though stratified in pressure). Neither of these assumptions is likely to be met under solar conditions. Consider, then, the more realistic case where we have a non-uniform density distribution.

(ii) Exponential Density Distribution

In contrast to the above, consider now the case in which the Alfvén speed is still assumed to be constant but where the density distribution is exponentially stratified (c.f. Rayleigh, 1900; see also Lamb, 1932 and Chandrasekhar, 1961, Sect. 92) such that

$$\rho_0(z) = \begin{cases} \rho_0 e^{-z/H_B}, & z > 0, \\ \rho_e e^{-z/H_e}, & z < 0, \end{cases} \qquad (2.29)$$

where H_B and H_e are arbitrary but related (see below) scale heights and are a direct result of the inclusion of gravity. They are arbitrary in the sense that they cannot, in the incompressible case, be determined by the ideal gas law and the equilibrium, as would be the case for a gas in a gravitationally stratified,compressible medium (see Chapter 4). For an incompressible medium the equation of state is not the ideal gas law, but is instead replaced by the assumption of incompressibility. That is, in the incompressible case the equation of state is that volumes do not change with variations in applied pressure or correspondingly the density (i.e., the mass per unit volume) does not change. In this respect, in an incompressible medium a gas should be treated as a fluid.

We observe that in Section 2.4(i),although the medium was gravitationally stratified there appeared to be no such scale heights. However, there we assumed a constant density distribution (c.f. Equation (2.29)) thereby effectively choosing the scale heights (since they are arbitrary) to be infinite.

Since the Alfvén speed is assumed constant and the density is no longer uniform, the magnetic field is also non-uniform, $\underline{B}_0 = B_0(z)\hat{\underline{x}}$, and the equilibrium is one of magnetohydrostatic balance, given by Equation (2.7). Once again pressure balance at the interface z = 0 dictates that the total (magnetic plus gas) pressure (as $z \to 0_+$) equals that in the field-free region below (as $z \to 0_-$) :

$$p_0(0_+) + \frac{B_0^2}{2\mu_0} = p_e(0_-), \tag{2.30}$$

where B_0 is the magnetic field strength at z = 0. The gas pressure in the upper magnetic region for a constant Alfvén speed is given by

$$p_0(z) = \rho_0\left[gH_B - \frac{1}{2}v_A^2\right]e^{-z/H_B} \tag{2.31}$$

while the gas pressure in the lower non-magnetic region is given by

$$p_e(z) = \rho_e g H_e e^{-z/H_e}. \tag{2.32}$$

Then by continuity of pressure at z=0 given by Equation (2.30) we obtain a relationship between the densities at the interface and the scale heights, namely

$$gH_B = \frac{\rho_e}{\rho_0} gH_e, \tag{2.33}$$

for finite scale heights H_e and H_B. We note that there is a condition from Equation (2.31) that for positive gas pressure in the upper magnetic region we require to satisfy the inequality

$$gH_B > \tfrac{1}{2} v_A^2. \qquad (2.34)$$

Then, for the stratification defined by Equation (2.29), the governing differential Equation (2.19) applied to the magnetic field region reduces to

$$\frac{d^2v_z}{dz^2} - \frac{1}{H_B}\frac{dv_z}{dz} + a_B v_z = 0, \qquad z > 0, \qquad (2.35)$$

where

$$a_B = k_x^2\left\{\frac{g/H_B - (\omega^2 - k_x^2 v_A^2)}{(\omega^2 - k_x^2 v_A^2)}\right\}. \qquad (2.36)$$

Equation (2.35) possesses the general solution

$$v_z(z) = \left(d_1 \exp\frac{z(1 - 4a_B H_B^2)^{1/2}}{2H_B} + d_2 \exp\frac{-z(1 - 4a_B H_B^2)^{1/2}}{2H_B}\right)\exp\left(\frac{z}{2H_B}\right), \qquad z > 0, \qquad (2.37)$$

where d_1 and d_2 are arbitrary constants. In the subsequent discussion we will assume that $4a_B H_B^2 < 1$. This assumption focuses attention on surface wave behaviour giving an exponential dependence of the disturbance. If $4a_B H_B^2 > 1$, then oscillatory-type disturbances may arise, corresponding to internal gravity modes. These will not be discussed here.

In the non-magnetic region, Equation (2.19) reduces to

$$\frac{d^2v_z}{dz^2} - \frac{1}{H_e}\frac{dv_z}{dz} + a_e v_z = 0, \qquad z < 0, \qquad (2.38)$$

where

$$a_e = k_x^2\left\{\frac{g/H_e - \omega^2}{\omega^2}\right\}. \qquad (2.39)$$

Equation (2.38) possesses the general solution

$$v_z(z) = \left(d_3 \exp \frac{z(1 - 4a_e H_e^2)^{1/2}}{2H_e} + d_4 \exp \frac{-z(1 - 4a_e H_e^2)^{1/2}}{2H_e} \right) \exp\left(\frac{z}{2H_e}\right), \quad z < 0, \tag{2.40}$$

where d_3 and d_4 are arbitrary constants. In the subsequent analysis we will assume that $4a_e H_e^2 < 1$.

The linearised form of the magnetic energy density of the perturbations is given by $\underline{B}_0.\underline{B}/\mu_0$. Since the equilibrium magnetic field only has an x-component, $\underline{B}_0 = B_0(z)\hat{\underline{x}}$, then the magnetic energy density is $B_0 B_x/\mu_0$. The x-component of the linearised perturbed induction Equation (2.8), when Fourier decomposed, gives

$$B_x = \frac{-v_z}{i\omega} \frac{dB_0}{dz}. \tag{2.41}$$

Thus, the magnetic energy density is related to

$$\frac{B_0 B_x}{\mu_0} = \frac{i v_z}{\omega} \frac{B_0}{\mu_0} \frac{dB_0}{dz}. \tag{2.42}$$

The requirement that the total [kinetic ($\propto \rho v_z^2$) plus magnetic ($\propto B_0 v_z dB_0/dz$)] energy density remains finite as $|z| \to \infty$, together with the assumptions (discussed in Section 2.4.1 entitled "Cutoff Curves") that $4a_B H_B^2 < 1$ and $4a_e H_e^2 < 1$, implies that $d_1 = d_4 = 0$. The vertical velocity component $v_z(z)$ is therefore of the form

$$v_z(z) = \begin{cases} d_2 \exp\left(\frac{1}{2H_B} - M_0\right) z, & z > 0, \\ d_3 \exp\left(\frac{1}{2H_e} + M_e\right) z, & z < 0, \end{cases} \tag{2.43}$$

where

$$M_0 = \frac{(1 - 4a_B H_B^2)^{1/2}}{2H_B}, \tag{2.44}$$

and

$$M_e = \frac{(1 - 4a_e H_e^2)^{1/2}}{2H_e} . \qquad (2.45)$$

We note that M_0, $M_e > 0$, since we take the positive square roots of $(1 - 4a_B H_B^2)^{1/2}$ and $(1 - 4a_e H_e^2)^{1/2}$. Notice that $v_z(z)$ declines in the lower dense region ($z<0$) but may or may not decline in the more tenuous upper region ($z>0$). We explore this aspect more fully in Section 2.4.2.

Applying the matching conditions as given previously in Section 2.4(i),namely continuity at $z=0$ of v_z and the total pressure perturbation (see (2.27)), to the solutions (2.43) yields the transcendental dispersion relation

$$\rho_0 \left\{ (\omega^2 - k_x^2 v_A^2)(\frac{1}{2H_B} - M_0) - g k_x^2 \right\} = \rho_e \left\{ \omega^2 (\frac{1}{2H_e} + M_e) - g k_x^2 \right\} . \qquad (2.46)$$

The dispersion relation (2.46) describes the parallel propagation of surface waves at a single, magnetic interface in a gravitationally stratified incompressible fluid, under the assumption of a constant Alfvén speed and exponential stratification in density. The dispersion relation (2.46) is written in such a way that quantities above the interface (in $z>0$) appear on the left-hand side of the equation, while those below the interface (in $z<0$) appear on the right-hand side of the equation. Throughout the thesis we shall adopt this style of presentation of the various dispersion relations that arise.

Equation (2.46) may be written in the alternative form

$$\frac{\omega^2}{k_x^2} = \frac{\rho_0}{\left(\rho_0 + \rho_e \frac{(M_e + 1/2H_e)}{(M_0 - 1/2H_B)}\right)} v_A^2 - g \frac{(\rho_0 - \rho_e)}{\rho_0 (M_0 - 1/2H_B) + \rho_e (M_e + 1/2H_e)} . \qquad (2.47)$$

This alternative form of the general dispersion relation proves to be more useful for comparing with other more complicated cases, such as the compressible cases which we shall consider in Chapters 3 and 4.

We note that in the case of a uniform density distribution or in the limit of zero gravity $H_B^{-1} = H_e^{-1} = 0$, and then $M_0 = M_e = k_x$. Thus, in the case of a uniform density distribution Equation (2.47) reduces to Equation (2.28), and in the limit of zero gravity it reduces to the dispersion relation (2.26) describing a hydromagnetic surface wave (Section 2.3).

2.4.1 Cutoff Curves

Before considering a numerical solution of the dispersion relation (2.47) it is necessary to examine the constraints under which the equation is derived. We require that $(1 - 4a_B H_B^2) > 0$ and $(1 - 4a_e H_e^2) > 0$. These constraints represent cutoff frequencies for the modes. If either $(1 - 4a_B H_B^2)$ or $(1 - 4a_e H_e^2)$ is negative, then solutions with an oscillatory structure arise; these are internal (or body) modes (Lighthill, 1978), modified by the presence of a magnetic field. They will not be discussed further in this thesis.

In much of the subsequent analysis, both in this chapter and elsewhere, it proves convenient to introduce the dimensionless frequency (squared) Ω^2, defined by

$$\Omega^2 = \frac{\omega^2}{gk_x}. \tag{2.48}$$

The condition $4a_e H_e^2 < 1$ generates a curve r_1 in the ω-k_x space which contains the allowed modes given by Equation (2.47). See Figure 2.2. Similarly, the condition $4a_B H_B^2 < 1$ generates the confining curve r_2. The form of these constraints depends upon whether $\omega > k_x v_A$ or $\omega < k_x v_A$. If $\omega > k_x v_A$, then in terms of Ω^2 we have

$$\max\left((k_x H_e) \frac{v_A^2}{gH_e}, r_1, r_2 \right) < \Omega^2, \tag{2.49}$$

where $k_x H_e$ is the dimensionless scale height for the lower non-magnetic region and v_A^2/gH_e is the non-dimensional Alfvén speed (squared).

However, if $\omega < k_x v_A$ then

$$r_1 < \Omega^2 < \min\left((k_x H_e)\frac{v_A^2}{gH_e},\ r_2\right). \qquad (2.50)$$

The curves for r_1 and r_2 are plots of

$$\Omega^2 = r_1 \equiv \frac{4k_x H_e}{1 + 4k_x^2 H_e^2}, \qquad \Omega^2 = r_2 \equiv \frac{4k_x H_B}{1 + 4k_x^2 H_B^2} + (k_x H_e)\frac{v_A^2}{gH_e}, \quad (2.51)$$

where $k_x H_B$ is the dimensionless wavenumber in terms of the scale height in the upper magnetic medium (related to that in the lower region by Equation (2.33)).

In the limit as $k_x H_e \to \infty$

$$r_1 \to 0 \qquad \text{and (provided } v_A \neq 0) \qquad r_2 \to \infty, \qquad (2.52)$$

while as $k_x H_e \to 0$

$$r_1 \to 0 \qquad \text{and} \qquad r_2 \to 0. \qquad (2.53)$$

If $v_A = 0$, then $r_2 \to 0$ as $k_x H_e \to \infty$. Additionally, we note that r_1 is independent of v_A and has a maximum at $\Omega^2 = 1$, $k_x H_e = \frac{1}{2}$.

2.4.2 The Surface Gravity Mode

It proves interesting to examine the dispersion relation (2.46) in the limit of zero magnetic field. With $B_0 = 0$, Equation (2.46) reduces to the dispersion relation

$$\rho_0\left\{\omega^2\left(\frac{1}{2H_0} - M_0\right) - gk_x^2\right\} = \rho_e\left\{\omega^2\left(\frac{1}{2H_e} + M_e\right) - gk_x^2\right\}, \qquad (2.54)$$

where now

$$M_0 = \frac{(1 - 4a_0 H_0^2)^{1/2}}{2H_0} \qquad (2.55)$$

is the non-magnetic version of M_0 given by the Equation (2.44).

In the notation of Equation (2.47), we may rewrite Equation (2.54) as

$$\frac{\omega^2}{k_x^2} = - g \frac{(\rho_0 - \rho_e)}{\rho_0 (M_0 - 1/2H_0) + \rho_e (M_e + 1/2H_e)} . \qquad (2.56)$$

It is interesting to observe that we can remove the transcendentality of Equation (2.56). This was first noticed by Bernstein and Book (1983) in their investigation of the effect of compressibility on the Rayleigh-Taylor instability. After much algebra, Equation (2.56) may be rewritten (see Appendix A.1) as a polynomial in Ω^2 :

$$(\Omega^4 - 1)\left\{k_x(\rho_0 + \rho_e)^2\Omega^4 - (\frac{\rho_0}{H_e} + \frac{\rho_e}{H_0})(\rho_0 + \rho_e)\Omega^2 - k_x(\rho_0 - \rho_e)^2\right\} = 0. \quad (2.57)$$

Bernstein and Book (1983), in their instability investigations, over-looked the factor $(\Omega^4 - 1)$ and considered the quadratic (in Ω^2) factor only of Equation (2.57); we consider the full expression as given by Equation (2.57).

Clearly, the process of removing the transcendental nature of Equation (2.56), through squaring several times, may introduce spurious roots which satisfy the polynomial (2.57) but not the original dispersion relation (2.56). Possible solutions to the polynomial (2.57) are $\Omega^2 = \pm 1$ together with those arising from the quadratic (in Ω^2), namely

$$k_x(\rho_0 + \rho_e)^2\Omega^4 - (\frac{\rho_0}{H_e} + \frac{\rho_e}{H_0})(\rho_0 + \rho_e)\Omega^2 - k_x(\rho_0 - \rho_e)^2 = 0. \qquad (2.58)$$

A stable (i.e., $\Omega^2 > 0$) solution to Equation (2.56) is $\omega^2 = gk_x$ (i.e., $\Omega^2 = 1$); this is termed the f-mode. It is shown Section 2.4.3 that the f-mode is able to propagate only when $\rho_0 > \rho_e$. The f-mode is illustrated in Figure 2.2; we shall discuss it in greater detail in the next section. Note now that in Figure 2.2 (and also in Figure 2.3) that for the non-magnetic case the curve r_2 tends to zero as $k_xH_e \to \infty$. When $\rho_0 > \rho_e$, there are no stable solutions to the Ω^2 - quadratic (2.58) which are also stable solutions to the dispersion relation (2.56).

If $\rho_0 < \rho_e$, then the solution $\omega^2 = gk_x$ of the polynomial (2.57) does not satisfy the dispersion relation (2.56) and the only stable ($\Omega^2 > 0$) solutions to the dispersion relation (2.56) are those resulting from the quadratic (2.58), namely

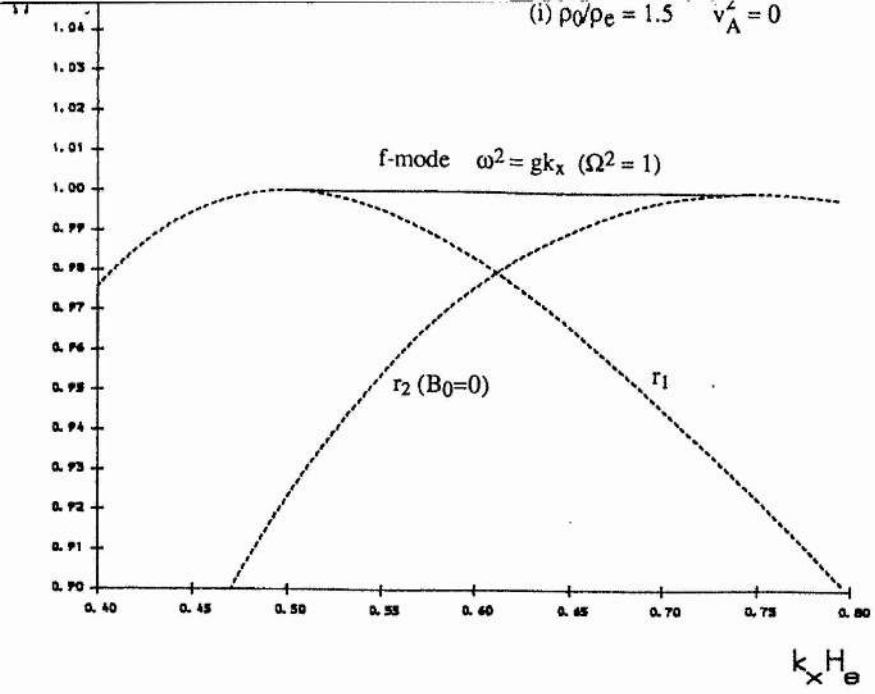

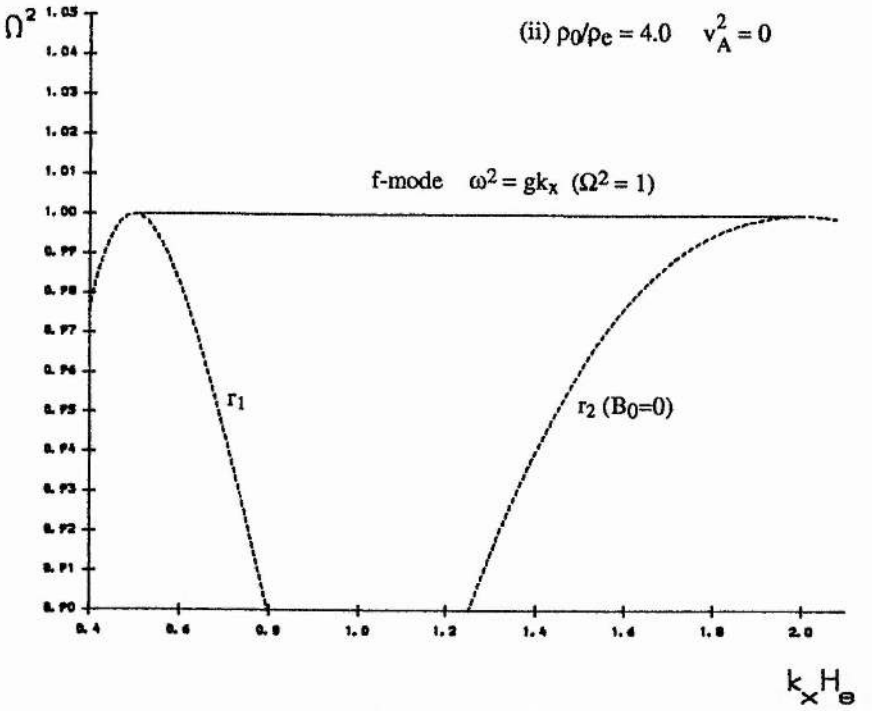

FIGURE 2.2 The f-mode ($\Omega^2 \equiv \omega^2/gk_x=1$) as a function of dimensionless horizontal wavenumber k_xH_e in the absence of a magnetic field. Case (i) $\rho_0/\rho_e = 1.5$; (ii) $\rho_0/\rho_e = 4.0$. Note the changed scales. The dashed curves r_1 and r_2 are cutoffs for the propagation of the f-mode determined by the requirements that $4a_0H_0^2 < 1$ and $4a_eH_e^2 < 1$ (see text). Solutions of the dispersion relation (2.56) must lie above the curves r_1 and r_2 $(B_0=0)$. Observe that the range of propagation wavenumber is reduced as ρ_0/ρ_e approaches unity; for $\rho_0<\rho_e$, the f-mode does not exist.

$$\Omega^2 = \frac{\frac{\rho_0}{k_x H_e} \pm \left\{ \frac{\rho_0^2}{k_x^2 H_e^2} + (\rho_0 - \rho_e)^2 \right\}^{1/2}}{(\rho_0 + \rho_e)} . \qquad (2.59)$$

In fact there is only one stable solution to Equation (2.59) which is also a solution to the dispersion relation (2.56). This mode is shown in Figure 2.3(i) and is the surface gravity wave. The mode asymptotes to a distinct limit at short wavelengths. As $k_x H_e \rightarrow \infty$, M_0 and $M_e \rightarrow k_x$, and dispersion relation (2.56) reduces to

$$\Omega^2 = - \frac{(\rho_0 - \rho_e)}{(\rho_0 + \rho_e)} , \qquad (2.60)$$

which is the familiar Rayleigh-Taylor dispersion relation (see Equation (2.28) with $v_A = 0$). We note that for $\rho_0 > \rho_e$, Equation (2.60) does not give a wave (i.e. $\Omega^2 < 0$) and so we can conclude that the f-mode (which propagates only for $\rho_0 > \rho_e$) must have an upper bound on its propagation. In fact, the f-mode is bounded both from above and below; we discuss this in the next section.

Figure 2.3(i) is drawn for the parameter value $\rho_0/\rho_e = 0.5$ for which Equation (2.60) gives $\Omega^2 = 1/3$ (i.e., $\Omega^2 \rightarrow 1/3$ as $k_x H_e \rightarrow \infty$). The mode may have a vertical velocity component, v_z, in the upper atmosphere ($z>0$) that is exponentially growing for small values of $k_x H_e$. The mode always has a vertical velocity component that declines in the lower atmosphere ($z<0$). This behaviour of the mode may easily be deduced from an examination of the vertical velocity component :

$$v_z(z) \propto \begin{cases} \exp\left\{ \frac{1}{2H_0} [1 - (1 - 4a_0 H_0^2)^{1/2}] z \right\}, & z > 0, \\ \exp\left\{ \frac{1}{2H_e} [1 + (1 - 4a_e H_e^2)^{1/2}] z \right\}, & z < 0, \end{cases} \qquad (2.61)$$

where we take the positive square roots of $(1 - 4a_0 H_0^2)^{1/2}$ and $(1 - 4a_e H_e^2)^{1/2}$.

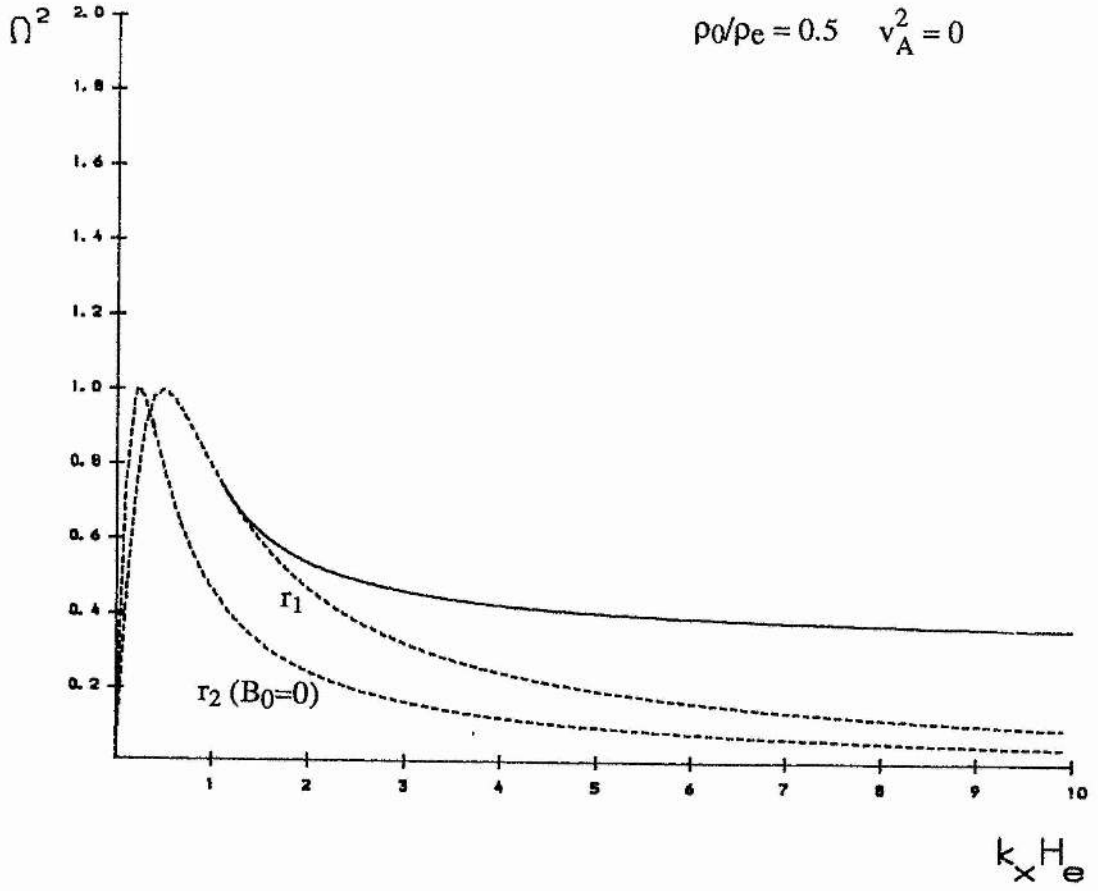

FIGURE 2.3(i) The non-dimensional frequency Ω^2 versus dimensionless horizontal wavenumber for the stable solution to the non-magnetic dispersion relation (2.54) when $\rho_0<\rho_e$. Here $\rho_0/\rho_e = 0.5$, giving $\Omega^2 \to 0$ as $k_xH_e \to 0$ and $\Omega^2 \to 1/3$ as $k_xH_e \to \infty$. The dashed curves r_1 and r_2 are determined from the requirements that $4a_0H_0^2 < 1$ and $4a_eH_e^2 < 1$.

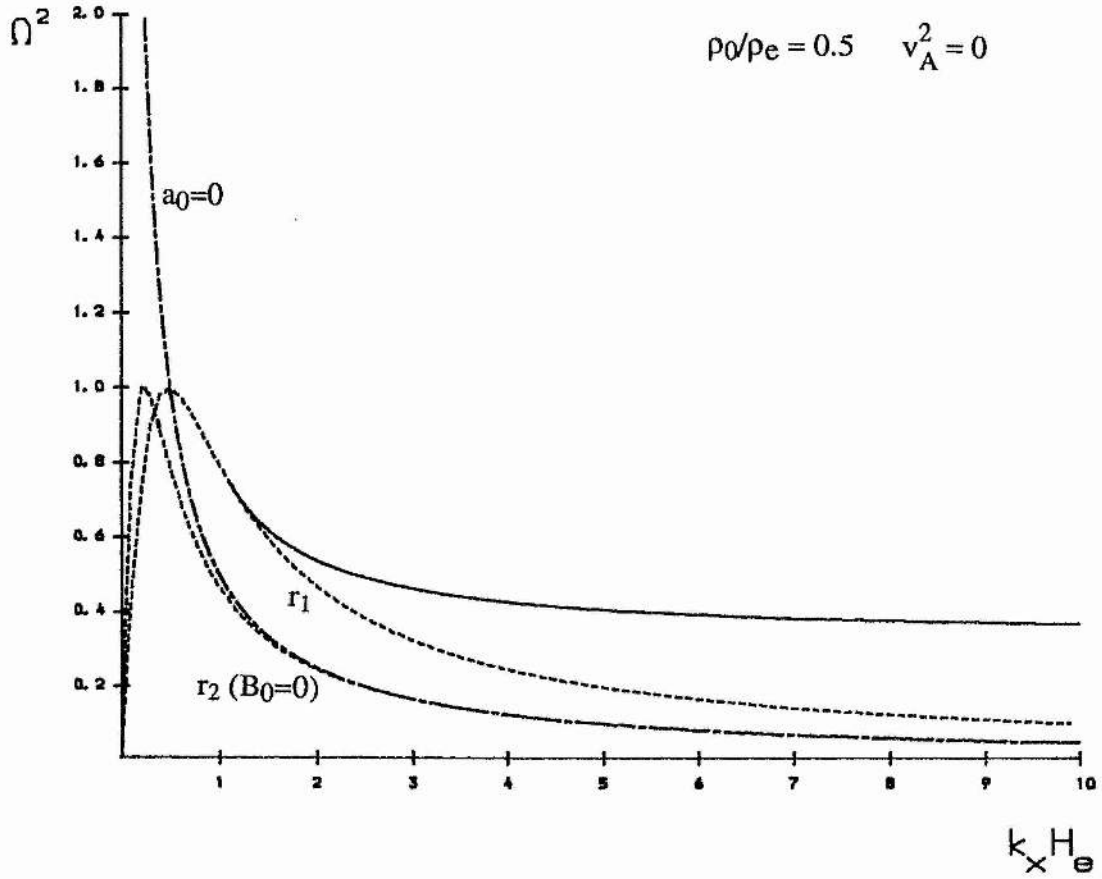

FIGURE 2.3(ii) As in (i) with the inclusion of the curve $a_0=0$, shown as a dash-dotted line. The curve $a_0=0$ divides the region of evanescence in the upper medium into a domain wherein the vertical velocity component is growing with height z from a domain where it is declining with height. Above and to the right of the curve $a_0=0$, a mode will have a vertical velocity component that is declining with height z.

Evidently, for $z<0$, v_z is always exponentially declining in nature. However, for $z>0$, v_z declines only if $a_0<0$. Thus $a_0=0$ determines the change in character from exponentially growing to exponentially declining. The curve $a_0=0$ is defined by

$$\Omega^2 = \frac{\rho_0}{\rho_e k_x H_e}. \tag{2.62}$$

The curve $a_0=0$ is drawn in Figure 2.3(ii), superimposed on the mode given in Figure 2.3(i). The $a_0=0$ curve (shown as a dash-dotted line) asymptotes to infinity as $k_xH_e \to 0$ and to the cutoff curve r_2 (with $B_0=0$) as $k_xH_e \to \infty$. Thus, from Equation (2.51) with $B_0=0$, the curve $a_0=0$ tends to zero as $k_xH_e \to \infty$.

Thus, for a mode to have declining v_z it must lie in the region $a_0<0$; that is, the mode must lie in the region

$$\Omega^2 > \frac{\rho_0}{\rho_e k_x H_e}, \tag{2.63}$$

which corresponds to the region above and to the right of the curve $a_0=0$ drawn in Figure 2.3(ii). We conclude, therefore, that since the mode lies entirely within the region defined by Equation (2.63), then the vertical velocity component, v_z, of the mode is always of an exponentially declining nature. This is illustrated in Figure 2.4 where the eigenmode is plotted for two values of k_xH_e.

Consider now the influence of a magnetic field on the surface gravity mode. Figure 2.5 illustrates how the surface gravity wave develops as the magnetic field strength is increased. The same scale is used on these figures as on those given previously in Figure 2.3 so that one may readily compare them to see how the mode develops from the non-magnetic case. Figure 2.5 clearly illustrates the fact that the curve r_1 is independent of v_A and has a maximum at $\Omega^2 = 1$, $k_xH_e = 0.5$.

In the limit as $k_xH_e \to \infty$, Equation (2.47) reduces to

$$\Omega^2 = \frac{\rho_0}{(\rho_0 + \rho_e)} \frac{k_x v_A^2}{g} - \frac{(\rho_0 - \rho_e)}{(\rho_0 + \rho_e)}, \tag{2.64}$$

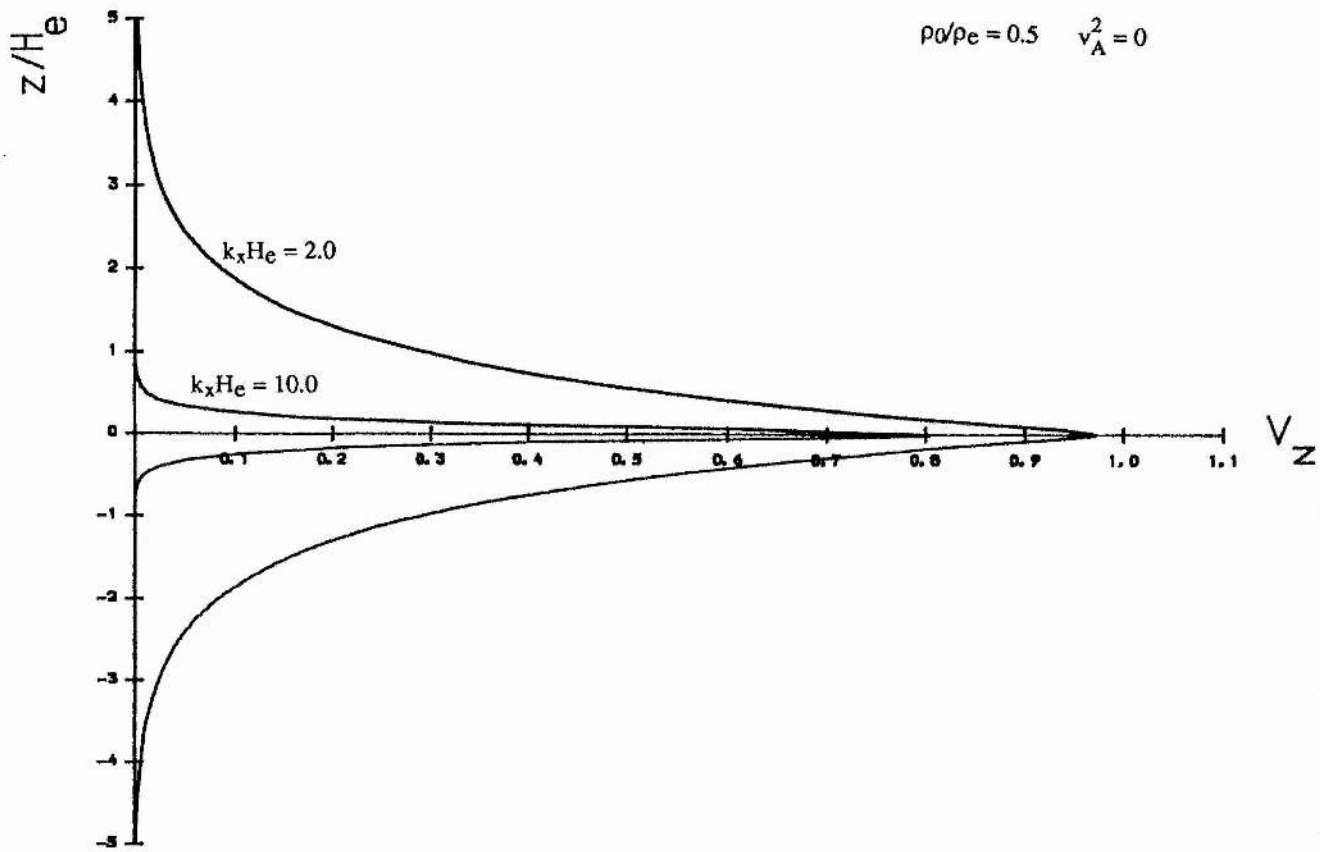

FIGURE 2.4 The eigenfunction $v_z(z)/v_z(0)$ for the surface gravity mode shown in Figure 2.3, at two values of k_xH_e.

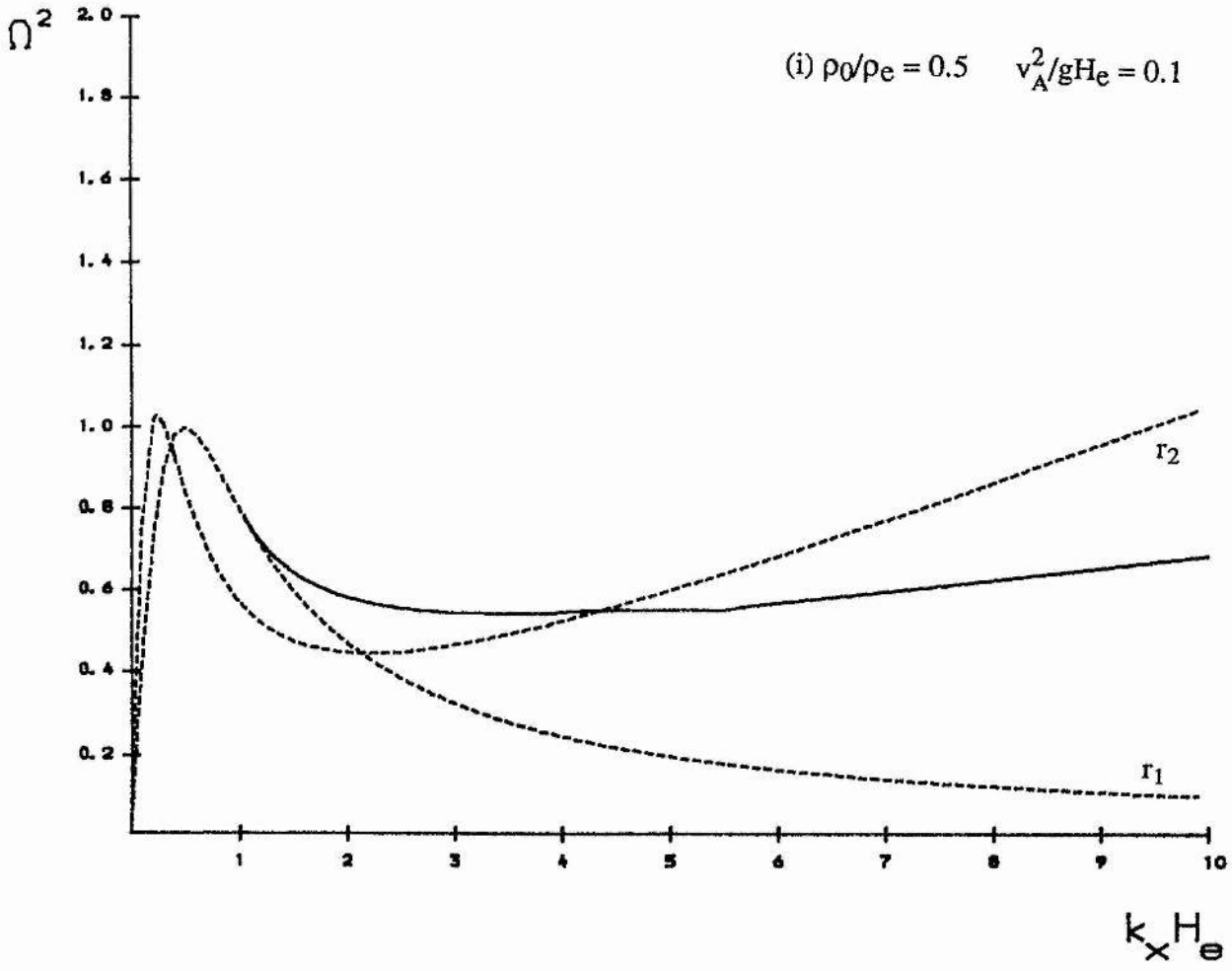

FIGURE 2.5(i) The non-dimensional frequency Ω^2 versus dimensionless horizontal wavenumber for the hydromagnetic surface gravity mode at a magnetic interface with a constant Alfvén speed and $\rho_0/\rho_e = 0.5$, $v_A^2/gH_e = 0.1$. The dashed curves r_1 and r_2 are determined from the requirements that $4a_BH_B^2 < 1$ and $4a_eH_e^2 < 1$.

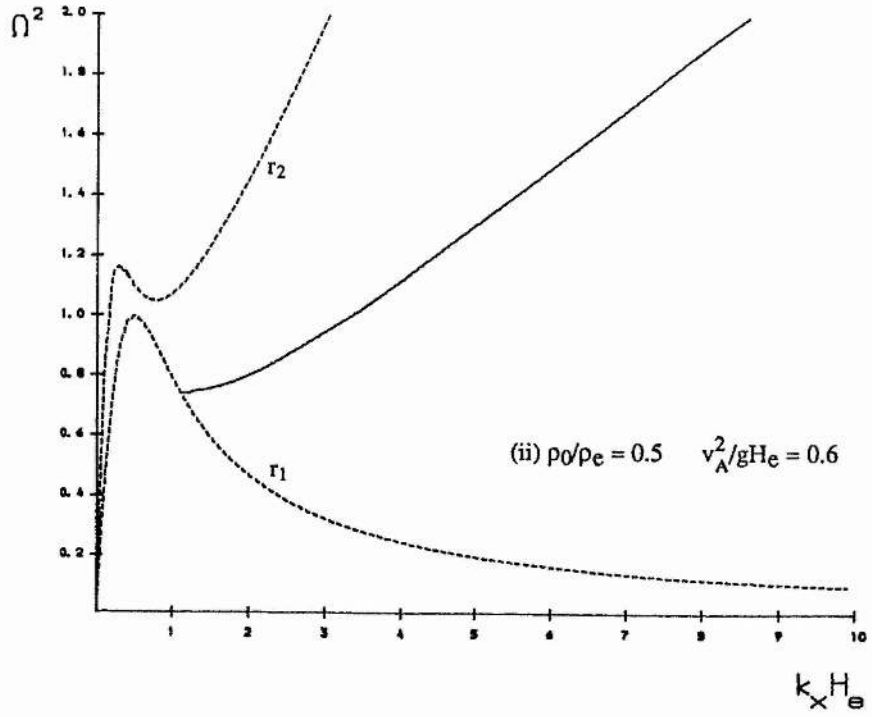

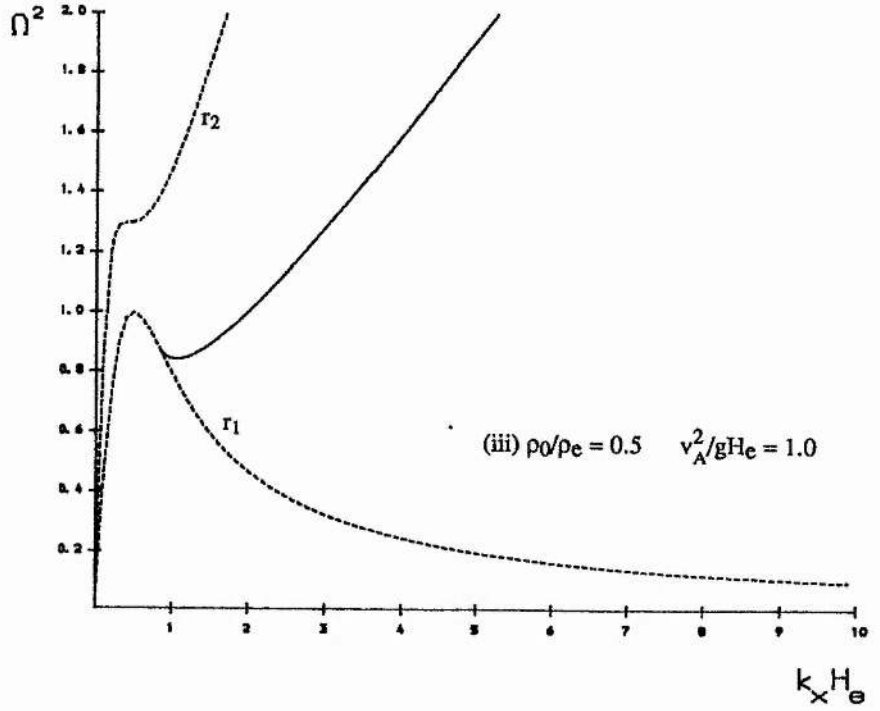

FIGURE 2.5(ii) & (iii) The non-dimensional frequency Ω^2 versus dimensionless horizontal wavenumber for the hydromagnetic surface gravity mode at a magnetic interface with a constant Alfvén speed and $\rho_0/\rho_e = 0.5$. Cases (ii) $v_A^2/gH_e = 0.6$ and (iii) $v_A^2/gH_e = 1.0$.

which is Equation (2.28); Equation (2.64) reduces to Equation (2.60) in the non-magnetic case. Now with the inclusion of a magnetic field the surface gravity mode no longer asymptotes to a finite value as $k_x H_e \to \infty$, but (as can be determined from Equation (2.64)) tends to infinity for large values of $k_x H_e$. This is illustrated, in particular, in Figures 2.5(ii) & (iii).

2.4.3 The f-Mode

In the absence of a magnetic field Equations (2.17) and (2.18) possess the solution, $v_z \propto e^{k_x z}$, $\omega^2 = gk_x$ (i.e. $\Omega^2 = 1$). The solution $\Omega^2 = 1$ is the f-mode. The f-mode is therefore an incompressible mode. However, in the presence of a horizontal magnetic field the f-mode's frequency is affected by the magnetic forces and departs slightly from $\omega^2 = gk_x$. In Chapter 4 (see also Miles and Roberts, 1991a,b) we shall consider this aspect of the f-mode's character for the case of a compressible plasma (see also Campbell and Roberts, 1989; Evans and Roberts, 1990a,b).

The f-mode will be a solution to the dispersion relation (2.46) in the limit of zero field provided the mode satisfies the conditions on $v_z(z)$ under which the dispersion relation was derived. In the case of zero magnetic field, Equation (2.46) with $\Omega^2 = 1$ reduces to

$$\rho_0 \left\{ \frac{1}{2k_x H_0} \left[1 - | 1 - 2k_x H_0 | \right] - 1 \right\} = \rho_e \left\{ \frac{1}{2k_x H_e} \left[1 + | 2k_x H_e - 1 | \right] - 1 \right\}. \tag{2.65}$$

A scrutiny of Equation (2.65) reveals that it is satisfied only if the horizontal wavenumber k_x lies in the interval

$$\frac{1}{2H_e} < k_x < \frac{1}{2H_0}. \tag{2.66}$$

With k_x lying in this interval there is a mode with $\omega^2 = gk_x$ and $v_z \propto e^{k_x z}$ that satisfies boundness of the kinetic energy density but the velocity itself is unbounded in the upper region (z>0). It follows immediately from the inequality (2.66) that the f-

mode can propagate only if $H_e > H_0$. Since the scale heights are related by Equation (2.33), namely (for $B_0 = 0$)

$$gH_0 = \frac{\rho_e}{\rho_0} gH_e, \tag{2.67}$$

and so the f-mode can propagate only if $\rho_0 > \rho_e$.

The restriction on the propagation of the f-mode is apparent in Figure 2.2. Figure 2.2 demonstrates clearly how the restriction on wavenumber for the propagation of the f-mode is tightened as ρ_0/ρ_e approaches unity. The dashed curves are cutoff curves for the propagation resulting from the assumptions that $4a_0H_0^2 < 1$ (giving the dashed curve r_2 (B_0=0)) and $4a_eH_e^2 < 1$ (giving the dashed curve r_1), with $a_B \rightarrow a_0$ and $H_B \rightarrow H_0$ in the limit of no magnetic field. Beyond these dashed curves the solutions to the dispersion relation (2.56) are complex.

We note that the f-mode is not a solution when we have a *uniform* density distribution, for which the dispersion relation (2.28) with $B_0 = 0$, reduces to

$$\frac{\omega^2}{gk_x} = - \frac{(\rho_0 - \rho_e)}{(\rho_0 + \rho_e)}. \tag{2.68}$$

Once again we recover the familiar Rayleigh-Taylor dispersion relation. We note that for $\rho_0 > \rho_e$ Equation (2.68) can give no wave solution since $\omega^2 < 0$. Clearly, $\omega^2 = gk_x$ is not a solution to Equation (2.68). This may be understood by considering the restriction on the f-mode's propagation given by Equation (2.66). With a uniform distribution of density the scale heights H_0 and H_e are effectively infinite. Then the range of existence for the f-mode given by Equation (2.66) is zero and thus the f-mode does not propagate for any horizontal wavenumber k_x.

We consider now the influence of the magnetic field on the f-mode. We seek an approximate solution to the dispersion relation (2.47), with the property that $\Omega^2 \rightarrow 1$ as $v_A^2/gH_e \rightarrow 0$, by writing

$$\Omega^2 \rightarrow 1 + \alpha \frac{v_A^2}{gH_e}, \qquad \frac{v_A^2}{gH_e} \rightarrow 0, \tag{2.69}$$

for constant α. Expanding the dispersion relation (2.47) for small v_A^2/gH_e allows us to determine α. After some detailed algebra (see Appendix A.2), we find that

$$\alpha = \frac{k_x H_e}{2} \frac{(2k_x H_e - 1)}{(k_x H_e - k_x H_0)}. \tag{2.70}$$

Since the conditions $2k_x H_e > 1$ and $\rho_0 > \rho_e$ (i.e. $H_e > H_0$) are imposed in deriving Equation (2.70), we see that α is positive. Thus, in the presence of a magnetic field the frequency of the f-mode is *increased*. Other investigations of the effect of a magnetic field on the f-mode's frequency have similarly found an increase (Campbell and Roberts, 1989; Evans and Roberts, 1990a,b).

In terms of the original variables, the first order correction to the f-mode in the presence of a magnetic field gives the result

$$\frac{\omega^2}{gk_x} \approx 1 + \frac{1}{2} \frac{(2k_x H_e - 1)}{(k_x H_e - k_x H_0)} \frac{k_x v_A^2}{g}, \tag{2.71}$$

valid for $2k_x H_e > 1$ and $\rho_0 > \rho_e$. We note that Equation (2.71) is valid only within the domain given by inequality (2.66), since otherwise the expansion (2.69) does not reduce to the f-mode as the magnetic field tends to zero.

Figure 2.6 compares the analytical result (2.71) with the results from a numerical solution of the dispersion relation (2.47). We note that the numerical solution (shown as the solid curve) departs from the non-magnetic solution, $\Omega^2 = 1$, and that this departure is accentuated as the magnetic field strength is increased (compare Figure 2.6(i) and Figure 2.6(ii)). The analytical approximation to the numerical solution, given by Equation (2.71) and shown as the dash-dotted curve, provides a reasonable approximation to the dispersion relation of the f-mode in the presence of a weak magnetic field. Thus in Figure 2.6(ii) (where $v_A^2/gH_e = 0.1$) there is a greater discrepancy between the solution and the analytical result, compared with Figure 2.6(i) ($v_A^2/gH_e = 0.05$) where the magnetic field is only 70% as strong.

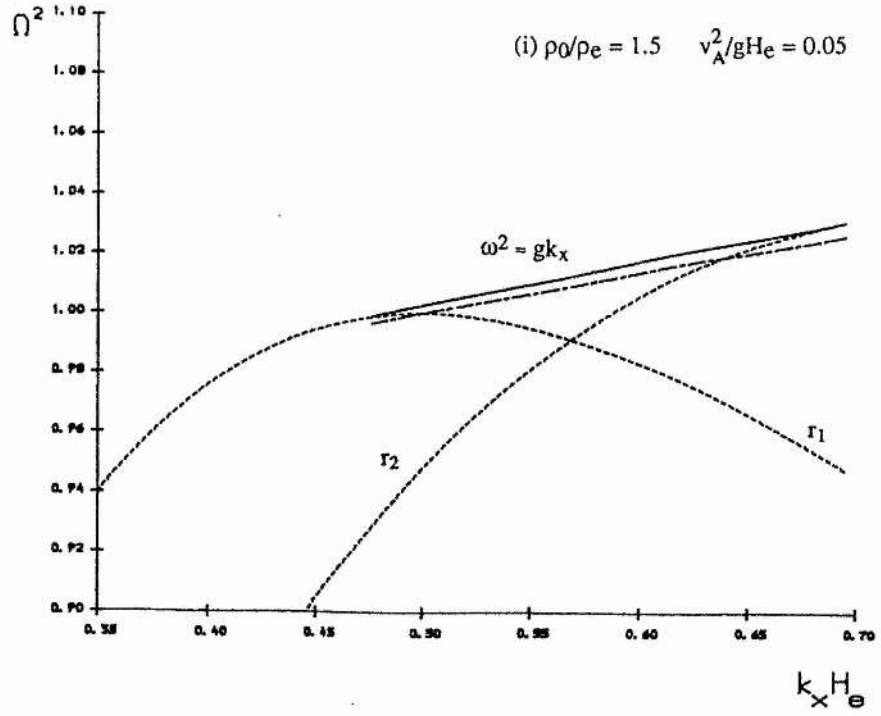

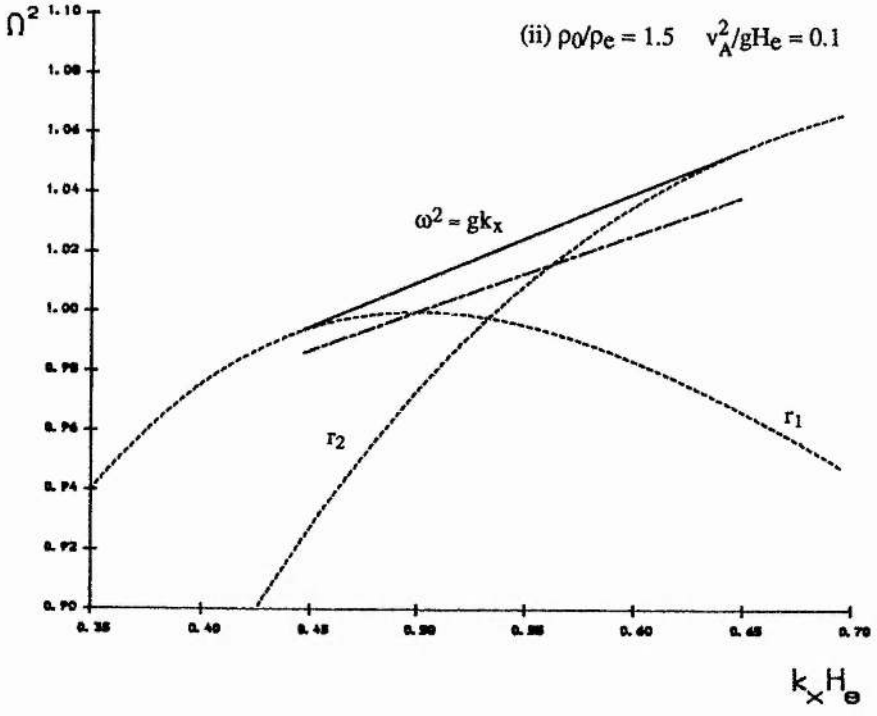

FIGURE 2.6 The effect of a weak magnetic field on the f-mode when $\rho_0/\rho_e = 1.5$. Case (i) $v_A^2/gH_e = 0.05$; (ii) $v_A^2/gH_e = 0.1$. The lower (dash-dotted) curve is that given by the analytical result (2.71) obtained in the text. The dashed curves labelled r_1 and r_2 are cutoff curves resulting from the constraints $4a_BH_B^2 < 1$ and $4a_eH_e^2 < 1$ in Equation (2.47).

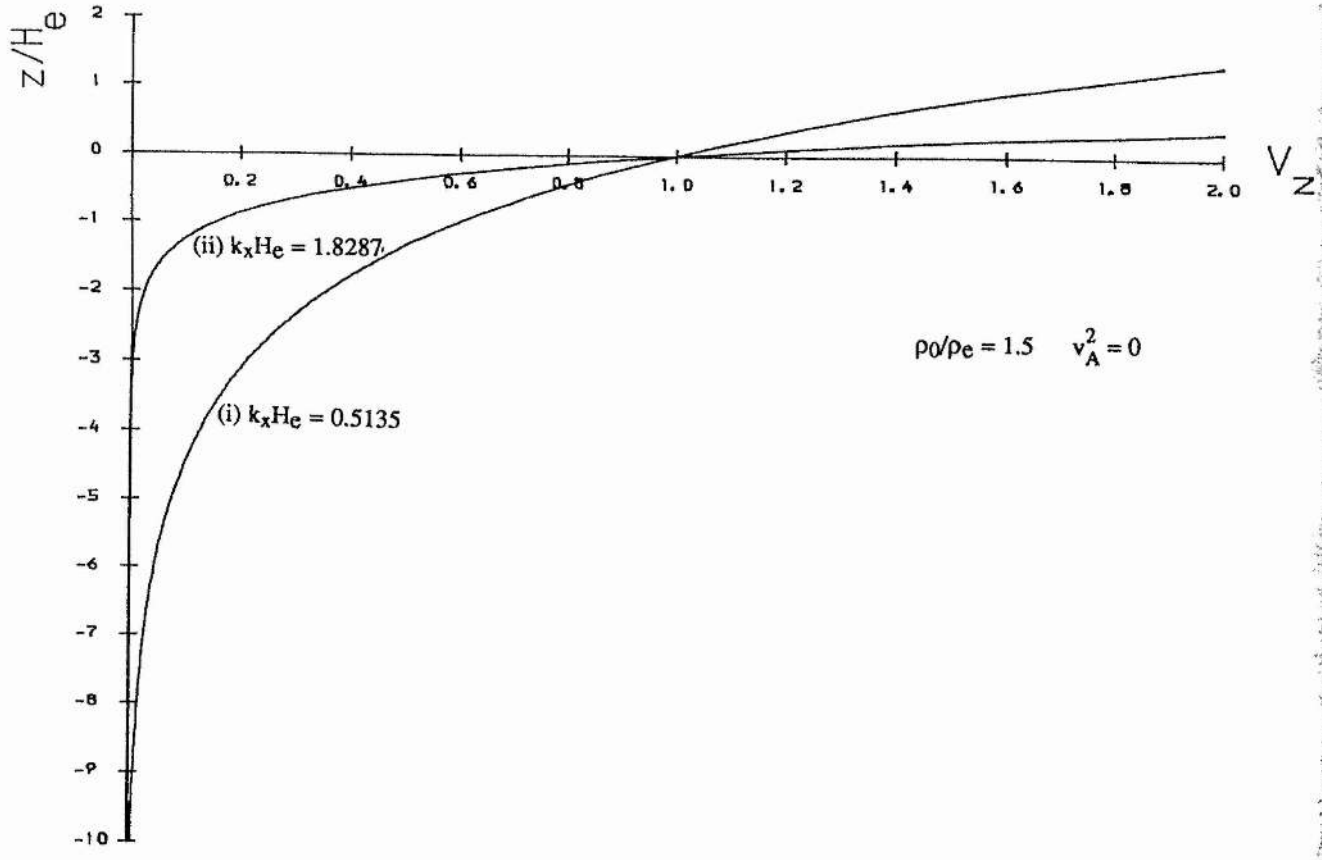

FIGURE 2.7 The eigenfunction $v_z(z)/v_z(0)$ for the f-mode with $\rho_0/\rho_e = 1.5$ (c.f. Figure 2.2(i)) and cases (i) $k_xH_e = 0.5135$ and (ii) $k_xH_e = 1.8287$, chosen close to the limits of allowable wavenumber.

We note also that the numerical solution can lie below $\Omega^2 = 1$ as well as above it. However, this possible negative correction to the result $\Omega^2 = 1$ is not allowed by the analytical solution which must always lie above $\Omega^2 = 1$. This is since the analytical result is valid only within the domain given by inequality (2.66); otherwise the expansion (2.69) does not reduce to the $\Omega^2 = 1$ as the magnetic field tends to zero. Thus $2k_xH_e > 1$ and Equation (2.71) is positive definite.

The vertical velocity of the disturbance, given by Equation (2.61), can be calculated as a function of height for any point on the dispersion curve. Figure 2.7 compares the eigenfunctions for the f-mode for two different values of the horizontal wavenumber. The eigenfunctions are for $k_xH_e = 0.5135$, just as the f-mode begins to propagate, and for $k_xH_e = 1.8287$ at the other extreme of its range of propagation. This figure shows clearly that the eigenfunction of the f-mode is depressed as the horizontal wavenumber is increased. We note that $v_z \not\to 0$ as $z \to \infty$. If we were to superimpose the curve $a_0=0$ on Figure 2.2 then the f-mode would lie entirely within the region $a_0>0$. That is, the f-mode lies in the region of the graph where its vertical velocity component, v_z, grows exponentially as $z \to \infty$. However, the conditions imposed on the solutions (2.61) ensure that the energy density (kinetic plus magnetic) remains finite as $|z| \to \infty$. The profiles of kinetic energy density for the eigenfunctions in Figure 2.7 are shown in Figure 2.8.

Figures 2.9 and 2.10 illustrate how the f-mode develops as the magnetic field strength is increased. Figures 2.9(i) and (ii) are exactly the same as those given earlier in Figure 2.6 except that here the analytical result has been omitted. They are presented again purely for convenience of comparison. We note that as the magnetic field strength is increased (through the parameter v_A^2/gH_e) so the f-mode's departure from $\Omega^2 = 1$ becomes greater. Now with the inclusion of a magnetic field, and unlike the non-magnetic case for $\rho_0 > \rho_e$, in addition to the f-mode (modified by the presence of magnetic field) we have a surface gravity mode (modified by the presence of magnetic field). The scales used in Figures 2.9 and 2.10(i) are such that the surface gravity mode is not apparent. This is since these figures have been drawn foremost to illustrate how

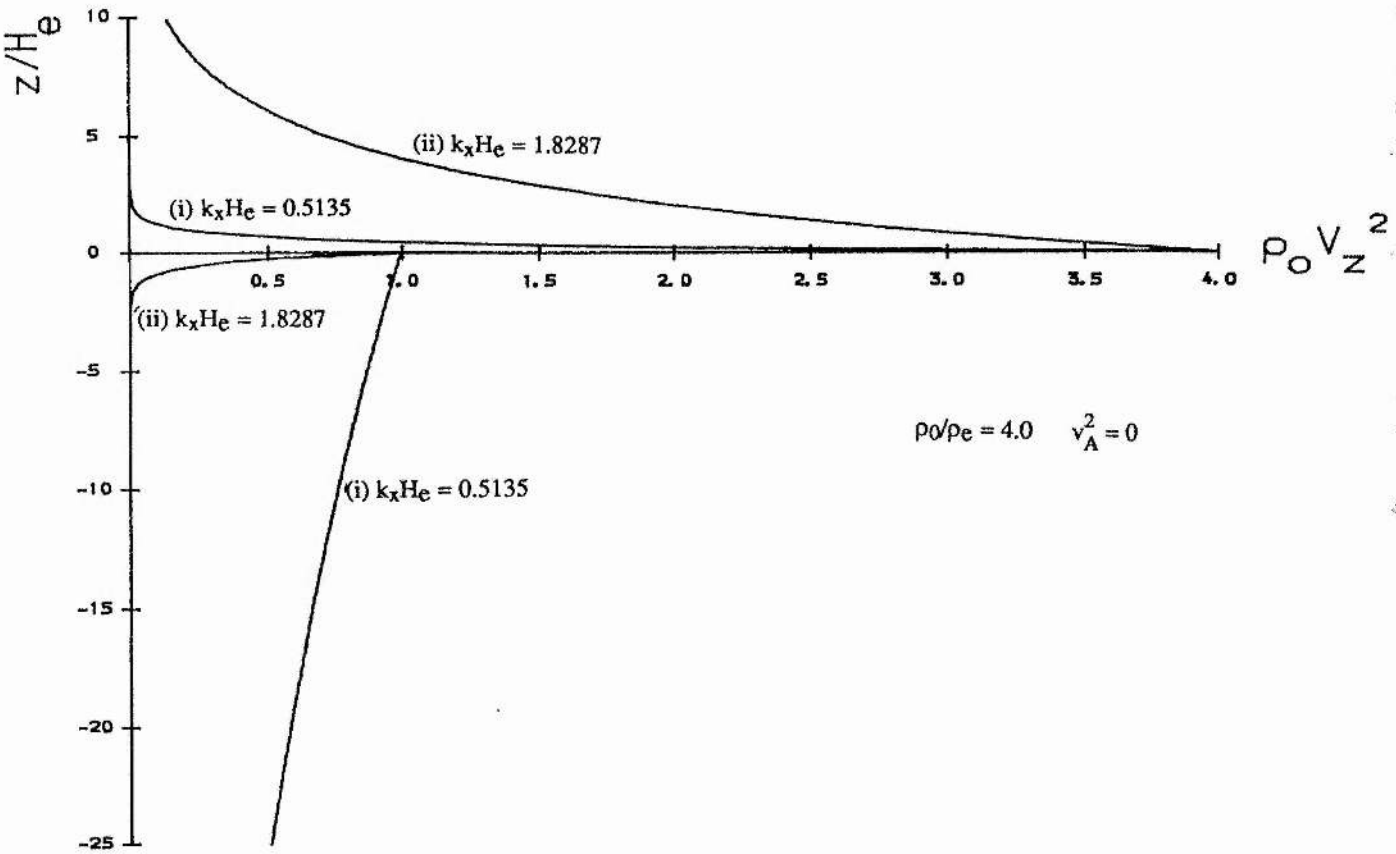

FIGURE 2.8 The profile of kinetic energy density, $\frac{1}{2}\rho(z)v_z^2$, of the f-mode with $\rho_0/\rho_e = 4.0$. Cases (i) $k_xH_e = 0.5135$, (ii) $k_xH_e = 1.8287$. The kinetic energy density is plotted in units of $\frac{1}{2}\rho_e v_z^2(0)$.

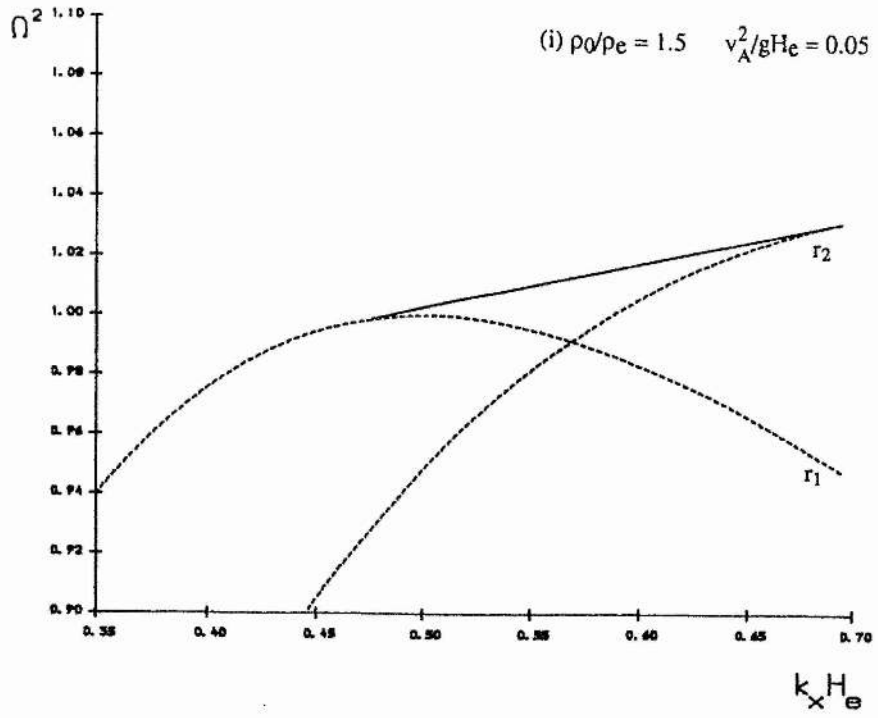

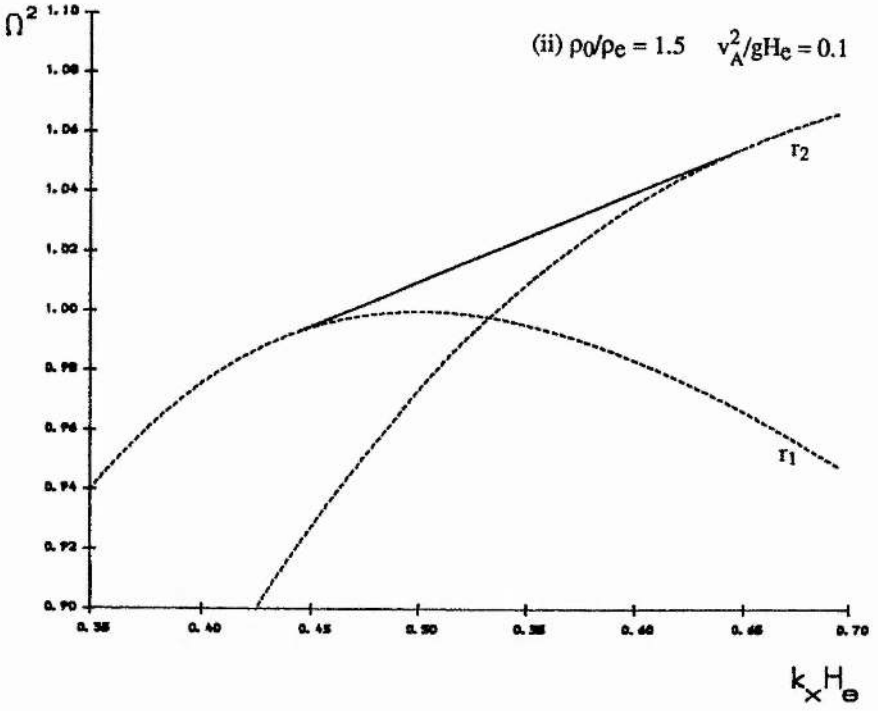

FIGURE 2.9(i) & (ii) The non-dimensional frequency Ω^2 versus dimensionless horizontal wavenumber for the f-mode (modified by the presence of a magnetic field) at a magnetic interface with a constant Alfvén speed and $\rho_0/\rho_e = 1.5$. Cases (i) $v_A^2/gH_e = 0.05$; (ii) $v_A^2/gH_e = 0.1$.

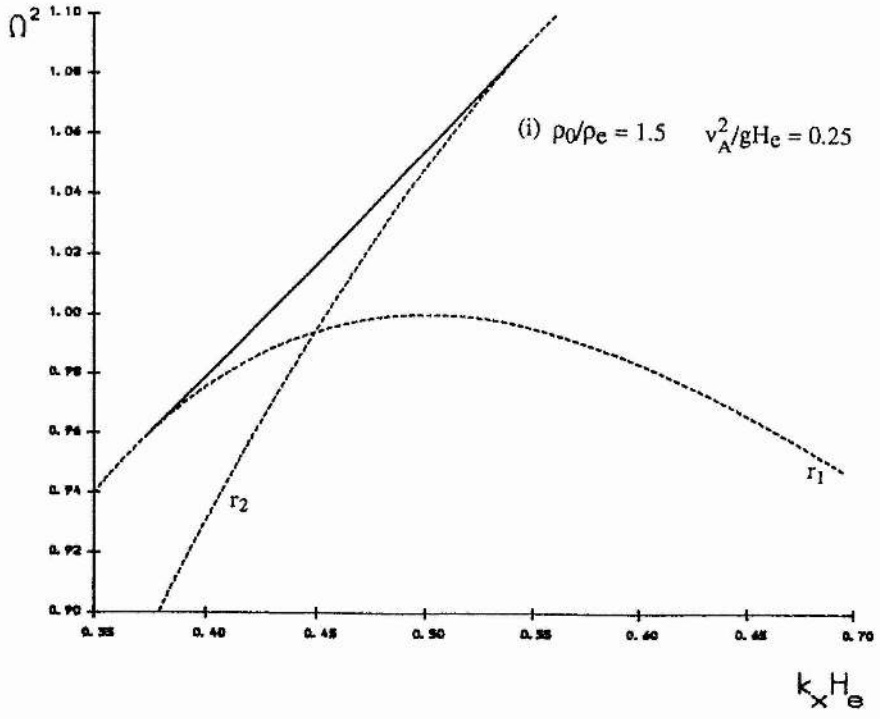

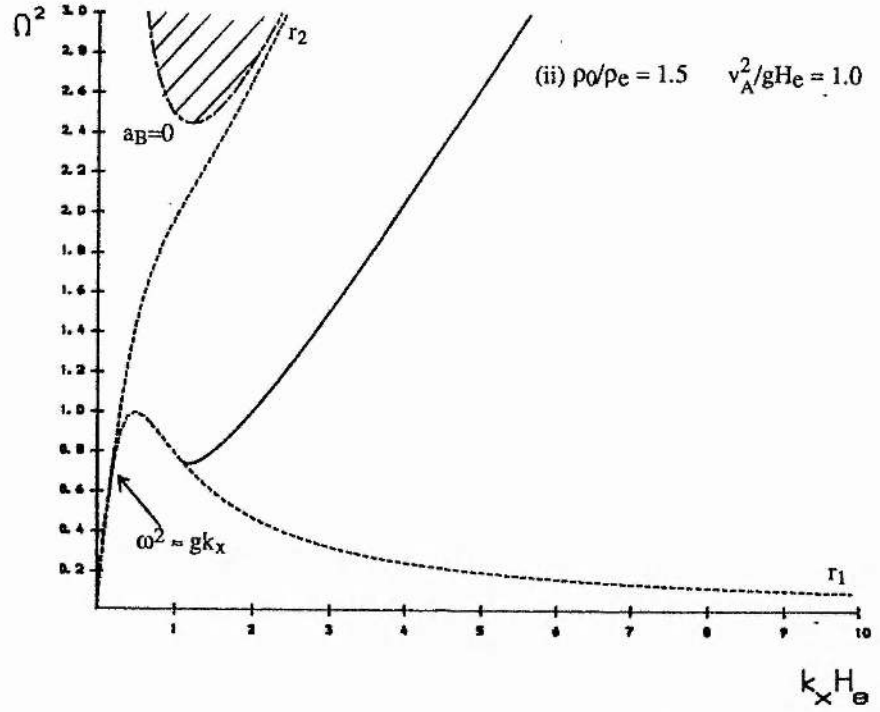

FIGURE 2.10(i) & (ii) The non-dimensional frequency Ω^2 versus dimensionless horizontal wavenumber for the f-mode at a magnetic interface with a constant Alfvén speed and $\rho_0/\rho_e = 1.5$. Cases (i) $v_A^2/gH_e = 0.25$ and (ii) $v_A^2/gH_e = 1.0$. In (ii) both the f-mode and the hydromagnetic surface gravity mode are present. In (ii) the curve $a_B=0$ is shown as a dash-dotted line.

the f-mode develops as the magnetic field increases in strength. However, in Figure 2.10(ii), drawn to a much larger scale, the surface gravity mode is seen. This is exactly the same mode as given in Figure 2.5 except that here $\rho_0/\rho_e = 1.5$. Once again as $k_xH_e \rightarrow \infty$ the mode asymptotes to infinity. Unfortunately, due to the larger scale the f-mode is almost indistinguishable and requires an indicator to show its presence.

Now we know that the surface gravity mode in Figure 2.5 has a vertical velocity component that declines in the upper atmosphere; thus the mode in Figure 2.10(ii), since it is the same mode, must also have a declining v_z. Also, we know that the f-mode, although modified by the presence of the magnetic field, has a growing v_z. The curve $a_B=0$ (the equivalent curve to $a_0=0$ with the inclusion of a magnetic field) determines where a mode changes in character from exponentially growing to exponentially declining. The curve $a_B=0$ is defined by

$$\Omega^2 = \frac{\rho_0}{\rho_e k_x H_e} + (k_x H_e)\frac{v_A^2}{gH_e}. \tag{2.72}$$

The curve $a_B=0$ is drawn in Figure 2.10(ii) as a dash-dotted line and asymptotes to infinity as $k_xH_e \rightarrow 0$ and $\Omega^2 \rightarrow \infty$ as $k_xH_e \rightarrow \infty$. Then for the mode to have declining v_z it must lie in the region $a_B<0$. The definition of the region $a_B<0$ depends upon whether $\omega > k_xv_A$ or $\omega < k_xv_A$. If $\omega > k_xv_A$ then the mode must lie in the region

$$\Omega^2 > \frac{\rho_0}{\rho_e k_x H_e} + (k_x H_e)\frac{v_A^2}{gH_e}, \tag{2.73}$$

which corresponds to the region inside the curve $a_B=0$ (indicated by the shaded area) drawn in Figure 2.10(ii). However, if $\omega < k_xv_A$ then the mode must lie in the region

$$\Omega^2 < \frac{\rho_0}{\rho_e k_x H_e} + (k_x H_e)\frac{v_A^2}{gH_e}, \tag{2.74}$$

corresponding to the region outside the curve $a_B=0$ (indicated by the non-shaded area) in Figure 2.10(ii). For Figure 2.10(ii), $v_A^2/gH_e = 1.0$ and so $\omega < k_xv_A$ for the surface

gravity mode (modified by the presence of magnetic field). Thus the region where $a_B<0$ is given by Equation (2.74). We conclude therefore, that since the surface gravity mode (modified by the presence of magnetic field) lies entirely in the region (i.e. the unshaded area of Figure 2.10(ii)) defined by Equation (2.74), the vertical velocity component, v_z, of the mode is always of an exponentially declining nature.

However, in Figure 2.10(ii) and if we were to impose the curve $a_B=0$ on Figures 2.9(i),(ii) and Figure 2.10(i) the f-mode (modified by the presence of magnetic field) would lie in the region corresponding to $a_B>0$, and therefore has a growing vertical velocity component. For example, in Figure 2.10(ii) the f-mode's frequency is such that $\omega > k_x v_A$ for $v_A^2/gH_e = 1.0$ and so the region where $a_B<0$ is given by Equation (2.73) (i.e. the shaded area of Figure 2.10(ii)). However, the f-mode does not lie in this region and therefore has a growing vertical velocity component. We note also, that in the non-magnetic case, the definition of the region where the vertical velocity component declines is given by Equation (2.73) which matches with Equation (2.63) as required.

(iii) Linear Density Distribution

We have seen that in the case of an exponentially stratified density distribution the f-mode's propagation is restricted to a range of horizontal wavenumber k_x. This restriction, however, may be an artefact of our modelling. Certainly the observations (Libbrecht *et al.* 1990) of the f-mode do not appear to have a lower bound on the horizontal wavenumber. There may, however, be an upper limit; thus far the f-mode has been observed up to about degree $l \approx 3500$.

We may be able to remove the lower bound on the f-mode by considering a density distribution for the lower region which gives a more realistic representation of the convection zone. A suitable density distribution for the convection region which models our expectations more closely is one in which the density increases as a linear power with depth. Consider, then, the following profile for the density distribution :

$$\rho_0(z) = \begin{cases} \rho_0 e^{-z/H_0}, & z > 0, \\ \rho_e (1 - \frac{z}{z_e})^n, & z < 0, \end{cases} \tag{2.75}$$

where n and z_e are positive constants. Then, with no magnetic field in either the upper or lower region, the equilibrium is one of hydrostatic balance given by

$$\frac{dp_0(z)}{dz} = -\rho_0(z)g. \tag{2.76}$$

The index n in Equation (2.75) is given by

$$n = \frac{z_e}{H_e} - 1 \tag{2.77}$$

and is determined through the equilibrium (2.76) together with the continuity of gas pressure at the interface.

For the region z<0 the governing ordinary differential Equation (2.19), with $v_A \equiv 0$, reduces to

$$\rho_0(z)\frac{d^2v_z}{dz^2} + \frac{d\rho}{dz}\frac{dv_z}{dz} - k_x^2\left\{\rho_0(z) + \frac{g}{\omega^2}\frac{d\rho_0}{dz}\right\}v_z = 0, \qquad z < 0, \tag{2.78}$$

which for the density distribution (2.75) gives

$$(z_e - z)\frac{d^2v_z}{dz^2} - n\frac{dv_z}{dz} - k_x^2\left\{(z_e - z) - \frac{n\,g}{\omega^2}\right\}v_z = 0, \qquad z < 0. \tag{2.79}$$

This second order differential equation with non-constant coefficients may be cast in the form of a confluent hypergeometric differential equation by transforming the dependent ($v_z(z)$) and independent (z) variables according to

$$V_z = v_z\, e^{k_x(z_e - z)}, \quad X = 2k_x(z_e - z). \tag{2.80}$$

Using these transformations Equation (2.79) becomes

$$X\frac{d^2V_z}{dX^2} + (b - X)\frac{dV_z}{dX} - aV_z = 0, \qquad z < 0. \tag{2.81}$$

This is the confluent hypergeometric differential equation or Kummer's equation (see, for example, Abramowitz and Stegun, 1965). The confluent hypergeometric differential equation has two singularities; a regular singularity at $X = 0$ and an irregularity singular at ∞. The parameters of the confluent hypergeometric differential Equation (2.81) satisfy

$$a = \frac{n}{2}\left(1 - \frac{gk_x}{\omega^2}\right), \qquad b = n. \tag{2.82}$$

The general solution to the confluent hypergeometric differential Equation (2.81), in terms of the original variable $v_z(z)$ about $z = z_e$ (i.e. $X = 0$) is given by (Abramowitz and Stegun, 1965)

$$v_z(z) = d_1M(a,b, X)e^{-k_x(z_e - z)} + d_2U(a,b, X)e^{-k_x(z_e - z)}, \quad z < 0, \tag{2.83}$$

where d_1 and d_2 are arbitrary constants and where M and U are the confluent hypergeometric functions (Kummer's functions). Note that the solution given by Equation (2.83) is valid only in a small neighbourhood about $X = 0$.

Once again we impose the condition that the energy density must remain finite as $z \to -\infty$. We note that for $z \to -\infty$ (i.e. $X \to \infty$) we have (Abramowitz and Stegun, 1965)

$$M(a, b, X) \sim e^X X^{a-b}, \qquad U(a, b, X) \sim X^{-a}, \tag{2.84}$$

so that the finite solution of Equation (2.83) as $z \to -\infty$ is

$$v_z(z) = d_2U(a,b, X)e^{-k_x(z_e - z)}, \qquad z < 0. \tag{2.85}$$

The solution in the upper region is exactly the same (see Equation (2.37)) as that for the exponential density case of Section 2.4(ii), except that now $v_A \equiv 0$ and so the vertical velocity component, $v_z(z)$, is of the form

$$v_z(z) = \begin{cases} d_1 \exp\left(\frac{1}{2H_0} - M_0\right) z, & z > 0, \\ d_2 U(a,b,X) e^{-k_x(z_e - z)}, & z < 0, \end{cases} \tag{2.86}$$

where M_0 is given by Equation (2.55), the non-magnetic version of Equation (2.44).

Once again we impose that the vertical velocity component, $v_z(z)$, is continuous at the interface z=0 and therefore from the governing ordinary differential Equation (2.19), with $v_A \equiv 0$, we must have that

$$\rho_0(z)\omega^2 \frac{dv_z}{dz} - gk_x^2 \rho_0(z) v_z(z), \tag{2.87}$$

is also continuous at z=0. We note, as expected, that this second matching condition given by Equation (2.87) is merely that given by Equation (2.27) with $v_A \equiv 0$. Applying these two matching conditions yields the transcendental dispersion relation

$$\rho_0 \left(\omega^2 \left(\frac{1}{2H_0} - M_0\right) - gk_x^2 \right) = \rho_e \left\{ \omega^2 \left(k_x + 2ak_x \frac{U(a+1,n+1,2k_x z_e)}{U(a,n,2k_x z_e)} \right) - gk_x^2 \right\}. \tag{2.88}$$

Alternatively, Equation (2.88) may be written as

$$\frac{\omega^2}{k_x^2} = -g \frac{(\rho_0 - \rho_e)}{\left\{ \rho_0 (M_0 - 1/2H_0) + \rho_e \left(k_x + 2ak_x \frac{U(a+1,n+1,2k_x z_e)}{U(a,n,2k_x z_e)} \right) \right\}}. \tag{2.89}$$

Now, as $\Omega^2 (= \omega^2/gk_x) \to 1$ we observe that $a \to 0$ and that the confluent hypergeometric function $U(0,n,2k_x z_e)$ is non-zero. This latter conclusion is established

by noting that (see, for example, Abramowitz and Stegun, 1965)

$$U(0,n,2k_x z_e) = \frac{\pi}{\sin n\pi}\left\{\frac{1}{\Gamma(n)\Gamma(1-n)} - (2k_x z_e)^{(1-n)}\frac{M(1-n,2-n,2k_x z_e)}{\Gamma(2-n)\Gamma(a)}\right\}, \quad a \to 0, \tag{2.90}$$

where

$$\lim_{a\to 0}\frac{1}{\Gamma(a)} = \lim_{a\to 0}\frac{a}{\Gamma(1+a)} = 0. \tag{2.91}$$

Thus

$$U(0,n,2k_x z_e) = \frac{\pi}{\sin n\pi}\left\{\frac{1}{\Gamma(n)\Gamma(1-n)}\right\} = 1. \tag{2.92}$$

Then, with $\Omega^2 \to 1$ the dispersion relation (2.88) reduces to

$$\rho_0\left\{\frac{1}{2k_x H_0}[1 - |1 - 2k_x H_0|] - 1\right\} = 0. \tag{2.93}$$

This is satisfied only if the horizontal wavenumber k_x satisfies

$$k_x < \frac{1}{2H_0}. \tag{2.94}$$

Thus, modelling the lower medium by the more realistic approach of a power law density distribution we have removed the upper restriction on the horizontal wavenumber k_x given in Equation (2.66). In terms of spherical harmonic degree l, the horizontal wavenumber k_x is given by

$$k_x^2 = \frac{l(l+1)}{R_0}, \tag{2.95}$$

where R_0 is the radius of the sun. Then for $R_0 = 7\times10^5$km and $H_0 = 100$km (the density scale height appropriate for the temperature minimum) the restriction given by

Equation (2.94) translates approximately into $l \leq 3500$. As stated earlier, the f-mode is indeed observed out to degree l of this order and perhaps a little larger.

2.5 Summary

In this chapter we have derived dispersion relations describing the parallel propagation of hydromagnetic surface modes at a single magnetic interface for the cases where gravity is both neglected and included. In the absence of gravity a single hydromagnetic surface wave exists which propagates with a phase-speed c_k which is intermediate between the Alfvén speeds of the two media either side of the interface. In the presence of gravity the surface wave is rendered dispersive and the possibility of instability occurs. When the media are uniform and there is no magnetic field the surface wave is Rayleigh-Taylor unstable if the fluid in the upper medium is denser than that in the lower region. The effect of including a magnetic field is to stabilise the surface wave at short wavelengths.

When there is a non-uniform distribution of density and in the absence of a magnetic field the transcendental dispersion relation may be written in polynomial form. There are two distinct modes, the f-mode and the surface gravity mode. If $\rho_0<\rho_e$, then the surface gravity mode exists. The mode develops, as the magnetic field strength is increased, into the hydromagnetic surface gravity mode. The mode always has a vertical velocity component that is exponentially declining.

If $\rho_0>\rho_e$, the f-mode may propagate but only for a restricted range of horizontal wavenumber, which again is determined by the ratio of the densities. When $\rho_0>\rho_e$, and only when a magnetic field is present, then in addition to the f-mode the surface gravity mode may propagate. This mode is unstable when $\rho_0>\rho_e$ and the magnetic field is absent. When we consider the lower medium to be modelled by a power law density profile, the upper restriction on the propagation of the f-mode is removed. The vertical velocity component of the f-mode is always exponentially growing in nature but both the f-mode and the surface gravity mode have decaying total (magnetic plus kinetic) energy.

Asymptotic solutions to the dispersion relation have been derived for the f-mode in the case of a low Alfvén velocity. The magnitude of the frequency shift increases monotonically with magnetic field strength. A numerical solution of the dispersion relation shows that the f-mode may lie below its non-magnetic value of unity (i.e. $\Omega^2 = 1$). Unfortunately, due to restrictions in its derivation, the analytic result gives $\Omega^2 \geq 1$.

Chapter 3 : The Influence of Compressibility on Magnetohydrodynamic Surface Waves

3.1 Introduction

A compressible flow is one in which the fluid density varies. The inclusion of compressibility is extremely important since the sun is a compressible plasma and therefore supports sound waves. In addition, the presence of magnetic fields makes the solar atmosphere even more elastic. With the inclusion of compression we have the restoring force of pressure which, together with the magnetic pressure and tension forces provided by the magnetic fields, sustains the wave motion. A local compression or rarefaction of the gas sets up a pressure gradient in the opposite direction to the motion, therefore attempting to restore the equilibrium.

In an incompressible fluid the propagation of pressure change is essentially instantaneous; in a compressible fluid the propagation takes place with finite velocity. For example, if the surface of an incompressible fluid is given some disturbance, the effect is observed at large distances in essentially zero time (since the sound speed is infinite). In a compressible fluid the effect propagates at finite velocity. A small disturbance produces compressions and rarefactions which propagate isotropically with the sound speed c_S defined by

$$c_S = \left(\frac{\gamma p_0}{\rho_0}\right)^{1/2}, \tag{3.1}$$

where p_0 and ρ_0 are the equilibrium values of pressure and density of the gas and γ the ratio of specific heat. A disturbance propagates equally in all directions from the source with the speed c_S. The gas undergoes variations in temperature, pressure and density and its motions are aligned with the direction of wave propagation, i.e. the waves are longitudinal. Thus in a compressible flow, in contrast to the incompressible case, since motion can cause pronounced changes in the density and temperature of the fluid, one needs to consider the thermodynamics of the flow.

The inclusion of magnetism, however, complicates the situation with the result that the propagation of any given disturbance is no longer isotropic. For a perfectly conducting gas, the magnetic field-lines and the fluid motions are "frozen" together and thus any possible initiation of a sound wave results in variations in the magnetic field as it is locally compressed or rarefied. Thus in the presence of a magnetic field, variations in the gas pressure lead to disturbances of the magnetic field-lines. Consequently sound waves are no longer able to propagate with the speed c_S and also the direction of the applied magnetic field renders propagation anisotropic. These variations in the magnetic field create magnetic tension which produces a disturbance that propagates along the magnetic field with a characteristic speed, the Alfvén speed v_A, defined earlier in Chapter 1 by

$$v_A = \left(\frac{B_0^2}{\mu_0 \rho_0} \right)^{1/2} . \tag{3.2}$$

Alfvén waves are transverse in the sense that the disturbance is perpendicular to the direction of motion. There are no density or pressure variations associated with the waves, i.e.Alfvén waves are incompressible.

Wave propagation in a compressible plasma permeated by a magnetic field involves two speeds, c_S and v_A. Moreover, combinations of these speeds occur, such as

$$c_f^2 = c_S^2 + v_A^2 \quad \text{and} \quad c_T^{-2} = c_S^{-2} + v_A^{-2}, \tag{3.3}$$

where $c_f\,(> c_T)$ is referred to as the fast magnetoacoustic speed. The fast speed c_f is both supersonic and super-Alfvénic, while the slow speed c_T is both subsonic and sub-Alfvénic. The speed c_T is also referred to as the cusp or tube speed (Roberts, 1981a). Thus in a compressible magnetic medium there are four characteristic speeds: the fast speed c_f, the sound speed c_S, the Alfvén speed v_A, and the cusp (or tube) speed c_T.

3.2 Governing Equations

The governing magnetohydrodynamic equations for a compressible, perfectly conducting plasma in the *absence of gravity* are (see Chapter 1)

$$\frac{\partial \underline{B}}{\partial t} = \underline{\nabla} \times (\underline{v} \times \underline{B}), \tag{3.4}$$

$$\rho \frac{D\underline{v}}{Dt} = -\underline{\nabla} p + \underline{J} \times \underline{B}, \tag{3.5}$$

$$\frac{Dp}{Dt} = c_s^2 \frac{D\rho}{Dt}, \tag{3.6}$$

and

$$\frac{D\rho}{Dt} + \rho (\underline{\nabla}.\underline{v}) = 0. \tag{3.7}$$

We consider small (adiabatic) perturbations of these equations from an equilibrium state in which the plasma is at rest. Then the equations for the perturbations are

$$\frac{\partial \underline{B}}{\partial t} = (\underline{B}_0 . \underline{\nabla})\, \underline{v} - (\underline{v} . \underline{\nabla})\, \underline{B}_0 - \underline{B}_0 \Delta, \tag{3.8}$$

$$\rho_0 \frac{\partial \underline{v}}{\partial t} = -\underline{\nabla} p_T + \frac{1}{\mu_0} (\underline{B}_0 . \underline{\nabla})\, \underline{B} + \frac{1}{\mu_0} (\underline{B} . \underline{\nabla})\, \underline{B}_0, \tag{3.9}$$

$$\frac{\partial p}{\partial t} + (\underline{v} . \underline{\nabla}) p_0 = c_s^2 \left(\frac{\partial \rho}{\partial t} + (\underline{v} . \underline{\nabla}) \rho_0 \right), \tag{3.10}$$

and

$$\frac{\partial \rho}{\partial t} + (\underline{v} . \underline{\nabla}) \rho_0 + \rho_0 \Delta = 0, \tag{3.11}$$

where $\Delta = \underline{\nabla}.\underline{v}$ is the divergence of the flow and is a measure of the compressibility of the plasma.

As in Chapter 2, we consider a horizontally structured magnetic field $\underline{B}_0 = B_0(z)\hat{\underline{x}}$. We Fourier decompose the perturbed velocity,total pressure and divergence as

$$\underline{v}(x,z,t) = (v_x(z), 0, v_z(z))e^{i(\omega t - k_x x)}, \tag{3.12}$$

$$p_T(x,z,t) = p_T(z)e^{i(\omega t - k_x x)}, \tag{3.13}$$

$$\Delta(x,z,t) = \Delta(z)e^{i(\omega t - k_x x)}, \tag{3.14}$$

where

$$\Delta(z) = \frac{dv_z(z)}{dz} - ik_x v_x(z). \tag{3.15}$$

By much the same derivation as used in Chapter 2 we may obtain the following two first order ordinary differential equations

$$i\frac{dp_T}{dz} = \frac{\rho_0}{\omega}(\omega^2 - k_x^2 v_A^2)\, v_z, \tag{3.16}$$

$$p_T = \frac{i\rho_0}{\omega}\left(\frac{(c_s^2 + v_A^2)(\omega^2 - k_x^2 c_T^2)}{(\omega^2 - k_x^2 c_s^2)}\frac{dv_z}{dz}\right). \tag{3.17}$$

Here p_T is the compressible form of the total pressure perturbation given by Equation (2.18) in Chapter 2. Eliminating p_T between Equations (3.16) and (3.17) then yields the second order ordinary differential equation for v_z, the amplitude of the horizontal velocity perturbation (see, for example, Roberts, 1981a)

$$\frac{d}{dz}\left\{\rho_0(z)\frac{(c_s^2(z) + v_A^2(z))(\omega^2 - k_x^2 c_T^2(z))}{(\omega^2 - k_x^2 c_s^2(z))}\frac{dv_z}{dz}\right\} + \rho_0(z)(\omega^2 - k_x^2 v_A^2(z))v_z = 0, \tag{3.18}$$

where k_x is the propagation vector for parallel propagation.

Alternatively, one may obtain Equation (3.18) by eliminating the compression term Δ from the following two ordinary differential equations, which in turn may be derived from the perturbed Equations (3.8)-(3.11)

$$\left(1 - \frac{k_x^2 c_s^2}{\omega^2}\right)\Delta = \frac{dv_z}{dz}, \tag{3.19}$$

$$c_s^2 \frac{d\Delta}{dz} - \frac{\gamma B_0}{\mu_0 \rho_0}\frac{dB_0}{dz}\Delta = (k_x^2 v_A^2 - \omega^2)v_z - \frac{1}{\rho_0}\frac{d}{dz}\left(\frac{B_0^2}{\mu_0}\frac{dv_z}{dz}\right). \tag{3.20}$$

Equation (3.18), although in a different form and for three-dimensional isentropic disturbances in a compressional non-uniform medium, has been given by a number of authors (e.g. Chen and Hasegawa, 1974), primarily with respect to magnetospheric and laboratory applications. An equivalent form in cylindrical geometry can be found in Goedbloed and Hagebeuk (1972), and the gravity modified form arises in Goedbloed (1971), Nye and Thomas (1976a,b), and Adam (1977). We note that in the incompressible limit ($\Delta = 0$, i.e. $c_s^2 \to \infty$) the governing differential Equation (3.18) reduces to Equation (2.19) (with $g = 0$) given in Chapter 2.

3.3 The Dispersion Relation

We consider an equilibrium state in which the magnetic field changes discontinuously from a constant B_0 to zero. The equilibrium pressure, density, temperature and magnetic field are taken to be in the form:

$$p_0(z), \rho_0(z), T_0(z), B_0(z) = \begin{cases} p_0, & \rho_0, & T_0, & B_0, & z > 0, \\ p_e, & \rho_e, & T_e, & 0, & z < 0, \end{cases} \tag{3.21}$$

representing a perfectly conducting plasma (in $z > 0$) with constant pressure p_0, density ρ_0 and temperature T_0 embedded in a unidirectional uniform magnetic field B_0 (see Figure 3.1).In the field-free region ($z < 0$) the pressure, density and temperature are p_e, ρ_e and T_e, respectively. The two sides are related by the requirement of total pressure

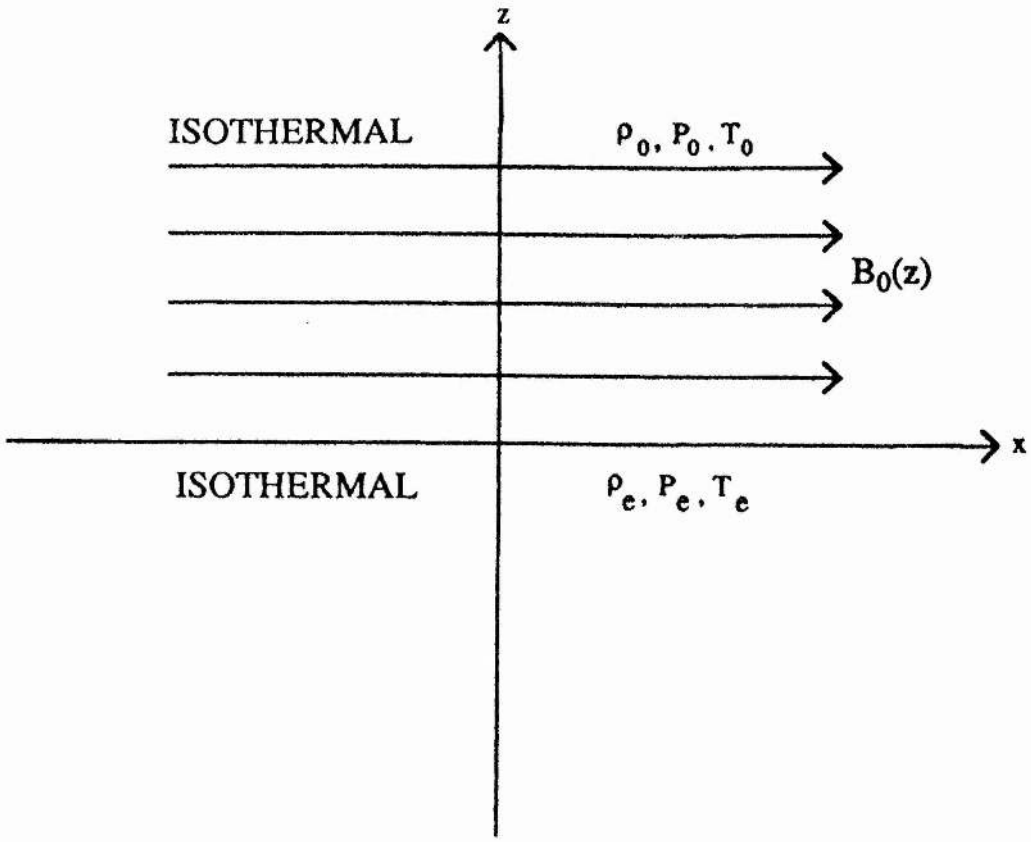

FIGURE 3.1 The equilibrium atmosphere of a single magnetic interface z=0 along which magnetoacoustic surface waves may propagate.

balance which, together with the gas law (see Equation (1.35) of Chapter 1), implies:

$$\frac{c_e^2}{c_0^2}\frac{\rho_e(0-)}{\rho_0(0+)} = 1 + \frac{1}{2}\frac{\gamma}{\beta}, \tag{3.22}$$

where $c_0 = (\gamma p_0/\rho_0)^{1/2}$ and $v_A = B_0/(\mu_0\rho_0)^{1/2}$ are the sound speed and Alfvén speed within the field and $c_e = (\gamma p_e/\rho_e)^{1/2}$ is the sound speed in the field-free medium. The ratio of the specific heats is γ, taken to be 5/3 in the numerical illustrations.

Then, linear, two-dimensional, isentropic perturbations about the equilibrium (3.21) are governed by Equation (3.18). It may be noted that the amplitude of the total (gas plus magnetic) pressure perturbation $p_T(z)$ is related to that of the velocity perturbation perpendicular to the field by (Roberts, 1981a)

$$p_T(z) = \frac{-i\rho_0(z)}{\omega}\frac{(c_s^2(z) + v_A^2(z))(\omega^2 - k_x^2c_T^2(z))}{(k_x^2c_s^2(z) - \omega^2)}\frac{dv_z}{dz}, \tag{3.23}$$

and the parallel motion v_x is related to the perpendicular motion v_z by

$$v_x(z) = \frac{k_x c_s^2(z)}{(k_x^2c_s^2(z) - \omega^2)}\frac{dv_z}{dz}. \tag{3.24}$$

For disturbances in the two uniform media Equation (3.18) reduces to:

$$(k_x^2v_A^2 - \omega^2)\left(\frac{d^2v_z}{dz^2} - m_0^2v_z\right) = 0, \qquad z > 0, \tag{3.25}$$

$$\omega^2\left(\frac{d^2v_z}{dz^2} - m_e^2v_z\right) = 0, \qquad z < 0, \tag{3.26}$$

where

$$m_0^2 = \frac{(k_x^2 v_A^2 - \omega^2)(k_x^2 c_0^2 - \omega^2)}{(c_0^2 + v_A^2)(k_x^2 c_T^2 - \omega^2)}, \tag{3.27}$$

and

$$m_e^2 = \frac{(k_x^2 c_e^2 - \omega^2)}{c_e^2}. \tag{3.28}$$

There are clearly two solutions to Equation (3.25): either v_z is arbitrary (in which case we have an Alfvén wave propagating with $\omega^2 = k_x^2 v_A^2$ in the field region) or $\omega^2 \neq k_x^2 v_A^2$ and the differential operator vanishes. The latter case gives:

$$\frac{d^2 v_z}{dz^2} - m_0^2 v_z = 0, \qquad z > 0, \tag{3.29}$$

$$\frac{d^2 v_z}{dz^2} - m_e^2 v_z = 0, \qquad z < 0, \tag{3.30}$$

with solutions

$$v_z(z) = \begin{cases} d_1 e^{-m_0 z}, & z > 0, \\ d_2 e^{m_e z}, & z < 0, \end{cases} \tag{3.31}$$

where in writing Equation (3.31) we have selected $m_0 > 0$ and $m_e > 0$ and imposed the condition that $v_z \to 0$ as $z \to \pm\infty$. Solutions (3.31) describe surface modes which propagate along $z = 0$. Laterally propagating modes are excluded by the condition on v_z imposed at infinity. This exponential decay or evanescent nature of surface wave velocity components in a direction perpendicular to the plane of propagation is characteristic of surface waves, as we have seen in Chapter 2.

Across the interface $z = 0$ we impose the condition that v_z is continuous, giving $d_1 = d_2$. Also, from a physical consideration of a balanced pressure force at $z = 0$, we require that the total pressure $p_T(z)$ is continuous across the interface $z = 0$. Indeed,

with v_z continuous across $z = 0$, Equation (3.18) implies (on integrating across the interface) that

$$\frac{\rho_0(z)(c_s^2(z) + v_A^2(z))(\omega^2 - k_x^2 c_T^2(z))}{(\omega^2 - k_x^2 c_s^2(z))} \frac{dv_z(z)}{dz} \tag{3.32}$$

is also continuous across $z = 0$. This quantity is in fact $-i\omega p_T(z)$ and is the compressible form of that given by (2.25) in Chapter 2.

The continuity of v_z and $p_T(z)$ together imply that (see, for example, Miles and Roberts (1989))

$$\frac{\omega^2}{k_x^2} = \frac{\rho_0}{(\rho_0 + \rho_e \frac{m_0}{m_e})} v_A^2, \tag{3.33}$$

where m_0 and m_e are both positive. This is the dispersion relation describing the parallel propagation of magnetoacoustic surface waves at a single magnetic interface one side of which is field-free. It has been obtained earlier by Wentzel (1979) and Roberts (1981a), who also derived the dispersion relation governing non-parallel ($k_y \neq 0$) propagation.

Note that Equation (3.33) may be rewritten in the form:

$$\frac{\omega^2}{k_x^2} = \frac{v_A^2}{R + 1}, \tag{3.34}$$

where $R = \frac{\rho_e m_0}{\rho_0 m_e} > 0$ is a function of ω^2. Equation (3.34) shows clearly that the longitudinal phase-speed, $\frac{\omega}{k_x}$, of a surface wave on a field-free interface lies below the Alfvén speed v_A.

An alternative form of (3.33) may be obtained by squaring both sides, giving a cubic in $c_{PH}^2 = \frac{\omega^2}{k_x^2}$, the square of the phase-speed c_{PH} ($= \frac{\omega}{k_x}$):

$$(c_0^2 + v_A^2)(c_T^2 - c_{PH}^2)(v_A^2 - c_{PH}^2)(c_e^2 - c_{PH}^2) = \left(\frac{\rho_e}{\rho_0}\right)^2 c_{PH}^4 c_e^2 (c_0^2 - c_{PH}^2). \tag{3.35}$$

The process of squaring may introduce spurious roots which satisfy (3.35) but not the original dispersion relation (3.33) and its constraints that m_0 and m_e are both positive. The dispersion relation (3.33) may possess one or two roots, depending on the relative magnitudes of the sound speeds (and thus the temperatures) in the two media.

The condition that $m_e > 0$ implies that $c_{PH} < c_e$, while the condition that $m_0 > 0$ yields $c_{PH} < c_T$ or $\min(c_0,v_A) < c_{PH} < \max(c_0,v_A)$. Additionally, as noted earlier, the longitudinal phase-speed must also lie below v_A. Thus $c_{PH} < \min(c_T,c_e)$ is a possibility; following Roberts (1981a), we shall refer to this as the *slow surface wave* . As may be easily seen from a graphical investigation of Equation (3.33), the slow surface wave always exists, whatever the magnitudes of c_e, c_0 and v_A (Roberts, 1981a). If $v_A > c_0$ and the field-free region is warmer than the magnetic medium (so that $c_e > c_0$), then a second mode may propagate with longitudinal phase-speed satisfying $c_0 < c_{PH} < \min(c_e,v_A)$; this is the *fast surface wave* (Roberts, 1981a).

3.4 Properties of The Modes

The variation of the longitudinal phase-speed c_{PH} with the parameter v_A/c_e is shown in Figure 3.2 for four values of c_0/c_e. It is immediately seen from this figure that propagation of both the fast and slow magnetoacoustic surface waves occurs only for $v_A/c_e > c_0/c_e$ (i.e. $v_A > c_0$). Note also the absence of the fast wave when $c_0/c_e > 1$, corresponding to the magnetic medium being warmer than the environment. In each case we note that $c_{PH} \to 0$ as $v_A/c_e \to 0$ for the slow surface wave; this is to be expected since the phase-speed for a surface wave must lie in the range $0 < \frac{\omega}{k_x} < v_A$, when there is a field-free region on one side of the interface.

Also evident in Figure 3.2 is that both surface waves propagate with phase-speeds which increase with increasing v_A/c_e, eventually asymptoting to distinct limits as $v_A/c_e \to \infty$. These two limits may be obtained from the dispersion relation (3.33) by letting $v_A/c_e \to \infty$:

$$\text{as } \frac{v_A}{c_e} \to \infty, \qquad \frac{\omega}{k_x c_e} \to \frac{c_0}{c_e} \quad \text{or} \quad \frac{\sqrt{2}\{(\gamma^2+1)^{1/2} - 1\}^{1/2}}{\gamma}. \tag{3.36}$$

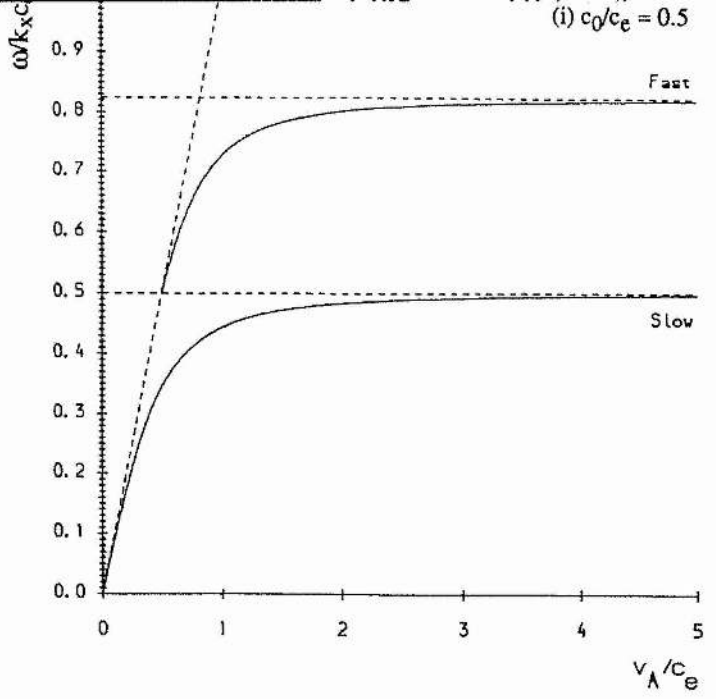

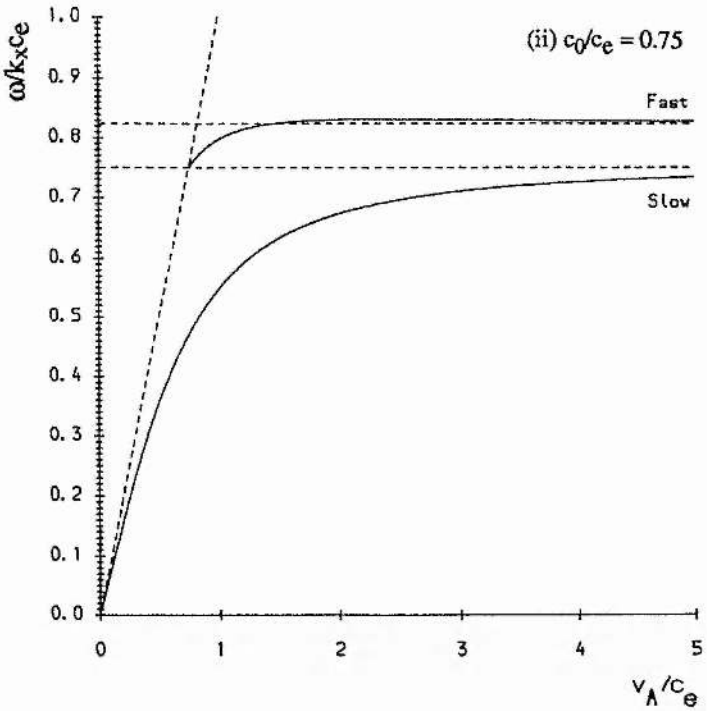

FIGURE 3.2(i) & (ii) The variation of the phase-speed of the fast and slow surface waves with the parameter v_A/c_e, for the cases (i) $c_0/c_e = 0.5$ and (ii) $c_0/c_e = 0.75$. We have taken $\gamma = 5/3$ throughout. The non-vertical asymptote is the line $\omega = k_x v_A$. The slow wave asymptotes for large v_A/c_e to the smaller of the values c_0/c_e, $\sqrt{2}\{(1+\gamma^2)^{1/2} - 1\}^{1/2}/\gamma$; the fast wave (when permitted to propagate) asymptotes to the larger of these values. The fast wave exists only when both $c_e > c_0$ and $v_A > c_0$.

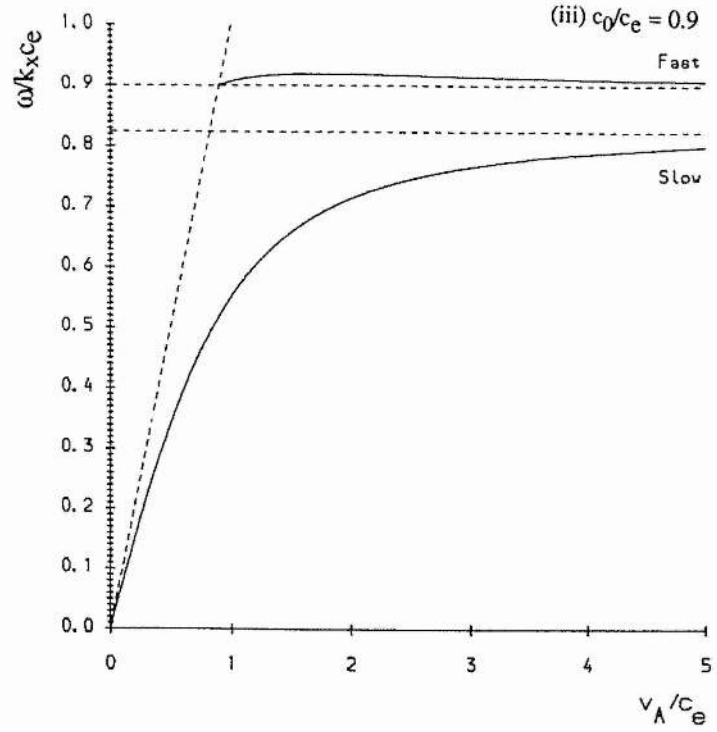

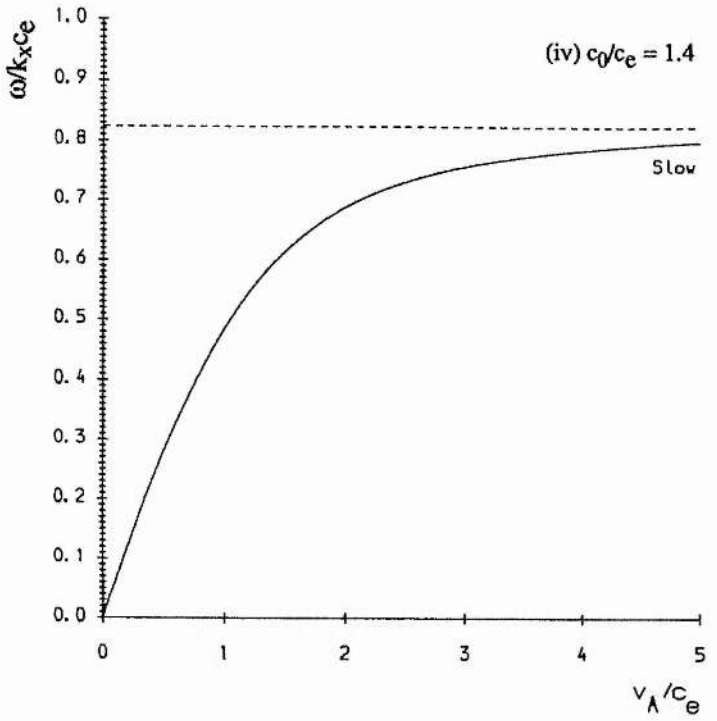

FIGURE 3.2(iii) & (iv) The variation of the phase-speed of the fast and slow surface waves with the parameter v_A/c_e, for the cases (iii) $c_0/c_e = 0.9$ and (iv) $c_0/c_e = 1.4$. Note in (iv) that $c_e < c_0$ and therefore only the slow wave exists. The non-vertical asymptote is the line $\omega = k_x v_A$.

Notice that the latter of these limiting values is independent of c_0/c_e; the asymptote to which the fast and slow surface waves tend for large v_A/c_e therefore depends upon the magnitude of c_0/c_e, be it greater or smaller than the value $\frac{\sqrt{2}\{(\gamma^2+1)^{1/2}-1\}^{1/2}}{\gamma}$. For example, in Figures 3.2(i) & (ii), where $c_0/c_e = 0.5$ and 0.75, respectively, the smaller of the two limiting values (for $\gamma = 5/3$) is c_0/c_e and so the slow surface wave will tend to c_0/c_e as $v_A \to \infty$. However, in Figures 3.2(iii) & (iv) the value of c_0/c_e exceeds the constant limit as $v_A \to \infty$, and thus it is the fast wave which asymptotes to the limit c_0/c_e, provided $c_e > c_0$.

Following on from Figure 3.2 it is interesting to consider the variation of c_{PH} with respect to c_0/c_e for different values of v_A/c_e. Such variations are shown in Figure 3.3 for four choices of v_A/c_e. Once again we observe that the fast magnetoacoustic surface wave propagates only for a range of values of c_0/c_e, namely below the point $c_0/c_e = v_A/c_e$ (i.e.$c_0 = v_A$). Since such a region always exists for non-zero v_A/c_e, a plot of c_{PH} against c_0/c_e always exhibits both fast and slow surface waves. Nonetheless, the condition that $c_0/c_e < 1$ (i.e.$c_e > c_0$) for the existence of a fast surface wave is apparent in Figure 3.3. Thus, in Figure 3.3(iv) the vertical asymptote is at $c_0/c_e = 1$, and not at $c_0/c_e = 1.4$ which might otherwise have been inferred from Figures 3.3(i),(ii) and (iii).

The slow surface wave propagates with a phase-speed which increases steadily from zero, reaches a maximum, and then declines away as $c_0/c_e \to \infty$. In contrast, the fast surface wave propagates for $c_0/c_e = 0$ with a longitudinal phase-speed given by:

$$\frac{c_{PH}^2}{c_e^2} = \frac{1 + v_A^2/c_e^2 - \left\{1 - 2v_A^2/c_e^2 + v_A^4/c_e^4(1+\gamma^2)\right\}^{1/2}}{2(1 - \gamma^2 v_A^2/4c_e^2)}. \qquad (3.37)$$

The fast wave's phase-speed decreases slowly before rising rapidly to reach its cut-off value, given by the intersection of the curves $c_{PH}/c_e = c_0/c_e$ (i.e.$c_{PH} = c_0$) and $c_0/c_e = v_A/c_e$ (i.e.$c_0 = v_A$).

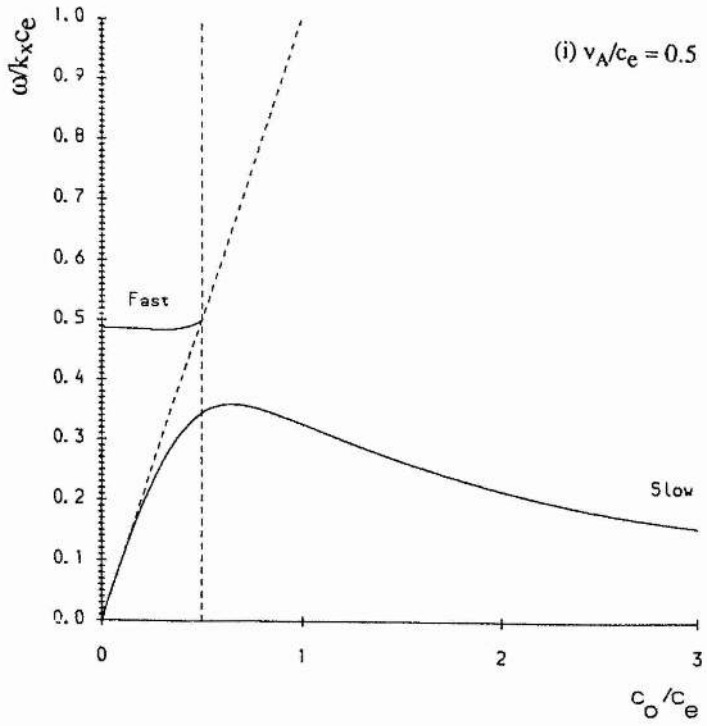

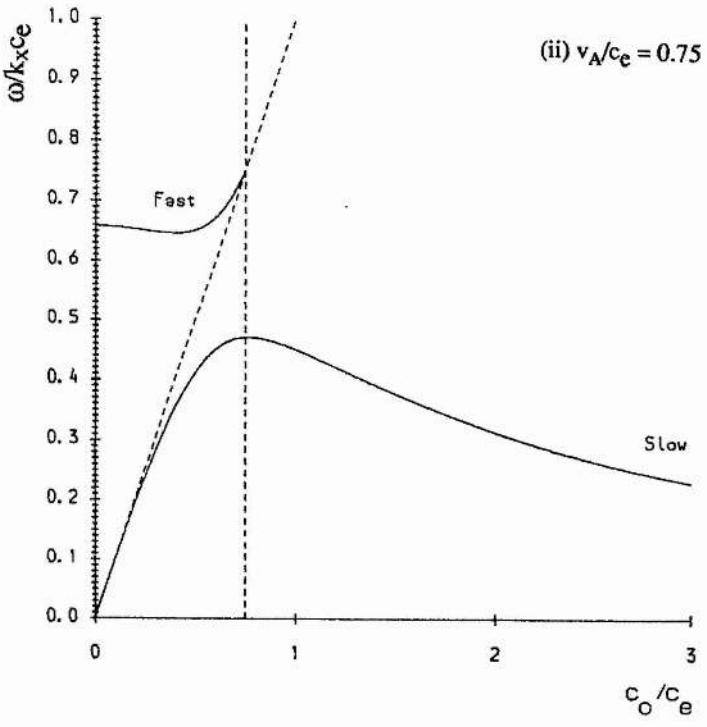

FIGURE 3.3(i) & (ii) The variation of the phase-speed of the fast and slow surface waves with the parameter c_0/c_e, for the cases (i) $v_A/c_e = 0.5$ and (ii) $v_A/c_e = 0.75$. The non-vertical asymptote is the line $\omega = k_x c_0$, the vertical asymptote the line $v_A = c_0$ (for $v_A/c_e \leq 1$).

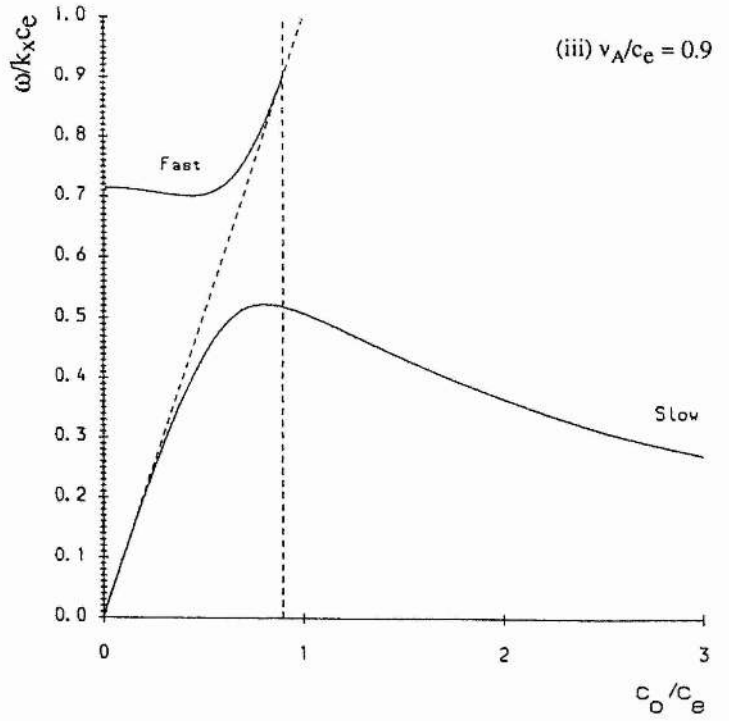

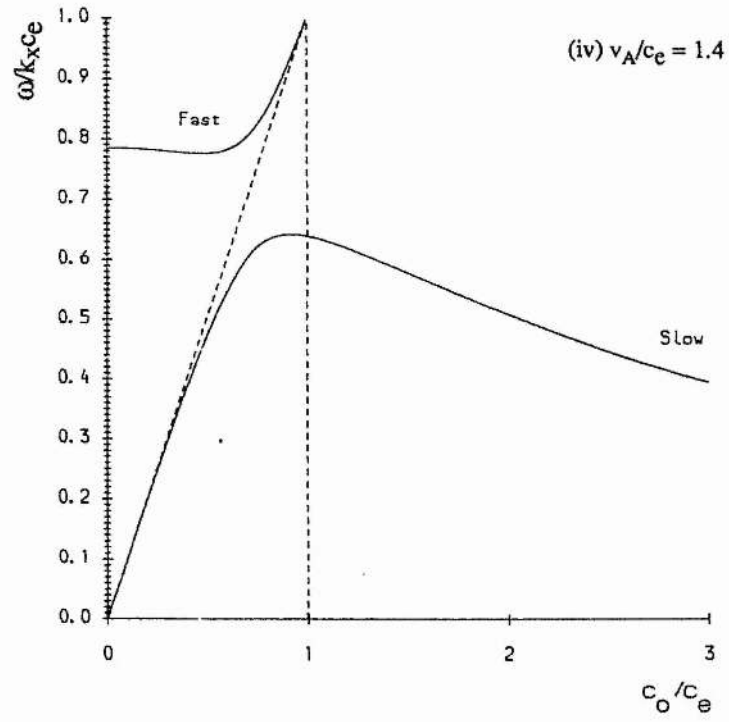

FIGURE 3.3(iii) & (iv) The variation of the phase-speed of the fast and slow surface waves with the parameter c_0/c_e, for the cases (iii) $v_A/c_e = 0.9$ and (iv) $v_A/c_e = 1.4$. The non-vertical asymptote is the line $\omega = k_x c_0$, the vertical asymptote the line $v_A = c_0$ (for $v_A/c_e \leq 1$).

Notice that as v_A/c_e is increased from 0.5 (Figure 3.3(i)) to 1.4 (Figure 3.3(iv)), the value of the phase-speed given by (3.37) increases. Thus the phase-speed for the fast surface wave occurs at a higher "initial" (i.e. $c_0/c_e = 0$) value as v_A/c_e is increased. However, there is a maximum to this "initial" speed, since in the limit of $v_A/c_e \to \infty$ Equation (3.37) gives $\frac{c_{PH}}{c_e} = \frac{\sqrt{2}\{(\gamma^2 + 1)^{1/2} - 1\}^{1/2}}{\gamma}$, the same limiting value that arises in Equation (3.36).

We turn now to a consideration of the distances from the interface that surface waves are able to penetrate. Magnetoacoustic surface waves penetrate a distance of the order of m_0^{-1} into the field region ($z > 0$) and a distance m_e^{-1} into the field-free region ($z < 0$). In terms of the parameters c_0/c_e and v_A/c_e, we have

$$m_0^{-1} = \frac{\lambda(c_0^2/c_e^2 + v_A^2/c_e^2)^{1/2}\,(c_T^2/c_e^2 - c_{PH}^2/c_e^2)^{1/2}}{2\pi(c_0^2/c_e^2 - c_{PH}^2/c_e^2)^{1/2}(1 - c_{PH}^2/c_e^2)^{1/2}}, \tag{3.38}$$

$$m_e^{-1} = \frac{\lambda}{2\pi(1 - c_{PH}^2/c_e^2)^{1/2}}, \tag{3.39}$$

where $\lambda\ (= 2\pi/k_x)$ is the wavelength of the mode.

Expressions (3.38) and (3.39) provide possible diagnostic information on the characteristics of fast and slow magnetoacoustic surface waves. In Figure 3.4 we display the variation of the penetration depths with increasing v_A/c_e for four values of c_0/c_e. In Figures 3.4(i), (ii) & (iii) we note the existence of asymptotes for the fast and slow waves into both the field and field-free regions. In each case, for large v_A/c_e, the greatest penetration is achieved by the fast surface wave into the field-free region, whilst the least penetration is by the slow surface wave into the magnetic field. Indeed, the slow wave penetrates into the field at an almost constant value, k_x^{-1}, for sufficiently large c_0/c_e.

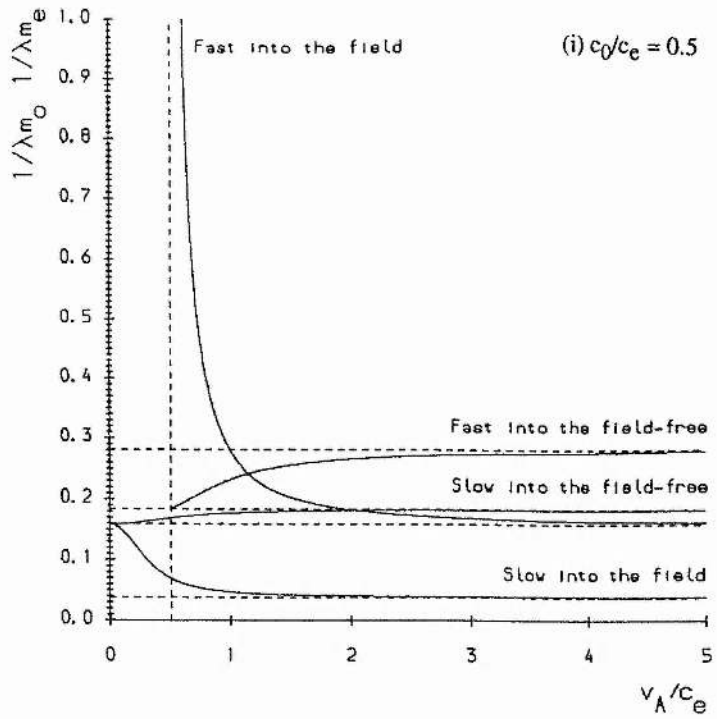

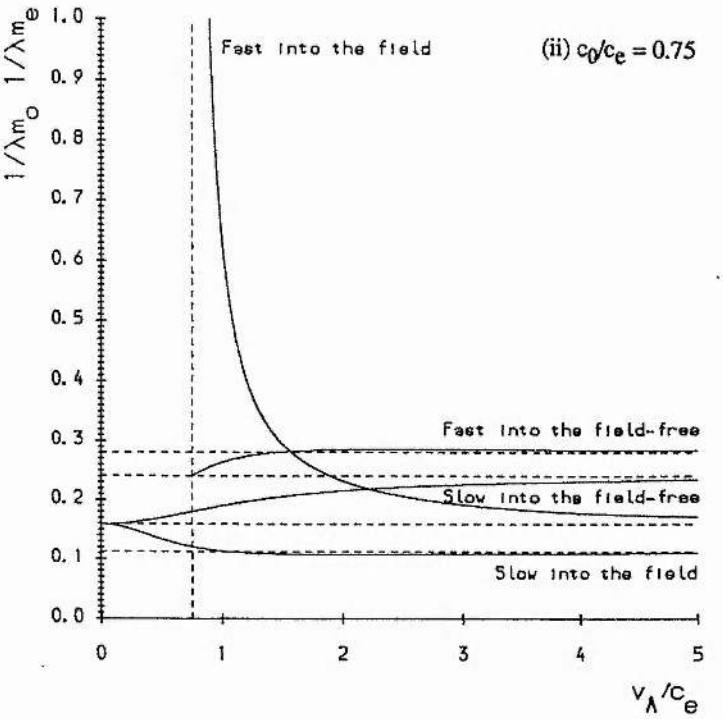

FIGURE 3.4(i) & (ii) The variation of the penetration depths of the fast and slow surface waves into the field-free and magnetic regions with v_A/c_e, for the cases (i) $c_0/c_e = 0.5$ and (ii) $c_0/c_e = 0.75$. The vertical asymptote is the line $v_A = c_0$ (for $c_0/c_e \leq 1$).

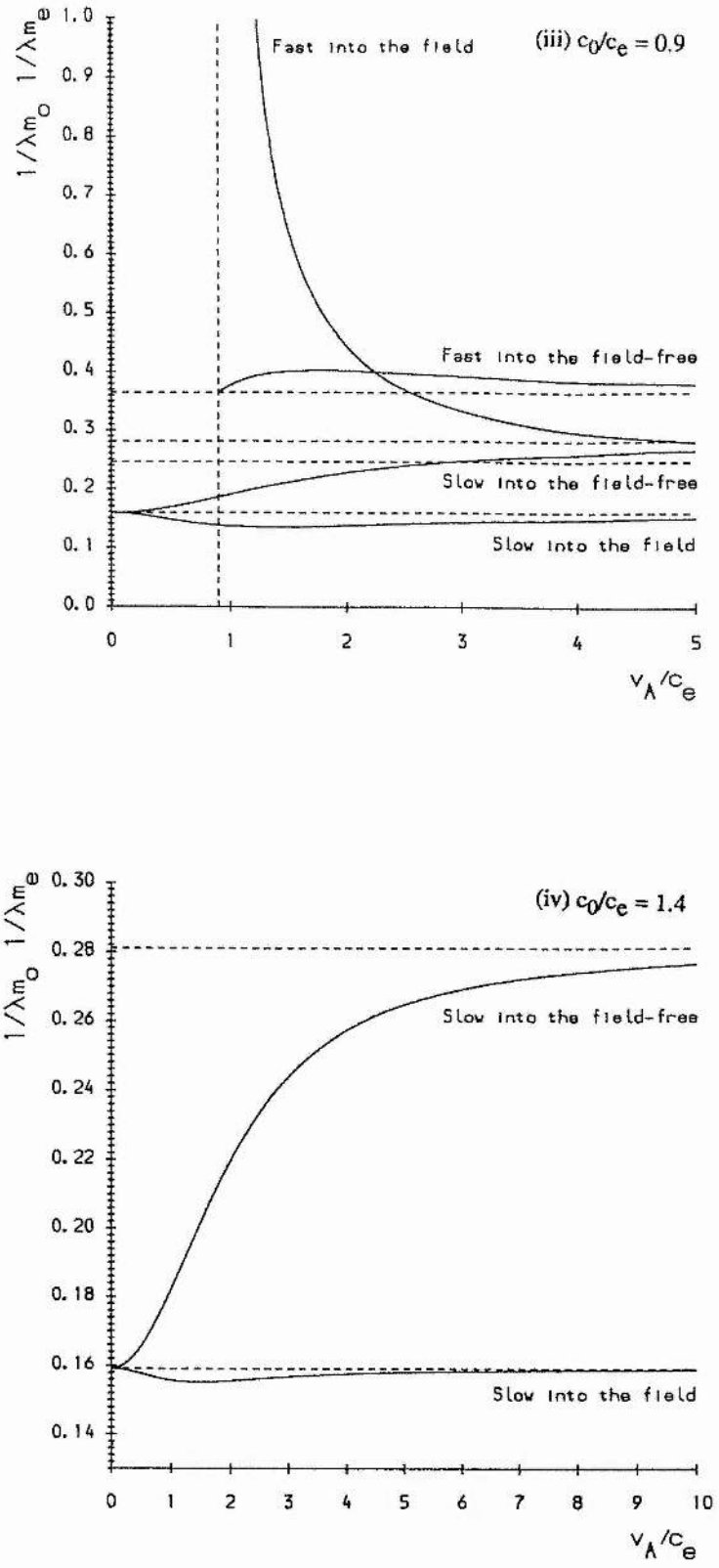

FIGURE 3.4(iii) & (iv) The variation of the penetration depths of the fast and slow surface waves into the field-free and magnetic regions with v_A/c_e, for the cases (iii) $c_0/c_e = 0.9$ and (iv) $c_0/c_e = 1.4$. The vertical asymptote is the line $v_A = c_0$ (for $c_0/c_e \leq 1$).

Note from (3.38) and (3.39) that as the critical cut-off point for propagation of the fast surface wave is approached (corresponding to $v_A/c_e \rightarrow c_0/c_e$), then $1/m_0\lambda \rightarrow \infty$ and so the fast surface wave penetrates to infinity into the field; the penetration of the fast wave into the field-free region falls to zero at the intersection of the asymptotes $v_A/c_e = c_0/c_e$ and $\frac{1}{\lambda m_e} = \frac{1}{2\pi(1 - c_0^2/c_e^2)^{1/2}}$.

The conclusion to be drawn from Figure 3.4 is that for sufficiently large values of the parameter v_A/c_e the penetrations of the fast and slow surface waves into the two regions may be ordered as follows: the fast surface wave penetrates more than the slow surface wave into either region, and they both penetrate deeper into the field-free region than into the field.

Further distinguishing features of magnetoacoustic surface waves may be obtained from a study of the total pressure perturbations and the velocity components in the waves. The amplitudes of the total pressure perturbation, $p_T(z)$, and the parallel velocity perturbation, v_x, are related to the perpendicular component, v_z, by

$$p_T(z) = \begin{cases} \dfrac{i\rho_0(k_x^2 v_A^2 - \omega^2)}{\omega m_0^2} \dfrac{dv_z}{dz}, & z > 0, \\ -\dfrac{i\rho_e \omega}{m_e^2} \dfrac{dv_z}{dz}, & z < 0, \end{cases} \tag{3.40}$$

$$v_x(z) = \begin{cases} \dfrac{ik_x c_0^2}{(k_x^2 c_0^2 - \omega^2)} \dfrac{dv_z}{dz}, & z > 0, \\ -\dfrac{ik_x}{m_e^2} \dfrac{dv_z}{dz}, & z < 0, \end{cases} \tag{3.41}$$

with v_z given in Equation (3.31).

Since

$$p_T(x,z,t) = p_T(z)e^{i(\omega t - k_x x)} \text{ and } v_z(x,z,t) = v_z(z)e^{i(\omega t - k_x x)},$$

we have immediately that

$$\frac{|p_T(z)|}{|d_1|} = \begin{cases} \frac{\rho_0}{\omega} \frac{(k_x^2 v_A^2 - \omega^2)}{m_0} e^{m_0 z}, & z > 0, \\ \frac{\rho_e}{m_e} \omega\, e^{-m_e z}, & z < 0, \end{cases} \tag{3.42}$$

and

$$\frac{|v_x(z)|}{|d_1|} = \begin{cases} \frac{k_x c_0^2 m_0}{(k_x^2 c_0^2 - \omega^2)} e^{m_0 z}, & z > 0, \\ \frac{k_x}{m_e} e^{-m_e z}, & z < 0. \end{cases} \tag{3.43}$$

Since $p_T(z)$ is continuous across the interface, we may eliminate the exponential terms in (3.42) by setting $z = 0$. Then the ratio of the total pressure perturbation in the fast surface wave to that in the slow surface wave is given by

$$\frac{|p_{T_f}|}{|p_{T_s}|} = \frac{c_{PH_f}}{c_{PH_s}} \frac{\lambda m_{e_s}}{\lambda m_{e_f}}, \tag{3.44}$$

where the subscripts f and s denote the fast and slow surface waves, respectively. In a similar fashion we may determine the ratio of the transverse to the parallel components of velocity:

$$\frac{|v_z|}{|v_x|} = \begin{cases} \frac{2\pi(c_0^2/c_e^2 - c_{PH}^2/c_e^2)}{\lambda m_0 c_0^2/c_e^2}, & z > 0, \\ \frac{\lambda m_e}{2\pi}, & z < 0. \end{cases} \tag{3.45}$$

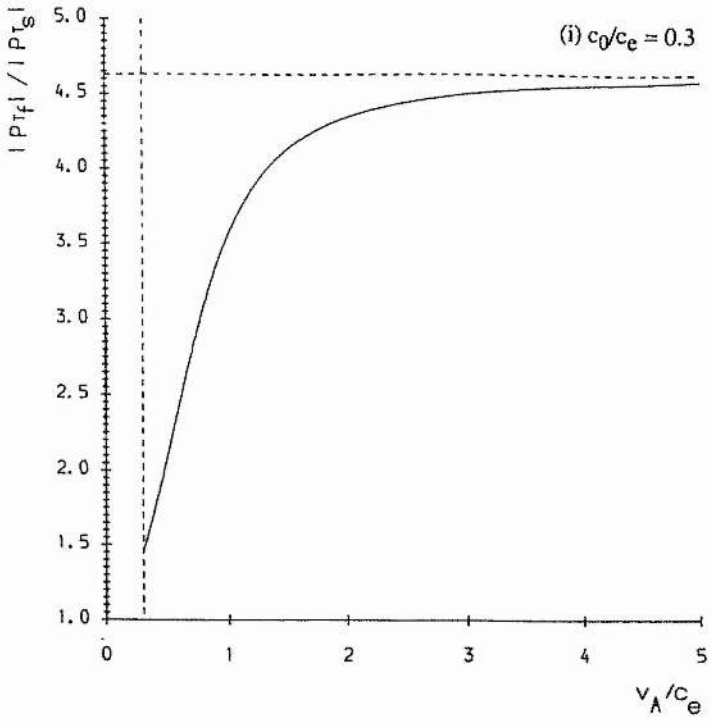

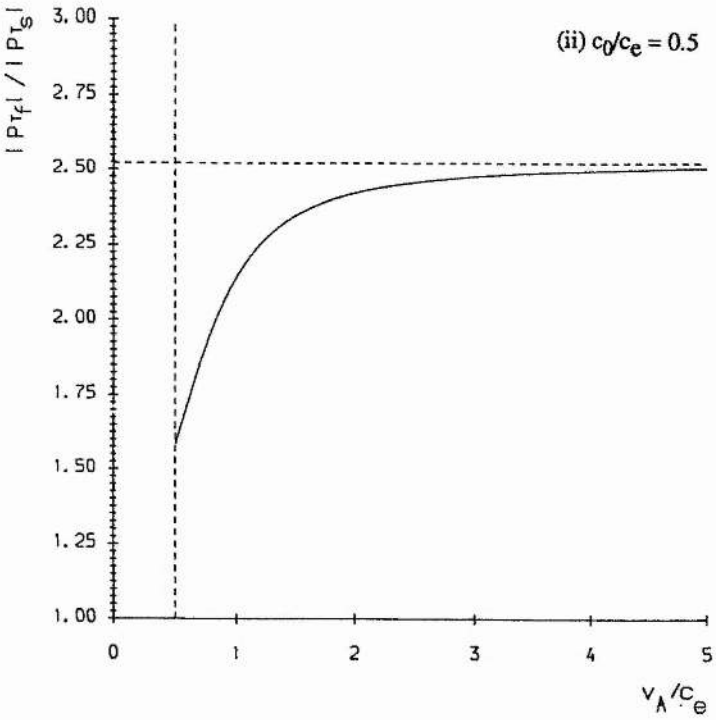

FIGURE 3.5(i) & (ii) The ratio of the magnitude of total (gas plus magnetic) pressure perturbation in the fast surface wave to that in the slow surface wave as a function of v_A/c_e, for the cases (i) $c_0/c_e = 0.3$ and (ii) $c_0/c_e = 0.5$. The vertical asymptote is the line $v_A = c_0$.

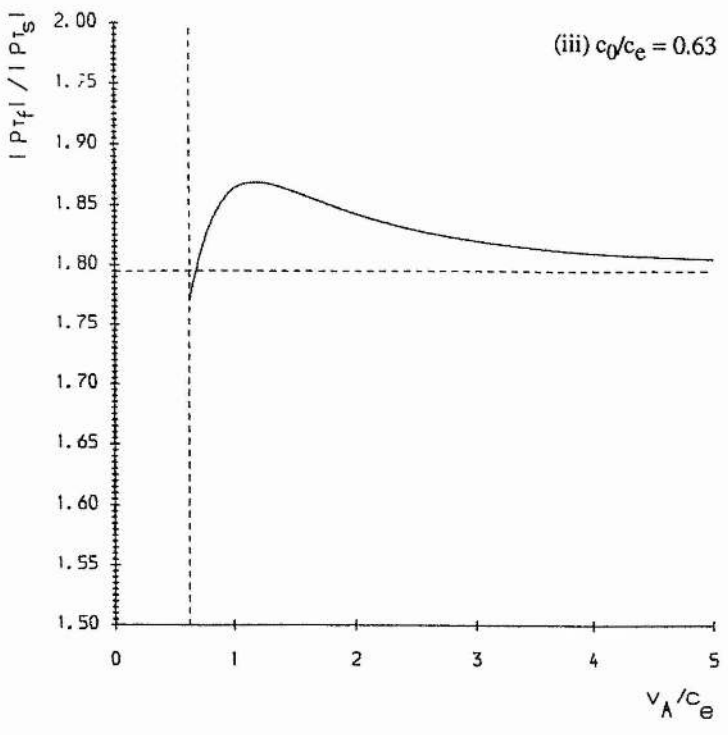

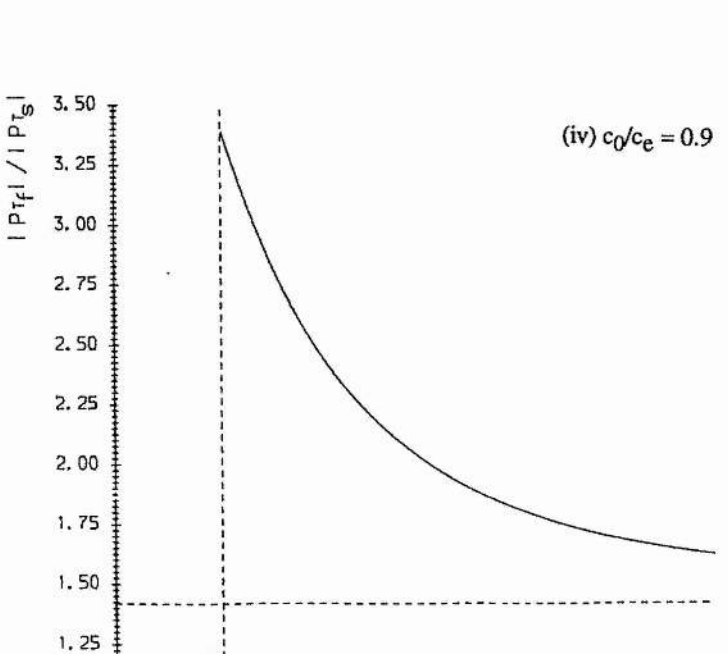

FIGURE 3.5(iii) & (iv) The ratio of the magnitude of total (gas plus magnetic) pressure perturbation in the fast surface wave to that in the slow surface wave as a function of v_A/c_e, for the cases (iii) $c_0/c_e = 0.63$ and (iv) $c_0/c_e = 0.9$.

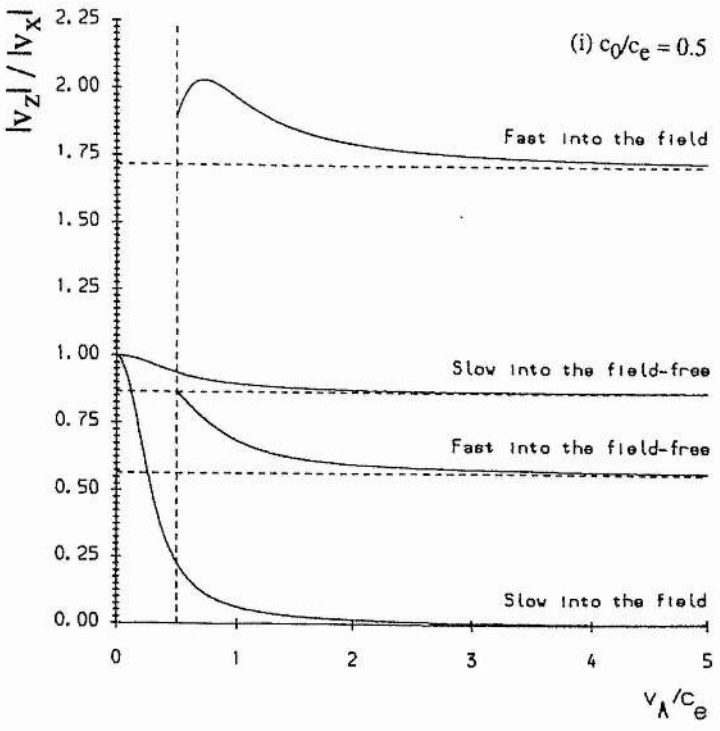

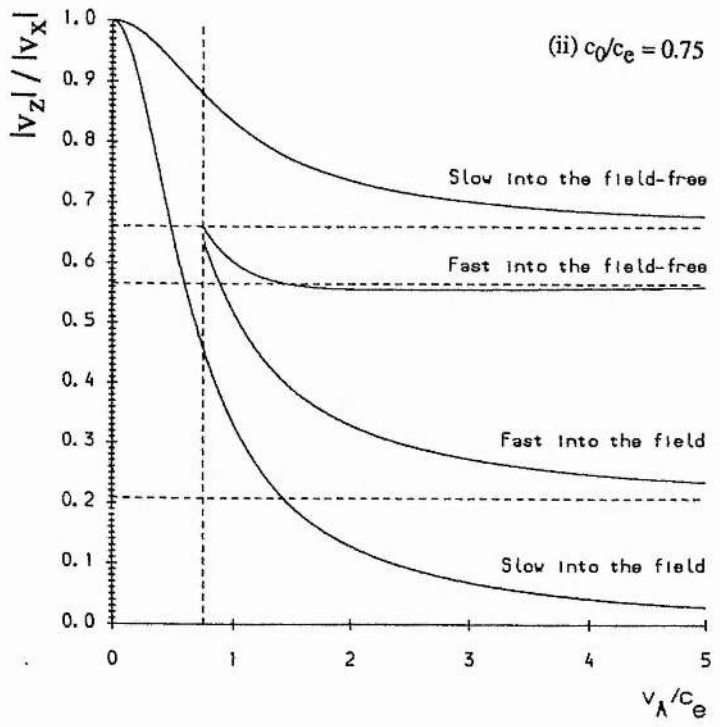

FIGURE 3.6(i) & (ii) The ratio of the magnitude of the perpendicular velocity to that of the parallel velocity for the fast and slow surface waves as a function of v_A/c_e, for the cases (i) $c_0/c_e = 0.5$, (ii) $c_0/c_e = 0.75$. The vertical asymptote is the line $v_A = c_0$.

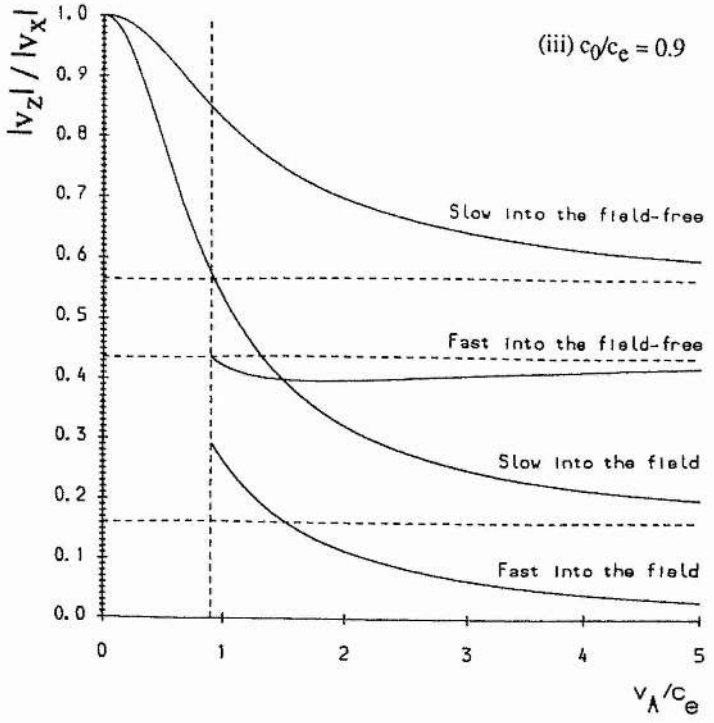

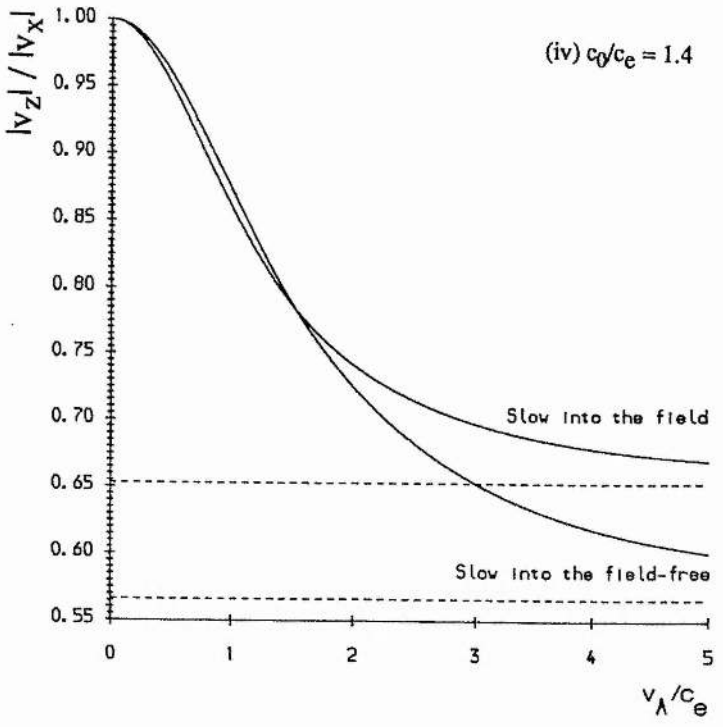

FIGURE 3.6(iii) & (iv) The ratio of the magnitude of the perpendicular velocity to that of the parallel velocity for the fast and slow surface waves as a function of v_A/c_e, for the cases (iii) $c_0/c_e = 0.9$, (iv) $c_0/c_e = 1.4$. The vertical asymptote is the line $v_A = c_0$.

The ratios given by Equations (3.44) and (3.45) are sketched in Figures 3.5 and 3.6. From the limits given in (3.36) (3.38) and (3.39)) it can be deduced that:

$$\text{as } \frac{v_A}{c_e} \to \infty, \qquad \frac{|p_{T_f}|}{|p_{T_s}|} \to \frac{\sqrt{2}/\gamma\{(\gamma^2+1)^{1/2}-1\}^{1/2}(1-c_0^2/c_e^2)^{1/2}}{c_0/c_e(1-2/\gamma^2\{(\gamma^2+1)^{1/2}-1\}^{1/2})}, \tag{3.46}$$

provided $\frac{c_0}{c_e} < \frac{\sqrt{2}\{(\gamma^2+1)^{1/2}-1\}^{1/2}}{\gamma}$ (as is the case for Figures 3.5(i),(ii) & (iii)). When the inequality is reversed, the right-hand side of Equation (3.46) is inverted; this is the case in Figure 3.5(iv).

It is clear from these curves that the total pressure perturbation in the fast surface wave is greater than that in the slow surface wave. As v_A/c_e increases their ratio may increase or decrease, depending on the value of c_0/c_e. Figures 3.5(i) & (ii) show an increase for increasing v_A/c_e, whilst in Figure 3.5(iv), where c_0/c_e has exceeded a critical value, we observe a decrease as v_A/c_e increases. At an intermediate value for c_0/c_e (e.g. $c_0/c_e = 0.63$ in Figure 3.5(iii)), $|p_{T_f}|/|p_{T_s}|$ is virtually constant.

Plots of the ratio of the velocities (v_x and v_z) in each region are given in Figure 3.6. These plots show clearly the anisotropic nature of the slow surface wave and the more isotropic character of the fast. In the magnetic field region the slow surface wave is always longitudinal in nature (i.e. $|v_x| > |v_z|$), whilst the fast surface wave is transverse for very strong fields (as seen in Figure 3.6(i), where the plasma beta $\beta \equiv 2c_0^2/\gamma v_A^2 = 0.012$ for $v_A/c_e = 5.0$) but becomes more longitudinal as the field strength weakens (as illustrated in Figure 3.6(iv), where $\beta \approx 1$ when $v_A/c_e = 1.0$). In the field-free region both surface waves are longitudinal in nature. The magnitudes of the two velocity components for the slow wave in the field-free region are comparable (i.e. $|v_z/v_x| \approx 1$) when the value of the plasma beta in the field region is small (e.g. $\beta = 0.012$ at $v_A/c_e = 5.0$ in Figure 3.6(i)).

3.5 Summary

Fast and slow magnetoacoustic surface waves may arise whenever a discontinuity occurs in the temperature or in the magnetic field, such as at a single magnetic interface. Whether only the slow surface wave or both surface modes propagate depends on the relative temperatures of the two media. In particular, if one side of the interface is field-free then the fast surface wave will not propagate if the Alfvén speed is less than the sound speed in the field (Roberts, 1981a). The fast surface wave penetrates more than the slow surface wave into either medium, and both penetrate more into the field-free medium than into the field for v_A/c_e large enough. Figure 3.5 suggests that the magnitude of the total pressure perturbation in the fast surface wave is greater than that of the slow. The slow mode is highly anisotropic in character, being predominantly longitudinal in nature, whereas the fast mode is more isotropic, polarized transversely in strong fields and longitudinally in weaker fields.

An important possible application of magnetoacoustic surface waves is to the running penumbral wave phenomenon. To draw conclusions from the results presented here requires a knowledge of the appropriate parameter ranges for v_A/c_e and c_0/c_e. These clearly depend on where the penumbral field resides in the atmosphere. However, there is no generally accepted model for the penumbra. Indeed, there is speculation not only on how high the penumbral field is elevated above the photosphere (if at all), but also how thick the field might be. Giovanelli (1982) considered the canopy base at the outer penumbral edge to be approximately 180km above the photosphere, with a penumbral thickness of 250km. More recently, Schmidt *et al* (1986) have proposed that the penumbral field is very shallow (about 80km deep) with a Wilson depression of only 60-120km. Such a model would mean that the canopy base would be level with the photosphere or possibly below it. Such uncertainties in the base height of the penumbral field have little effect on the value of the sound speed in the penumbra, but the Alfvén speed (varying inversely with the square root of the density) may change considerably as we proceed up from the photosphere. Spruit (1986) gives typical values for both the sound and Alfvén speeds at the photosphere of

approximately 7.0kms^{-1}.Nye and Thomas (1974), in their linear model for the penumbra, give values of 8.0kms^{-1} and 5.0kms^{-1} for the sound and Alfvén speeds (respectively) at the photospheric level, and 6·5kms^{-1} and 8.0kms^{-1} at approximately 200km above the photosphere. These values suggest that appropriate ranges for the sound and Alfvén speeds are $5.0\text{kms}^{-1} \leq c_0 \leq 7.0\text{kms}^{-1}$ and $4.0\text{kms}^{-1} \leq v_A \leq 10.0\text{kms}^{-1}$, say. Taking $c_0/c_e \approx 0.9$, Figure 3.2(iii) gives a value for the longitudinal phase-speed of the fast wave of approximately $0.9c_e$, i.e. $\omega/k_x \approx c_0$. This suggests a longitudinal phase-speed of at most 7kms^{-1}. Observed values for the longitudinal phase-speeds of running penumbral waves are typically between 10.0 and 20.0kms^{-1}. Thus the calculated value is too low. The reason for this is clear from Chapter 2, where we have shown that gravity has a significant effect both on the phase-speed and on the amplitude of waves (see also Nye and Thomas (1974, 1976a,b) and Small and Roberts (1984)). Thus any direct application of the study of magnetoacoustic surface waves to sunspot phenomena requires a detailed study of the modes in a stratified atmosphere. The present study, then, provides us with a basis from which to explore gravitational effects on magnetoacoustic surface waves, to which we now turn our attention.

Chapter 4 : The Influence of Gravity on Magnetoacoustic Surface Waves

4.1 Introduction

There is a widespread interest in the behaviour of surface waves (see the review by Roberts, 1991) and their possible application to observations of waves in the solar atmosphere. The 'running penumbral wave' sunspot phenomenon (see the discussion in Chapters 1 and 3) and chromospheric canopy modes are perhaps the most likely applications of surface wave theory. A theoretical understanding of magnetoacoustic surface waves in a gravitationally stratified atmosphere permeated by a magnetic field is therefore of natural interest. In any case, an understanding of surface waves in a stratified atmosphere is an essential prerequisite to any application to the photospheric and chromospheric plasmas. We present in this chapter (see also Miles and Roberts 1991a,b) a detailed systematic investigation of magnetic surface waves on a single horizontal magnetic interface in a stratified atmosphere. We shall refer to such waves as magnetoacoustic-gravity surface waves.

The presence of gravity modifies the equilibrium state of a medium and so the behaviour of a surface wave is changed in two ways: first, because the wave samples a non-uniform medium, and secondly because additional forces - buoyancy forces - arise to modify the propagation of the wave. These two effects seriously complicate any description of the waves. In general, any disturbance in the solar atmosphere is subject to the three restoring forces of buoyancy, compressibility and magnetism. The inclusion of gravity not only introduces a preferred direction additional to that determined by the magnetic field, but also imposes length and time scales in the system. Consequently, the nature of the propagation of magnetoacoustic-gravity surface waves is necessarily complicated, a reflection of the highly anisotropic character of a magnetically structured and stratified atmosphere. The length scales introduced by the gravitational field are defined by the equilibrium density and pressure profiles, while

the imposed time scales arise from the acoustic cutoff frequency and the buoyancy (Brunt-Väisälä) frequency. See the discussion in Chapter 1.

We consider the propagation of magnetoacoustic-gravity surface waves parallel to an applied horizontal magnetic field at an isothermal magnetic interface one side of which is field-free. The field strength of the horizontal magnetic field is assumed to decrease exponentially with height in such a manner that the Alfvén speed is constant. Such an equilibrium profile is amenable to an analytical investigation yielding a relatively simple, though transcendental, dispersion relation. It is the derivation of this relation and an unfolding of its properties that provides the topic of investigation in this chapter.

4.2 Governing Equations

The governing magnetohydrodynamic equations for a compressible perfectly conducting plasma in the presence of gravity are those given in Chapter 1,namely

$$\frac{\partial \underline{B}}{\partial t} = \underline{\nabla} \times (\underline{v} \times \underline{B}), \tag{4.1}$$

$$\rho \frac{D\underline{v}}{Dt} = - \underline{\nabla} p + \underline{J} \times \underline{B} + \rho \underline{g}, \tag{4.2}$$

$$\frac{Dp}{Dt} = \frac{\gamma p}{\rho} \frac{D\rho}{Dt}, \tag{4.3}$$

and

$$\frac{D\rho}{Dt} + \rho (\underline{\nabla}.\underline{v}) = 0. \tag{4.4}$$

We consider small adiabatic perturbations of these equations about an equilibrium state which is at rest. Then the perturbed equations are

$$\frac{\partial \underline{B}}{\partial t} = (\underline{B}_0 . \underline{\nabla}) \underline{v} - (\underline{v} . \underline{\nabla}) \underline{B}_0 - \underline{B}_0 \Delta, \tag{4.5}$$

$$\rho_0 \frac{\partial \underline{v}}{\partial t} = - \underline{\nabla} p_T + \frac{1}{\mu_0} (\underline{B}_0 . \underline{\nabla}) \underline{B} + \frac{1}{\mu_0} (\underline{B} . \underline{\nabla}) \underline{B}_0 + \rho \underline{g}, \tag{4.6}$$

$$\frac{\partial p}{\partial t} + (\underline{v} \cdot \underline{\nabla})p_0 = c_s^2\left(\frac{\partial \rho}{\partial t} + (\underline{v} \cdot \underline{\nabla})\rho_0\right), \tag{4.7}$$

and

$$\frac{\partial \rho}{\partial t} + (\underline{v} \cdot \underline{\nabla})\rho_0 + \rho_0\Delta = 0, \tag{4.8}$$

where $c_s^2(z) = (\gamma p_0/\rho_0)^{1/2}$ denotes the sound speed in the equilibrium state, $\Delta \equiv \text{div } \underline{v}$.

As in Chapter 3, we consider two dimensional perturbations of the form $\underline{v} = (v_x(z),0,v_z(z))\exp i(\omega t - k_x x)$, taking $k_y = 0$. We may then reduce the above system of equations to two first order ordinary differential equations for $v_z(z)$ and $p_T(z)$, the amplitude of the total pressure perturbation:

$$i\left(\frac{dp_T}{dz} + g\frac{k_x^2}{\omega^2}p_T\right) = \frac{\rho_0}{\omega}\left(\omega^2 - k_x^2v_A^2 + \frac{g}{\rho_0}\frac{d\rho_0}{dz}\right)v_z + \frac{g\rho_0}{\omega}\left(1 - \frac{k_x^2v_A^2}{\omega^2}\right)\frac{dv_z}{dz}, \tag{4.9}$$

$$p_T = \frac{i\rho_0}{\omega}\left(\frac{(c_s^2 + v_A^2)(\omega^2 - k_x^2c_T^2)}{(\omega^2 - k_x^2c_s^2)}\frac{dv_z}{dz} - \frac{\omega^2 g v_z}{(\omega^2 - k_x^2c_s^2)}\right). \tag{4.10}$$

In the above, $v_A(z)$ denotes the Alfvén speed ($v_A^2 = B_0^2/\mu_0\rho_0$) and $c_T(z)$ the cusp speed ($c_T^{-2} = c_s^{-2} + v_A^{-2}$); see Chapter 1.

Eliminating the total pressure p_T leads to the second-order ordinary differential equation (Adam, 1977; Small and Roberts, 1984; Roberts, 1985; c.f., Goedbloed, 1971)

$$\frac{d}{dz}\left\{\frac{\rho_0(z)(c_s^2(z) + v_A^2(z))(\omega^2 - k_x^2c_T^2(z))}{(\omega^2 - k_x^2c_s^2(z))}\frac{dv_z}{dz}\right\}$$

$$+\left\{\rho_0(z)(\omega^2 - k_x^2v_A^2(z)) - \frac{g^2k_x^2\rho_0(z)}{(\omega^2 - k_x^2c_s^2(z))} - gk_x^2\frac{d}{dz}\left(\frac{\rho_0(z)c_s^2(z)}{\omega^2 - k_x^2c_s^2(z)}\right)\right\}v_z = 0. \tag{4.11}$$

Alternatively, one can also derive Equation (4.11) by eliminating Δ (= div $\underline{v}$) from the following two ordinary differential equations, which in turn can be obtained from Equations (4.5)-(4.8)

$$\left(1 - \frac{k_x^2 c_s^2}{\omega^2}\right)\Delta = \frac{dv_z}{dz} - \frac{gk_x^2}{\omega^2} v_z , \tag{4.12}$$

$$c_s^2 \frac{d\Delta}{dz} - (\gamma - 1)g\Delta - \frac{\gamma B_0}{\mu_0 \rho_0}\frac{dB_0}{dz}\Delta = g\frac{dv_z}{dz} + (k_x^2 v_A^2 - \omega^2)v_z - \frac{1}{\rho_0}\frac{d}{dz}\left(\frac{B_0^2}{\mu_0}\frac{dv_z}{dz}\right) . \tag{4.13}$$

The ordinary differential Equations (4.12) and (4.13) describe magnetoacoustic waves in a stratified gas. They also describe gravity waves and their unstable counterpart, convection. Equation (4.11) possesses a complex structure reflecting the fact that the medium is compressible, magnetic and stratified in temperature and density.

4.3 The Dispersion Relation

Consider a plane-parallel stratified atmosphere with gas pressure $p_0(z)$ and density $\rho_0(z)$ within which is embedded a horizontal magnetic field $\underline{B}_0(z)$. The equilibrium is one of magnetohydrostatic balance determined by

$$\frac{d}{dz}\left(p_0(z) + \frac{B_0^2(z)}{2\mu_0}\right) = -\rho_0(z)g, \tag{4.14}$$

demonstrating that the magnetic pressure may provide support against gravity $-g\hat{\underline{z}}$.

Once again we consider a magnetic interface located at z=0 (see Figure 4.1). The region (z>0) above the interface is taken to be isothermal at temperature T_0 and permeated by a non-uniform horizontal magnetic field $\underline{B}_0(z) = (B_0(z),0,0)$, the strength of which declines exponentially at the same rate as the square root of the gas density,thus producing an Alfvén speed that is constant (see also Yu,1965; Thomas,1983). The field-free medium (z<0) below the interface is also isothermal but of a possibly different temperature, T_e, to that above the interface.

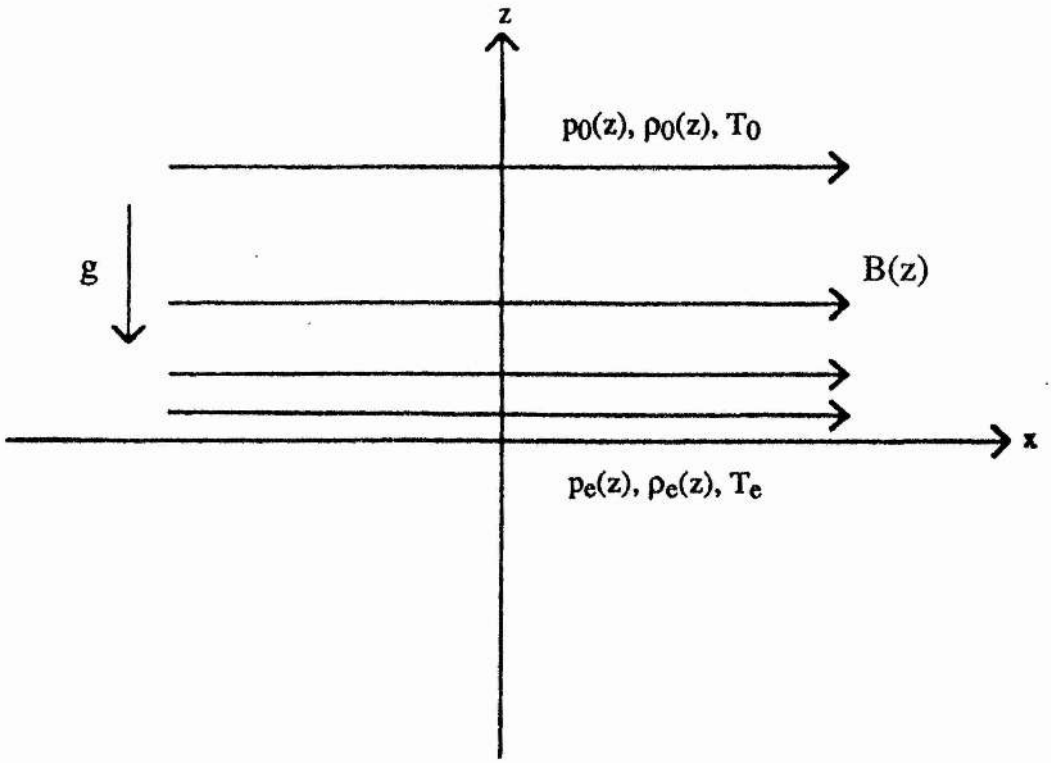

FIGURE 4.1 The equilibrium model of a single magnetic interface z = 0 in a stratified atmosphere. The temperatures T_0 and T_e either side of the interface are taken to be isothermal.

Pressure balance at the interface $z = 0$ dictates that the total (magnetic plus gas) pressure (as $z \to 0_+$) equals that in the field-free region below (as $z \to 0_-$) :

$$p_0(0_+) + \frac{B_0^2}{2\mu_0} = p_e(0_-), \tag{4.15}$$

where B_0 is the magnetic field strength at $z = 0$. Equation (4.15) coupled with the ideal gas law (Equation (1.35) of Chapter 1) gives a relationship between the densities on either side of the interface, namely

$$\frac{c_e^2}{c_0^2}\frac{\rho_e(0_-)}{\rho_0(0_+)} = 1 + \frac{1}{2}\frac{\gamma}{\beta}, \tag{4.16}$$

where $\beta = c_0^2/v_A^2$ is the squared ratio of the sound speed c_0 $(=(\gamma p_0/\rho_0)^{1/2})$ to the Alfvén speed $v_A = \dfrac{B_0}{(\mu_0\rho_0(0_+))^{1/2}}$ at the base of the magnetic atmosphere, and c_e $(=(\gamma p_e/\rho_e)^{1/2})$ is the sound speed in the field-free region.

The assumptions of constant sound and Alfvén speeds imply a density profile of the form

$$\rho_0(z) = \begin{cases} \rho_0 e^{-z/H_B}, & z > 0, \\ \rho_e e^{-z/H_e}, & z < 0, \end{cases} \tag{4.17}$$

where H_B and H_e are the density scale-heights above and below the interface, respectively. It proves convenient to introduce a magnetically-modified adiabatic exponent Γ, defined by

$$\Gamma = \frac{2\beta\gamma}{2\beta + \gamma}. \tag{4.18}$$

In the absence of a magnetic field, $\Gamma = \gamma$. In Equation (4.17) we have written $\rho_e \equiv \rho_e(0_-)$ and $\rho_0 \equiv \rho_0(0_+)$.

In contrast to the incompressible case of Chapter 2, the scale heights here are determined through the equilibrium, given by Equation (4.14), and the ideal gas law,

given by Equation (1.35) (which is absent in the incompressible case). Then, from the equilibrium with a constant Alfvén speed we have

$$\frac{\Gamma g}{c_s^2}\frac{d\rho_0}{dz} + g\rho_0(z) = 0, \tag{4.19}$$

and thus

$$\rho_0(z) \propto e^{-\lambda z}, \tag{4.20}$$

where

$$\lambda = \frac{\Gamma g}{c_s^2}. \tag{4.21}$$

We define $H = \lambda^{-1}$ to be the density scale height, representing the vertical distance over which the density falls by a factor e. Then the scale heights above and below the interface are defined by $H_B = c_0^2/\Gamma g$ and $H_e = c_e^2/\gamma g$, respectively. In the absence of a magnetic field $H_B = H_0$ ($\equiv c_0^2/\gamma g$)).

For the stratification (4.17), the governing ordinary differential Equation (4.11) for the magnetic field region reduces to (see also Yu, 1965 ; Campbell and Roberts, 1989)

$$\frac{d^2v_z}{dz^2} - \frac{1}{H_B}\frac{dv_z}{dz} + A_B v_z = 0, \qquad z > 0, \tag{4.22}$$

where

$$A_B = \frac{(\Gamma - 1)g^2k_x^2 + (\omega^2 - k_x^2v_A^2)(\omega^2 - k_x^2c_0^2)}{(c_0^2 + v_A^2)(\omega^2 - k_x^2c_T^2)} \tag{4.23}$$

is the compressible equivalent of the incompressible version, denoted by a_B, and given by Equation (2.36) in Chapter 2.

Equation (4.22) possesses the general solution

$$v_z(z) = \left(d_1\exp\frac{z(1 - 4A_BH_B^2)^{1/2}}{2H_B} + d_2\exp\frac{-z(1 - 4A_BH_B^2)^{1/2}}{2H_B}\right)\exp\left(\frac{z}{2H_B}\right), \qquad z > 0, \tag{4.24}$$

where d_1 and d_2 are arbitrary constants. We restrict attention to the circumstance that $4A_BH_B^2 < 1$, corresponding to a surface mode behaviour.

In the non-magnetic region Equation (4.11) reduces to

$$\frac{d^2v_z}{dz^2} - \frac{1}{H_e}\frac{dv_z}{dz} + A_e v_z = 0, \qquad z < 0, \tag{4.25}$$

where

$$A_e = \frac{(\gamma - 1)g^2k_x^2 + \omega^2(\omega^2 - k_x^2c_e^2)}{\omega^2 c_e^2} \tag{4.26}$$

is the compressible equivalent of the incompressible version, a_e, given by Equation (2.39) in Chapter 2.

Equation (4.25) possesses the general solution

$$v_z(z) = \left(d_3 \exp \frac{z(1 - 4A_eH_e^2)^{1/2}}{2H_e} + d_4 \exp \frac{-z(1 - 4A_eH_e^2)^{1/2}}{2H_e} \right) \exp\left(\frac{z}{2H_e}\right), \qquad z < 0, \tag{4.27}$$

where d_3 and d_4 are arbitrary constants. We assume that $4A_eH_e^2 < 1$.

The requirement that the total (kinetic plus magnetic) energy density remains finite as $|z| \to \infty$, together with the assumptions (see Section 4.4 entitled "Cutoff Curves" for a discussion) that $4A_BH_B^2 < 1$ and $4A_eH_e^2 < 1$, implies that $d_1=d_4=0$. The vertical velocity component $v_z(z)$ is therefore of the form

$$v_z(z) = \begin{cases} d_2 \exp\left(\dfrac{1}{2H_B} - M_0\right) z, & z > 0, \\ d_3 \exp\left(\dfrac{1}{2H_e} + M_e\right) z, & z < 0, \end{cases} \tag{4.28}$$

where

$$M_0 = \frac{(1 - 4A_BH_B^2)^{1/2}}{2H_B}, \tag{4.29}$$

and

$$M_e = \frac{(1 - 4A_eH_e^2)^{1/2}}{2H_e}. \tag{4.30}$$

We note that M_0, $M_e > 0$, since we take the positive square roots of $(1 - 4A_BH_B^2)^{1/2}$ and $(1 - 4A_eH_e^2)^{1/2}$. Notice that $v_z(z)$ declines in the dense region ($z<0$) but may or may not decline in the more tenuous region ($z>0$). We explore this aspect more fully in Section 4.5.

We require that the normal component of velocity across the interface $z = 0$ be continuous; so $d_2 = d_3$. Additionally, integration of Equation (4.11) about a small neighbourhood of the interface shows that

$$\frac{\rho_0(z)(c_S^2(z) + v_A^2(z))(\omega^2 - k_x^2c_T^2(z))}{(k_x^2c_S^2(z) - \omega^2)} \frac{dv_z(z)}{dz} - \frac{k_x^2g\rho_0(z)c_S^2(z)v_z(z)}{(k_x^2c_S^2(z) - \omega^2)} \tag{4.31}$$

is continuous across $z = 0$. Application of these matching conditions to the solution (4.28) then yields the transcendental dispersion relation

$$\frac{\rho_0(c_0^2 + v_A^2)(k_x^2c_T^2 - \omega^2)(\frac{1}{2H_B} - M_0)}{(k_x^2c_0^2 - \omega^2)} + \frac{k_x^2g\rho_0c_0^2}{(k_x^2c_0^2 - \omega^2)}$$

$$= \frac{\rho_e c_e^2}{(k_x^2c_e^2 - \omega^2)}\left\{k_x^2g - (\frac{1}{2H_e} + M_e)\omega^2\right\}. \tag{4.32}$$

It may be noted that the Lamb modes $\omega = k_xc_0$ and $\omega = k_xc_e$ (Lamb,1932) do not satisfy this dispersion relation but act as separatices in the usual diagnostic diagram (see, for example, Roberts, 1985; see also Section 4.5).

The dispersion relation (4.32) describes the parallel propagation of surface waves at a single magnetic interface in a gravitationally stratified atmosphere under the assumption of a constant Alfvén speed in the magnetic region.

An alternative form of the dispersion relation is

$$\frac{\omega^2}{k_x^2} = \frac{\rho_0}{\left(\rho_0 + \rho_e \dfrac{(M_e + 1/2H_e)\, m_0^2}{(M_0 - 1/2H_B)\, m_e^2}\right)} v_A^2 - g \frac{\left\{ \dfrac{\rho_0 c_0^2}{(k_x^2 c_0^2 - \omega^2)} - \dfrac{\rho_e c_e^2}{(k_x^2 c_e^2 - \omega^2)} \right\}}{\rho_0 \dfrac{(M_0 - 1/2H_B)}{m_0^2} + \rho_e \dfrac{(M_e + 1/2H_e)}{m_e^2}}, \tag{4.33}$$

where

$$m_0^2 = \frac{(k_x^2 v_A^2 - \omega^2)(k_x^2 c_0^2 - \omega^2)}{(c_0^2 + v_A^2)(k_x^2 c_T^2 - \omega^2)}, \tag{4.34}$$

and

$$m_e^2 = \frac{(k_x^2 c_e^2 - \omega^2)}{c_e^2}. \tag{4.35}$$

The form (4.33) of the dispersion relation, is useful for comparing with the non-magnetic case (which we consider in Sections 4.5 and 4.6) and with zero gravity and the incompressible limits of the dispersion relation, to which we now turn.

4.3.1 The Zero-Gravity Limit : Magnetoacoustic Surface Waves

It is of interest to examine the general dispersion relation (4.33) in some limiting cases. For example, in the limit of *zero gravity* we have $H_B^{-1} = H_0^{-1} = 0$ and

$$A_B \to -m_0^2 \,, \; A_e \to -m_e^2 \qquad \text{as } g \to 0. \tag{4.36}$$

Then Equation (4.33) reduces to

$$\frac{\omega^2}{k_x^2} = \frac{\rho_0}{(\rho_0 + \rho_e \frac{m_0}{m_e})} v_A^2, \tag{4.37}$$

where $m_0, m_e > 0$. Thus, we recover the dispersion relation describing the parallel propagation of surface waves on a magnetic interface one side of which is field-free (see Chapter 3).

The dispersion relation (4.37) for surface waves in an unstratified medium implies that the longitudinal phase-speed ω/k_x, of a surface wave must lie below the Alfvén speed. In fact, as discussed in Chapter 3, there may be *two* surface waves (Roberts, 1981a). The interface always supports a *slow* surface wave, satisfying $\omega/k_x < \min(c_T, c_e)$. But if $v_A > c_0$ and $c_e > c_0$, then a second mode, the *fast* surface wave, may propagate with a longitudinal phase-speed satisfying $c_0 < \omega/k_x < \min(c_e, v_A)$. The properties of magnetoacoustic surface waves are described in detail in Chapter 3 (see also Miles and Roberts, 1989). The investigation of their properties has been extended to non-parallel propagation in Jain and Roberts (1991); see also Uberoi (1982) for the cold plasma approximation and Uberoi (1972) for the incompressible case.

4.3.2 Incompressible Limit

Another case of the dispersion relation (4.33) that is of interest is that of an *incompressible* medium, corresponding to $c_0, c_e \to \infty$. Consider the special case of a fluid with *uniform* distributions of density, so that $\rho_0(z) = \rho_0$ and $\rho_e(z) = \rho_e$. Then, with non-zero gravity but c_0 and c_e large, we obtain

$$m_0, m_e, M_0, M_e \to k_x, \tag{4.38}$$

and so Equation (4.33) reduces to the

$$\frac{\omega^2}{k_x^2} = \frac{\rho_0}{(\rho_0 + \rho_e)} v_A^2 - \frac{g}{k_x} \frac{(\rho_0 - \rho_e)}{(\rho_0 + \rho_e)}. \tag{4.39}$$

Thus we recover the dispersion relation describing the propagation of hydromagnetic surface waves in a stratified fluid (see Section 2.4 of Chapter 2).

4.4 Cutoff Curves

Before considering a numerical solution of the general dispersion relation (4.33) it is necessary to examine the constraints under which the equation is derived. We require that $(1 - 4A_BH_B^2) > 0$ and $(1 - 4A_eH_e^2) > 0$. These constraints represent the cutoff frequencies for the modes. If either $(1 - 4A_BH_B^2)$ or $(1 - 4A_eH_e^2)$ is negative, then solutions with oscillatory structure arise; these are internal (or body) modes (Lighthill, 1978), modified by the presence of a magnetic field. They will not be discussed further here.

The condition $4A_eH_e^2 < 1$ generates curves R_1 and R_2 in the ω-k_x space which contain the allowed modes given by Equation (4.33). Similarly, the condition $4A_BH_B^2 < 1$ generates confining curves R_3 and R_4. These conditions are the compressible equivalent of the conditions that $4a_eH_e^2 < 1$ and $4a_BH_B^2 < 1$ which generated the curves r_1 and r_2 in the incompressible case (see Chapter 2, Section 2.4.1).

The form of these constraints depends upon whether $\omega > k_xc_T$ or $\omega < k_xc_T$. Thus, if $\omega > k_xc_T$ then

$$\max\left(\frac{c_T}{c_e},\, R_1,\, R_3\right) \le \frac{\omega}{k_xc_e} \le \min\,(R_2, R_4). \tag{4.40}$$

However, if $\omega < k_xc_T$ then either

$$R_1 \le \frac{\omega}{k_xc_e} \le \min\left(\frac{c_T}{c_e},\, R_2,\, R_3\right), \tag{4.41}$$

or

$$\max\,(R_1, R_4) \le \frac{\omega}{k_xc_e} \le \min\left(\frac{c_T}{c_e},\, R_2\right). \tag{4.42}$$

Here R_1^2 and R_2^2 are given by

$$R_{1,2}^2 = \frac{\left(1+4k_x^2H_e^2\right) \mp \left\{(1+4k_x^2H_e^2)^2 - 64k_x^2H_e^2\frac{(\gamma-1)}{\gamma^2}\right\}^{1/2}}{8k_x^2H_e^2}, \tag{4.43}$$

and R_3^2 and R_4^2 satisfy

$$1 - \frac{\frac{c_0^4}{4}}{\frac{c_e^4}{\Gamma^2}} \left\{ \frac{(\Gamma-1) + \gamma^2 k_x^2 H_e^2 \left(R_{3,4}^2 - \frac{c_0^2}{c_e^2} \right) \left(R_{3,4}^2 - \frac{v_A^2}{c_e^2} \right)}{\left(\frac{c_0^2}{c_e^2} + \frac{v_A^2}{c_e^2} \right) \left(R_{3,4}^2 - \frac{c_T^2}{c_e^2} \right)} \right\} = 0. \qquad (4.44)$$

In the limit as $k_x H_e \to \infty$, which includes the case $g \to 0$, we obtain

$$R_1 \to 0, \quad R_2 \to 1 \qquad (4.45)$$

and

$$R_3^2 \to \min\left(\frac{c_0^2}{c_e^2}, \frac{v_A^2}{c_e^2} \right), \quad R_4^2 \to \max\left(\frac{c_0^2}{c_e^2}, \frac{v_A^2}{c_e^2} \right). \qquad (4.46)$$

In the limit as $k_x H_e \to 0$ we find that

$$R_1^2 \to \frac{4(\gamma-1)}{\gamma^2}, \quad R_2^2 \to \infty \qquad (4.47)$$

and

$$R_3^2 \to \frac{\frac{c_0^2}{c_e^2} \left(\Gamma^2 \frac{v_A^2}{c_e^2} + 4 \frac{c_0^2}{c_e^2} (\Gamma-1) \right)}{\Gamma^2 \left(\frac{c_0^2}{c_e^2} + \frac{v_A^2}{c_e^2} \right)}, \quad R_4^2 \to \infty. \qquad (4.48)$$

Thus, for example, with $c_0/c_e = 0.9$ and $v_A/c_e = 0.5$ (as used later in the numerical solutions) we have

$$R_1 \to 0, \quad R_2 \to 1, \quad R_3 \to 0.9, \quad R_4 \to 0.5 \qquad \text{as } k_x H_e \to \infty, \qquad (4.49)$$

and

$$R_1 \to 0.98, \quad R_2 \to \infty, \quad R_3 \to 0.81, \quad R_4 \to \infty \qquad \text{as } k_x H_e \to 0. \tag{4.50}$$

In the above, and in all the subsequent illustrations, we have taken $\gamma = 5/3$.

4.5 The Surface Gravity Mode

It is also interesting to examine the dispersion relation (4.33) in the limit of *zero magnetic field*. With $B_0 = 0$, the dispersion relation given by Equation (4.32) reduces to

$$\frac{\rho_0 c_0^2}{(k_x^2 c_0^2 - \omega^2)}\left(k_x^2 g - (M_0 - \frac{1}{2H_0})\omega^2\right) = \frac{\rho_e c_e^2}{(k_x^2 c_e^2 - \omega^2)}\left(k_x^2 g - (M_e + \frac{1}{2H_e})\omega^2\right), \tag{4.51}$$

where now

$$M_0 = \frac{(1 - 4A_0 H_0^2)^{1/2}}{2H_0} \tag{4.52}$$

is the non-magnetic version of M_0 given by Equation (4.29).

We note immediately that since there is no magnetic field there can be no magnetoacoustic surface mode solutions to this dispersion relation. In the notation of Equation (4.33), we may rewrite Equation (4.51) as

$$\frac{\omega^2}{k_x^2} = -g \frac{\left\{\dfrac{\rho_0 c_0^2}{(k_x^2 c_0^2 - \omega^2)} - \dfrac{\rho_e c_e^2}{(k_x^2 c_e^2 - \omega^2)}\right\}}{\rho_0 \dfrac{(M_0 - 1/2H_0)}{m_0^2} + \rho_e \dfrac{(M_e + 1/2H_e)}{m_e^2}}. \tag{4.53}$$

It is interesting to observe that we can remove the transcendentality of Equation (4.53). This was first noted by Bernstein and Book (1983) in their investigation of the

effect of compressibility on the Rayleigh-Taylor instability. After much algebra (see Appendix A.3), Equation (4.53) may be rewritten as a polynomial in Ω^2 :

$$(\Omega^4-1)(\Omega^2 g-k_x c_0^2)^2(\Omega^2 g-k_x c_e^2)^2[\Omega^8-2S\Omega^6+(S^2+2\gamma-1)\Omega^4-2(\gamma-1)S\Omega^2-D^2]=0, \tag{4.54}$$

where $\Omega^2 = \omega^2/gk_x$, as defined previously in Chapter 2 by Equation (2.48), $S = k_x (c_0^2+ c_e^2)/g$ and $D = k_x (c_0^2- c_e^2)/g$. Bernstein and Book (1983), in their instability investigations, considered only the quartic (in Ω^2) factor of Equation (4.54); we consider the full expression as given by Equation (4.54).

Clearly, the process of removing the transcendental nature of Equation (4.53), through squaring several times, may introduce spurious roots which satisfy the polynomial (4.54) but not the original dispersion relation (4.53). For example, Equation (4.54) possesses the solutions $\Omega^2 = k_x c_0^2/g$ and $\Omega^2 = k_x c_e^2/g$, roots of which are the Lamb modes $\omega = k_x c_0$ and $\omega = k_x c_e$. However, although these are solutions to the polynomial Equation (4.54) they do not satisfy the transcendental dispersion relation Equation (4.53).

The other possible solutions to the polynomial (4.54) are $\Omega^2 = \pm 1$ and those arising from the quartic (in Ω^2), namely

$$\Omega^8 - 2S\Omega^6 + (S^2 + 2\gamma - 1)\Omega^4 - 2(\gamma - 1)S\Omega^2 - D^2 = 0. \tag{4.55}$$

This quartic is the compressible counterpart of the incompressible quadratic (2.58) investigated previously in Chapter 2.

Once again, as for the incompressible case, a stable (i.e. $\Omega^2 > 0$) solution to Equation (4.54) is the f-mode, $\omega^2 = gk_x$ (i.e., $\Omega^2 = 1$). It was shown in Chapter 2 for the incompressible case that the f-mode was able to propagate only when $\rho_0 > \rho_e$. This is also the case here for the compressible problem, as we detail in Section 4.6. For the compressible problem the inequality in densities may be expressed as an inequality in sound speeds: the f-mode is able to propagate only when $\rho_0 > \rho_e$, i.e., $c_e > c_0$. Note

this is the same as one of the two conditions in the zero-gravity case for the fast magnetoacoustic surface mode to propagate (see Chapter 3). The f-mode is illustrated in Figure 4.2; we shall discuss it in greater detail in Section 4.6. There are no stable solutions to the Ω^2-quartic (4.55), which are also stable solutions to the dispersion relation (4.53), when $\rho_0 > \rho_e$. This is completely analogous to the incompressible case (Chapter 2) where, when $\rho_0 > \rho_e$, there are no stable solutions to the Ω^2-quadratic (2.58) which are also stable solutions to the dispersion relation (2.56).

If $\rho_0 < \rho_e$, then the opposite is true; that is, the solution $\omega^2 = gk_x$ of the polynomial (4.54) does not satisfy the dispersion relation (4.53), and the only stable solutions to the dispersion relation (4.53) are those resulting from the quartic (4.55). In fact, when $\rho_0 < \rho_e$ there is again only one stable solution of relation (4.53). This is the surface gravity wave; its dispersive phase-speed is shown in Figure 4.3(i). Once again this is exactly the same as for the incompressible counterpart of the surface gravity wave described previously in Chapter 2. The mode asymptotes to distinct limits at short and long wavelengths. We discuss these limits in turn.

Consider, first, the short wavelength limit. As $k_x \to \infty$, $S \to \infty$ and $D \to \infty$; then the dominant terms in the quartic (4.55) reduce it to

$$S^2 \Omega^4 - D^2 = 0, \tag{4.56}$$

the stable solution of which, for $\rho_0 < \rho_e$, is the familiar Rayleigh-Taylor dispersion relation

$$\frac{\omega^2}{k_x^2} = -\frac{g}{k_x} \frac{(\rho_0 - \rho_e)}{(\rho_0 + \rho_e)}, \tag{4.57}$$

as determined earlier (Equation 2.60)) for the short wavelength limit in the incompressible case. In terms of Figure 4.3, this result means that the dimensionless phase-speed $\omega/k_x c_e \to 0$ as $k_x H_e \to \infty$.

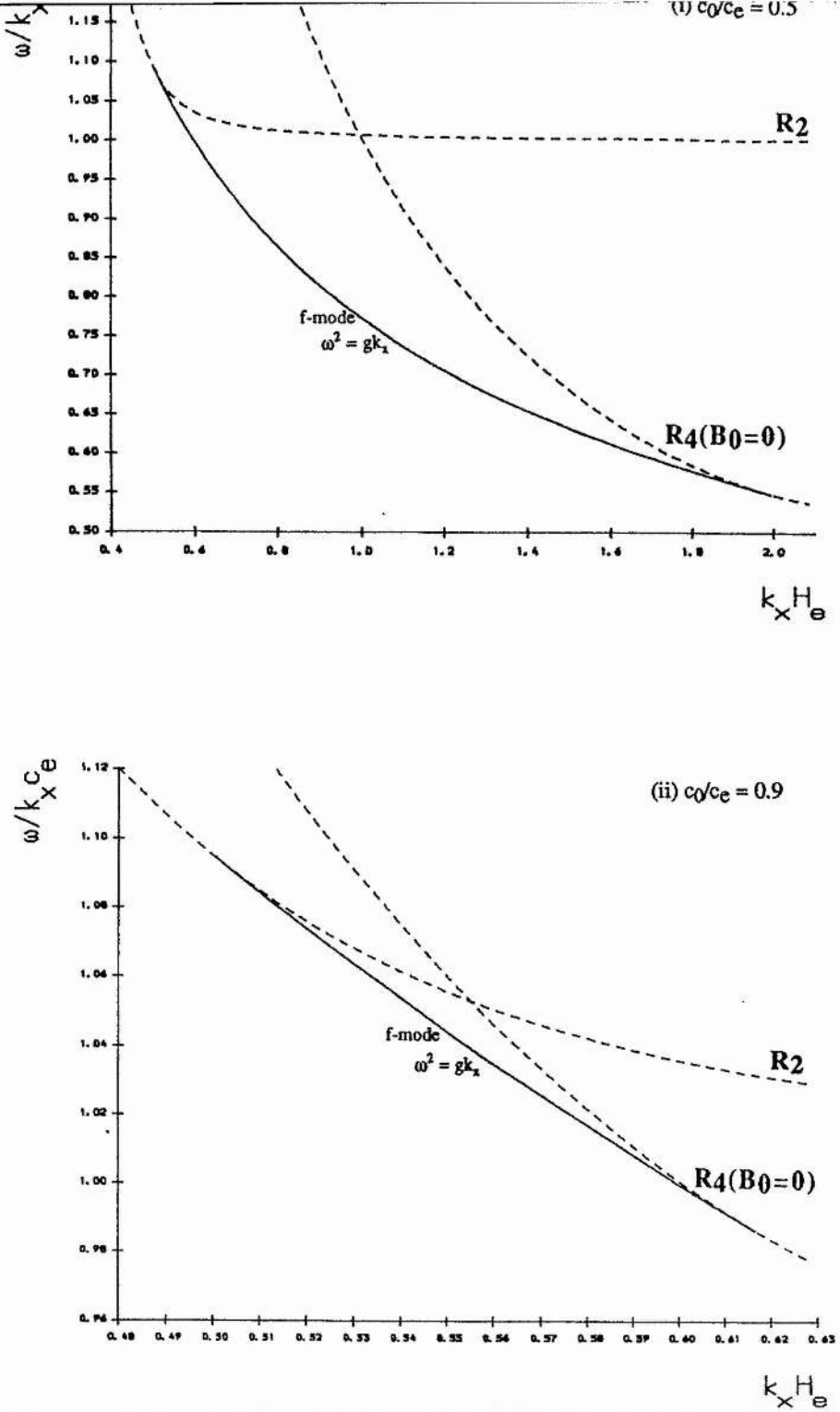

FIGURE 4.2 The dimensionless phase-speed $\omega/k_x c_e$ of the f-mode ($\omega^2=gk_x$) as a function of dimensionless horizontal wavenumber $k_x H_e$ in the absence of a magnetic field. Case (i) $c_0/c_e = 0.5$ and (ii) $c_0/c_e = 0.9$. Note the changed scales. The dashed curves are cutoffs for the propagation of the f-mode determined by the requirements that $4A_0H_0^2 < 1$ and $4A_eH_e^2 < 1$ (see text). Observe that the range in wavenumber for propagation is reduced as c_0/c_e approaches unity; for $c_0 > c_e$, the f-mode does not exist. We have taken $\gamma = 5/3$ in this and subsequent figures.

In the long wavelength limit, as $k_x \to 0$, the quartic (4.55) reduces to

$$(2\gamma-1)\Omega^4 - 2(\gamma-1)S\Omega^2 - D^2 = 0, \tag{4.58}$$

which possesses the solution

$$\frac{\omega^2}{k_x^2 c_e^2} = \frac{(\gamma-1)(\rho_0+\rho_e) + \{(\gamma-1)^2(\rho_0+\rho_e)^2 + (2\gamma-1)(\rho_0-\rho_e)^2\}^{1/2}}{\rho_0(2\gamma-1)}. \tag{4.59}$$

Figure 4.3(i) is drawn for the parameter value $c_0/c_e = 1.4$ for which Equation (4.59) gives $\omega^2/k_x^2c_e^2 \simeq 1.9$ (i.e., $\omega/k_xc_e \to 1.38$ as $k_x \to 0$). The mode has the property that its vertical velocity component in the upper atmosphere ($z>0$) changes in character from exponentially growing for small values of k_xH_e to exponentially declining for large values of k_xH_e. The mode always declines in the lower atmosphere ($z<0$). This is illustrated in Figure 4.4 where the eigenfunctions for the mode are plotted at three values of k_xH_e.

This behaviour of the mode may be easily understood from an examination of the vertical velocity component :

$$v_z(z) \propto \begin{cases} \exp\left\{\frac{1}{2H_0}[1 - (1 - 4A_0H_0^2)^{1/2}]z\right\}, & z > 0, \\ \exp\left\{\frac{1}{2H_e}[1 + (1 - 4A_eH_e^2)^{1/2}]z\right\}, & z < 0, \end{cases} \tag{4.60}$$

where we take the positive square roots of $(1 - 4A_0H_0^2)^{1/2}$ and $(1 - 4A_eH_e^2)^{1/2}$. Evidently, for $z<0$, v_z is always exponentially declining in nature. However, for $z>0$, v_z declines only if $A_0<0$. Thus $A_0=0$ determines where the mode changes in character from exponentially growing to exponentially declining. The curve $A_0=0$ is drawn in Figure 4.3(ii), superimposed on the mode displayed in Figure 4.3(i). The curve is contained within the cutoff curves R_3 (with $B_0=0$) and R_4 (with $B_0=0$), asymptoting to

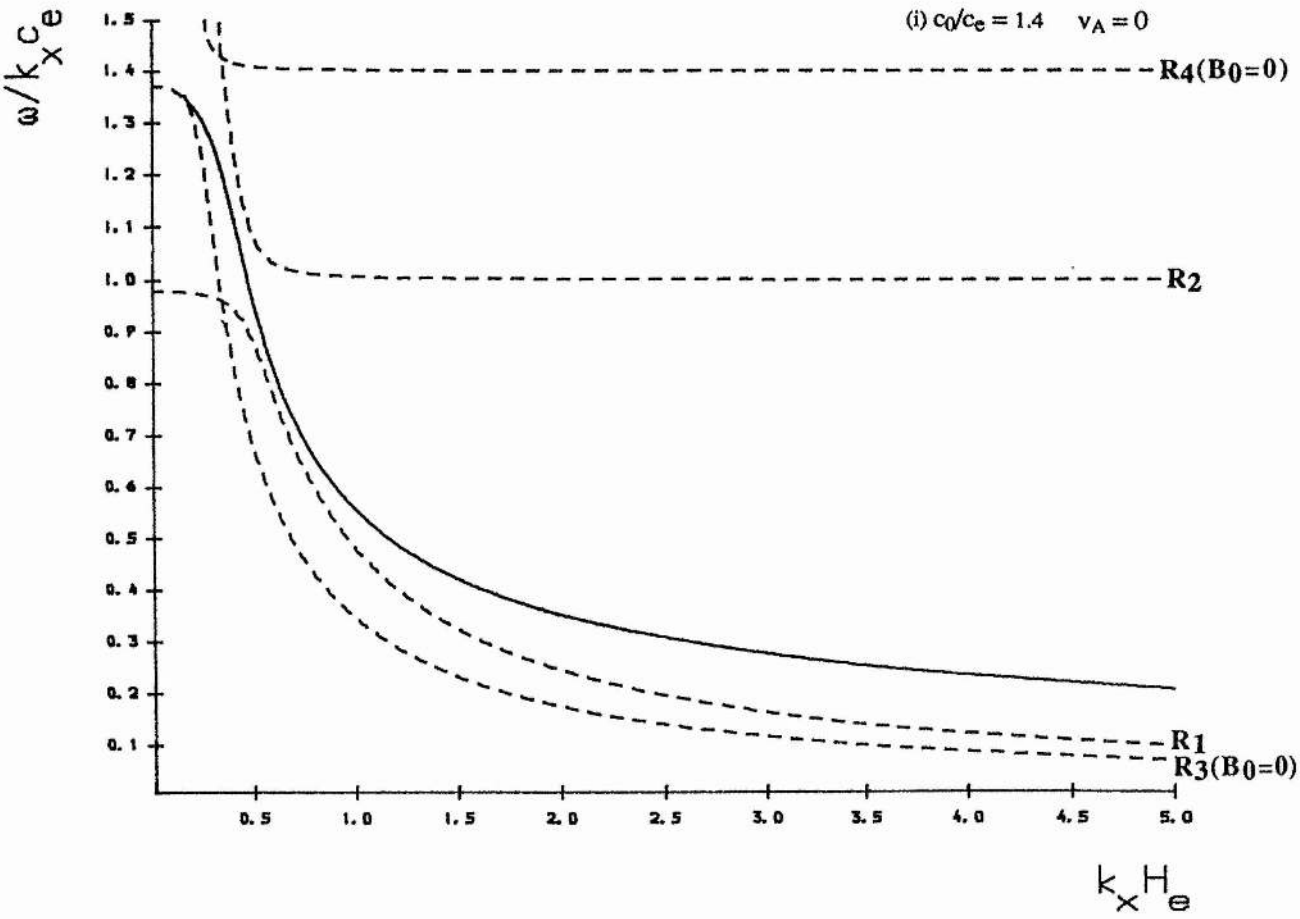

FIGURE 4.3(i) The dimensionless phase-speed versus dimensionless horizontal wavenumber for the stable solution to the non-magnetic dispersion relation (4.53) when $\rho_0 < \rho_e$ (i.e. $c_0 > c_e$). Here $c_0/c_e = 1.4$ giving $\omega/k_x c_e \to 1.38$ as $k_x H_e \to 0$ and $\omega/k_x c_e \to 0$ as $k_x H_e \to \infty$. The dashed curves R_1,R_2, R_3 and R_4 are determined from the requirements that $4A_0H_0^2 < 1$ and $4A_eH_e^2 < 1$.

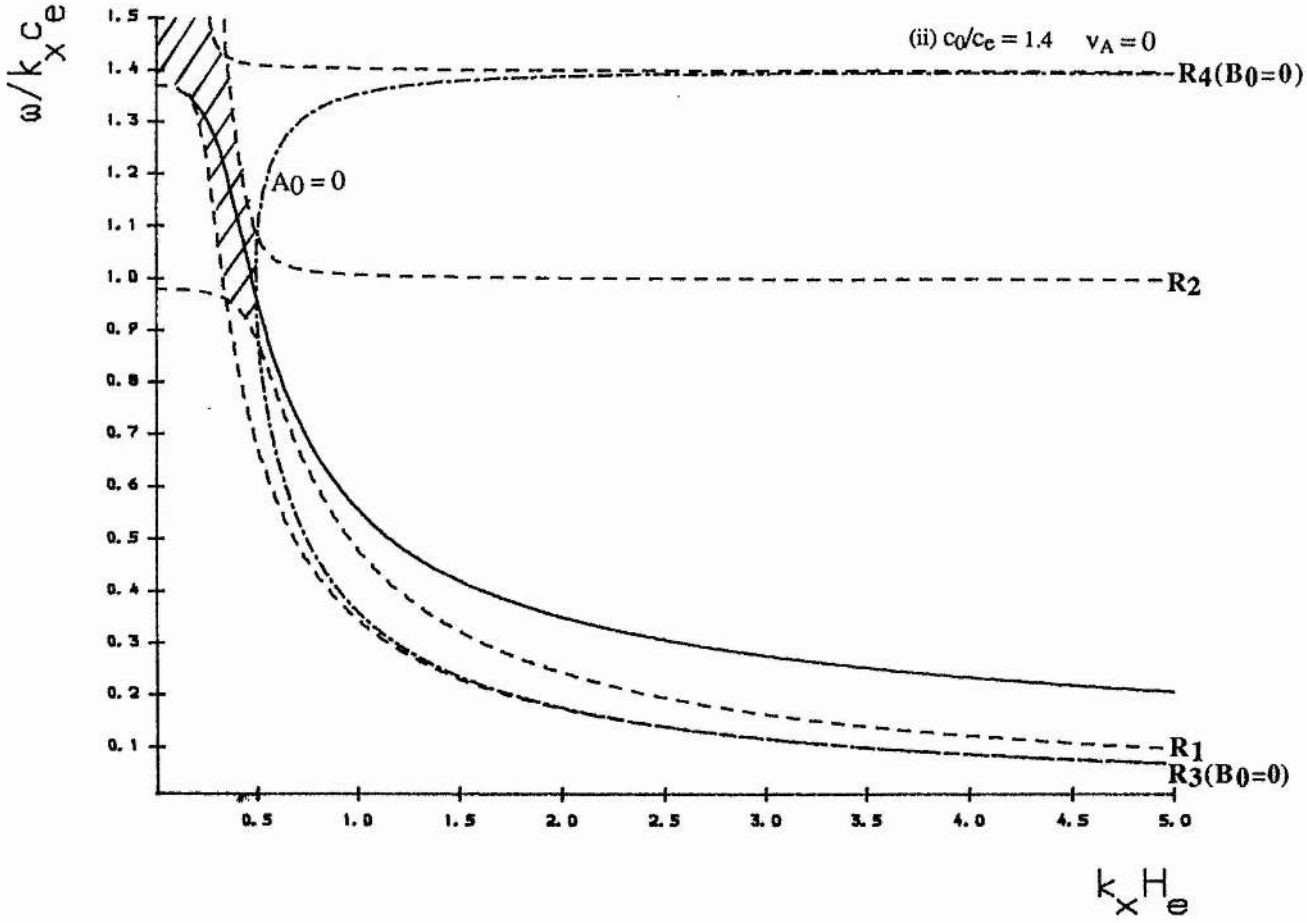

FIGURE 4.3(ii) As in (i) with the inclusion of the curve A_0=0, shown as a dash dotted line. The curve A_0=0 divides the region of evanescence in the upper medium into a domain wherein the vertical velocity component is growing with height z from a domain where it is declining with height. Together with the conditions imposed by the cutoff curves, this means that the mode has a growing v_z only in the region shown shaded. Elsewhere on the dispersion curve v_z declines with height.

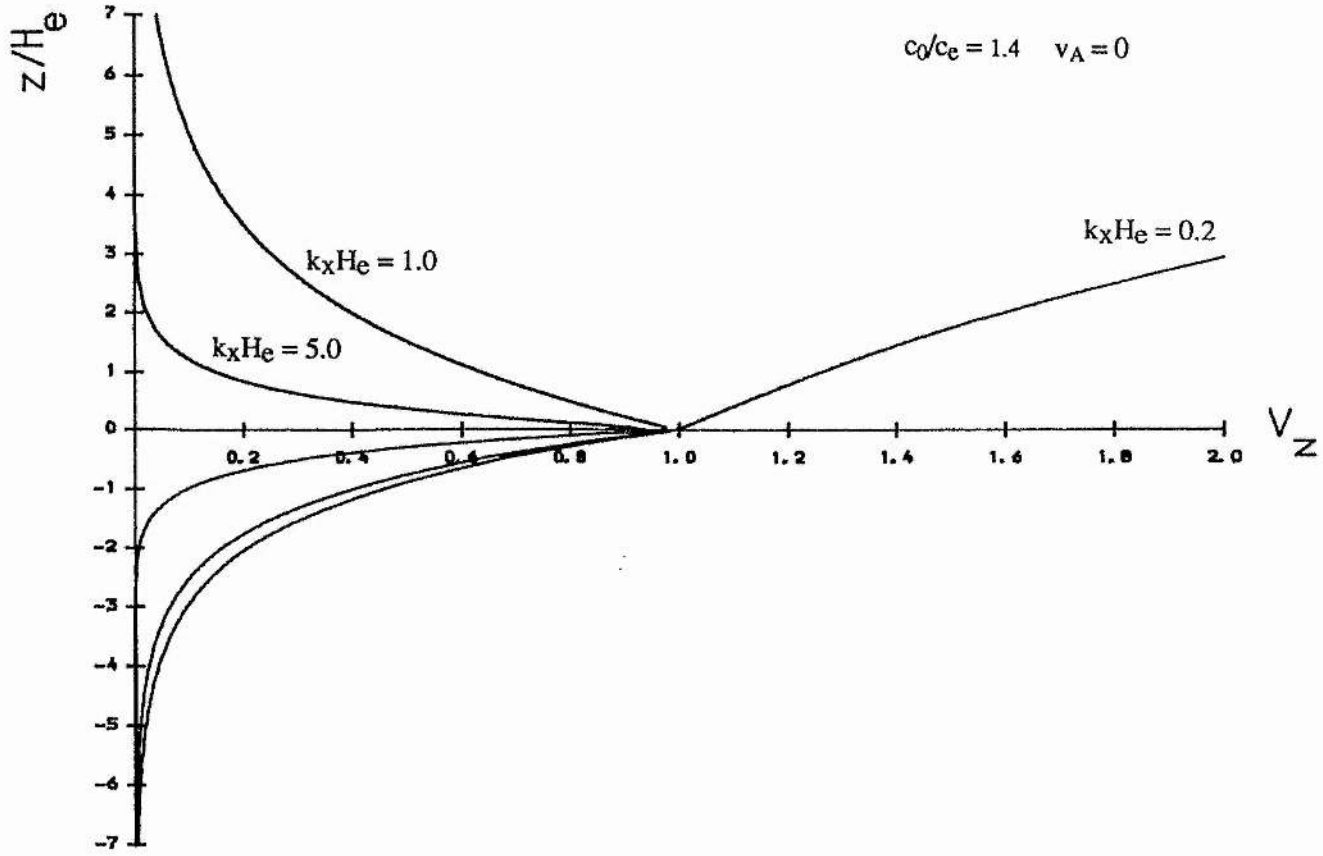

FIGURE 4.4 The eigenfunction $v_z(z)/v_z(0)$ for the gravity surface mode shown in Figure 4.3 at three values of k_xH_e. As the value of k_xH_e is increased (i.e., as we move from left to right in Figure 4.3), so the eigenfunction of the mode switches from spatial growth to decay. There is a critical value of k_xH_e. If k_xH_e exceeds $2\left(\frac{\gamma-1}{\gamma^2}\right)^{1/2}\left(\frac{\rho_0}{\rho_e}\right)^2$, then the mode will have a decaying character. For $c_0 = 1.4c_e$, this critical value of k_xH_e is approximately 0.5.

these curves as $k_x H_e \to \infty$. Now for real solutions in the lower atmosphere the mode must lie within the region defined by R_1 and R_2, while for real solutions in the upper atmosphere the mode must lie within the region defined by R_3 ($B_0=0$) and R_4 ($B_0=0$). For the mode to have a declining v_z it must also lie within the region defined by the curve $A_0=0$. Thus, in Figure 4.3(ii) the *unshaded* region, defined by $A_0<0$ and satisfying

$$\max(R_3(B_0=0), R_1) \leq \frac{\omega}{k_x c_e} \leq \min(R_2, R_4(B_0=0)), \tag{4.61}$$

defines the region where the mode has a *declining* vertical velocity component. The shaded region represents the region where the mode has a spatially growing vertical velocity component.

The turning point of the curve $A_0=0$ is given by

$$\frac{\omega}{k_x c_e} = \frac{\rho_e}{\rho_0\sqrt{2}}, \quad k_x H_e = 2\left(\frac{\gamma-1}{\gamma^2}\right)^{1/2}\left(\frac{\rho_0}{\rho_e}\right)^2; \tag{4.62}$$

for the parameter values of Figure 4.3(ii) this gives

$$\frac{\omega}{k_x c_e} \simeq 0.99, \quad k_x H_e \simeq 0.5. \tag{4.63}$$

Thus, for both Figures 4.3(i) &(ii), the mode has a growing vertical velocity component in the region $k_x H_e < 0.5$.

Figure 4.3 is in fact equivalent to the more familiar ω-k_x diagnostic diagram (see, for example, Roberts, 1985). In Figure 4.5 we present the standard diagnostic diagram for an isothermal atmosphere with sound speed c_s. Included in Figure 4.5 is the curve A=0 defined by

$$\frac{k_x^2\omega_g^2}{\omega^2} + \frac{(\omega^2 - k_x^2 c_s^2)}{c_s^2} = 0, \tag{4.64}$$

where $\omega_g (= (\gamma-1)^{1/2} c_S/\gamma H)$ is the buoyancy (Brunt-Väisälä) frequency of an isothermal atmosphere. As in Figure 4.3, cutoff curves divide the ω-k_x space into regions of evanescence and regions of propagation. However, in contrast to Figure 4.3, there is only a single pair of cutoff curves in Figure 4.5. This is because the standard diagnostic diagram is usually drawn for one medium only (and not for two media as in Figure 4.3). Application of Figure 4.5 to the upper atmosphere gives the curves R_4 ($B_0=0$) and R_3 ($B_0=0$) of Figure 4.3(i); the curve R_4 corresponds to the upper (acoustic branch) cutoff curve of Figure 4.5, and the curve R_3 corresponds to the lower (gravity branch) cutoff curve of Figure 4.5.

As $k_x \to 0$, the upper cutoff curve tends to $\omega_a (= c_S/2H)$, the acoustic cutoff frequency for an isothermal atmosphere, while the lower cutoff curve tends to zero. As $k_x \to \infty$, the upper cutoff curve tends to $\omega = k_x c_S$, the Lamb frequency for the atmosphere, while the lower cutoff curve tends to the buoyancy frequency ω_g. Note that $\omega_a > \omega_g$. The time scales ω_g^{-1} and ω_a^{-1} arise in the atmosphere because of the presence of the gravitational field. The region above the upper cutoff curve is one in which sound waves may propagate. The region below the lower cutoff curve is where gravity (or g-modes) may exist. As in Figure 4.3, the region bounded by these cutoff curves is where surface modes may occur, corresponding to vertical evanescence (non-propagation). The curve $A=0$ divides the region of evanescence still further, and asymptotes to $\omega = k_x c_S$ and to $\omega = \omega_g$ as $k_x \to \infty$. In the region enclosed by the cutoff curves and where $A<0$ a mode possesses a decaying vertical velocity component; in the shaded region a mode has a growing vertical velocity component.

The turning point of the curve $A=0$ is given by

$$\omega = \omega_g\sqrt{2}\ ,\ k_x = \frac{2\omega_g}{c_S}. \qquad (4.65)$$

Thus, in Figure 4.5, if $k_x < 2\omega_g/c_S$ then the mode will have a growing vertical velocity component.

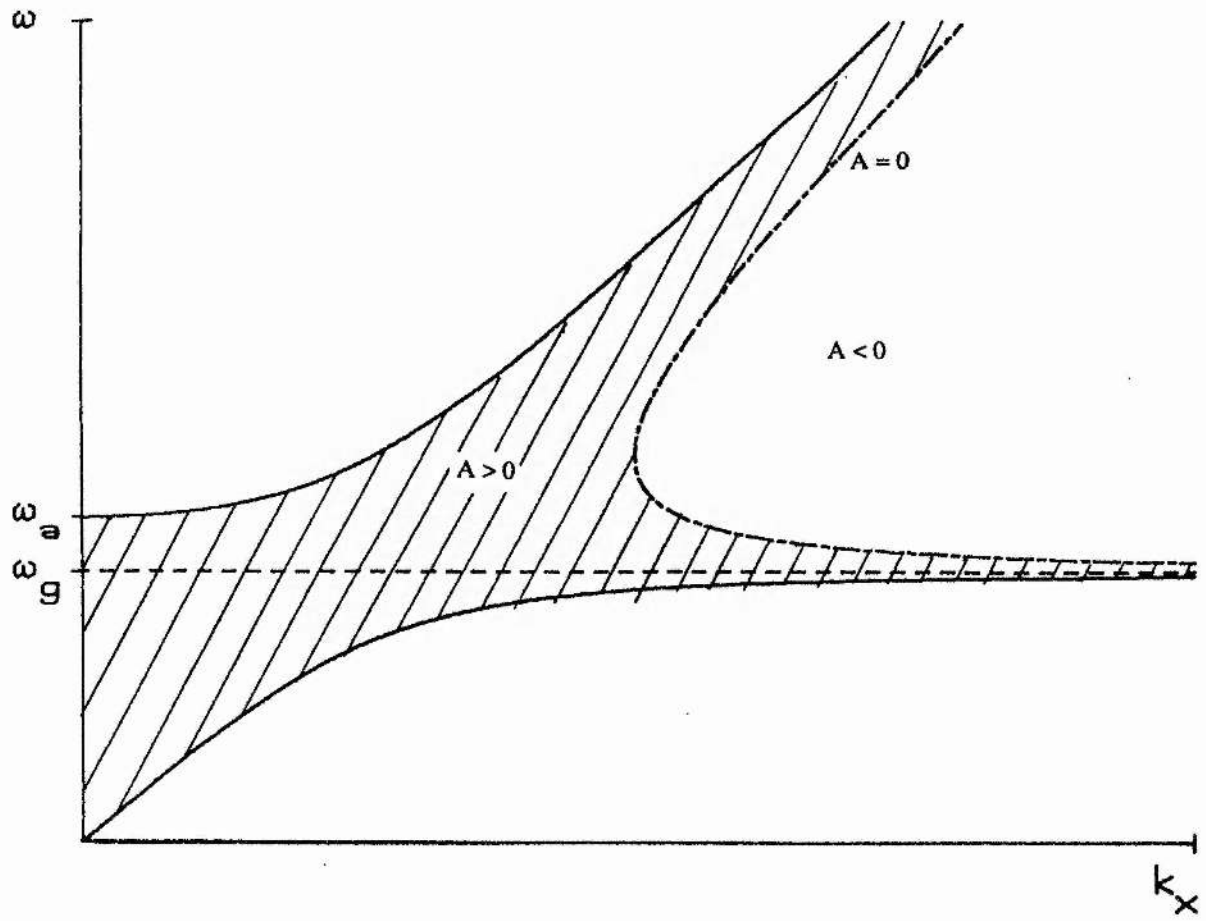

FIGURE 4.5 The familiar diagnostic diagram for an isothermal atmosphere, with the inclusion of the curve (shown as a dash-dotted line) A=0 defined by Equation (4.64). Evanescent (non-propagating) modes exist only within the region defined by the cutoff curves (the solid lines). The unshaded region defined by A<0 is where an evanescent mode will have a vertical velocity component that declines with height (c.f. Figure 4.3(ii)).

Thus we conclude that in the absence of a magnetic field, the dispersion relation (4.33) reduces to (4.53) and possesses two distinct stable modes, the f-mode and the surface gravity mode, only one of which may propagate at any given circumstance depending on the ratio of the densities. This is exactly the same situation as for the incompressible case investigated earlier in Chapter 2 (see Section 2.4.2). If $\rho_0 < \rho_e$, then the surface gravity mode will propagate; if $\rho_0 > \rho_e$ the f-mode exists, although only within a certain range of horizontal wavenumber k_x. It is to this mode that we now switch our attention.

4.6 The f-Mode

In the absence of a magnetic field Equations (4.12) and (4.13) possess the solution $\Delta = 0$, $v_z \propto e^{k_x z}$, $\omega^2 = gk_x$ (i.e. $\Omega^2 = 1$). The solution $\Omega^2 = 1$ is the f-mode. The f-mode is incompressible ($\Delta = 0$) and its frequency and spatial dependence are independent of the form of the thermal stratification. In the presence of a horizontal magnetic field the f-mode is no longer incompressible and its frequency is affected by the magnetic forces and the compressibility of the gas (Campbell and Roberts, 1989; Evans and Roberts, 1990a,b).

The f-mode will be a solution to the dispersion relation (4.33) in the limit of zero field provided the mode satisfies the conditions on $v_z(z)$ under which the dispersion relation was derived. In the case of zero magnetic field, Equation (4.33) with $\Omega^2 = 1$ reduces to

$$\frac{1}{(\gamma k_x H_e c_0^2/c_e^2 - 1)} \left\{ \frac{1}{2k_x H_e c_0^2/c_e^2} [1 - |1 - 2k_x H_e c_0^2/c_e^2|] - 1 \right\}$$

$$= \frac{1}{(\gamma k_x H_e - 1)} \left\{ \frac{1}{2k_x H_e} [1 + |2k_x H_e - 1|] - 1 \right\}. \qquad (4.66)$$

A scrutiny of Equation (4.66) reveals that it is satisfied only if $1 < 2k_xH_e < c_e^2/c_0^2$; that is, Equation (4.66) is satisfied only if the horizontal wavenumber lies in the interval

$$\frac{1}{2H_e} < k_x < \frac{1}{2H_0}, \tag{4.67}$$

(c.f. Equation (2.66) in Chapter 2).

With k_x lying in this interval there is a mode with $\omega^2 = gk_x$ and $v_z \propto e^{k_x z}$ that satisfies boundness of the kinetic energy density but the velocity itself is unbounded in the upper atmosphere ($z>0$). It follows immediately from the inequality (4.67) that the f-mode can propagate only if $H_e > H_0$, i.e. if $c_e > c_0$ or (equivalently) $\rho_0 > \rho_e$. Thus the field-free region must be warmer and more tenuous than the overlying atmosphere for the f-mode to exist in an isothermal non-magnetic medium. This is the same condition that pertains for the existence of fast magnetoacoustic surface waves on an unstratified field-free interface (Chapter 3; see also Roberts, 1981a, Miles and Roberts, 1989).

The restriction on the propagation of the f-mode is illustrated in Figure 4.2, which shows the variation of the phase-speed with the horizontal wavenumber for two values of the parameter c_0/c_e.Figure 4.2 demonstrates clearly how the restriction on wavenumber for the propagation of the f-mode is tightened as c_0/c_e approaches unity. The dashed curves are cutoff curves for the propagation resulting from the assumptions that $4A_0H_0^2 < 1$ (giving the dashed curve R_4 ($B_0=0$)) and $4A_eH_e^2 < 1$ (giving the dashed curve R_2), with $A_B \to A_0$ and $H_B \to H_0$ in the limit of no magnetic field. Beyond these dashed curves the solutions to the dispersion relation (4.53) are complex valued.

We consider now the influence of the magnetic field on the f-mode. We seek an approximate solution to the dispersion relation (4.66), with the property that $\Omega^2 \to 1$ as $v_A/c_e \to 0$, by writing

$$\Omega^2 \to 1 + \alpha v_A^2/c_e^2, \qquad v_A/c_e \to 0, \tag{4.68}$$

for constant α. Expanding the dispersion relation (4.33) for small v_A/c_e allows us to determine α. After some detailed algebra, we find that (see Appendix A.4)

$$\alpha = \frac{\gamma\,(2k_xH_e-1)}{2(1-c_0^2/c_e^2)}\,. \tag{4.69}$$

The conditions $2k_xH_e > 1$ and $c_0^2/c_e^2 < 1$ are imposed in deriving the dispersion relation (4.66), and so we see that α is positive. Thus, in the presence of a magnetic field the frequency of the f-mode is *increased*. Other investigations of the effect of a magnetic field on the f-mode frequency have similarly found an increase (Campbell and Roberts, 1989; Evans and Roberts, 1990a,b).

In terms of the original variables, the first order correction to the f-mode in the presence of a magnetic field gives the result

$$\frac{\omega^2}{gk_x} \approx 1 + \frac{\gamma}{2}\frac{(2k_xH_e - 1)}{(c_e^2 - c_0^2)}\,v_A^2, \tag{4.70}$$

valid for $c_e > c_0$ and $2k_xH_e > 1$ (c.f. the incompressible result (2.71) in Chapter 2). The result (4.70) is in fact identical to that for the incompressible case given by (2.71) in Chapter 2. This is not surprising since the result (4.70) is evidently independent of compressibility γ, and so also holds when $\gamma \to \infty$. We note that Equation (4.70) is valid only within the domain given by inequality (4.67), since otherwise the expansion (4.68) does not reduce to the f-mode as the magnetic field tends to zero.

Figure 4.6 compares the analytical result (4.70) with the results from a numerical solution of the dispersion relation (4.33). For Figure 4.6(i), where $c_0/c_e = 0.9$ and $v_A/c_e = 0.1$, the analytical and numerical results are virtually identical, resulting in the two curves being indistinguishable. Thus, the approximation (4.70) is accurate for small values of the magnetic field and so Equation (4.70) provides a good approximation to the dispersion relation of the f-mode in the presence of a weak field. In Figure 4.6(ii) the strength of the magnetic field is increased slightly to give $v_A/c_e = 0.2$. There is now a small but noticeable difference between the analytical and

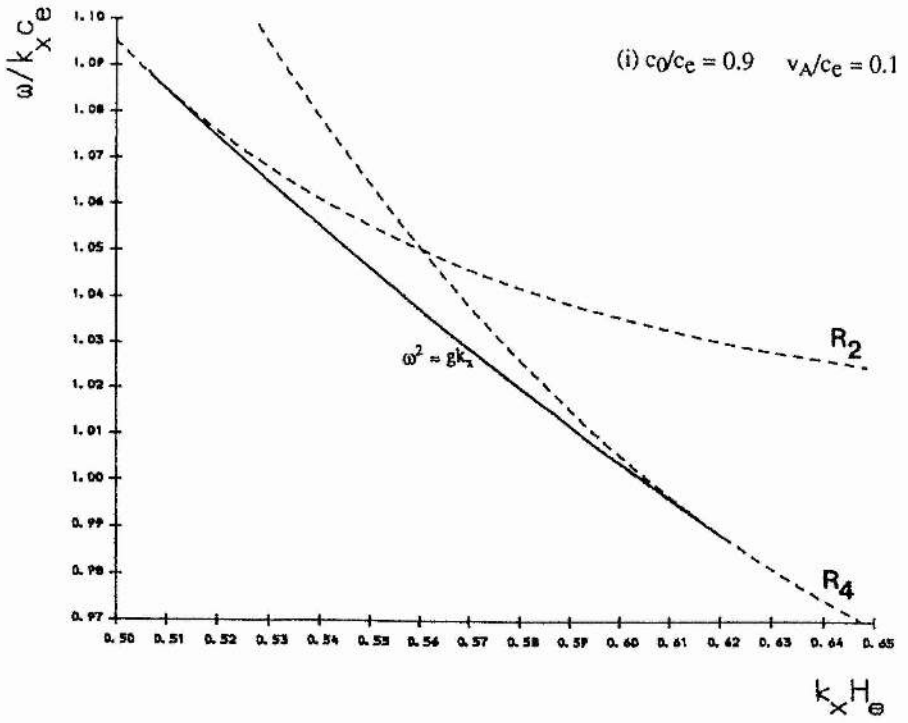

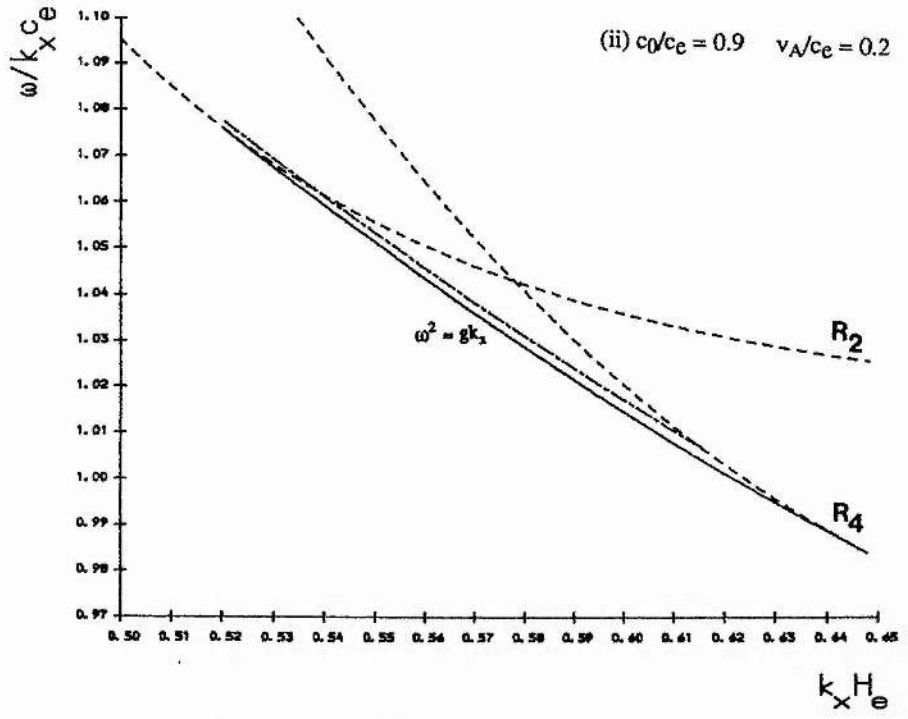

FIGURE 4.6 The effect of a weak magnetic field on the f-mode when $c_0/c_e = 0.9$. For case (i) $v_A/c_e = 0.1$ the numerical and analytical curves overlie one another. For case (ii) $v_A/c_e = 0.2$ the upper (dashed) curve is that given by the analytical result (4.70) obtained in the text. The dashed curves labelled R_2 and R_4 are cutoff curves resulting from the constraints $4A_B H_B^2 < 1$ and $4A_e H_e^2 < 1$ in Equation (4.33).

numerical results. The upper (dashed) curve is the analytical result, satisfying the bounds given by Equation (4.67), while the lower (full) curve is that found from the numerical results. Comparing Figure 4.6(ii) with the non-magnetic curve in Figure 4.2(ii), we note that the effect of including the magnetic field is two-fold: the restriction in the horizontal wavenumber has been lessened and shifted to the right, thereby resulting in a smaller maximum longitudinal phase-speed.

The vertical velocity of the disturbance, given by Equation (4.60), can be calculated as a function of height for any point on the dispersion curve. Figure 4.7(i) compares the eigenfunctions for the f-mode for two different values of the horizontal wavenumber. The eigenfunctions are for $k_xH_e = 0.5135$, just as the f-mode begins to propagate, and for $k_xH_e = 1.8287$ at the other extreme of its range of propagation. The figure shows clearly that the eigenfunction of the f-mode is depressed as the horizontal wavenumber is increased. We note that $v_z \not\to 0$ as $z \to \infty$. If we were to impose the curve $A_0=0$ on Figure 4.2 then the f-mode would lie entirely within the region $A_0>0$. However, the conditions imposed on the solutions (4.60) ensure that the energy density (kinetic plus magnetic) remains finite as $|z| \to \infty$. The profiles of kinetic energy density for the eigenfunctions in Figure 4.7(i) are shown in Figure 4.7(ii).

4.7 Magnetoacoustic-gravity Surface Modes

We turn now to an examination of all of the modes given by the numerical solution of the dispersion relation (4.33). This includes the f-mode modified by magnetism, as discussed above, and makes clear the complex interconnections that exist between the various surface waves. The behaviour of the modes is explored over the ranges of the various parameters.

Figure 4.8 illustrates the variation of the phase-speed with the parameter k_xH_e, taking $c_0 < c_e$ (specifically $c_0/c_e = 0.9$) for three values of v_A/c_e (Figures 4.8(i),(ii) & (iii)) and taking $c_0 > c_e$ (specifically $c_0/c_e = 1.4$) for case (iv) where $v_A/c_e = 0.75$ (Figure 4.8(iv)).The dashed horizontal lines correspond to $\omega = k_xc_T$ and the asymptotes to which the surface modes tend as $k_xH_e \to \infty$. These asymptotes correspond to the

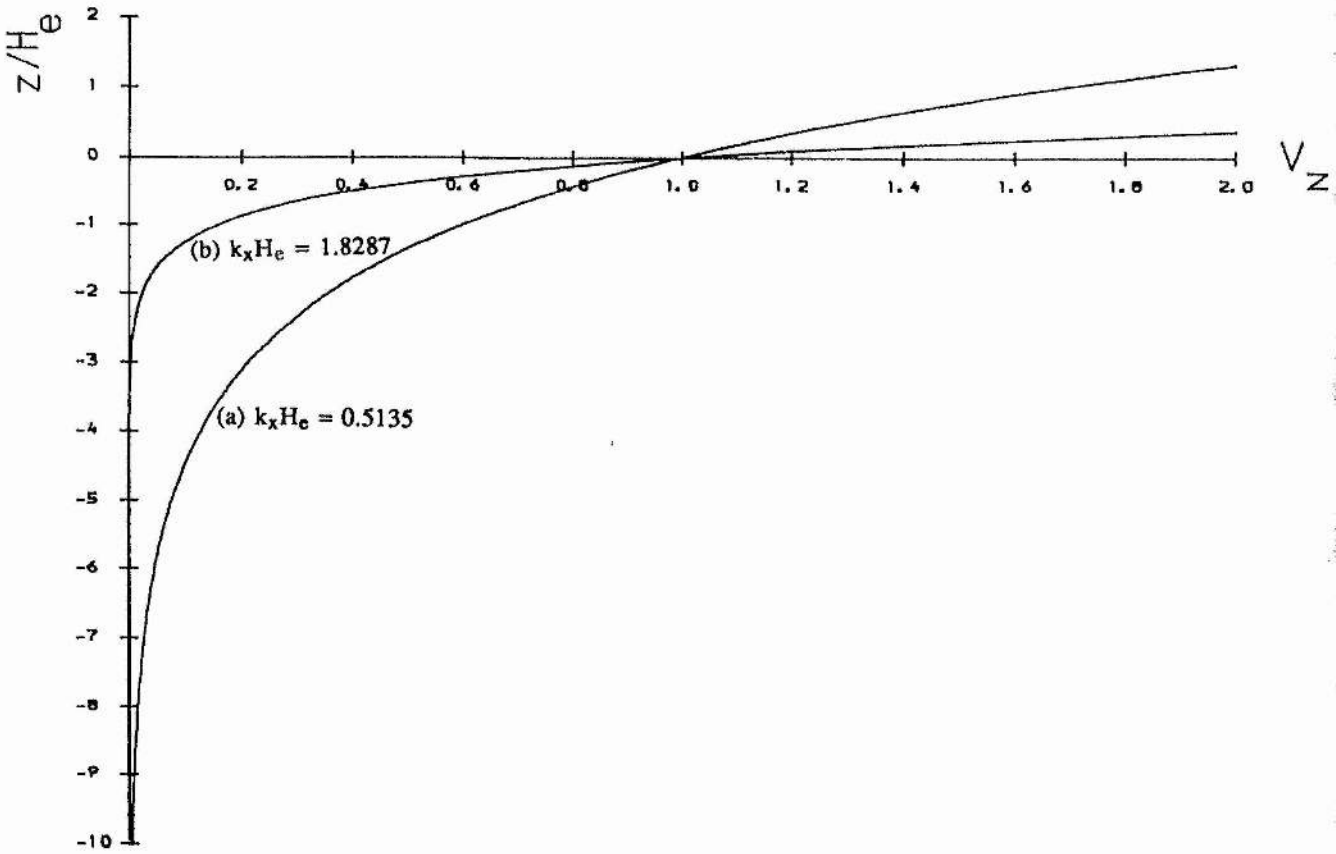

FIGURE 4.7(i) The eigenfunction $v_z(z)/v_z(0)$ for the f-mode with $c_0/c_e = 0.5$ (c.f. Figure 4.2(i)) and cases (a) $k_xH_e = 0.5135$ and (b) $k_xH_e = 1.8287$, chosen close to the limits of allowable wavenumber.

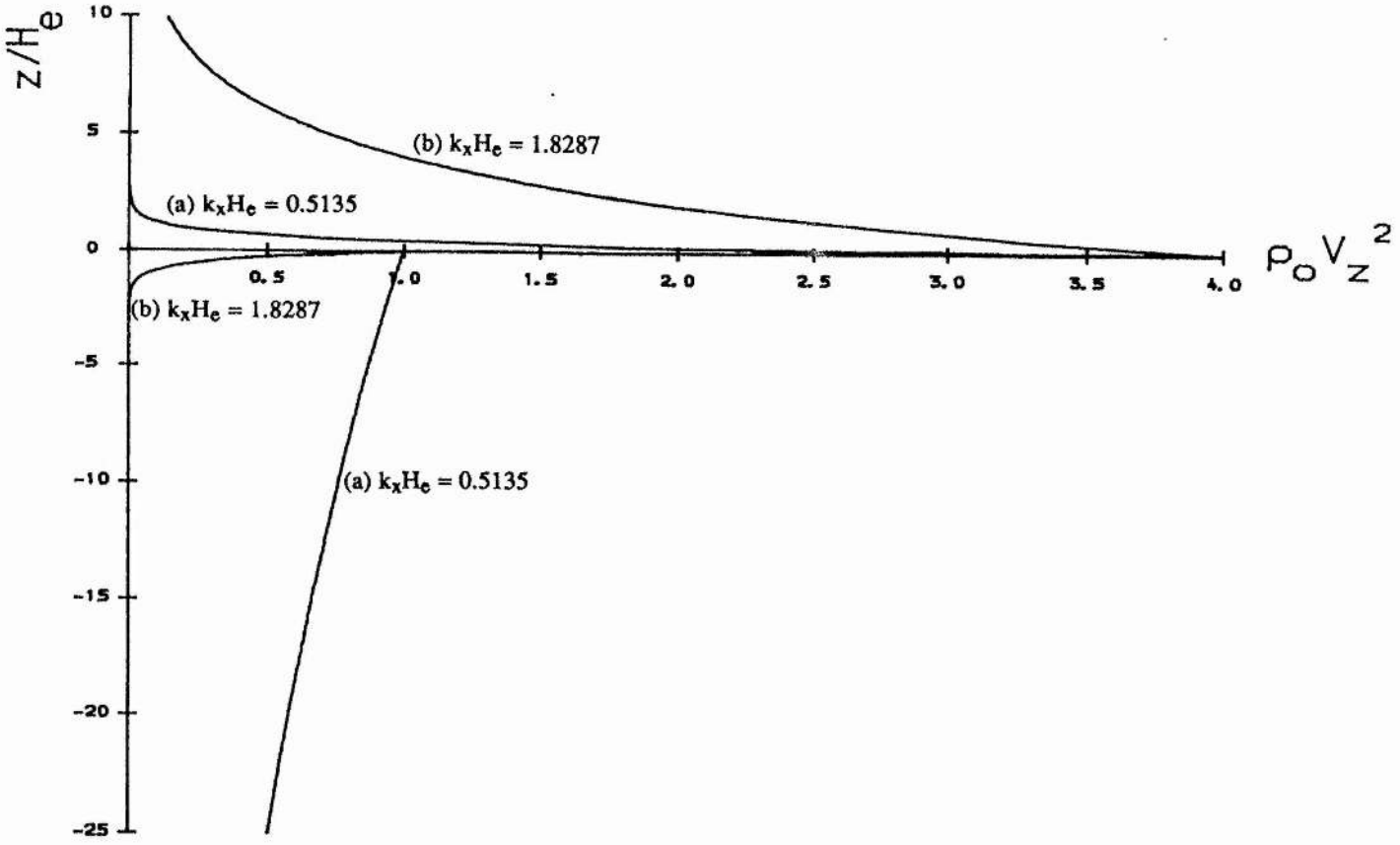

FIGURE 4.7(ii) The profile of kinetic energy density, $\frac{1}{2}\rho(z)v_z^2$, of the f-mode for the eigenfunctions in (i), with $c_0/c_e = 0.5$. (a) $k_xH_e = 0.5135$, (b) $k_xH_e = 1.8287$. The kinetic energy density is plotted in units of $\frac{1}{2}\rho_e v_z^2(0)$.

phase-speeds which the fast and slow magnetoacoustic surface modes possess in the zero-gravity case, as determined by the transcendental dispersion relation (4.37).

Recall that in the zero gravity case (discussed in detail in Chapter 3) that whereas the slow mode always occurs, the fast magnetoacoustic surface wave propagates only when *both* $v_A > c_0$ and $c_e > c_0$. This is evident here. For example, in Figures 4.8(i) & (ii), for which $v_A < c_0$, one mode only (the slow surface wave) propagates for large k_xH_e (which includes $g \to 0$). By contrast, in Figure 4.8(iii), where $v_A > c_0$ and $c_e > c_0$, both surface waves propagate in the zero gravity limit and therefore for large k_xH_e. We note also the absence of the fast surface mode as $k_xH_e \to \infty$ when $c_e < c_0$ (see Figure 4.8(iv)), which again is consistent with the zero gravity investigations.

The lower phase-speed curves in Figure 4.8 are readily identified as the slow magnetoacoustic-gravity surface wave, that is, the slow magnetoacoustic surface wave modified by the presence of gravity. Similarly, the upper phase-speed curve in Figure 4.8(iii) can be described as the fast magnetoacoustic-gravity mode. In Figure 4.8(i) & (ii), however, the upper phase-speed curve is more akin to the f-mode modified by the magnetic field. We see that as the magnetic field strength is increased (through the parameter v_A/c_e) and k_xH_e is increased, so *the f-mode develops into the fast magnetoacoustic-gravity surface mode.*

The upper mode in Figure 4.8(iv) is the magnetic equivalent to the surface gravity wave in Figure 4.3. In the non-magnetic case the surface gravity wave occurs only when $c_0 > c_e$ (i.e. $\rho_0 < \rho_e$) and so the f-mode is not a solution to the dispersion relation (4.53). The fast magnetoacoustic-gravity surface wave develops from the f-mode. Therefore in the magnetic case when $c_0 > c_e$, the fast magnetoacoustic-gravity surface wave is not a solution to the dispersion relation (4.33).

By comparing Figures 4.2(ii), 4.6 and 4.8(i),(ii) & (iii), we may see the development of the f-mode from the non-magnetic case ($\omega^2 = gk_x$) of Figure 4.2(ii), through the gradual increase of the magnetic field strength (Figure 4.6), to its eventual merger with the fast magnetoacoustic surface wave (as $k_xH_e \to \infty$) in Figure 4.8(iii).

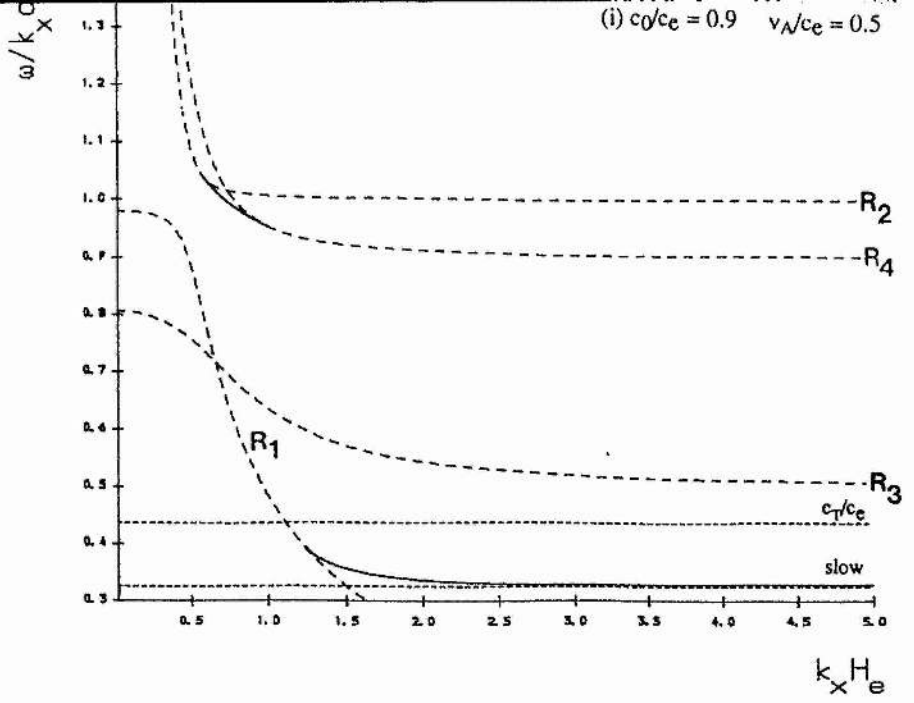

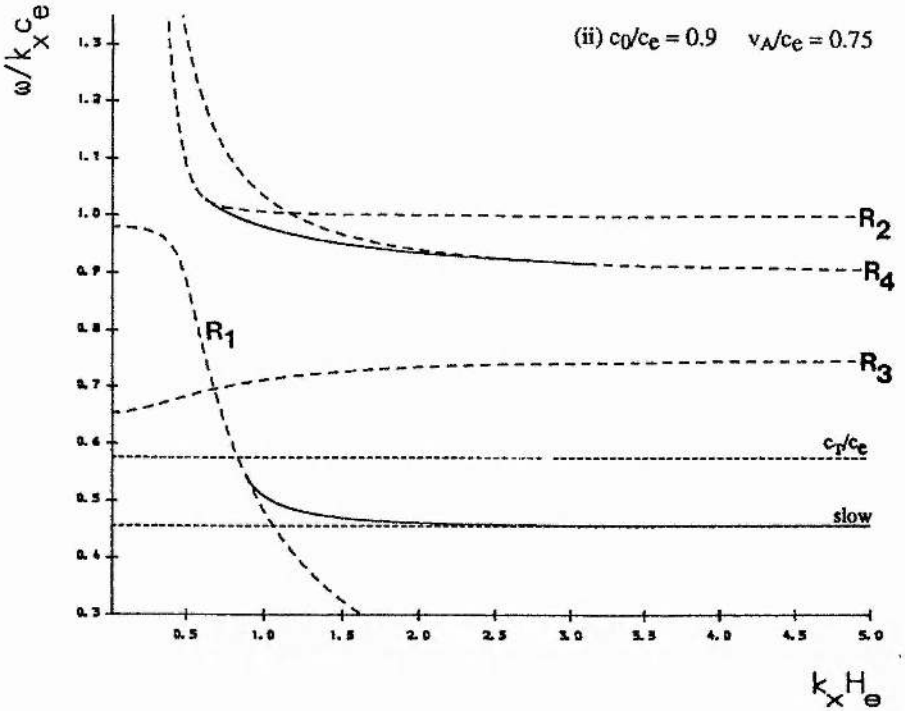

FIGURE 4.8(i) & (ii) The phase-speeds of magnetoacoustic-gravity surface modes at an isothermal magnetic interface with a constant Alfvén speed. Cases (i) $c_0/c_e = 0.9$, $v_A/c_e = 0.5$ and (ii) $c_0/c_e = 0.9$, $v_A/c_e = 0.75$. The horizontal dashed lines are $\omega = k_x c_T$ and the asymptotes to which the surface modes tend as $k_x H_e \to \infty$, as determined by the case g=0 (see Equation (4.37)). The dashed curves R_1, R_2, R_3 and R_4 are determined from the requirements that $4A_B H_B^2 < 1$ and $4A_e H_e^2 < 1$.

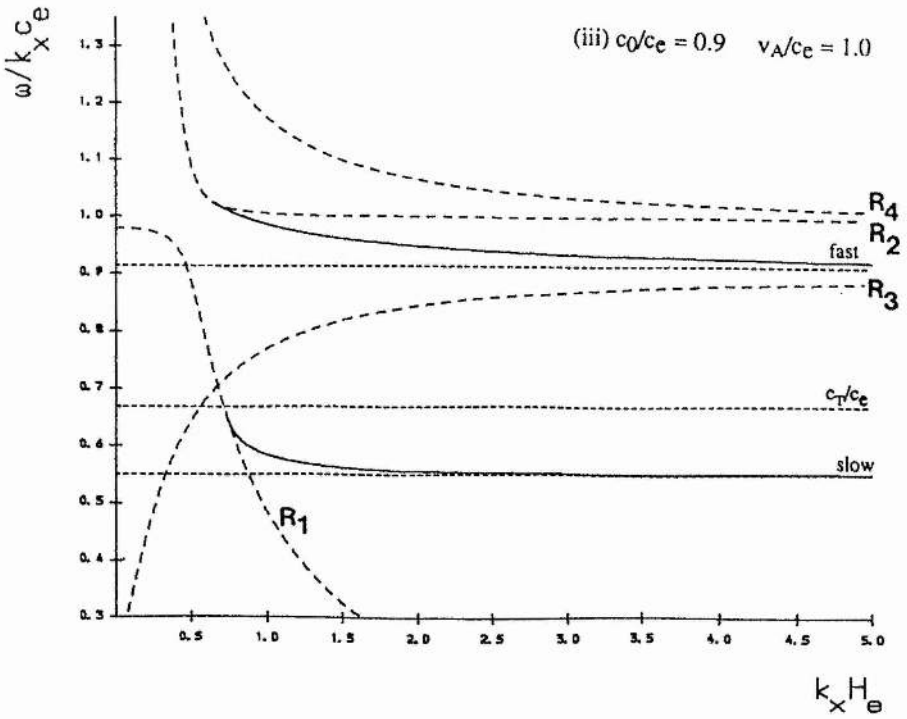

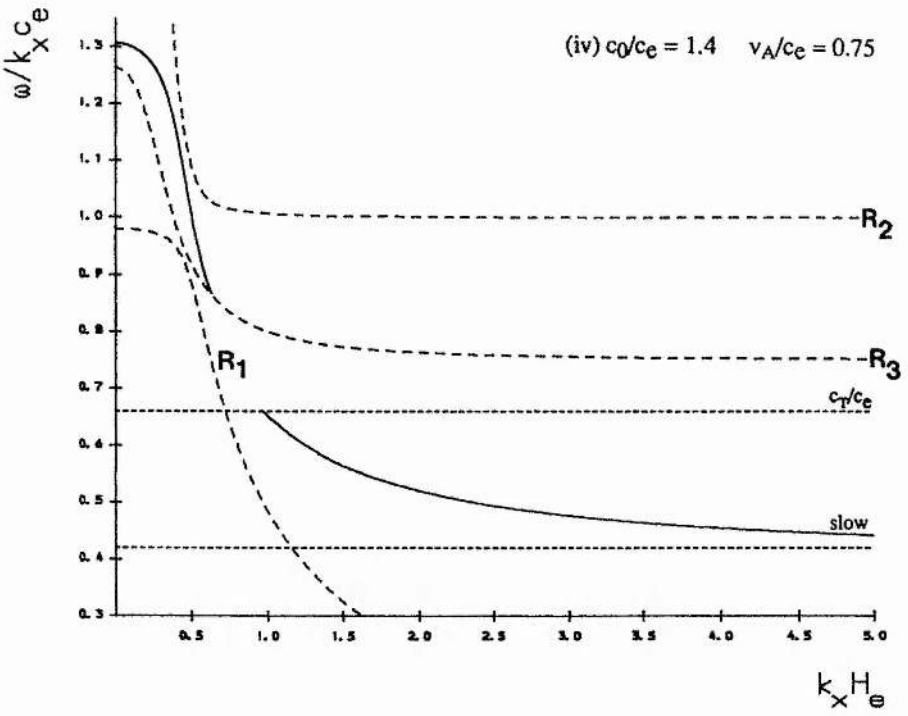

FIGURE 4.8(iii) & (iv) The phase-speeds of magnetoacoustic-gravity surface modes at an isothermal magnetic interface with a constant Alfvén speed. Cases (iii) $c_0/c_e = 0.9$, $v_A/c_e = 1.0$, and (iv) $c_0/c_e = 1.4$, $v_A/c_e = 0.75$. The horizontal dashed lines are $\omega = k_x c_T$ and the asymptotes to which the surface modes tend as $k_x H_e \rightarrow \infty$, as determined by the case g=0 (see Equation (4.37)).

It is of interest to see how the results we have obtained compare with the well-known dispersion relation for surface waves in an *incompressible* medium with uniform distribution of densities (see Equation (4.39)). Unfortunately, such a comparison is difficult to make directly from Figure 4.8. Accordingly, in Figure 4.9, we have re-presented our dispersion curves, normalised in units appropriate for such a comparison. Of particular interest is the slow surface wave. Figure 4.9 illustrates the phase-speed (in units of the Alfvén speed v_A) as a function of wavenumber k_x (in units of g/v_A^2) for increasing values of the sound speed c_0 within the field, holding fixed the sound speed c_e in the field-free region. Comparing the slow surface wave (shown as a solid curve in Figure 4.9) with its incompressible counterpart (determined by Equation (4.39) and shown in Figure 4.9 as a dot-dashed curve) we see a close similarity between the two, the two curves merging together as we approach the incompressible extreme of large c_0/v_A. We expect this result, since for fixed γ (= 5/3) as we increase the sound speed, the scale-height is also increased and so the density has a weaker exponential dependence, and ultimately tends to a constant (as is the case described by Equation (4.39)).

It can be seen from Equation (4.39) that the incompressible mode asymptotes to c_k/v_A as $k_x v_A^2/g \rightarrow \infty$. We note that as the value of c_0/v_A is increased the trend of the modes switches from monotonically increasing (Figures 4.9(i),(ii) & (iii)) to monotonically decreasing (Figure 4.9(iv)). This can most easily be explained by considering the incompressible Equation (4.39). Clearly, if $\rho_0 > \rho_e$ then the mode asymptotes to c_k/v_A as $k_x v_A^2/g \rightarrow \infty$ from below, whereas if $\rho_0 < \rho_e$ then the mode asymptotes from above. It should be noted that the restrictions of the cutoff curves R_1 and R_2 do not apply to the incompressible Equation (4.39); consequently the incompressible mode propagates beyond the cutoff curves in Figure 4.9.

It is also of interest to see how the results we have obtained here in the compressible case compare with those for surface waves in an incompressible medium with a non-uniform distribution of densities (see Section 2.4(ii) of Chapter 2). This comparison is best done from the two distinct regimes of $\rho_0 < \rho_e$ and $\rho_0 > \rho_e$. If $\rho_0 < \rho_e$

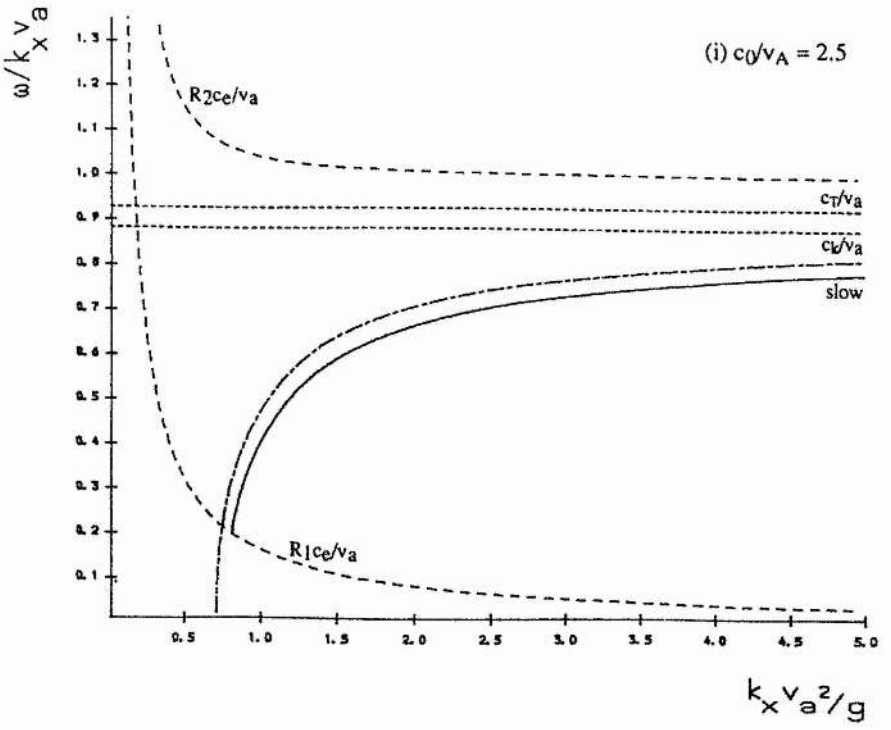

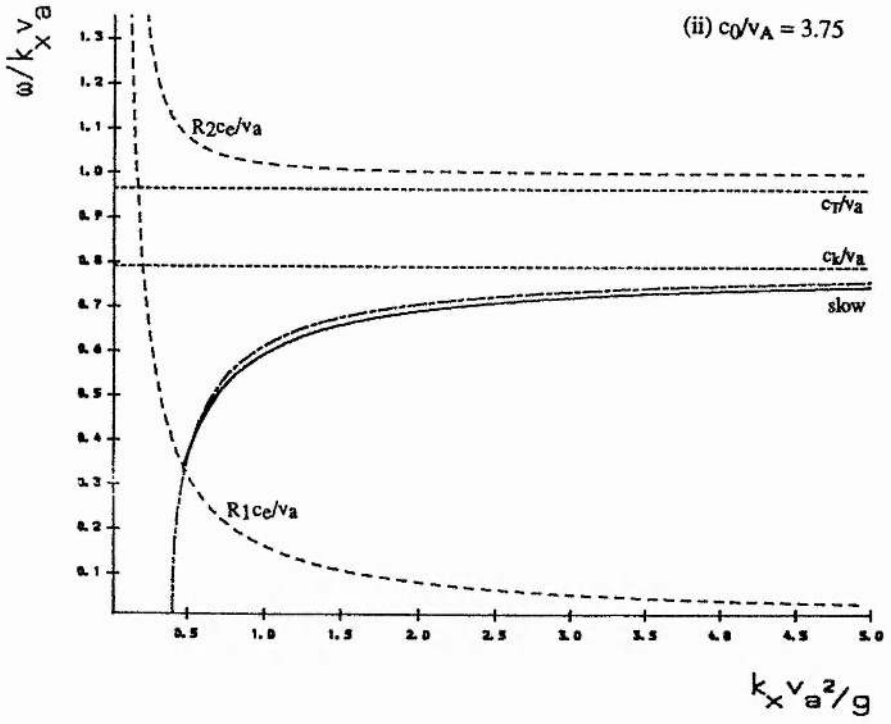

FIGURE 4.9(i) & (ii) The phase-speeds of magnetoacoustic-gravity surface modes normalised with respect to the Alfvén speed, with $c_e/v_A = 5.0$. Cases (i) $c_0/v_A = 2.5$ and (ii) $c_0/v_A = 3.75$. The solid curve is the slow surface mode, the dot-dashed one its incompressible counterpart (determined by Equation (4.39)). For the sake of clarity, the fast mode has been omitted.

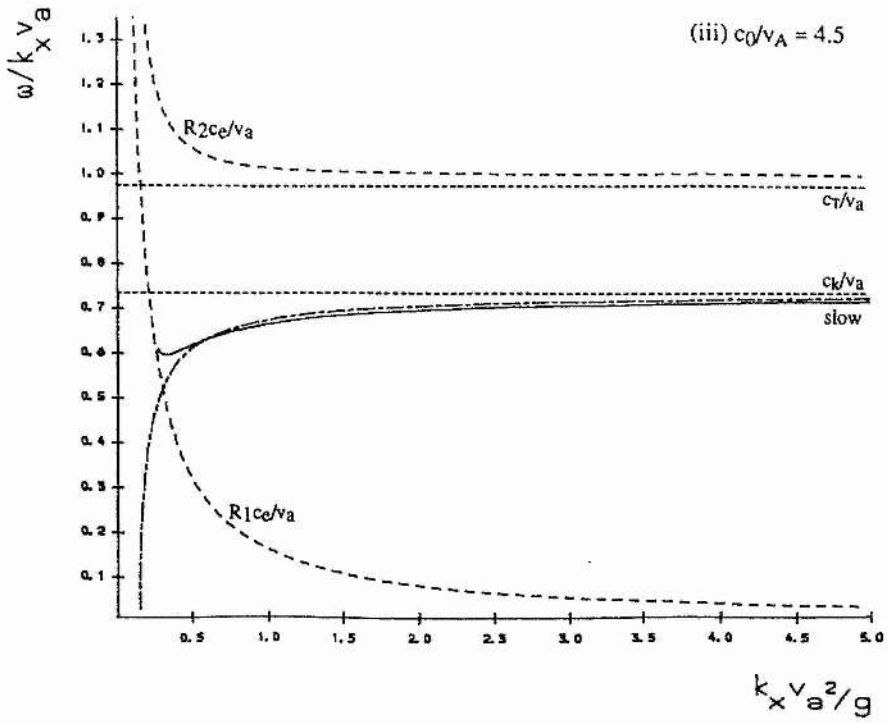

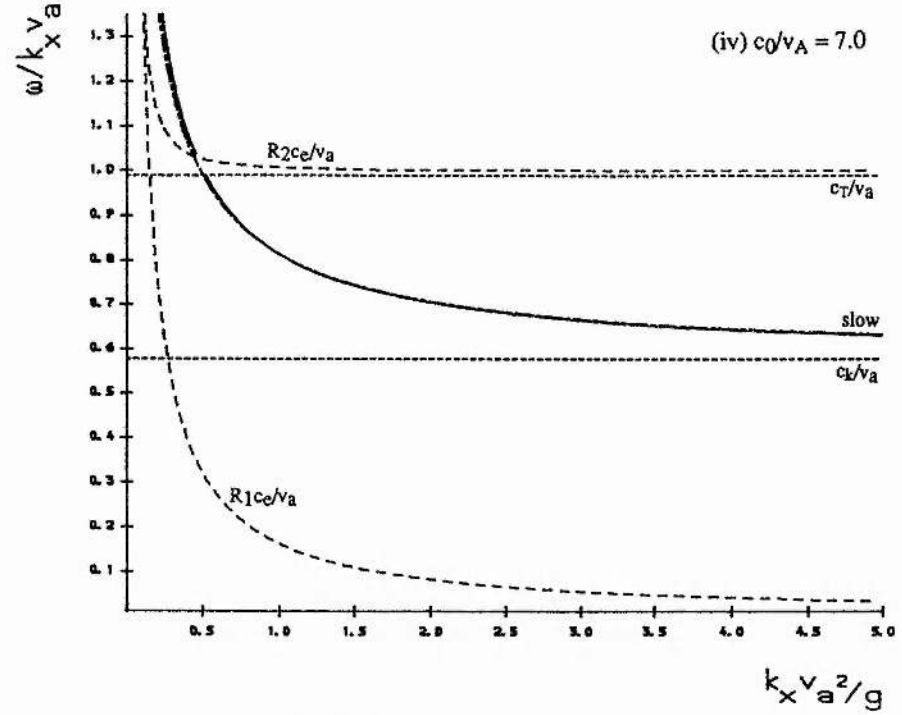

FIGURE 4.9(iii) & (iv) The phase-speeds of magnetoacoustic-gravity surface modes normalised with respect to the Alfvén speed, with $c_e/v_A = 5.0$. Cases (iii) $c_0/v_A = 4.5$ and (iv) $c_0/v_A = 7.0$. The solid curve is the slow surface mode, the dot-dashed one its incompressible counterpart (determined by Equation (4.39)). For the sake of clarity, the fast mode has been omitted.

and in the presence of a magnetic field, then in the compressible case we have only the slow magnetoacoustic-gravity surface wave which for the incompressible case is the hydromagnetic surface gravity mode (see Section 2.4.2 of Chapter 2). If $\rho_0 > \rho_e$ and in the presence of a magnetic field, then for the compressible case we have in addition to the slow mode that the fast magnetoacoustic-gravity surface wave may propagate if $v_A > c_0$; else if $v_A < c_0$, in addition to the slow mode the modified f-mode (modified by the presence of the magnetic field) propagates. When $v_A > c_0$ the fast magnetoacoustic-gravity surface mode that propagates has developed from the modified f-mode that propagates when $v_A < c_0$. Then in the incompressible case if $\rho_0 > \rho_e$ (see Section 2.4.3 of Chapter 2), the fast magnetoacoustic-gravity surface mode vanishes (its phase-speed is infinite) but the modified f-mode is still present in addition to the hydromagnetic surface gravity mode.

Finally, in Figure 4.10 we compare and contrast the eigenfunctions of the f-mode (in the presence of a magnetic field) with those of the fast and slow magnetoacoustic-gravity surface waves. The eigenfunction of the f-mode (modified by the presence of the magnetic field) at $k_xH_e = 1.0$ in Figure 4.8(iii) is shown together with the eigenfunctions of the fast and slow magnetoacoustic-gravity surface modes at $k_xH_e = 5.0$ (Figure 4.8(iii)). The curves are plotted for a fixed ratio of the sound speeds, namely $c_0/c_e = 0.9$, and field strength $v_A/c_e = 1.0$. We note that the f-mode (in the presence of a magnetic field) and the fast magnetoacoustic-gravity surface mode have similar profiles, demonstrating the connection which exists between them. By contrast, there is a marked difference between the eigenfunctions of the f-mode and the slow magnetoacoustic-gravity surface mode, the latter having a much more symmetric profile.

Observe that the f-mode (in the presence of a magnetic field) has a declining vertical velocity component (c.f. Figure 4.7(i)). This is the case only when both $v_A > c_0$ and $c_e > c_0$. If we were to superimpose the curve $A_B=0$, say - the curve equivalent to $A_0=0$ but with the inclusion of a magnetic field - on Figure 4.8(iii), then the upper mode (which "includes" the f-mode) is found to lie entirely within the region $A_B < 0$.

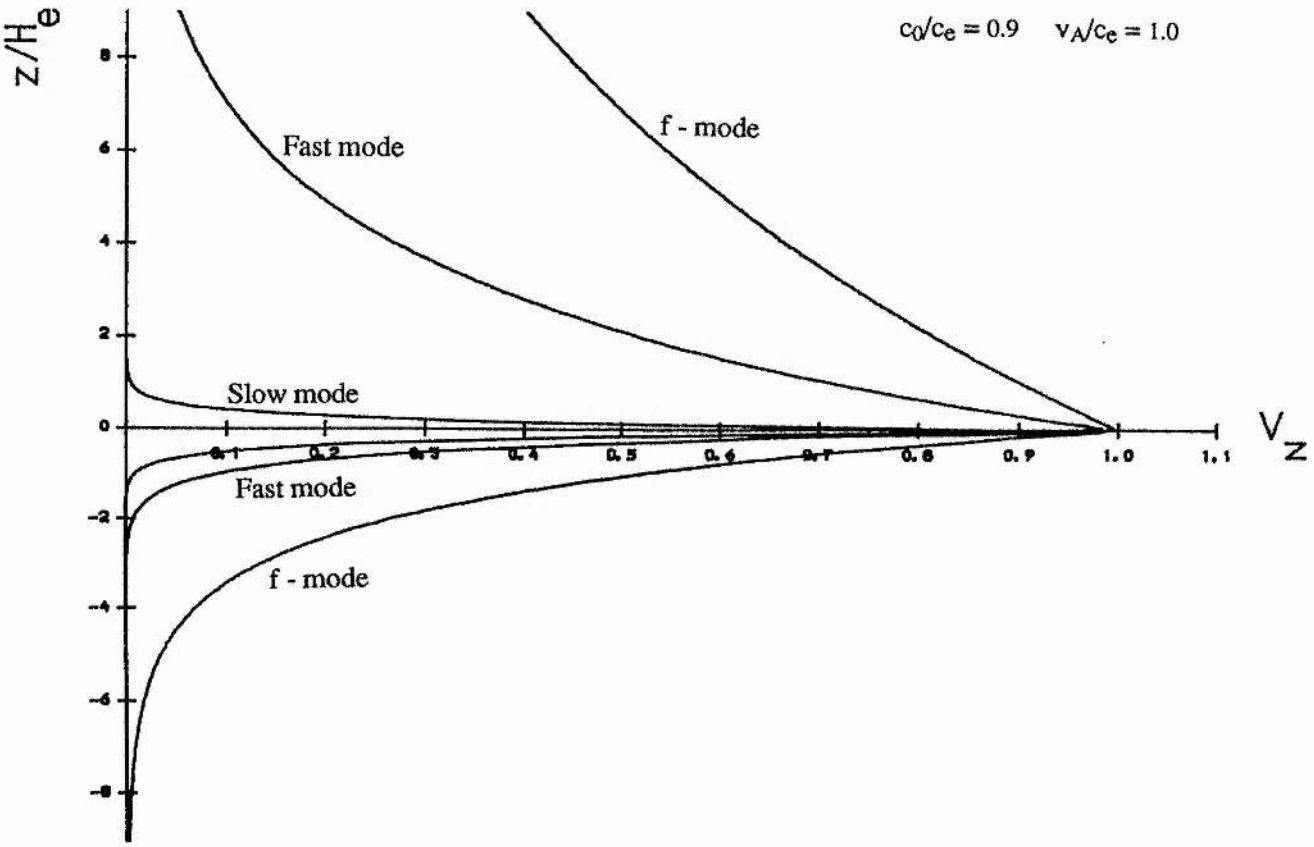

FIGURE 4.10 The eigenfunctions for the case $c_0/c_e = 0.9$ and $v_A/c_e = 1.0$ of the f-mode (modified by the magnetic field) with $k_xH_e = 1.0$ and the slow and fast magnetoacoustic-gravity surface modes with $k_xH_e = 5.0$ (c.f. Figure. 4.8(iii)). The eigenfunctions are plotted in units of $v_z(0)$.

However, if we were to superimpose the curve $A_B=0$ on Figures 4.8(i) & (ii) then the upper mode would lie in the region $A_B>0$ and therefore have a growing vertical velocity component. The fast magnetoacoustic-gravity surface wave will always lie in the region $A_B<0$ since it must satisfy the above conditions, namely that both $v_A > c_0$ and $c_e > c_0$. In fact, both the slow and fast magnetoacoustic-gravity surface waves always have a bounded vertical velocity component.

4.8 Summary

We have derived a dispersion relation describing the parallel propagation of magnetoacoustic-gravity surface modes and the f-mode at a single magnetic interface. In the absence of a magnetic field the transcendental dispersion relation may be written in polynomial form. There are two distinct modes, only one of which may propagate (depending on the ratio of the densities and therefore on the ratio of the sound speeds). If $\rho_0<\rho_e$, then the surface gravity mode exists. If $\rho_0>\rho_e$, then the f-mode may propagate but only for a restricted range of horizontal wavenumber, determined by the ratio of the sound speeds. As in the non-magnetic case, in the presence of a magnetic field the f-mode cannot propagate if the magnetic region is warmer than the field-free medium.

Asymptotic solutions to the dispersion relation have been derived for the f-mode in the case of low Alfvén velocity. The magnitude of the frequency shift increases monotonically with magnetic field strength. Numerical solutions of the dispersion relation indicate that the restriction on the f-mode decreases as the magnetic field strength is increased. The f-mode changes its character as the magnetic field strength is increased, and eventually develops into the fast magnetoacoustic-gravity surface wave.

It as been shown that the domain of evanescence for the kinetic energy density of a mode can be divided into two regions corresponding to whether a mode has a growing or decaying vertical velocity component. The vertical velocity component of the f-mode and the modified f-mode (modified by the presence of the magnetic field) are always exponentially growing in nature. However, the fast magnetoacoustic-gravity

surface wave (having developed from the f-mode) and the slow magnetoacoustic-gravity surface wave always have a decaying vertical velocity component. All the modes have decaying total (magnetic plus kinetic) energy.

Dispersion curves for the fast and slow magnetoacoustic-gravity surface waves show that both modes propagate with phase-speeds which decrease as the horizontal wavenumber is increased, gradually asymptoting to distinct limits as $k_x H_e \rightarrow \infty$, provided both $c_e > c_0$ and $v_A > c_0$. If either of these latter conditions is not met then the propagation of the fast magnetoacoustic-gravity surface mode is restricted in wavenumber and only the slow magnetoacoustic surface wave exists as $k_x H_e \rightarrow \infty$.

Chapter 5 : Magnetoacoustic-Gravity Surface Waves With a Uniform Magnetic Field

5.1 Introduction

In Chapter 4 we derived the analytical dispersion relation for magnetoacoustic-gravity surface waves for the case of an isothermal interface with a uniform Alfvén speed residing above a field-free region. In this chapter we once again consider such an interface but now with the upper region permeated by a uniform, horizontal magnetic field. The Alfvén speed is then no longer a constant but increases exponentially with height at a rate half that of the exponentially decreasing density.

Much as in the uniform Alfvén speed case of Chapter 4, when the field-free region is warmer than the upper magnetic atmosphere we find that the same three surface modes may propagate on the interface. These modes are the fast and slow magnetoacoustic-gravity surface modes and the f-mode modified by the presence of the uniform magnetic field. However, in contrast to Chapter 4 we also find harmonic modes, akin to the usual p-modes in helioseismology but here confined to the chromosphere. These modes again only occur when the field-free region is warmer than the magnetic medium. These are trapped modes resulting from the increasing Alfvén speed with height into the atmosphere.

Nye and Thomas (1976b) similarly found such trapped modes in their study of running penumbral waves, which they modelled as modes trapped by an increasing sound speed into the convection zone and by an increasing Alfvén speed into the penumbral atmosphere. We view the modes discussed by Nye and Thomas as p-modes influenced by the presence of a horizontal magnetic field (see also Evans and Roberts, 1990b). These modes are absent in the case of zero gravity whereas the surface modes considered here exist even in the absence of gravity, with no trapping (i.e. wave reflection or refraction) being required. The surface modes owe their existence solely to the presence of the discontinuity (or rapid variation) in the magnetic field.

5.2 The Dispersion Relation

Consider a single magnetic interface, situated at z=0, in an atmosphere stratified by gravity acting in the negative z-direction. We assume an equilibrium state in which the temperature and magnetic field are given by

$$T_0(z), B_0(z) = \begin{cases} T_0, & B_0, \quad z > 0, \\ T_e, & 0, \quad z < 0, \end{cases} \tag{5.1}$$

where T_0, B_0 and T_e are constants. See Figure 5.1. In contrast to the model discussed in Chapter 4, since the magnetic field is uniform in this case it provides no support against gravity. The equilibrium, therefore, is one of hydrostatic balance determined by

$$\frac{dp_0(z)}{dz} = -\rho_0(z)g, \tag{5.2}$$

and the ideal gas law,

$$p_0(z) = \frac{k_B}{m_{av}} \rho_0(z)T_0(z), \tag{5.3}$$

where $p_0(z)$ and $\rho_0(z)$ are the gas pressure and density, k_B Boltzmann's constant and m_{av} the mean particle mass of the plasma.

Pressure balance at the interface z = 0 means that the total (magnetic plus gas) pressure above the interface must equal the gas pressure in the field-free region below. This requirement of pressure balance, together with the ideal gas law, leads to a relationship between the densities on either side of the interface, namely

$$\frac{c_e^2}{c_0^2} \frac{\rho_e(0_-)}{\rho_0(0_+)} = 1 + \frac{1}{2}\frac{\gamma}{\beta}, \tag{5.4}$$

where $\beta = c_0^2/v_A^2$ is the squared ratio of the sound speed c_0 $(=(\gamma p_0/\rho_0)^{1/2})$ to the Alfvén speed $v_A = \dfrac{B_0}{(\mu_0\rho_0(0_+))^{1/2}}$ at the base of the magnetic atmosphere, and c_e $(=(\gamma p_e/\rho_e)^{1/2})$ is the sound speed in the field-free region.

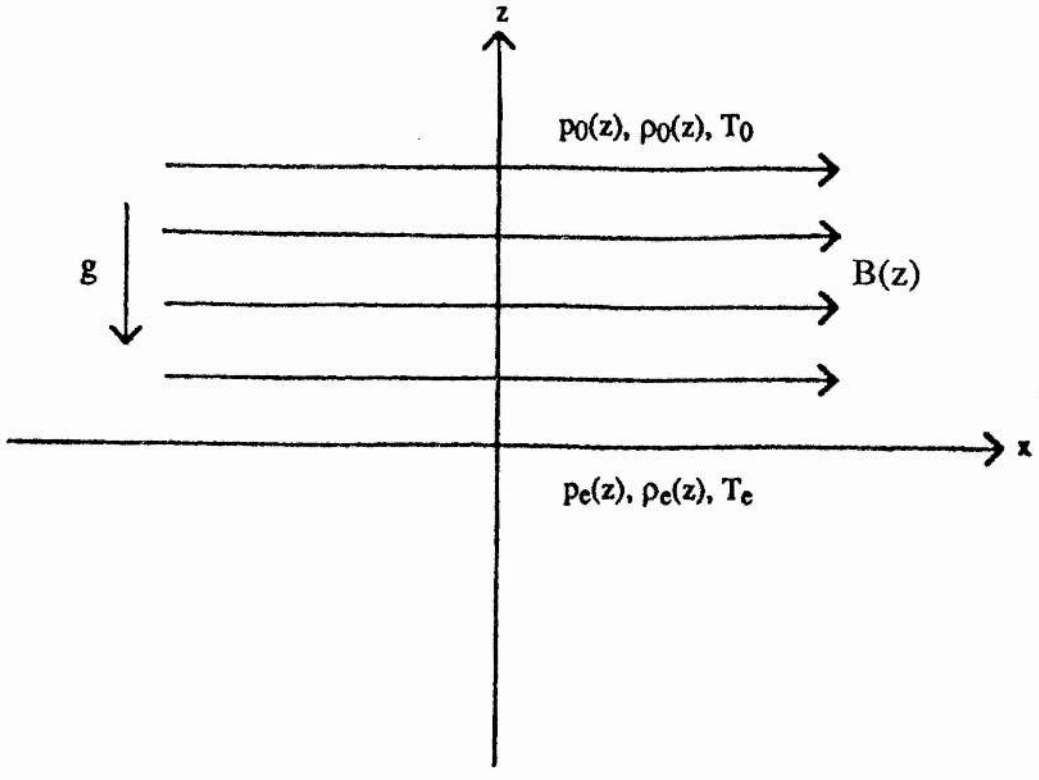

FIGURE 5.1 The equilibrium model of a single magnetic interface z = 0 in a stratified atmosphere with a uniform horizontal magnetic field in z > 0.

The density and Alfvén speed profiles are

$$\rho_0(z),\, v_A(z) = \begin{cases} \rho_0 e^{-z/H_0}, & v_A\, e^{z/2H_0}, \quad z > 0, \\ \rho_e\, e^{-z/H_e}, & 0, \qquad z < 0, \end{cases} \tag{5.5}$$

where H_0 ($= c_0^2/\gamma_g$) and H_e ($= c_e^2/\gamma_g$) are the isothermal scale-heights above ($z>0$) and below ($z<0$) the interface, respectively.

Two-dimensional, linear, isentropic perturbations of the form

$$\underline{v}(x,z,t) = (v_x(z),\, 0,\, v_z(z))e^{i(\omega t - k_x x)}, \tag{5.6}$$

for frequency ω and horizontal wavenumber k_x, satisfy the second-order ordinary differential equation (Adam, 1977; Small and Roberts, 1984; Roberts, 1985; c.f., Goedbloed, 1971)

$$\frac{d}{dz}\left\{\frac{\rho_0(z)(c_S^2(z) + v_A^2(z))(\omega^2 - k_x^2 c_T^2(z))}{(\omega^2 - k_x^2 c_S^2(z))}\,\frac{dv_z}{dz}\right\}$$

$$+\left\{\rho_0(z)(\omega^2 - k_x^2 v_A^2(z)) - \frac{g^2 k_x^2 \rho_0(z)}{(\omega^2 - k_x^2 c_S^2(z))} - g k_x^2 \frac{d}{dz}\left(\frac{\rho_0(z) c_S^2(z)}{\omega^2 - k_x^2 c_S^2(z)}\right)\right\} v_z = 0, \tag{5.7}$$

where $c_T^2 = c_S^2 v_A^2/(c_S^2 + v_A^2)$ is the square of the cusp speed.

For the profile (5.5) the governing ordinary differential Equation (5.7) for the magnetic field region (i.e. $z > 0$) reduces to (Nye and Thomas, 1976a; Evans and Roberts, 1990b)

$$\left\{c_0^2\omega^2 + (\omega^2 - k_x^2c_0^2)v_A^2e^{z/H_0}\right\}\frac{d^2v_z}{dz^2} - \frac{c_0^2\omega^2}{H_0}\frac{dv_z}{dz}$$

$$+ \left\{(\omega^2 - k_x^2c_0^2)(\omega^2 - k_x^2v_A^2e^{z/H_0}) - gk_x^2(g - c_0^2/H_0)\right\}v_z = 0, \qquad z > 0. \quad (5.8)$$

If a second order homogeneous linear differential equation has at most three regular singularities, assumed to be at 0,1 and ∞, then the equation can be reduced to the hypergeometric differential equation (Erdélyi, 1953). Thus the second order differential Equation (5.8) with non-constant coefficients may be cast in the form of a hypergeometric differential equation by transforming the dependent ($v_z(z)$) and independent (z) variables according to (Adam, 1975; Nye and Thomas, 1976a)

$$V_z = v_z\, e^{zK_0/H_0}, \quad X = X_0\, e^{-z/H_0}, \qquad (5.9)$$

where

$$X_0 = \frac{\beta\Omega_0^2}{(K_0^2 - \Omega_0^2)}. \qquad (5.10)$$

Here $\Omega_0 = H_0\omega/c_0$ and $K_0 = H_0k_x$ are the non-dimensional frequency and horizontal wavenumber, respectively.

Using the transformations (5.9), Equation (5.8) reduces to

$$\frac{X}{H_0}e^{-zK_0/H_0}\left\{X(1-X)\frac{d^2V_z}{dX^2} + [r - (p+q+1)X]\frac{dV_z}{dX} - pqV_z\right\} = 0, \quad z > 0, \qquad (5.11)$$

and so

$$X(1-X)\frac{d^2V_z}{dX^2} + [r - (p+q+1)X]\frac{dV_z}{dX} - pqV_z = 0; \qquad (5.12)$$

this is the hypergeometric differential equation (see, for example, Abramowitz and Stegun, 1965). The hypergeometric differential equation has three regular singularities at X = 0,1 and ∞. For the specific problem we are interested in here the parameters of the hypergeometric differential Equation (5.12) satisfy

$$p + q = r = 2K_0 + 1, \tag{5.13}$$

$$p,q = \frac{1}{2} + K_0 \pm \frac{1}{2}\left\{\left[1 - \left(\frac{\omega}{\omega_{a_0}}\right)^2\right] + 4K_0^2\left[1 - \left(\frac{\omega_{g_0}}{\omega}\right)^2\right]\right\}^{1/2}, \tag{5.14}$$

where $\omega_{a_0} = c_0/2H_0$ and $\omega_{g_0} = (\gamma\text{-}1)^{1/2}\, c_0/\gamma H_0$ are the acoustic and buoyancy (Brunt-Väisälä) frequencies for the isothermal, magnetic medium. These time scales are imposed in the atmosphere due to the presence of the gravitational field. We note that if ω lies in the range $\omega_{g_0} < \omega < \omega_{a_0}$, then the parameters p and q are purely real. However, in general p and q will be complex conjugates.

The non-trivial solution to Equation (5.11) is the general solution to the hypergeometric differential Equation (5.12), which in terms of the original variable $v_z(z)$ about $X = 0$ is given by (Abramowitz and Stegun, 1965)

$$v_z(z) = d_1 F(p,q; r; X)e^{-zK_0H_0} + d_2 X_0^{-2K_0} F(1\text{-}p,1\text{-}q; 2\text{-}r; X)e^{zK_0/H_0}, \quad z > 0, \tag{5.15}$$

where d_1 and d_2 are arbitrary constants and F is the hypergeometric function defined by the Gauss hypergeometric series (Abramowitz and Stegun, 1965)

$$F(p,q; r; X) = 1 + \frac{pq}{r}X + \frac{p(p+1)q(q+1)}{r(r+1)}\frac{X^2}{2!} + \ldots \tag{5.16}$$

which is absolutely convergent in $|X| < 1$. The parameters p, q and r may be complex and are independent of the variable X. The series is not defined when $r = -m$ ($m=0,1,2,3,\ldots$), provided p or q is a negative integer n with $n<m$. The Gauss series reduces to a polynomial of degree n in X when p or q is equal to -n ($n=0,1,2,3,\ldots$). For $X \leq -1$ the following linear transformation of (5.16) may be used (Abramowitz and Stegun, 1965)

$$F(p,q;\, r;\, X) = \frac{\Gamma(r)\Gamma(q-p)}{\Gamma(q)\Gamma(r-p)}(-X)^{-p}\, F(p,1-r+p;\, 1-q+p;\, \frac{1}{X})$$

$$+\frac{\Gamma(r)\Gamma(p-q)}{\Gamma(p)\Gamma(r-q)}(-X)^{-q}\, F(q,1-r+q;\, 1-p+q;\, \frac{1}{X}),\quad (|\arg(-X)| < \pi). \tag{5.17}$$

Alternatively, an integral representation may be used to analytically continue the F function into the region $X \leq -1$ (see Abramowitz and Stegun, 1965)

$$F(p,q;\, r;\, X) = \frac{\Gamma(r)}{\Gamma(q)\Gamma(r-q)}\int_0^1 t^{q-1}(1-t)^{r-q-1}(1-Xt)^{-p}dt, \qquad (\mathrm{Re}(r)>\mathrm{Re}(q)>0). \tag{5.18}$$

For $X \geq 1$ there is a logarithmic singularity at the regular singularity $X=1$ (Abramowitz and Stegun, 1965). The region $X \geq 1$ corresponds to

$$\frac{\beta\Omega_0^2}{(K_0^2 - \Omega_0^2)} \geq 1, \tag{5.19}$$

that is, to the region

$$c_T^2 \leq \frac{\omega^2}{k_x^2} \leq c_0^2, \tag{5.20}$$

for the horizontal phase-speed $\frac{\omega}{k_x}$. In this range the solution for v_z is singular and so resonance may occur making resistive and viscous effects important. Provided the phase-speed lies outside the range given by (5.20) the solution for v_z will be everywhere bounded. We note that the regular singularity at $X = \infty$ corresponds to $\omega^2/k_x^2 = c_0^2$ and is therefore included in the range (5.20).

For the lower half plane (i.e. $z < 0$), where there is no magnetic field, the governing ordinary differential Equation (5.7) reduces (as in Chapter 4) to one with constant coefficients :

$$\frac{d^2v_z}{dz^2} - \frac{1}{H_e}\frac{dv_z}{dz} + A_e v_z = 0, \qquad z<0, \tag{5.21}$$

where A_e is given by (see Equation (4.26) of Chapter 4)

$$A_e = \frac{(\gamma - 1)g^2k_x^2 + \omega^2(\omega^2 - k_x^2c_e^2)}{\omega^2c_e^2} = k_x^2\left(\frac{\omega_{ge}}{\omega}\right)^2 - m_e^2, \qquad (5.22)$$

where

$$m_e^2 = \frac{k_x^2c_e^2 - \omega^2}{c_e^2}; \qquad (5.23)$$

$\omega_{ge} = (\gamma\text{-}1)^{1/2}c_e/\gamma H_e$ is the buoyancy frequency in the lower, isothermal, non-magnetic region.

Equation (5.21) possesses the general solution (see Equation (4.27) of Chapter 4)

$$v_z(z) = \left(d_3\exp\frac{z(1 - 4A_eH_e^2)^{1/2}}{2H_e} + d_4\exp\frac{-z(1 - 4A_eH_e^2)^{1/2}}{2H_e}\right)\exp(\frac{z}{2H_e}), \quad z < 0, \qquad (5.24)$$

where d_3 and d_4 are arbitrary constants.

We impose the condition that the total (kinetic plus magnetic) energy density remains finite as $|z| \to \infty$, and restrict attention to the circumstances of $(1\text{-}4A_eH_e^2) < 0$. These two conditions, imply that $d_2 = d_4 = 0$. We note that the condition that the total energy density remains finite as $|z| \to \infty$ (i.e. $X \to 0$) has the effect of removing the singularity in the solution (5.15). Thus, the vertical velocity component $v_z(z)$ in the two regions is given by

$$v_z(z) = \begin{cases} d_1F(p,q; r; X)e^{-zK_0/H_0}, & z > 0, \\ d_3\exp\left(\frac{1}{2H_e} + M_e\right)z, & z < 0, \end{cases} \qquad (5.25)$$

where

$$M_e = \frac{(1 - 4A_eH_e^2)^{1/2}}{2H_e}. \qquad (5.26)$$

We note that $M_e > 0$, since we take the positive square root of $(1 - 4A_eH_e^2)^{1/2}$. We note also that the solution in the field-free region (i.e. $z < 0$) is exactly as that in Chapter 4. It may be shown from Equation (5.25) that $v_z \to 0$ as $|z| \to \infty$ (see also Evans and Roberts, 1990b).

Matching the normal component of velocity across the interface gives

$$d_1F(p,q; r; X_0) = d_3, \tag{5.27}$$

while integrating Equation (5.7) about the interface $z = 0$ yields the second matching condition (see also Chapter 4), namely that

$$\frac{\rho_0(z)(c_s^2(z) + v_A^2(z))(\omega^2 - k_x^2c_T^2(z))}{(k_x^2c_s^2(z) - \omega^2)}\frac{dv_z}{dz} - \frac{k_x^2g\rho_0(z)c_s^2(z)}{(k_x^2c_s^2(z) - \omega^2)}v_z(z) \tag{5.28}$$

is continuous across $z = 0$. This quantity is in fact $i\omega p_T(z) - g\rho_0(z)v_z(z)$, where

$$p_T(z) = -\frac{i\rho_0(z)}{\omega}\frac{(c_s^2(z) + v_A^2(z))(\omega^2 - k_x^2c_T^2(z))}{(k_x^2c_s^2(z) - \omega^2)}v_z(z) + \frac{i\omega\rho_0(z)g}{(k_x^2c_s^2(z) - \omega^2)}v_z(z) \tag{5.29}$$

is the perturbation in total (gas plus magnetic) pressure.

Applying the two matching conditions to the solution (5.25) determines the transcendental dispersion relation (see also Small and Roberts, 1984):

$$\frac{\rho_0(c_0^2 + v_A^2)(\omega^2 - k_x^2c_T^2)}{(k_x^2c_0^2 - \omega^2)}\left\{k_x + \frac{pq}{r}\frac{X_0}{H_0}\frac{F(p+1,q+1; r+1; X_0)}{F(p,q; r; X_0)}\right\}$$

$$+\frac{k_x^2g\rho_0c_0^2}{(k_x^2c_0^2 - \omega^2)} = \frac{\rho_e c_e^2}{(k_x^2c_e^2 - \omega^2)}\left\{k_x^2g - (\frac{1}{2H_e} + M_e)\omega^2\right\}. \tag{5.30}$$

The dispersion relation (5.30) describes the parallel propagation of surface waves at a single magnetic interface in a gravitationally stratified atmosphere under the assumption of a uniform magnetic field and isothermal upper and lower atmospheres. As in Chapter 4, for the dispersion relation given there, it may be noted that the Lamb modes $\omega = k_x c_0$ and $\omega = k_x c_e$ (Lamb,1932) do not satisfy the dispersion relation (5.30).

We note briefly two special cases of Equation (5.30). In the limit as $g \to 0$, $A_e \to -m_e^2$ and then Equation (5.30) reduces after much algebra (see Appendix A.5) to

$$\rho_0(k_x^2 v_A^2 - \omega^2)m_e - \omega^2 \rho_e m_0 = 0, \tag{5.31}$$

where $m_0, m_e > 0$ and

$$m_0^2 = \frac{(k_x^2 c_0^2 - \omega^2)(k_x^2 v_A^2 - \omega^2)}{(c_0^2 + v_A^2)(k_x^2 c_T^2 - \omega^2)}. \tag{5.32}$$

Thus, we recover the dispersion relation describing the parallel propagation of surface waves on a magnetic interface one side of which is field-free. This was derived earlier in Chapter 3.

Also of interest is the *incompressible* limit ($c_0, c_e \to \infty$). Consider the special case of a fluid having a uniform density distribution so that $\rho_0(z) = \rho_0$ and $\rho_e(z) = \rho_e$. Then, in the incompressible limit m_e and $M_e \to k_x$, while the quantities $F(p+1,q+1; r+1; X_0)$, $F(p,q; r; X_0)$ and X_0 remain finite. However, $pq/rH_0 \to 0$ and so Equation (5.30) reduces (see Section 4.3.2 of Chapter 4)

$$\frac{\omega^2}{k_x^2} = c_k^2 - \frac{g}{k_x}\frac{(\rho_0 - \rho_e)}{(\rho_0 + \rho_e)}, \tag{5.33}$$

where

$$c_k^2 = \frac{\rho_0}{(\rho_0 + \rho_e)} v_A^2. \tag{5.34}$$

Thus, we recover the familiar dispersion relation of a uniform incompressible fluid.

5.3 Cutoff Curves

The transcendental dispersion relation (5.30) is solved subject to the constraints that $\omega \neq k_x c_0$, $\omega \neq k_x c_e$ and that $(1 - 4A_e H_e^2) > 0$. Much as in Chapter 4, this latter constraint gives rise to non-horizontal dashed curves, labelled R_1 and R_2 in Figure 5.2. We note that the confining curves R_3 and R_4 of Chapter 4 no longer occur since they result from the condition that $(1 - 4A_B H_B^2) > 0$, which does not apply here. The curves R_1 and R_2 denote cutoff curves for the propagation of the modes; beyond these curves, i.e. for $(1 - 4A_e H_e^2) < 0$, complex solutions may arise and correspond to internal modes. In this respect the plots in Figure 5.2 can be compared with the standard diagnostic diagram for acoustic-gravity waves in an isothermal atmosphere, dividing the ω-k_x plane into regions of evanescence and propagation (see, for example, Roberts, 1985). The plots in Figure 5.2 are the equivalent diagrams when a magnetic field is included. The area above the upper dashed curve R_2 corresponds to a region where magnetoacoustic waves may propagate, whilst that below the lower dashed curve R_1 is a region in which magnetogravity waves may exist. The area bounded by the two curves is one in which magnetoacoustic surface waves (i.e. evanescent modes) are permitted to propagate.

The form of these constraints depends upon whether $\omega > k_x c_T$ or $\omega < k_x c_T$. Thus, if $\omega > k_x c_T$ then the non-dimensional longitudinal phase-speed $\omega/k_x c_e$ must satisfy

$$\max\left(\frac{c_T}{c_e},\, R_1\right) \leq \frac{\omega}{k_x c_e} \leq R_2, \tag{5.35}$$

when a solution exists. If $\omega < k_x c_T$, then the constraint becomes

$$R_1 \leq \frac{\omega}{k_x c_e} \leq \min\left(\frac{c_T}{c_e},\, R_2\right). \tag{5.36}$$

Here R_1^2 and R_2^2 are given by

$$R_{1,2}^2 = \frac{\left(1+4k_x^2H_e^2\right) \mp \left\{(1+4k_x^2H_e^2)^2 - 64k_x^2H_e^{\frac{2(\gamma-1)}{\gamma^2}}\right\}^{1/2}}{8k_x^2H_e^2}, \qquad (5.37)$$

as given previously in Equation (4.43) of Chapter 4.

In the limit as $k_xH_e \to \infty$, which includes the case $g \to 0$, we obtain

$$R_1 \to 0, \quad R_2 \to 1. \qquad (5.38)$$

In the limit $k_xH_e \to 0$:

$$R_1 \to \frac{2(\gamma-1)^{1/2}}{\gamma}, \quad R_2 \to \infty. \qquad (5.39)$$

For $\gamma = 5/3$, $R_1 \to 0.98$ as $k_xH_e \to 0$.

5.4 Numerical Method

The dispersion relation (5.30) is solved numerically, regarding it as a function of frequency ω for given values of the horizontal wavenumber k_x. The approach taken involved determining an interval for k_x in which the dispersion relation contains a root (i.e. ω), and then using an numerical technique to converge to the root.

The main difficulty in the numerical solution is the evaluation of the hypergeometric function F. For $|X| < 1$, the F function is evaluated by using Gauss's series (5.16). The series converges rapidly for $|X| < 1$. The stopping criterion was decided upon by summing the next ten terms of the series and comparing with a required tolerance. If the sum was less than the required tolerance the summation was stopped. Typically, about ten to twenty terms were required for a tolerance of 10^{-6}.

For $X \leq -1$, the F function can be evaluated from the integral representation (5.18). We could have also employed the analytical continuation of the series given by Equation (5.17). However, since the parameters p and q for this problem can be

complex conjugates this would have meant writing a routine to solve the gamma function with complex argument. Accordingly, it was decided to evaluate the F function directly from the hypergeometric differential Equation (5.12), rather than write extra routines for the complex gamma functions. The ordinary differential equation was solved using a fourth order, variable step, Runge-Kutta-Mersion scheme.

Having determined the bracketed roots the Van Wijngaarden-Dekker-Brent Method (more commonly referred to as Brent's Method) was used to obtain convergence to the roots (see "Numerical Recipes: The Art of Scientific Computing" by Press *et al.*, 1987). This method was developed in the 1960s at the Mathematical Centre in Amsterdam. Brent's Method combines root bracketing, bisection and inverse quadratic interpolation to converge from the neighbourhood of a zero crossing. The method is guaranteed to converge, so long as the function can be evaluated within the initial interval known to contain a root.

5.5 Magnetoacoustic-gravity Surface Waves

Consider now the behaviour of the modes determined through a numerical investigation of the dispersion relation (5.30). We set $\gamma = 5/3$ throughout. The variation of the longitudinal phase-speed (non-dimensionalised with respect to the sound speed in the field-free region),$\omega/k_x c_e$, with the non-dimensional horizontal wavenumber $k_x H_e$ is shown in Figure 5.2. In Figures 5.2(i) & (ii), where $c_e > c_0$ and $v_A > c_0$, the upper horizontal dashed line corresponds to $\omega = k_x c_0$. The lower horizontal dashed line is the asymptote to which the slow magnetoacoustic-gravity surface mode tends as $k_x H_e \rightarrow \infty$, and is determined by Equation (5.31) (see also Chapter 3). The other horizontal dashed line in Figures 5.2(i) & (ii) is the line $\omega = k_x c_T$. We note that although the higher harmonic modes in Figures 5.2(i) & (ii) asymptote to $\omega/k_x c_e = c_0/c_e = 0.9$ as $k_x H_e \rightarrow \infty$, the solution $\omega = k_x c_0$ is not itself permitted (as stated previously); thus in Figures 5.2(i) & (ii) as $k_x H_e \rightarrow \infty$ *only* the slow mode exists. This result is as expected from the zero-gravity case (Chapter 3) for which the fast and slow magnetoacoustic surface modes both propagate only when $c_e > c_0$ and $v_A > c_0$.Thus, in

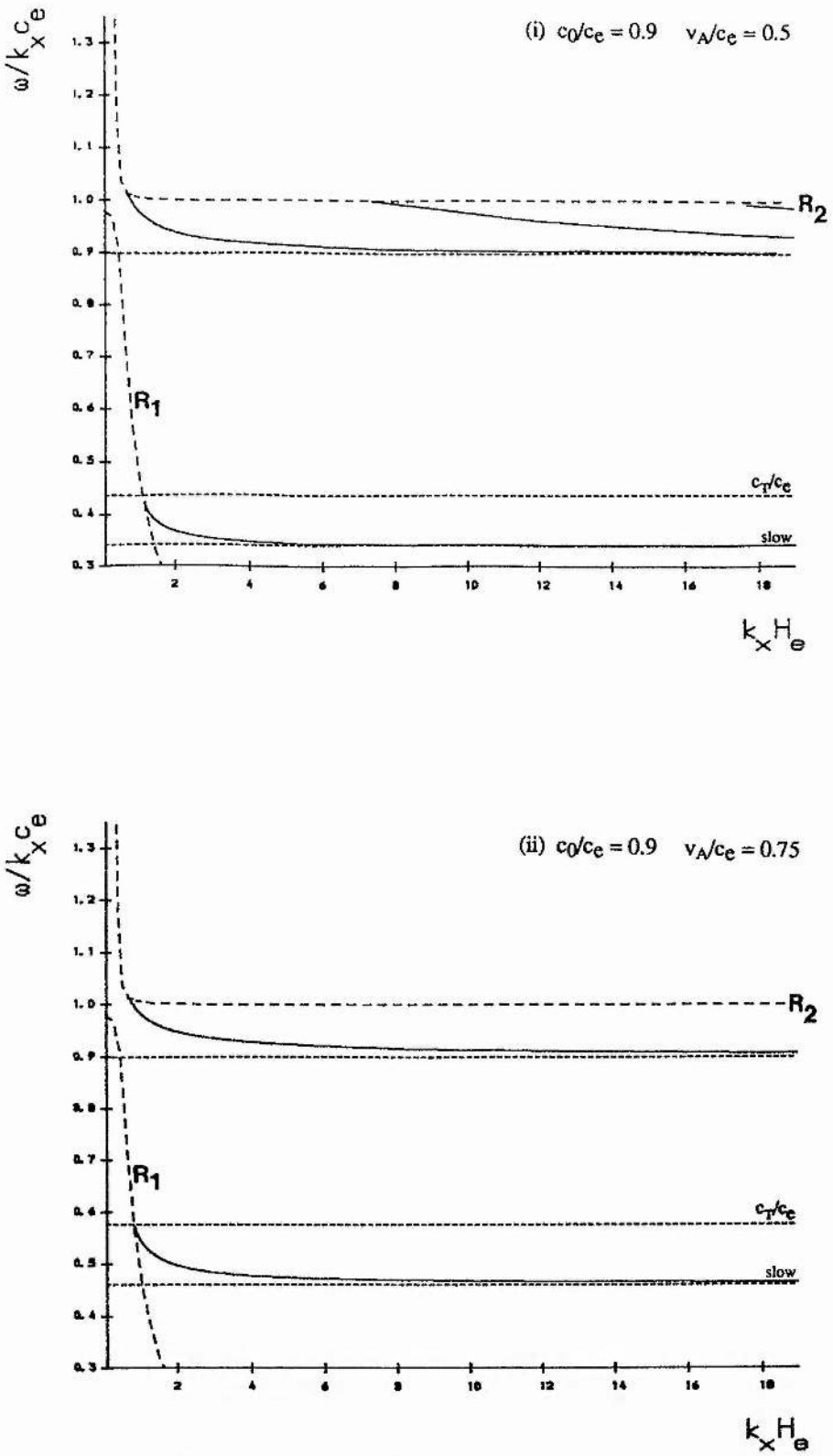

FIGURE 5.2(i) & (ii) The variation of the non-dimensional longitudinal phase-speed for magnetoacoustic-gravity modes with the non-dimensional horizontal wavenumber for the cases (i) $c_0/c_e = 0.9$, $v_A/c_e = 0.5$ and (ii) $c_0/c_e = 0.9$,$v_A/c_e = 0.75$. The dashed curves R_1 and R_2 are cutoff curves for the propagation of the modes determined by the assumption that $4A_eH_e^2 < 1$ (see text).

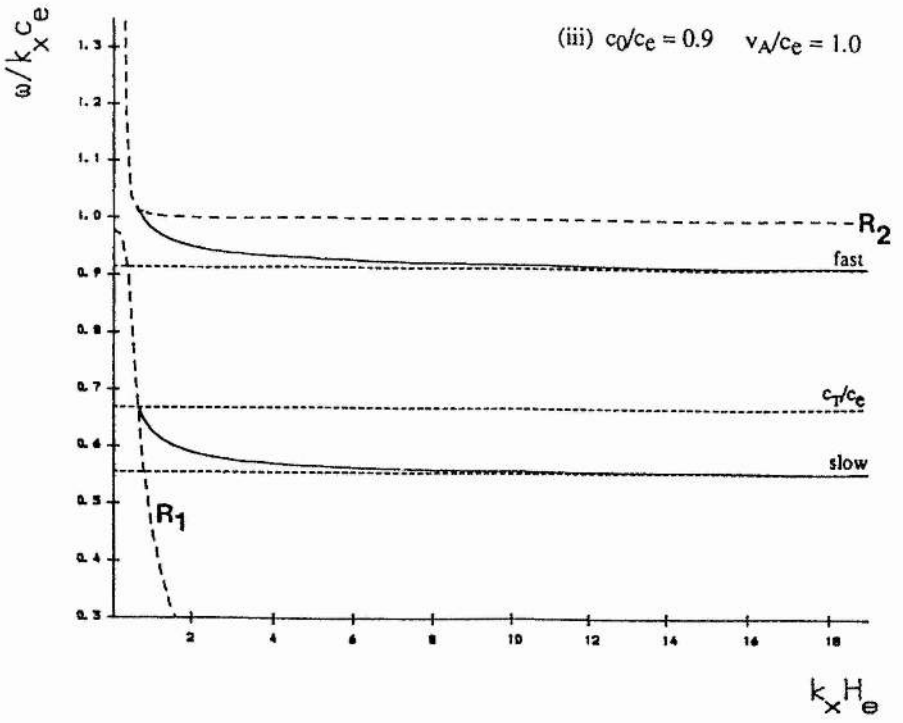

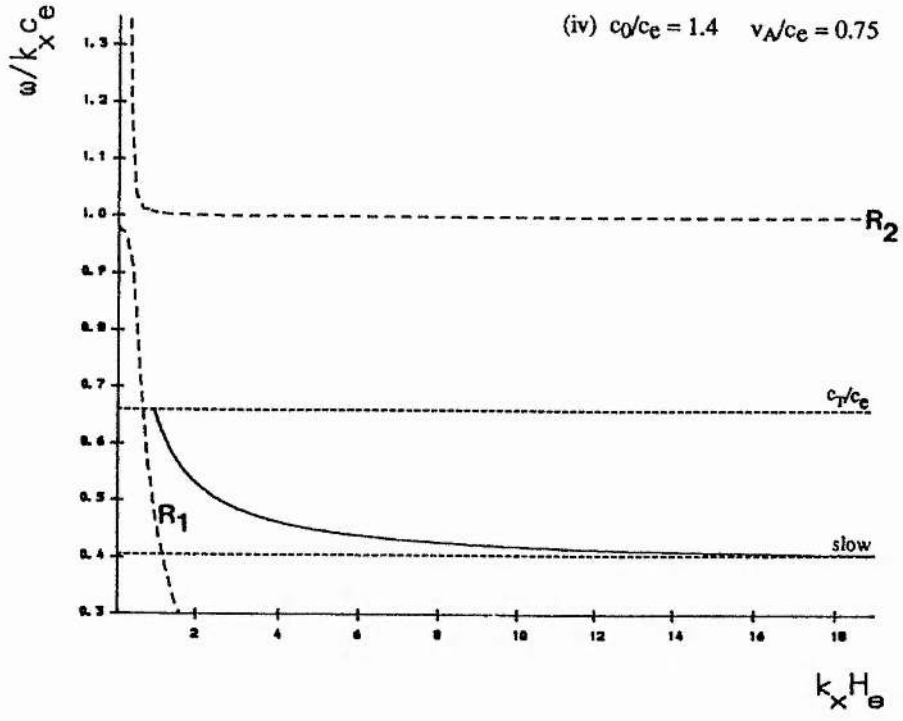

FIGURE 5.2(iii) & (iv) The variation of the non-dimensional longitudinal phase-speed for magnetoacoustic-gravity modes with the non-dimensional horizontal wavenumber for the cases (iii) $c_0/c_e = 0.9$, $v_A/c_e = 1.0$, and (iv) $c_0/c_e = 1.4$, $v_A/c_e = 0.75$. The dashed curves R_1 and R_2 are cutoff curves for the propagation of the modes determined by the assumption that $4A_eH_e^2 < 1$ (see text).

Figure 5.2(iii), where these conditions are met, we see that as $k_x H_e \rightarrow \infty$ both the slow and fast magnetoacoustic surface modes propagate. The upper horizontal dashed line in this case (Figure 5.2(iii)) is the limit to which the fast magnetoacoustic-gravity surface mode asymptotes as $k_x H_e \rightarrow \infty$. Finally, in Figure 5.2(iv), where $c_e < c_0$ and $v_A < c_0$, we find (as expected from the zero gravity analysis of Chapter 3) that only the slow magnetoacoustic surface mode propagates as $k_x H_e \rightarrow \infty$. We note that none of the modes lie in the region defined by Equation (5.20), where the solution for v_z is singular.

It is evident from Figures 5.2(i) & (ii) that the harmonic modes are confined to the region defined by

$$\frac{c_0}{c_e} \leq \frac{\omega}{k_x c_e} \leq R_2. \tag{5.40}$$

We note that as the value of v_A/c_e is increased, the second and subsequent harmonics originate at higher values of the non-dimensional wavenumber $k_x H_e$. Thus, for example, in Figure 5.2(ii) only the first harmonic is seen for the range of $k_x H_e$ shown. We observe also the absence of the harmonic modes in Figure 5.2(iv), where $c_0/c_e > 1$, i.e. $c_0/c_e > R_2$ as $k_x H_e \rightarrow \infty$, and so the inequality Equation (5.40) is violated. We identify the first of these harmonic modes as the f-mode modified by the presence of a uniform horizontal magnetic field. In Chapter 4 we discovered that as the magnetic field strength is increased the f-mode develops into the fast magnetoacoustic-gravity surface mode, eventually becoming the fast magnetoacoustic surface mode as the effect of the gravitational field diminishes. Similarly, in this study, we find that as the magnetic field strength is increased, from $v_A/c_e = 0.5$ in Figure 5.2(i) to $v_A/c_e = 1.0$ in Figure 5.2(iii), the first harmonic mode in Figure 5.2(i) develops into the upper mode in Figure 5.2(iii). That is, the modified f-mode (modified by the presence of the magnetic field) in Figure 5.2(i) changes in character as v_A/c_e is increased, becoming the fast magnetoacoustic-gravity surface wave in Figure 5.2(iii).

The eigenfunctions of the first two harmonics in Figure 5.2(i) are given in Figure 5.3. The eigenfunctions are plotted against a non-dimensional height, z/H_e.

Figure 5.3(i) shows the eigenfunction for the first or fundamental harmonic in Figure 5.2(i) (at $k_xH_e = 2.0$). We note that the eigenfunction has no nodes, a characteristic of an eigenfunction for a surface mode. We recognise the eigenfunction as that of the f-mode in the presence of a magnetic field. Figure 5.3(ii) gives the eigenfunction for the second of the harmonics in Figure 5.2(i) (at $k_xH_e = 10.0$). We observe that this eigenfunction has one node, similar to that of the eigenfunction of the first (n=1) p-mode. This eigenfunction, then, is characteristic of a trapped mode, the trapping in this case arising due to refraction caused by the increasing Alfvén speed (and therefore increasing magnetoacoustic speed) with height into the atmosphere. These modes are therefore not present in the model investigated in Chapter 4, since the Alfvén speed is constant there and consequently no trapping of the modes can take place. A plot of the eigenfunction for the third harmonic (not shown) from Figure 5.2(i) would show a trapped mode with two nodes.

Finally, in Figure 5.4, we compare and contrast the eigenfunctions of the f-mode (in the presence of a magnetic field) with the fast and slow magnetoacoustic-gravity surface waves. The eigenfunction of the f-mode (modified by the presence of the magnetic field) at $k_xH_e = 1.0$ in Figure 5.2(iii) is shown with that of the fast and slow magnetoacoustic-gravity surface modes at $k_xH_e = 5.0$ in Figure 5.2(iii). The curves are plotted for a fixed ratio of the sound speeds, namely $c_0/c_e = 0.9$, and Alfvén speed $v_A/c_e = 1.0$. We note, as in Chapter 4, that the f-mode and the fast magnetoacoustic-gravity surface mode have similar profiles, demonstrating the association which exists between them.

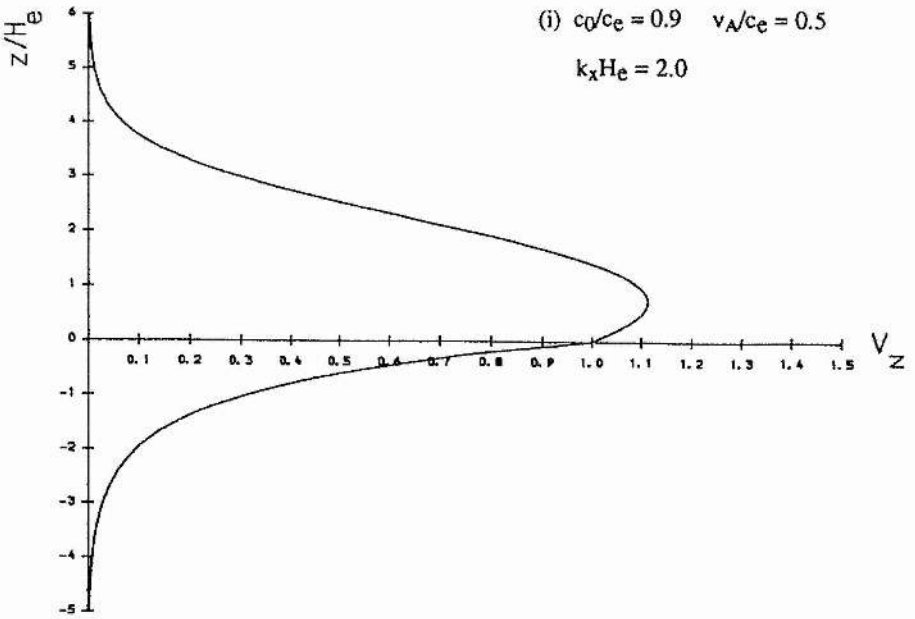

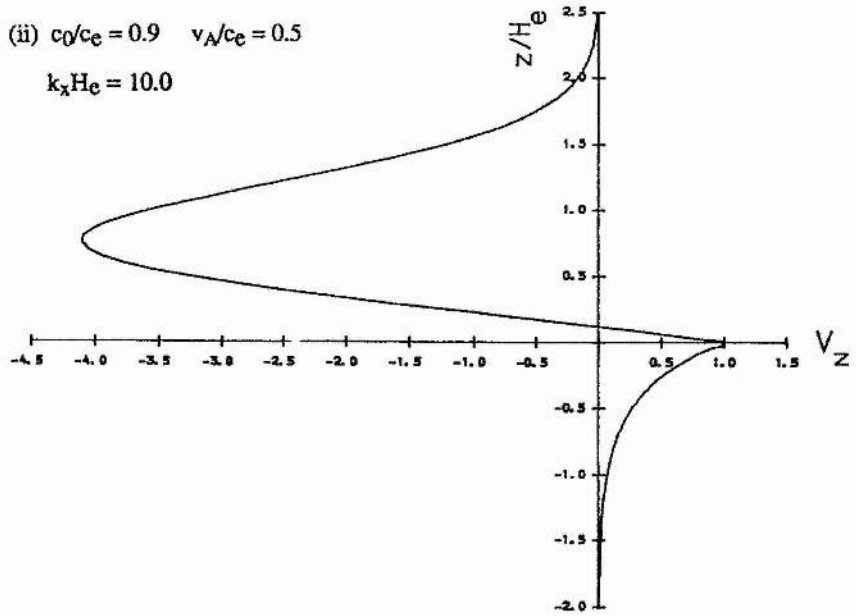

FIGURE 5.3 The modes of oscillation for the harmonics in Figure 5.2(i) with fixed values $c_0/c_e = 0.9$, $v_A/c_e = 0.5$, for (i) $k_xH_e = 2.0$ and (ii) $k_xH_e = 10.0$. The modes are plotted in units of $v_z(0)$.

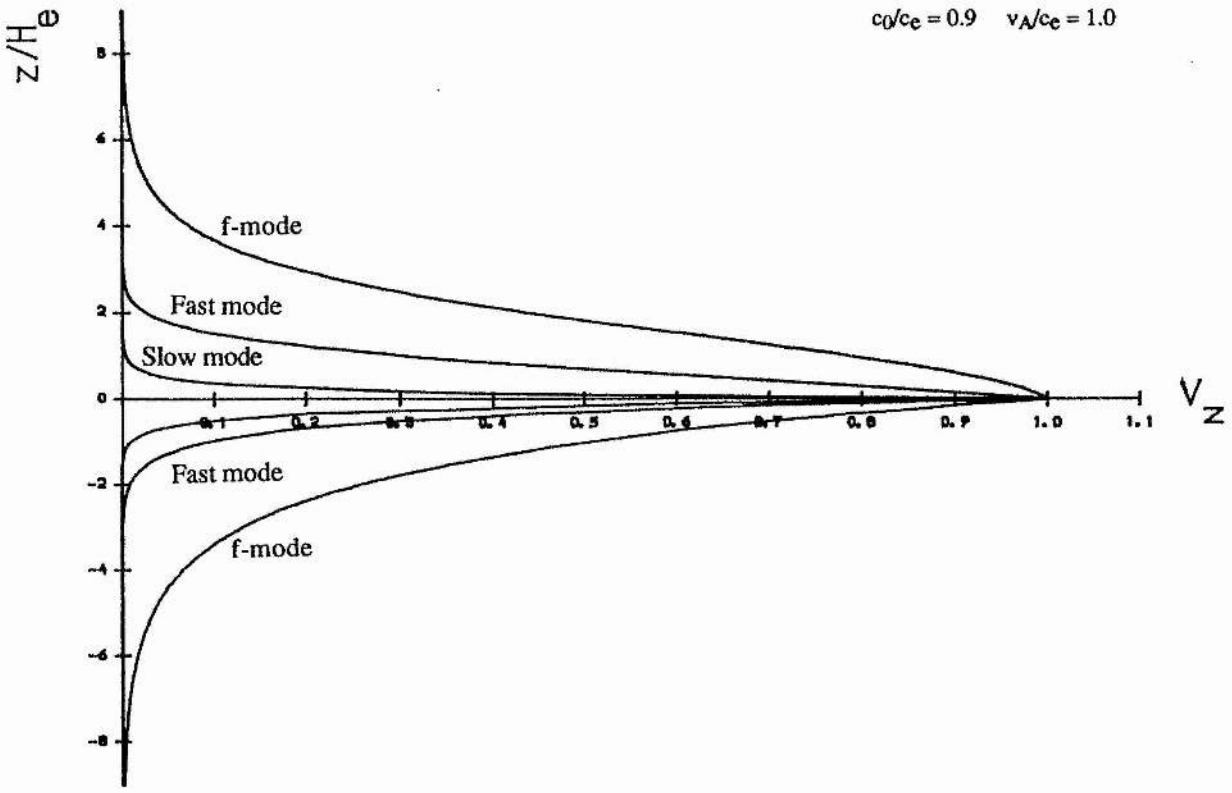

FIGURE 5.4 The eigenfunctions for the f-mode (modified by the magnetic field) with $k_xH_e = 1.0$ and the slow and fast magnetoacoustic-gravity surface modes with $k_xH_e = 5.0$. The eigenfunctions are plotted in units of $v_z(0)$ for $c_0/c_e = 0.9$ and $v_A/c_e = 1.0$.

5.6 Summary

We have derived a dispersion relation describing the parallel propagation of magnetoacoustic-gravity surface modes and the f-mode at a single magnetic interface. The model presented in Chapter 4 of a non-uniform magnetic field in the photosphere-chromosphere decaying away with height is a good global model for the solar atmosphere. The model consider in this chapter, where the atmosphere has a uniform magnetic field, is probably a better representation of the expected behaviour more local to the surface of the sun. Both the model of Chapter 4 and that discussed here yield similar features for some of the wave structures. For example, in the presence of a magnetic field, the f-mode fails to propagate if the magnetic region is warmer than the field-free medium (i.e. $c_0 > c_e$). Also, the f-mode changes its character as the magnetic field strength is increased, and eventually develops into the fast magnetoacoustic-gravity surface wave. Dispersion curves for the fast and slow magnetoacoustic-gravity surface waves show that both modes propagate with phase-speeds which decrease as the horizontal wavenumber is increased, gradually asymptoting to distinct limits as $k_x H_e \rightarrow \infty$, provided both $c_e > c_0$ and $v_A > c_0$. If either of the latter two conditions is not met then the propagation of the fast magnetoacoustic-gravity surface mode is restricted, and only the slow magnetoacoustic surface wave exists as $k_x H_e \rightarrow \infty$.

In contrast to the constant Alfvén speed model of Chapter 4, the increasing Alfvén speed model discussed here results in the trapping of modes due to refraction. These trapped modes are in some respects similar to the usual p-modes in helioseismology and may be relevant to the recent discussions of the possibility of a chromospheric cavity (see, for example, Kumar *et al.*, 1991; Woodard and Libbrecht, 1991). These modes only occur when the field-free region is warmer than the magnetic medium (i.e. when $c_e > c_0$).

Chapter 6 : Concluding Remarks

6.1 Summary of the Modes

We have investigated the nature of parallel (parallel to the applied magnetic field $\underline{B}_0 = B_0(z)\hat{\underline{x}}$) propagation of surface waves at a single discontinuous interface for both an incompressible and compressible plasma for the cases when gravity is both included and neglected. There are many interconnections between the various surface modes. Thus, before considering any applications of the theory developed in the thesis, it is worth summarising all the modes discussed to illustrate which modes develop into others as we move from the incompressible case through to the compressible case, with and without the effect of including gravity along the way.

In the simplest situation of incompressible media with constant but different densities either side of the interface and with no gravity acting, a single hydromagnetic surface wave exists which propagates with a phase-speed c_k (given by Equation (2.26) of Chapter 2). This is the classical result of a hydromagnetic surface wave propagating at a speed which is intermediate between the two Alfvén speeds either side of the interface. The inclusion of gravity has two effects on the hydromagnetic surface wave. The surface wave now samples a non-uniform medium, and also additional forces - buoyancy forces - arise to modify the propagation of the surface wave. In the presence of gravity the hydromagnetic surface wave becomes dispersive (i.e. ω/k_x is no longer independent of the horizontal wavenumber k_x) and there is also the possibility of the Rayleigh-Taylor instability (i.e. $\omega^2<0$) occurring at long wavelengths if a dense fluid rests on top of a light fluid. The effect of the magnetic field is to stabilize the interface against short wavelength oscillations.

In the incompressible case with a non-uniform distribution of density and in the absence of a magnetic field the transcendental dispersion relation may be written as a polynomial. There are two genuine (i.e. physically and mathematically acceptable) roots of this polynomial, the f-mode ($\Omega^2=\omega^2/gk_x=1$) and the surface gravity mode. Depending on the ratio of the densities, only one of these modes may exist. If $\rho_e > \rho_0$,

then only the surface gravity mode will propagate, while if $\rho_e < \rho_0$ then only the f-mode exists, though only for a restricted range of horizontal wavenumber k_x. This restriction is purely an artifact of the model. If we model the lower region by a power law density profile which is more representative of the convection zone, then the upper restriction on the wavenumber k_x for the propagation of the f-mode is removed. When a magnetic field is included and $\rho_e < \rho_0$, then in addition to the f-mode (now modified by the presence of the magnetic field) the surface gravity mode (also modified by the presence of the magnetic field) stabilised by the magnetic field also propagates.

The dispersion relation for the f-mode in the presence of a magnetic field is only approximated by $\Omega^2=\omega^2/gk_x=1$; the exact relation is not known. Observationally the f-mode's frequency is seen to lie *below* $\Omega^2=1$, but all the analytical solutions (Campbell and Roberts, 1989 and Evans and Roberts, 1990b) show a departure that is *above* $\Omega^2=1$. Similarly, an asymptotic solution to the dispersion relation derived here shows that for the case of a low Alfvén velocity the frequency shift increases monotonically with the magnetic field strength.

Consider the effect of compression on these modes, in the first instance neglecting gravitational stratification. With the inclusion of compression we have the additional restoring force of pressure, which together with the magnetic pressure and tension forces provided by the magnetic field sustains the wave motion. There is now the possibility that the interface may support one or two surface modes; the slow magnetoacoustic mode, which we may view has having developed from the incompressible hydromagnetic surface wave, and the fast magnetoacoustic mode, which we may view as being a new surface wave established by the inclusion of compressibility. Whether both modes propagate depends once more on the ordering of the densities (and hence for a compressible medium on the sound speeds) in the two media. In particular, if one side of the interface is field-free then, in addition to the slow mode, the fast magnetoacoustic mode will propagate, though only if the Alfvén speed is greater than the sound speed in the magnetic field region and if the sound speed in the

field-free region is greater than that in the magnetic atmosphere (i.e. if the field-free region is warmer than the magnetic medium).

The fast magnetoacoustic surface mode has the property that it penetrates more than the slow mode into either media, while both penetrate more into the field-free region than into the magnetic medium. The slow magnetoacoustic surface wave is highly anisotropic in character, being predominantly longitudinal in nature, whereas the fast mode is more isotropic, being polarized transversely in strong fields and longitudinally in weaker fields. Consider next the effect of gravity on these modes.

In general, any disturbance in the solar atmosphere is subject to the three restoring forces of buoyancy, compressibility and magnetism. Consequently, the nature of the propagation of magnetoacoustic-gravity surface waves is necessarily complicated, a reflection of the highly anisotropic character of a magnetically structured and stratified atmosphere. As with the incompressible case, in the absence of a magnetic field the transcendental dispersion relation may be written as a polynomial. Once again, as for the incompressible case, there are two solutions to this polynomial which are also solutions to the original transcendental dispersion relation. Yet again, depending on the ratio of the densities only one of these modes may exist in any given circumstance. If $\rho_e > \rho_0$, then only the surface gravity mode exists; while if $\rho_e < \rho_0$, then the f-mode will propagate (but, as for the incompressible case, only within a restricted range of horizontal wavenumber k_x).

However, when a magnetic field is included such that the Alfvén speed is constant and $\rho_e < \rho_0$, then in addition to the f-mode (now modified by the presence of the magnetic field) a surface gravity mode (also modified by the presence of the magnetic field) is stabilised by the magnetic field and may also propagate. This is exactly the same as in the incompressible case. The surface gravity mode in the compressible context is now "labelled" the slow magnetoacoustic-gravity surface wave, whilst the f-mode develops into the fast magnetoacoustic-gravity surface wave as the magnetic field strength increases. We note, however, that both the slow magnetoacoustic-gravity surface wave and either the f-mode (when $v_A < c_0$), modified

by the magnetic field, or the fast magnetoacoustic-gravity surface wave (when $v_A > c_0$) will propagate only when $\rho_e < \rho_0$ (or correspondingly when $c_e > c_0$). This finds a correspondence in the condition that pertains in the non-gravity case, when the counterparts of the modes, namely the slow and fast magnetoacoustic surface waves, both exist only when $v_A > c_0$ and $c_e > c_0$. In the non-gravity case, when $c_e > c_0$ but $v_A < c_0$, then only the slow magnetoacoustic mode exists but in the gravity case the f-mode (which does not exist in the non-gravity case), although modified by the presence of the magnetic field, may also propagate.

The following diagrams show the connections between the various modes, and hopefully makes the above summary of the modes even clearer.

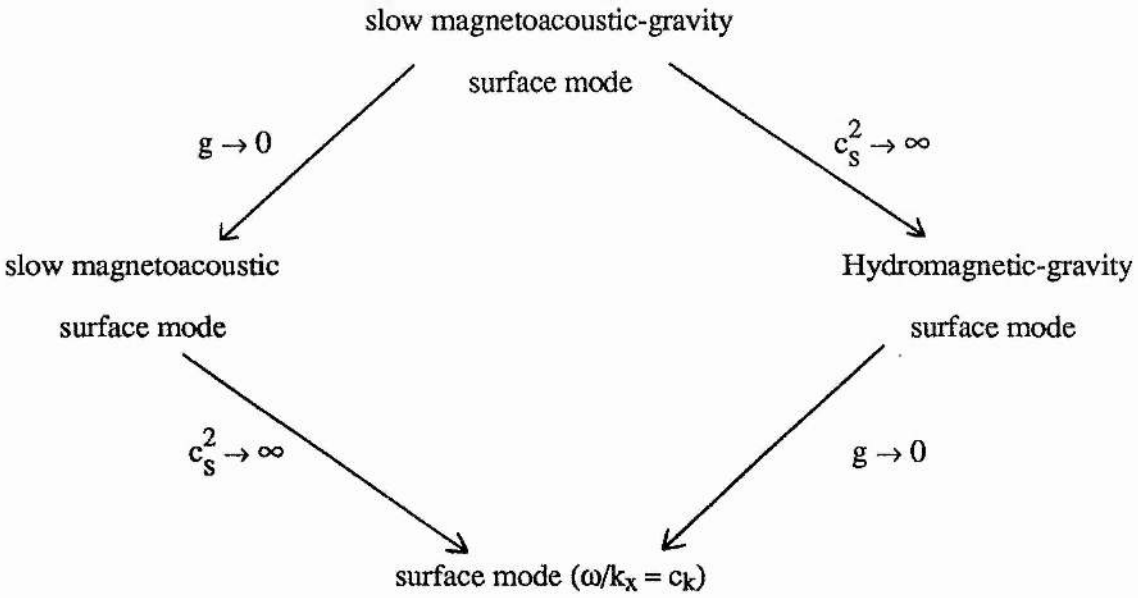

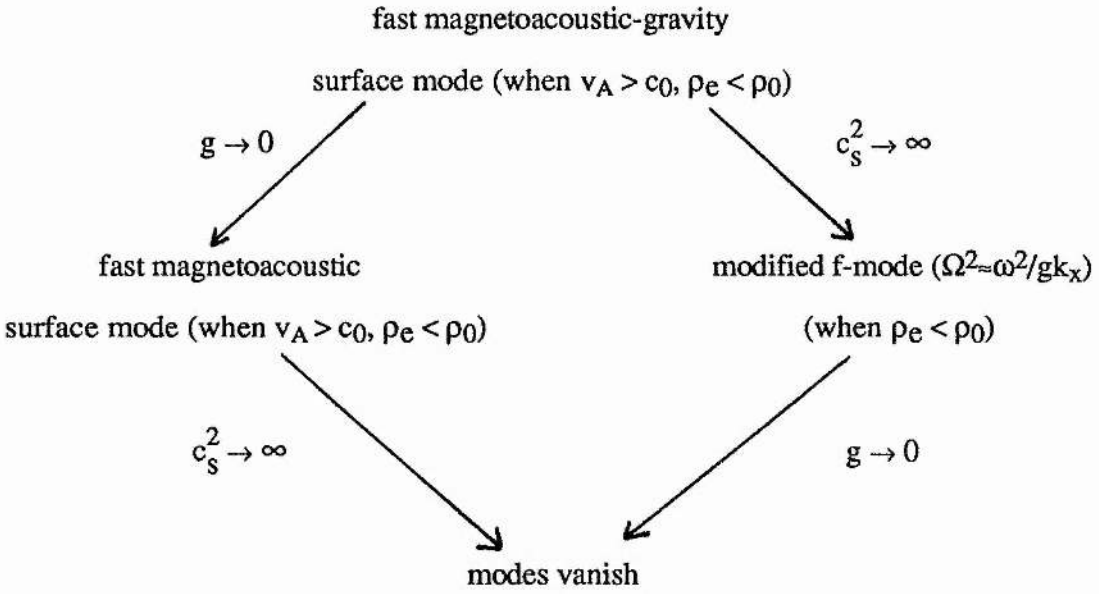

Finally, we have discussed the case where all three restoring forces are present, as above, except that we considered the magnetic medium to be modelled by a uniform magnetic field (so that the Alfvén speed increases exponentially with height). As a result of this increasing Alfvén speed, refraction of the waves can take place and we obtained harmonic-type trapped modes, in addition to the surface modes mentioned above. The harmonic modes propagate only when $v_A > c_0$ and $\rho_e < \rho_0$, which are the same criteria for the existence of the f-mode in the presence of a magnetic field. This is not surprising since the first of these harmonics is the modified f-mode (modified by the presence of the uniform magnetic field). Apart from these harmonics the uniform magnetic field model yields surface modes, which exhibit much the same characteristics as in the constant Alfvén speed case.

In the light of the investigations on surface waves in a gravitationally stratified atmosphere carried out in Chapters 4 and 5, let us now return to the question of whether we can successfully model running penumbral waves as surface waves. The filamentary nature of the penumbra makes it very difficult to model consistently and there is no generally accepted model. The sound speed and in particular the Alfvén speed, which varies inversely with the square root of the density, clearly depend on the height of the penumbral field. Giovanelli (1982) considered the canopy base at its

outermost edge to lie at about 180km above the photosphere, with a thickness of about 250km. By contrast, Schmidt *et al.* (1986) have suggested a much shallower penumbral field of only 80km deep with a Wilson depression in the range 60-120km. This would place the canopy base of the penumbral field around the photospheric base at the very most. Clearly, then, it is not easy to determine appropriate sound and Alfvén speeds. Spruit (1986) suggests typical values for both the sound and Alfvén speeds of around $7kms^{-1}$. Nye and Thomas (1974), in a linear model for heights ranging between the photosphere base and 200km above the photosphere, give the sound and Alfvén speeds as lying in the ranges $6.5\text{-}8kms^{-1}$ and $5\text{-}8kms^{-1}$, respectively.

In our calculations, where we have non-dimensionalised with respect to the sound speed in the field-free region (i.e. c_e), we are interested in the ratios c_0/c_e and v_A/c_e. We shall consider the field-free region to be slightly warmer than the overlying magnetic region and take $c_0/c_e = 0.9$. Then from Figures 5.2(i),(ii) & (iii), we note that the largest possible horizontal phase-speed is given by $\omega/k_x = c_e$, which is the magnetically modified f-mode in Figures 5.2(i) & (ii), and the fast magnetoacoustic-gravity surface mode in Figure 5.2(iii). Thus, for example, in order to fit the observed range of horizontal phase-speeds for the running penumbral wave of $8\text{-}25kms^{-1}$ in the chromosphere, we require the sound speed in the field-free region to also lie in this range. This places the penumbral field at the photospheric level or below, as suggested by Schmidt *et al.* (1986). However, as stated earlier, the observed horizontal phase-speeds for the running penumbral wave at the photospheric level lie in the range 40-90 kms^{-1}. Thus agreement between the theory and the observations may only be possible if we consider the observations to include the effect of flows such as the Evershed flow (Thomas, 1981).

At photospheric levels the Evershed flow consists of a radial horizontal outflow from the sunspot to the surroundings, while at chromospheric levels, the direction is reversed and material flows into the sunspot umbra. Radial outflows of up to $6kms^{-1}$ are found in the photosphere, inflows of up to $20kms^{-1}$ in the chromosphere. Also,

Alissandrakis *et al.* (1988) have shown that at transition zone temperatures (10^5 K), the flow has the same characteristics as the inward chromospheric flow but with a higher flow velocity. Thus with such a flow present, the actual horizontal phase-speeds for the running penumbral waves in photosphere would be in the range 35-85kms^{-1} say, while those in the chromospheric region would lie in the range 20-40kms^{-1}.

It could be possible that we may be able to match the observed phase-speeds for the running penumbral waves by considering non-parallel propagation. Although running penumbral waves are seen to be mainly field aligned, it is worth considering such an analysis, especially when such an investigation is readily available.

6.2 Discussion

The investigations carried out in Chapter 3 on the parallel propagation of magnetoacoustic surface waves in a non-gravitationally stratified atmosphere have recently been extended by Jain and Roberts (1991) to take into account non-parallel propagation. Previous investigations in this area have been considered by Uberoi (1982) and Somasundaram and Uberoi (1982). Uberoi (1982) considered only a low beta plasma drawing the conclusion that there were no surfaces waves for the case when the angle of propagation to the applied magnetic field was zero (i.e. parallel propagation) or as the angle of propagation approached $\pi/2$,with the phase-speeds decreasing as the angle of propagation approached $\pi/2$. Somasundaram and Uberoi (1982) investigated the longitudinal phase-speed of magnetoacoustic surface waves for various propagation angles and field strengths either side of the interface.

In a similar analysis to that of Somasundaram and Uberoi (1982), Jain and Roberts (1991) considered the occurrence of magnetoacoustic surface waves at a single magnetic interface for non-parallel propagation. They considered propagation in a plane at an angle θ to the applied non-uniform magnetic field $\underline{B}_0=B_0(x)\hat{\underline{z}}$. They investigated the dependence of the phase-speed (ω/K) and penetration depths of the magnetoacoustic surface waves on the angle of propagation to the magnetic field for various sound and Alfvén speeds.The wavenumber K lies in the yz-plane and is defined by $\underline{K} = (0,k_y,k_z)$.

Thus if propagation takes place at an angle θ to the magnetic field, the wave vector has components $k_y = K\sin\theta$ and $k_z = K\cos\theta$.

For the case of two magnetic fields of different strengths either side of the interface, Jain and Roberts (1991) they obtained the dispersion relation (see also Roberts, 1981a)

$$\frac{\omega^2}{k_z^2} = \frac{\rho_0 v_A^2 (m_e^2 + k_y^2)^{1/2} + \rho_e v_{Ae}^2 (m_0^2 + k_y^2)^{1/2}}{\rho_0 (m_e^2 + k_y^2)^{1/2} + \rho_e (m_0^2 + k_y^2)^{1/2}}, \qquad (6.1)$$

where for evanescent solutions it is required that $(m_0^2 + k_y^2)^{1/2} > 0$ and $(m_e^2 + k_y^2)^{1/2} > 0$. m_0 has been defined previously in Chapter 3 by Equation (3.27), and m_e is equivalent to the definition of m_0 except that the sound and Alfvén speeds are c_e and v_{Ae}, respectively.

For parallel propagation ($k_y = 0$), with one side of the interface field-free ($v_{Ae} = 0$, say), the above dispersion relation (6.1) reduces to Equation (3.33) obtained in Chapter 3. Note the change in geometry; Jain and Roberts consider the magnetic field to be directed along the z-axis whereas in this thesis the magnetic field lies parallel to the x-axis. Thus in Jain and Roberts the wavenumber k_z is equivalent to the wavenumber k_x in this thesis.

The dispersion relation given by Equation (6.1) may be rewritten as (Roberts, 1981a, Jain and Roberts, 1991)

$$\frac{\omega^2}{K^2} = \left[v_{Ae}^2 + \frac{1}{R+1} (v_A^2 - v_{Ae}^2) \right] \cos^2\theta, \qquad (6.2)$$

where $R > 0$ (a function of θ and the phase-speed ω/K) and is given by

$$R = \left(\frac{\rho_e}{\rho_0}\right) \left(\frac{m_0^2 + k_y^2}{m_e^2 + k_y^2} \right)^{1/2}. \qquad (6.3)$$

We note that for parallel propagation, Equations (6.2) reduces to Equations (3.34) of Chapter 3. It is clear from Equation (6.2) that the phase speed ω/K lies in the interval

$[v_A\cos\theta, v_{Ae}\cos\theta]$, which is equivalent to saying that the longitudinal phase-speed ω/k_z lies in the interval $[v_A, v_{Ae}]$, as noted earlier in Chapter 3. Then, with one side of the interface field-free (e.g. $v_{Ae} = 0$) the phase speed ω/K must satisfy

$$\frac{\omega}{K} \leq v_A\cos\theta \tag{6.4}$$

and therefore for $\theta=\pi/2$ there are no waves. Thus magnetoacoustic surface waves cannot propagate across the magnetic field. We note that for parallel propagation the inequality (6.4) reduces to give the result that the longitudinal phase-speed, ω/k_z, of a surface wave on a field-free interface lies below the Alfvén speed v_A, as pointed out in Chapter 3.

By a similar analysis to that carried out in Chapter 3, Jain and Roberts deduced from the restrictions $(m_0^2 + k_y^2)^{1/2} > 0$ and $(m_e^2 + k_y^2)^{1/2} > 0$ that both the slow and fast magnetoacoustic surface waves can exist only when both $c_e > c_0$ and $v_A > c_0$. This is exactly the same as for the parallel case given in Chapter 3. The slow mode must satisfy (Jain and Roberts, 1991)

$$\frac{\omega}{K} < \min(c_T\cos\theta, c_e) \tag{6.5}$$

while the fast mode when it is allowed to propagate must satisfy (Jain and Roberts, 1991)

$$c_0\cos\theta < \frac{\omega}{K} < \min(v_A\cos\theta, c_e). \tag{6.6}$$

Once again, these conditions reduce in the parallel case to those obtained previously in Chapter 3 from the requirements that $m_0, m_e > 0$.

Jain and Roberts (1991) observe that both the slow and fast magnetoacoustic surface waves propagate with phase-speeds that decrease as the angle θ approaches $\pi/2$. This is not surprising since we have already deduced that there are no surface waves for $\theta=\pi/2$. Thus the surface waves cannot propagate across the magnetic field and attain their highest phase-speed when propagating parallel to the magnetic field.

They also note that the penetration depths of both the slow and fast modes decrease with increasing angle θ. They come to the same conclusion as stated in Chapter 3 for the parallel propagation case that the fast mode penetrates more than the slow mode into either region and that both modes penetrate deeper into the field-free region than into the more dense magnetic field region.

Jain and Roberts (1991) also considered the case of a low beta plasma for the case of parallel propagation at an interface with different field strengths either side of the interface. They concluded that no surface waves exist in the low beta case. This is in agreement with the earlier result by Uberoi (1982) for non-parallel propagation, in which there is no mode when θ approaches zero.

Returning to our question of whether we can model running penumbral waves as magnetoacoustic surface waves, it is clear that we cannot obtained any higher phase-speeds in the non-parallel case. This is clearly true by (6.4) which demonstrates that the phase-speeds of the surface waves are greatest when propagating parallel to the magnetic field. It is true that the analysis of Jain and Roberts (1991) and others does not include the effect of gravity, but this will probably have no major bearing on the magnitude of the phase-speeds. No studies to date have considered the effect of gravity on the non-parallel propagation of magnetoacoustic surface waves. In the investigations carried out in Chapters 4 and 5 where gravity was included for the case of parallel propagation, we found that the phase-speeds did not increase sufficiently to match those observed for the running penumbral wave. Presumably then the same will be true when gravity is included in the non-parallel case, especially if a similar condition to (6.4) exists when gravity is included, i.e. the phase-speed of the modes decreases with increasing angle of propagation.

If an investigation into the inclusion of gravity is to be undertaken for the non-parallel case, then from the experience of the parallel case, the problem where a uniform magnetic field is considered could prove difficult to tackle. The governing ordinary differential equation will once again have non-constant coefficients, but now the Alfvén wave is coupled into the equation. When the Alfvén speed is constant or if attention is

restricted to parallel propagation, then the Alfvén mode will factorise out. The non-constant coefficient differential equation for the parallel case (see Equation (5.8) of Chapter 5) can be cast in the form of a hypergeometric differential equation through a suitable variable change. Therefore it would seem natural to assume that a similar transformation to a hypergeometric differential equation could be performed for the non-parallel case. Clearly the change of variable must involve a function of θ such that when $\theta=0$ the change of variable (see Equation (5.9) of Chapter 5) for the parallel case is recovered. However, this is not to say that it will prove easy to obtain such a transformation. Indeed, as yet, such a change of variable has not been found.

Another possible extension of the work carried out in this thesis is to consider the unstable aspect (i.e. $\omega^2 < 0$). The nature of compressible effects on the Rayleigh-Taylor instability in the absence of magnetic fields has been investigated by Bernstein and Book (1983) and Baker (1983). However, there has been some disagreement about the effect of compressibility on the growth rate of the instability. Bernstein and Book (1983) concluded that the growth rates increased with compressibility while Baker (1983) concluded that in the absence of a magnetic field, compressibility can neither enhance nor decrease the growth rate. Indeed Bernstein and Book (1983) have stated that "thus far research on the general nature of the compressibility effects in the Rayleigh-Taylor instability is inconclusive".

Recently Gonzalez and Gratton (1990), in a sequel to Gratton's *et al.* (1988) investigation of the stability of internal modes, have considered the stability of magnetoacoustic surface waves for a plasma-vacuum interface, mainly with a view to laboratory applications. However, in general there has been little consideration of magnetic effects on the Rayleigh-Taylor instability. An extension therefore of the compressible analysis to include magnetic effects, especially in the astrophysical context, is required. In the light of the investigations presented in this thesis, we are conveniently placed to carry out such an investigation for both the incompressible and compressible cases.

Appendices

A.1 Removal of the Transcendental Nature of the Incompressible Dispersion Relation When There is no Magnetic Field

In the limit of no magnetic field the transcendental dispersion relation given by Equation (2.46) of Chapter 2 reduces to

$$\frac{\omega^2}{k_x^2} = - g \frac{(\rho_0 - \rho_e)}{\rho_0 (M_0 - 1/2H_0) + \rho_e (M_e + 1/2H_e)}, \qquad \text{(A1.I)}$$

where

$$M_0 = \frac{(1 - 4a_0H_0^2)^{1/2}}{2H_0}, \qquad \text{(A1.II)}$$

$$M_e = \frac{(1 - 4a_eH_e^2)^{1/2}}{2H_e}, \qquad \text{(A1.III)}$$

and

$$a_0 = k_x^2\left\{\frac{g/H_0 - \omega^2}{\omega^2}\right\}, \qquad \text{(A1.IV)}$$

$$a_e = k_x^2\left\{\frac{g/H_e - \omega^2}{\omega^2}\right\}. \qquad \text{(A1.V)}$$

Then by removing the radicals in the dispersion relation (A1.I) defined by Equations (A1.II)-(A1.V) the dispersion relation may be rewritten as

$$\Omega\left\{\frac{\rho_0}{k_xH_0}\left(\Omega^2 (1 + 4k_x^2H_0^2) - 4k_xH_0\right)^{1/2} + \frac{\rho_e}{k_xH_e}\left(\Omega^2 (1 + 4k_x^2H_e^2) - 4k_xH_e\right)^{1/2}\right\}$$

$$= \Omega^2\left\{\frac{\rho_0}{k_xH_0} - \frac{\rho_e}{k_xH_e}\right\} - 2(\rho_0 - \rho_e), \qquad \text{(A1.VI)}$$

where $\Omega^2 = \frac{\omega^2}{gk_x}$.

For ease of algebraic manipulation, let

$$A = \frac{\rho_0^2}{k_x^2 H_0^2}\left(\Omega^2\,(1 + 4k_x^2 H_0^2) - 4k_x H_0\right), \qquad \text{(A1.VII)}$$

$$B = \frac{\rho_e^2}{k_x^2 H_e^2}\left(\Omega^2\,(1 + 4k_x^2 H_e^2) - 4k_x H_e\right), \qquad \text{(A1.VIII)}$$

$$C = \frac{\rho_0}{k_x H_0} - \frac{\rho_e}{k_x H_e}, \qquad \text{(A1.IX)}$$

and

$$D = \rho_0 - \rho_e. \qquad \text{(A1.X)}$$

Then Equation (A1.VI) may be written as

$$\Omega\,(A^{1/2} + B^{1/2}) = C\Omega^2 - 2D. \qquad \text{(A1.XI)}$$

Squaring both sides of Equation (A1.XI) and rewriting yields

$$2\Omega^2 A^{1/2} B^{1/2} = C^2\Omega^4 - \Omega^2(A + B + 4CD) + 4D^2. \qquad \text{(A1.XII)}$$

Squaring both sides for a second time finally removes all the square roots to yield

$$\begin{aligned} &2\Omega^6 C^2(A + B) - \Omega^4(A - B)^2 - 8\Omega^4 CD(A + B) - 8\Omega^2 D^2(A + B) \\ &\quad = \Omega^8 C^4 - 8\Omega^6 C^3 D + 24\Omega^4 C^2 D^2 - 32\Omega^2 CD^3 + 16D^4. \end{aligned} \qquad \text{(A1.XIII)}$$

By explicitly writing A and B, Equation (A1.XIII) may then be expressed as the following polynomial in Ω^2:

$$\left\{ C^4 - 2C^2\left(\frac{\rho_0^2}{k_x^2H_0^2}(1 + 4k_x^2H_0^2) + \frac{\rho_e^2}{k_x^2H_e^2}(1 + 4k_x^2H_e^2)\right)\right.$$

$$\left. + \frac{\rho_0^2}{k_x^2H_0^2}(1 + 4k_x^2H_0^2) - \frac{\rho_e^2}{k_x^2H_e^2}(1 + 4k_x^2H_e^2)\right\}\ \Omega^8$$

$$+ 8\left\{ CD\left(\frac{\rho_0^2}{k_x^2H_0^2}(1 + 4k_x^2H_0^2) + \frac{\rho_e^2}{k_x^2H_e^2}(1 + 4k_x^2H_e^2)\right) + C^2(\rho_0 + \rho_e) - C^3D\right.$$

$$\left. - D\left(\frac{\rho_0^2}{k_x^2H_0^2}(1 + 4k_x^2H_0^2) - \frac{\rho_e^2}{k_x^2H_e^2}(1 + 4k_x^2H_e^2)\right)\right\}\ \Omega^6$$

$$+ 8D\left\{ D\left(\frac{\rho_0^2}{k_x^2H_0^2}(1 + 4k_x^2H_0^2) + \frac{\rho_e^2}{k_x^2H_e^2}(1 + 4k_x^2H_e^2)\right) - 4C(\rho_0 + \rho_e)\right.$$

$$\left. + (2 + 3C^2)D\right\}\ \Omega^4 - 32D^2\left\{ (\rho_0 + \rho_e) + CD\right\}\ \Omega^2 + 16D^4 = 0. \qquad \text{(A1.XIV)}$$

It is not apparent at first sight that (A1.XIV) possesses the factor $(\Omega^4 - 1)$. However, once this factor is realised we may rewrite Equation (A1.XIV) in the form

$$(\Omega^4 - 1)(a\Omega^4 + b\Omega^2 + a + c) = 0, \qquad \text{(A1.XV)}$$

where a, b and c are the coefficients of Ω^8, Ω^6 and Ω^4 in Equation (A1.XIV), respectively. Written explicitly, after some algebra, it can be determined that the coefficients a, b and a + c of Equation (A1.XV) are

$$a = \frac{\rho_0}{H_0}\frac{\rho_e}{H_e}\left(\rho_0^2 + \rho_e^2\right) - \rho_0^2\rho_e^2\left(\frac{1}{H_0^2} + \frac{1}{H_e^2}\right) + k_x^2\left(\rho_0^2 - \rho_e^2\right)^2, \qquad \text{(A1.XVI)}$$

$$b = -2k_x\rho_0\rho_e(\rho_0 - \rho_e)^2\left(\frac{1}{H_0} + \frac{1}{H_e}\right), \qquad \text{(A1.XVII)}$$

and

$$a + c = -k_x^2(\rho_0 - \rho_e)^4. \qquad \text{(A1.XVIII)}$$

Then, by using the fact that the two sides of the interface are related by Equation (2.66), that is

$$g\rho_0 H_0 = g\rho_e H_e, \qquad \text{(A1.XIX)}$$

the coefficients a, b and a + c simplify and Equation (A1.XV) reduces to

$$(\Omega^4 - 1)\left\{k_x(\rho_0 + \rho_e)^2\Omega^4 - \left(\frac{\rho_0}{H_e} + \frac{\rho_e}{H_0}\right)(\rho_0 + \rho_e)\Omega^2 - k_x(\rho_0 - \rho_e)^2\right\} = 0. \qquad \text{(A1.XX)}$$

This is the polynomial given by Equation (2.57) in Chapter 2.

A.2 Analytical Correction to the f-Mode Due to the Presence of a Magnetic Field for the Incompressible Case

For the purposes of this calculation it is convenient to rewrite the dispersion relation (2.47) as

$$\Omega^2 = \frac{\rho_0}{\left(\rho_0 + \rho_e \frac{(M_e/k_x + 1/2k_xH_e)}{(M_0/k_x - 1/2k_xH_B)}\right)} (k_xH_e) \frac{v_A^2}{gH_e}$$

$$- \frac{(\rho_0 - \rho_e)}{\rho_0 (M_0/k_x - 1/2k_xH_B) + \rho_e (M_e/k_x + 1/2k_xH_e)}, \tag{A2.I}$$

where

$$\frac{M_0}{k_x} = \frac{(1 - 4a_BH_B^2)^{1/2}}{2k_xH_B}, \tag{A2.II}$$

$$\frac{M_e}{k_x} = \frac{(1 - 4a_eH_e^2)^{1/2}}{2k_xH_e}, \tag{A2.III}$$

and

$$a_B = k_x \left\{ \frac{1/H_B - k_x \left(\Omega^2 - (k_xH_e) \frac{v_A^2}{gH_e} \right)}{\left(\Omega^2 - (k_xH_e) \frac{v_A^2}{gH_e} \right)} \right\}, \tag{A2.IV}$$

$$a_e = k_x \left\{ \frac{1/H_e - k_x\Omega^2}{\Omega^2} \right\}. \tag{A2.V}$$

The scale heights H_B ($\equiv H_0$ when $v_A=0$) and H_e are related by

$$H_B = H_0 + \frac{1}{2} H_e \frac{v_A^2}{gH_e}, \tag{A2.VI}$$

and from Equation (2.33) we note that the densities are related to the scale heights by

$$\frac{\rho_e}{\rho_0} = \frac{H_0}{H_e} + \frac{1}{2}\frac{v_A^2}{gH_e}. \qquad \text{(A2.VII)}$$

For ease of algebraic manipulation, let

$$A = \frac{1}{2k_xH_B} - \frac{M_0}{k_x}, \qquad \text{(A2.VIII)}$$

$$B = \frac{1}{2k_xH_e} + \frac{M_e}{k_x}, \qquad \text{(A2.IX)}$$

and

$$V = \frac{v_A^2}{gH_e}. \qquad \text{(A2.X)}$$

Then, using this notation, Equation (A2.I) may be written as

$$\Omega^2 \left\{ (2k_xH_0 + Vk_xH_e)B - 2Ak_xH_e \right\} = 2k_xH_0 - 2k_xH_e + Vk_xH_e - 2AVk_x^2H_e^2, \qquad \text{(A2.XI)}$$

where

$$A = \frac{1}{(2k_xH_0 + Vk_xH_e)}\left[1 - \left\{ 1 + (2k_xH_0 + Vk_xH_e)^2 - \frac{2(2k_xH_0 + Vk_xH_e)}{(\Omega^2 - Vk_xH_e)} \right\}^{1/2} \right], \qquad \text{(A2.XII)}$$

and

$$B = \frac{1}{2k_xH_e}\left[1 + \left\{ 1 + 4k_x^2H_e^2 - \frac{4k_xH_e}{\Omega^2} \right\}^{1/2} \right]. \qquad \text{(A2.XIII)}$$

Now let $\Omega^2 = 1 + \alpha V$, where α is a constant, and expand the dispersion relation (A2.XI) for small values of V (i.e. v_A^2/gH_e). Consider firstly the expansion of A. We rewrite A as

$$A = \frac{1}{(2k_xH_0 + Vk_xH_e)}\left[1 - \{h(V)\}^{1/2} \right], \qquad \text{(A2.XIV)}$$

where

$$h(V) = 1 + (2k_xH_0+Vk_xH_e)^2 - \frac{2(2k_xH_0+Vk_xH_e)}{(1+(\alpha-k_xH_e)V)}. \qquad \text{(A2.XV)}$$

Then, by Maclaurin series, the expansion of h(V) to terms O(V) is

$$\{h(V)\}^{1/2} = \{h(0)\}^{1/2}\left[1 + \frac{1}{2}V\{h(0)\}^{-1}\frac{dh(0)}{dV}\right], \qquad \text{(A2.XVI)}$$

that is

$$\{h(V)\}^{1/2} = \pm|1-2k_xH_0|\left\{1 + \frac{(2k_xH_0\alpha - k_xH_e)}{(1 - 2k_xH_0)^2}V\right\}, \qquad \text{(A2.XVII)}$$

where we take the the positive root, since we take the positive square root of Equation (A2.II). Then the expansion for A up to terms of O(V) is

$$A = \frac{1}{(2k_xH_0 + Vk_xH_e)}\left[1 - |1-2k_xH_0|\left\{1 + \frac{(2k_xH_0\alpha - k_xH_e)}{(1 - 2k_xH_0)^2}V\right\}\right]. \qquad \text{(A2.XVIII)}$$

Similarly we write B as

$$B = \frac{1}{2k_xH_e}\left[1 + \{f(V)\}^{1/2}\right], \qquad \text{(A2.XIX)}$$

where

$$f(V) = 1 + 4k_x^2H_e^2 - \frac{4k_xH_e}{(1+\alpha V)}. \qquad \text{(A2.XX)}$$

Then, once again by Maclaurin series, the expansion of f(V) to terms O(V) gives

$$\{f(V)\}^{1/2} = \pm|2k_xH_e - 1|\left\{1 + \frac{2k_xH_e\alpha}{(2k_xH_e - 1)^2}V\right\}. \qquad \text{(A2.XXI)}$$

Once again we take the positive root, since we take the positive square root of Equation (A2.III). Then the expansion for B up to terms of O(V) is

$$B = \frac{1}{2k_xH_e}\left[1 + |2k_xH_e - 1|\left\{1 + \frac{2k_xH_e\alpha}{(2k_xH_e - 1)^2}V\right\}\right]. \qquad \text{(A2.XXII)}$$

Substituting (A2.XVIII) and (A2.XXII) into the dispersion relation (A2.XI) gives

$$(1+\alpha V)\frac{(2k_xH_0 + Vk_xH_e)}{2k_xH_e}\left[1 + |2k_xH_e - 1|\left\{1 + \frac{2k_xH_e\alpha}{(2k_xH_e - 1)^2}V\right\}\right]$$

$$- (1+\alpha V)\frac{2k_xH_e}{(2k_xH_0 + Vk_xH_e)}\left[1 - |1-2k_xH_0|\left\{1 + \frac{(2k_xH_0\alpha - k_xH_e)}{(1 - 2k_xH_0)^2}V\right\}\right]$$

$$= 2k_xH_0-2k_xH_e+Vk_xH_e-\frac{2Vk_x^2H_e^2}{(2k_xH_0+Vk_xH_e)}\left[1-|1-2k_xH_0|\left\{1 + \frac{(2k_xH_0\alpha - k_xH_e)}{(1-2k_xH_0)^2}V\right\}\right].$$

(A2.XXIII)

Then comparing coefficients of $O(V^0)$ gives

$$\frac{2k_xH_0}{2k_xH_e}\left[1 + |2k_xH_e - 1|\right] - \frac{2k_xH_e}{2k_xH_0}\left[1 - |1 - 2k_xH_0|\right] = 2k_xH_0 - 2k_xH_e.$$

(A2.XXIV)

We note that Equation (A2.XXIV) is satisfied only if $(2k_xH_e - 1) > 0$ and $(1 - 2k_xH_0) > 0$. That is, $\Omega^2 = 1$ is a solution if the horizontal wavenumber lies in the range

$$\frac{1}{2H_e} < k_x < \frac{1}{2H_0}. \qquad \text{(A2.XXV)}$$

Then by comparing coefficients of O(V) in Equation (A2.XXIII) and taking $(2k_xH_e - 1) > 0$ and $(1 - 2k_xH_0) > 0$ we determine α as

$$\alpha = \frac{k_xH_e}{2}\frac{(2k_xH_e - 1)}{(k_xH_e - k_xH_0)}, \qquad \text{(A2.XXVI)}$$

which is Equation (2.70) of Chapter 2. Thus the first order correction to the f-mode in the presence of a magnetic field is

$$\Omega^2 \approx 1 + \frac{1}{2}\frac{(2k_xH_e - 1)}{(k_xH_e - k_xH_0)}\frac{k_xv_A^2}{g}, \qquad \text{(A2.XXVII)}$$

which is Equation (2.71) of Chapter 2.

A.3 Removal of the Transcendental Nature of the Compressible Dispersion Relation When There is no Magnetic Field

In the limit of no magnetic field the transcendental dispersion relation given by Equation (4.33) of Chapter 4 reduces to

$$\frac{\omega^2}{k_x^2} = -g\frac{\left\{\dfrac{\rho_0 c_0^2}{(k_x^2c_0^2 - \omega^2)} - \dfrac{\rho_e c_e^2}{(k_x^2c_e^2 - \omega^2)}\right\}}{\rho_0\dfrac{(M_0 - 1/2H_0)}{m_0^2} + \rho_e\dfrac{(M_e + 1/2H_e)}{m_e^2}}, \qquad \text{(A3.I)}$$

where

$$M_0 = \frac{(1 - 4A_0H_0^2)^{1/2}}{2H_0}, \qquad \text{(A3.II)}$$

$$M_e = \frac{(1 - 4A_eH_e^2)^{1/2}}{2H_e}, \qquad \text{(A3.III)}$$

and

$$A_0 = \frac{(\gamma - 1)g^2k_x^2 + \omega^2(\omega^2 - k_x^2c_0^2)}{\omega^2c_0^2}, \qquad \text{(A3.IV)}$$

$$A_e = \frac{(\gamma - 1)g^2k_x^2 + \omega^2(\omega^2 - k_x^2c_e^2)}{\omega^2c_e^2}, \qquad \text{(A3.V)}$$

and

$$m_0^2 = \frac{(k_x^2c_0^2 - \omega^2)}{c_0^2}, \qquad \text{(A3.VI)}$$

$$m_e^2 = \frac{(k_x^2c_e^2 - \omega^2)}{c_e^2}. \qquad \text{(A3.VII)}$$

Then by removing the radicals in the dispersion relation (A3.I) defined by Equations (A3.II)-(A3.VII) the dispersion relation may be rewritten as

$$\Omega^2\left(\frac{\rho_0 c_0^2}{(k_x c_0^2 - g\Omega^2)}\right)\left\{\frac{\gamma^2 g^2}{k_x^2 c_0^4} - 4\left(\frac{(\gamma - 1)g - \Omega^2(k_x c_0^2 - g\Omega^2)}{\Omega^2 k_x c_0^2}\right)\right\}^{1/2}$$

$$+\Omega^2\left(\frac{\rho_e c_e^2}{(k_x c_e^2 - g\Omega^2)}\right)\left\{\frac{\gamma^2 g^2}{k_x^2 c_e^4} - 4\left(\frac{(\gamma - 1)g - \Omega^2(k_x c_e^2 - g\Omega^2)}{\Omega^2 k_x c_e^2}\right)\right\}^{1/2}$$

$$= \Omega^2\left\{\frac{\gamma g \rho_0}{(k_x c_0^2 - g\Omega^2)} - \frac{\gamma g \rho_e}{(k_x c_e^2 - g\Omega^2)}\right\} - 2\left\{\frac{\rho_0 c_0^2}{(k_x c_0^2 - g\Omega^2)} - \frac{\rho_e c_e^2}{(k_x c_e^2 - g\Omega^2)}\right\}, \quad \text{(A3.VIII)}$$

where $\Omega^2 = \frac{\omega^2}{gk_x}$.

For ease of algebraic manipulation, let

$$A = \frac{\rho_0^2 c_0^4}{(k_x c_0^2 - g\Omega^2)^2}\left\{\frac{\gamma^2 g^2}{k_x^2 c_0^4} - 4\left(\frac{(\gamma - 1)g - \Omega^2(k_x c_0^2 - g\Omega^2)}{\Omega^2 k_x c_0^2}\right)\right\}, \quad \text{(A3.IX)}$$

$$B = \frac{\rho_e^2 c_e^4}{(k_x c_e^2 - g\Omega^2)^2}\left\{\frac{\gamma^2 g^2}{k_x^2 c_e^4} - 4\left(\frac{(\gamma - 1)g - \Omega^2(k_x c_e^2 - g\Omega^2)}{\Omega^2 k_x c_e^2}\right)\right\}, \quad \text{(A3.X)}$$

$$C = \frac{\gamma g \rho_0}{(k_x c_0^2 - g\Omega^2)} - \frac{\gamma g \rho_e}{(k_x c_e^2 - g\Omega^2)}, \quad \text{(A3.XI)}$$

and

$$D = \frac{\rho_0 c_0^2}{(k_x c_0^2 - g\Omega^2)} - \frac{\rho_e c_e^2}{(k_x c_e^2 - g\Omega^2)}. \quad \text{(A3.XII)}$$

Then Equation (A3.VIII) may be written as

$$\Omega\,(A^{1/2}+ B^{1/2}) = C\Omega^2 - 2D. \qquad \text{(A3.XIII)}$$

Squaring both sides of Equation (A3.XIII) and rewriting yields

$$2\Omega^2A^{1/2}B^{1/2} = C^2\Omega^4 - \Omega^2(A + B + 4CD) + 4D^2. \qquad \text{(A3.XIV)}$$

Squaring both sides for a second time finally removes all the square roots to yield

$$\begin{aligned} &2\Omega^6C^2(A + B) - \Omega^4(A - B)^2 - 8\Omega^4CD(A + B) - 8\Omega^2D^2(A + B) \\ &= \Omega^8C^4 - 8\Omega^6C^3D + 24\Omega^4C^2D^2 - 32\Omega^2CD^3 + 16D^4. \end{aligned} \qquad \text{(A3.XV)}$$

By explicitly writing A, B and C, Equation (A3.XV) may then be expressed as a polynomial in Ω^2. This polynomial is of tenth order in Ω^2 and for the sake of clarity shall not be quoted. However, as in the incompressible case the polynomial may be factorised.

We note that the expressions for A, B and C either contain the factor $(k_xc_0^2 - g\Omega^2)$ or the factor $(k_xc_e^2 - g\Omega^2)$ and therefore on squaring and multiplying out by these denominators the resulting polynomial has the factor $(k_xc_0^2 - g\Omega^2)^2(k_xc_e^2 - g\Omega^2)^2$. In addition, as in the incompressible case and although not apparent at first sight, the resulting polynomial also possesses the factor $(\Omega^4 - 1)$. Once these factors are realised we may rewrite Equation (A3.XV) in the form:

$$(\Omega^4-1)(\Omega^2g-k_xc_0^2)^2(\Omega^2g-k_xc_e^2)^2[\Omega^8-2s\Omega^6+ (s^2+2\gamma-1)\Omega^4-2(\gamma-1)s\Omega^2-d^2] = 0, \qquad \text{(A3.XVI)}$$

which is Equation (4.54) of Chapter 4 and where $s = k_x(c_0^2+ c_e^2)/g$ and $d = k_x(c_0^2- c_e^2)/g$.

A.4 Analytical Correction to the f-Mode Due to the Presence of a Magnetic Field for the Compressible Case

As in Appendix A.2 for the incompressible case, for the purposes of this calculation it is convenient to rewrite the dispersion relation (4.33) of Chapter 4 as

$$\Omega^2 = \frac{1}{\left(1 + \frac{\rho_e}{\rho_0}\frac{(M_e/k_x + 1/2k_xH_e)m_0^2/k_x^2}{(M_0/k_x - 1/2k_xH_B)m_e^2/k_x^2}\right)}(k_xH_e)\frac{v_A^2}{gH_e}$$

$$- \frac{\left\{\frac{\gamma k_xH_0}{(\gamma k_xH_0 - \Omega^2)} - \frac{\rho_e}{\rho_0}\frac{\gamma k_xH_e}{(\gamma k_xH_e - \Omega^2)}\right\}}{\frac{(M_0/k_x - 1/2k_xH_B)}{m_0^2/k_x^2} + \frac{\rho_e}{\rho_0}\frac{(M_e/k_x + 1/2k_xH_e)}{m_e^2/k_x^2}}, \qquad \text{(A4.I)}$$

where

$$\frac{M_0}{k_x} = \frac{(1 - 4A_BH_B^2)^{1/2}}{2k_xH_B}, \qquad \text{(A4.II)}$$

$$\frac{M_e}{k_x} = \frac{(1 - 4A_eH_e^2)^{1/2}}{2k_xH_e}, \qquad \text{(A4.III)}$$

and

$$A_B = k_x^2\left\{\frac{\left(\frac{\gamma k_xH_0}{k_xH_B} - 1\right) + \left(\Omega^2 - (k_xH_e)\frac{v_A^2}{gH_e}\right)(\Omega^2 - \gamma k_xH_0)}{\Omega^2\left(\gamma k_xH_0 + (k_xH_e)\frac{v_A^2}{gH_e}\right) - \gamma k_xH_0\,(k_xH_e)\frac{v_A^2}{gH_e}}\right\}, \qquad \text{(A4.IV)}$$

$$A_e = k_x^2\left\{\frac{(\gamma - 1) + \Omega^2(\Omega^2 - \gamma k_xH_e)}{\gamma k_xH_e\Omega^2}\right\}, \qquad \text{(A4.V)}$$

and

$$\frac{m_0^2}{k_x^2} = \left\{ \frac{\left((k_x H_e) \frac{v_A^2}{gH_e} - \Omega^2 \right)(\gamma k_x H_0 - \Omega^2)}{\gamma k_x H_0 (k_x H_e) \frac{v_A^2}{gH_e} - \Omega^2 \left(\gamma k_x H_0 + (k_x H_e) \frac{v_A^2}{gH_e} \right)} \right\}, \tag{A4.VI}$$

$$\frac{m_e^2}{k_x^2} = \frac{(\gamma k_x H_e - \Omega^2)}{\gamma k_x H_e}. \tag{A4.VII}$$

As in the incompressible case of Appendix A.2, the scale heights H_B ($\equiv H_0$ when $v_A=0$) and H_e are related by

$$H_B = H_0 + \frac{1}{2} H_e \frac{v_A^2}{gH_e}, \tag{A4.VIII}$$

and the densities are related to the scale heights by

$$\frac{\rho_e}{\rho_0} = \frac{H_0}{H_e} + \frac{1}{2} \frac{v_A^2}{gH_e}. \tag{A4.IX}$$

Once again for ease of algebraic manipulation, let

$$A = \frac{1}{2k_x H_B} - \frac{M_0}{k_x}, \tag{A4.X}$$

$$B = \frac{1}{2k_x H_e} + \frac{M_e}{k_x}, \tag{A4.XI}$$

and

$$V = \frac{v_A^2}{gH_e}. \tag{A4.XII}$$

Then using this notation, Equation (A4.I) may be written as

$$\Omega^2 \left\{ \frac{m_0^2}{k_x^2} (2k_x H_0 + V k_x H_e) B - 2 \frac{m_e^2}{k_x^2} A k_x H_e \right\}$$

$$= \gamma k_x H_e \frac{m_0^2 m_e^2}{k_x^2 k_x^2} \left\{ \frac{2k_x H_0 + V k_x H_e}{(\gamma k_x H_e - \Omega^2)} - \frac{2k_x H_0}{(\gamma k_x H_0 - \Omega^2)} \right\} - 2 \frac{m_e^2}{k_x^2} A V k_x^2 H_e^2, \tag{A4.XIII}$$

where

$$(2k_xH_0 + Vk_xH_e)A =$$

$$1-\left\{1+(2k_xH_0+Vk_xH_e)^2-(2k_xH_0+Vk_xH_e)^2\left(\frac{\left(\frac{2\gamma k_xH_0}{2k_xH_0 + Vk_xH_e} - 1\right) + \Omega^4}{\Omega^2(\gamma k_xH_0+Vk_xH_e)- \gamma k_xH_0Vk_xH_e}\right)\right\}^{1/2}, \tag{A4.XIV}$$

and

$$B = \frac{1}{2k_xH_e}\left[1 + \left\{1 + 4k_x^2H_e^2 - 4k_xH_e\left(\frac{(\gamma - 1) + \Omega^4}{\gamma\Omega^2}\right)\right\}^{1/2}\right]. \tag{A4.XV}$$

Now let $\Omega^2 = 1 + \alpha V$, where α is a constant, and expand the dispersion relation (A4.XIII) for small values of V (i.e. v_A^2/gH_e). Consider firstly the expansion of A. We rewrite A as

$$A = \frac{1}{(2k_xH_0 + Vk_xH_e)}\left[1 - \{h(V)\}^{1/2}\right], \tag{A4.XVI}$$

where

$$h(V) = 1+(2k_xH_0+Vk_xH_e)^2-(2k_xH_0+Vk_xH_e)^2\left(\frac{\left(\frac{2\gamma k_xH_0}{2k_xH_0 + Vk_xH_e} - 1\right) + \Omega^4}{\Omega^2(\gamma k_xH_0+Vk_xH_e)- \gamma k_xH_0Vk_xH_e}\right). \tag{A4.XVII}$$

Then, by Maclaurin series, the expansion of h(V) to terms O(V) is

$$\{h(V)\}^{1/2} = \{h(0)\}^{1/2}\left[1 + \frac{1}{2}V\{h(0)\}^{-1}\frac{dh(0)}{dV}\right], \tag{A4.XVIII}$$

that is

$$\{h(V)\}^{1/2} = \pm|1 - 2k_xH_0|\left\{1 + \frac{(\gamma - 2)(2k_xH_0\alpha - k_xH_e)}{\gamma(1 - 2k_xH_0)^2}V\right\}, \tag{A4.XIX}$$

where we take the the positive root, since we take the positive square root of Equation (A4.II). Then the expansion for A up to terms of O(V) is

$$A = \frac{1}{(2k_xH_0 + Vk_xH_e)}\left[1 - |1-2k_xH_0|\left\{1 + \frac{(\gamma - 2)(\gamma k_xH_e - 2k_xH_0\alpha)}{(1 - 2k_xH_0)^2}\, V\right\}\right]. \tag{A4.XX}$$

Similarly we write B as

$$B = \frac{1}{2k_xH_e}\left[1 + \{f(V)\}^{1/2}\right], \tag{A4.XXI}$$

where

$$f(V) = 1 + 4k_x^2H_e^2 - 4k_xH_e\left(\frac{(\gamma - 1) + \Omega^4}{\gamma\Omega^2}\right). \tag{A4.XXII}$$

Then, once again by Maclaurin series, the expansion of f(V) to terms O(V) gives

$$\{f(V)\}^{1/2} = \pm|2k_xH_e - 1|\left\{1 + \frac{2(\gamma - 2)k_xH_e\alpha}{\gamma(2k_xH_e - 1)^2}\, V\right\}. \tag{A4.XXIII}$$

Once again we take the positive root, since we take the positive square root of Equation (A4.III). Then the expansion for B up to terms of O(V) is

$$B = \frac{1}{2k_xH_e}\left[1 + |2k_xH_e - 1|\left\{1 + \frac{2(\gamma - 2)k_xH_e\alpha}{\gamma(2k_xH_e - 1)^2}\, V\right\}\right]. \tag{A4.XXIV}$$

Then as in the incompressible case we substitute (A4.XX) and (A4.XXIV) into the dispersion relation (A4.XIII) and equate coefficients of V. Comparing coefficients of $O(V^0)$ gives

$$\frac{(\gamma k_xH_0 - 1)}{\gamma k_xH_0}(2k_xH_0)\left[1 + |2k_xH_e - 1|\right] - \frac{(\gamma k_xH_e - \Omega^2)}{\gamma k_xH_e}(2k_xH_e)\left[1 - |1 - 2k_xH_0|\right]$$

$$= \frac{(\gamma k_xH_0 - 1)}{\gamma k_xH_0}(2k_xH_0) - \frac{(\gamma k_xH_e - \Omega^2)}{\gamma k_xH_e}(2k_xH_e). \tag{A4.XXV}$$

We note that Equation (A4.XXV) is satisfied only if $(2k_xH_e - 1) > 0$ and $(1 - 2k_xH_0) > 0$. That is, $\Omega^2 = 1$ is a solution if the horizontal wavenumber lies in the range

$$\frac{1}{2H_e} < k_x < \frac{1}{2H_0}. \qquad \text{(A4.XXVI)}$$

Then by comparing coefficients of O(V) in Equation (A4.XIII) and taking $(2k_xH_e - 1) > 0$ and $(1 - 2k_xH_0) > 0$ we determine α to be

$$\alpha = \frac{k_xH_e}{2}\frac{(2k_xH_e - 1)}{(k_xH_e - k_xH_0)}. \qquad \text{(A4.XXVII)}$$

Then the first order correction to the f-mode in the presence of a magnetic field gives the result

$$\frac{\omega^2}{gk_x} \approx 1 + \frac{\gamma}{2}\frac{(2k_xH_e - 1)}{(c_e^2 - c_0^2)}\, v_A^2, \qquad \text{(A4.XXVIII)}$$

which is Equation (4.70) of Chapter 4. However, we note that since $H_e = c_e^2/\gamma g$ and $H_0 = c_0^2/\gamma g$ and so Equation (A4.XXVIII) may be rewritten as

$$\Omega^2 \approx 1 + \frac{1}{2}\frac{(2k_xH_e - 1)}{(k_xH_e - k_xH_0)}\frac{k_xv_A^2}{g}, \qquad \text{(A4.XXIX)}$$

which is the Equation (A2.XXVII) of Appendix A.2 and Equation (2.71) of Chapter 2, obtained in the incompressible calculation. Thus the first order correction to the f-mode due to the presence of a magnetic field is the same as in the incompressible case.

A.5 The Zero-Gravity Limit for the Case of a Uniform Magnetic Field

In the limit as $g \to 0$ the transcendental dispersion relation given by Equation (5.30) of Chapter 5 reduces to

$$\frac{\rho_0(k_x^2 v_A^2 - \omega^2)}{m_0^2}\left\{k_x + X_0 \lim_{g\to 0}\left[\frac{pq}{r}\frac{1}{H_0}\frac{F(p+1,\, q+1;\, r+1;\, X_0)}{F(p,\, q;\, r;\, X_0)}\right]\right\} = \frac{\rho_e}{m_e}\omega^2. \tag{A5.I}$$

Thus, in order to determine the dispersion relation in the limit as $g \to 0$ requires a knowledge of the hypergeometric functions in this limit. However, directly taking the limit as $g \to 0$ of the hypergeometric functions is not possible since all three parameters p, q and r become infinite in this limit. Instead, following a suggestion by Dr. A. W. Hood, we work from the hypergeometric differential Equation (5.12), i.e.

$$X(1-X)\frac{d^2V_z}{dX^2} + [r - (p+q+1)X]\frac{dV_z}{dX} - pqV_z = 0. \tag{A5.II}$$

This may be rewritten as

$$\frac{d^2V_z}{dX^2} + \left\{\frac{r}{X} + \frac{1}{(X-1)}\right\}\frac{dV_z}{dX} - \frac{pq}{X(1-X)}V_z = 0. \tag{A5.III}$$

Introduce the transformation

$$V_z = \frac{Y}{(X-1)^{1/2}X^{r/2}}. \tag{A5.IV}$$

Then Equation (A5.III) reduces to

$$\frac{d^2Y}{dX^2} - H_0^2 h(X,H_0)Y = 0, \tag{A5.V}$$

where

$$h(X,H_0) = \frac{X^2\left(\frac{r^2-4pq-1}{H_0^2}\right) - 2X\left(\frac{r^2-2pq-r}{H_0^2}\right) + \frac{r(r-2)}{H_0^2}}{4X^2(X-1)^2}. \qquad \text{(A5.VI)}$$

Now, with p,q and r defined by Equations (5.13) and (5.14), we have

$$\frac{r^2-4pq-1}{H_0^2} = 4\left\{\frac{k_x^2c_0^2 - \omega^2}{c_0^2} - \frac{(\gamma-1)}{\gamma^2}\frac{k_x^2c_0^2}{H_0^2\omega^2}\right\}, \qquad \text{(A5.VII)}$$

$$\frac{r^2-2pq-r}{H_0^2} = 2\left\{\frac{2k_x^2c_0^2 - \omega^2}{c_0^2} - \frac{(\gamma-1)}{\gamma^2}\frac{k_x^2c_0^2}{H_0^2\omega^2}\right\}, \qquad \text{(A5.VIII)}$$

and

$$\frac{r(r-2)}{H_0^2} = 4k_x^2 - \frac{1}{H_0^2}, \qquad \text{(A5.IX)}$$

where

$$X = X_0e^{-z/H_0} = \frac{c_0^2\omega^2}{v_A^2(k_x^2c_0^2 - \omega^2)}\, e^{-z/H_0}, \quad z > 0. \qquad \text{(A5.X)}$$

We seek a solution to Equation (A5.V) of the form

$$Y = \exp\{H_0G(X,H_0)\}, \qquad \text{(A5.XI)}$$

where

$$G(X,H_0) = G_1(X) + \frac{1}{H_0}G_2(X) + ..., \qquad \text{(A5.XII)}$$

is such that as $H_0 \to \infty$ (i.e. $g \to 0$), $G(X,H_0) \to G_1(X)$. To determine $G_1(X)$ we substitute (A5.XI) into (A5.V). Then

$$\frac{1}{H_0}\frac{d^2G}{dX^2} + \left(\frac{dG}{dX}\right)^2 - h(X,H_0) = 0. \qquad \text{(A5.XIII)}$$

In the limit as $H_0 \to \infty$, Equation (A5.XIII) gives $G_1(X)$ as

$$\left(\frac{dG_1}{dX}\right)^2 = \lim_{H_0\to\infty} h(X,H_0), \qquad \text{(A5.XIV)}$$

that is,

$$\left(\frac{dG_1}{dX}\right)^2 = \frac{X(k_x^2c_0^2 - \omega^2) - k_x^2c_0^2}{c_0^2X^2(X-1)}. \qquad \text{(A5.XV)}$$

Now, from the transformation (A5.IV), we have

$$\frac{dV_z/dX}{V_z} = \frac{dY/dX}{Y} - \frac{1}{2}\left\{\frac{X + r(X-1)}{X(X-1)}\right\}, \qquad \text{(A5.XVI)}$$

where

$$V_z(z) = d_1F(p,q; r; X)e^{-zK_0/H_0}, \quad z > 0. \qquad \text{(A5.XVII)}$$

Thus,

$$\left.\frac{dV_z/dX}{V_z}\right|_{z=0} = \frac{pq}{r}\frac{F(p+1, q+1; r+1; X_0)}{F(p,q; r; X_0)}, \qquad \text{(A5.XVIII)}$$

and so Equation (A5.XVI) in the limit as $H_0 \to \infty$ (i.e. $g \to 0$) becomes

$$\lim_{H_0\to\infty}\left[\frac{pq}{r}\frac{1}{H_0}\frac{F(p+1, q+1; r+1; X_0)}{F(p, q; r; X_0)}\right]$$

$$= \lim_{H_0\to\infty}\left\{\frac{dY/dX}{H_0Y}\right\}\Bigg|_{z=0} - \frac{1}{2}\lim_{H_0\to\infty}\left\{\frac{X + r(X-1)}{H_0X(X-1)}\right\}\Bigg|_{z=0}. \qquad \text{(A5.XIX)}$$

Now

$$\lim_{H_0\to\infty}\left\{\frac{dY/dX}{H_0Y}\right\}\Bigg|_{z=0} = \lim_{H_0\to\infty}\frac{dG_1}{dX}\Bigg|_{z=0}, \qquad \text{(A5.XX)}$$

where dG_1/dX is given by Equation (A5.XV). Thus Equation (A5.XIX) reads

$$\lim_{H_0\to\infty}\left[\frac{pq}{r}\,\frac{1}{H_0}\,\frac{F(p+1,\,q+1;\,r+1;\,X_0)}{F(p,q;\,r;\,X_0)}\right]$$

$$= \pm\left\{\frac{X_0(k_x^2c_0^2 - \omega^2) - k_x^2c_0^2}{c_0^2X_0^2(X_0 - 1)}\right\}^{1/2} - \frac{1}{2}\lim_{H_0\to\infty}\left\{\frac{X_0/H_0 + (2k_x + 1/H_0)(X_0 - 1)}{(X_0 - 1)}\right\}. \qquad \text{(A5.XXI)}$$

Finally, after some algebra this reduces to give

$$\lim_{H_0\to\infty}\left[\frac{pq}{r}\,\frac{1}{H_0}\,\frac{F(p+1,\,q+1;\,r+1;\,X_0)}{F(p,q;\,r;\,X_0)}\right] = \pm\,\frac{1}{X_0}\,[m_0 - k_x]. \qquad \text{(A5.XXII)}$$

Then taking the positive root of Equation (A5.XXII) and substituting into Equation (A5.I) yields the result

$$\rho_0(k_x^2v_A^2 - \omega^2)m_e - \omega^2\rho_e m_0 = 0, \qquad \text{(A5.XXIII)}$$

which is the dispersion relation applicable in the absence of gravity (i.e. Equation (3.33) of Chapter 3).

References

Abdelatif, T. E. : 1988, *Astrophys. J.*, **333**, 395.

Abramowitz, M. and Stegun, I. A .: 1965, *Handbook of Mathematical Functions*, Dover.

Adam, J .A. : 1975, *Ph.D. Thesis*, University of London.

Adam, J. A. : 1977, *Solar Phys.* **52**, 293.

Alissandrakis, C. E.; Dialetis, D.; Mein, P.; Schmieder, B. and Simon, G.: 1988, *Astron. Astrophys.* **201**, 339.

Amagishi, Y. : 1986, *Phys. Rev. Letters* **57**, 2807.

Appert, K., Collins, G. A., Hellsten, T., Vaclavik, J. and Villard, L. : 1986,*Plasma Phys. Contr. Fusion* **28**, 133.

Baker, L. : 1983, *Phys. Fluids* **26**, 950.

Barston, E. M. : 1964, *Ann. Phys.* **29**, 282.

Behannon, K. W. : 1978, *Rev. Geophys. Space Phys.* **16**, 125.

Bernstein, I. B. and Book, D. L. : 1983, *Phys. Fluids* **26**, 453.

Cadez, V. M. and Okretic, V. K. : 1989, *J. Plasma Phys.* **41**, 23.

Cally, P. S. : 1985, *Australian J. Phys.* **38**, 825.

Cally, P. S. : 1986, *Solar Phys.* **103**, 27.

Campbell, W .R. and Roberts, B. : 1989, *Astrophys. J.* **338**, 538.

Chandrasekhar, S. : 1961, *Hydrodynamics and Hydromagnetic Stability*, Clarendon Press, Oxford.

Chen, L. and Hasegawa, A. : 1974, *J. Geophys. Res.* **79**, 1033.

Christensen-Dalsgaard, J., Gough, D. O. and Toomre, J. : 1985, *Science* **229**, 923.

Cowling, T. G.: 1941, *Mon. Not. R. Astron. Soc.* **101**, 367.

Deubner, F-L. and Gough, D. O. : 1984, *Ann. Rev. Astron. Astrophys.* **22**, 593.

Dungey, J. W. and Loughhead, R .E. : 1954, *Australian J. Phys.* **7**, 5.

Duvall, T. L., Harvey, J. W., Libbrecht, K. G., Popp, B. D. and Pomerantz, M. A .: 1988, *Astrophys. J.* **324**, 1158.

Edwin, P. M. and Roberts, B. : 1983, *Solar Phys.* **88**, 179.

Edwin, P. M. and Roberts, B. : 1986, in S. Vukovic (ed), *Surface Waves in Plasmas and Solids*, World Scientific, p.78.

Edwin, P. M. and Roberts, B. : 1987, *Proc. 21st ESLAB Symp.*, ESA SP-275, p.169.

Evans, D. J. and Roberts, B. : 1990a, *Astrophys. J.*, **348**, 346.

Evans, D. J. and Roberts, B. : 1990b, *Astrophys. J.*, **356**, 704.

Erdélyi, A. : 1953, *Higher Transcendental Functions, Vol I*, McGraw-Hill, p.56.

Galloway, D. J. : 1978, *Mon. Not. R. Astron. Soc.* **184**, 49.

Giovanelli, R. G. : 1972, *Solar Phys.* **27**, 71.

Giovanelli, R. G. : 1974, in *Chromospheric Fine Structure, IAU Symp.* **56**, 137.

Giovanelli, R. G. : 1982, *Solar Phys.* **52**, 293.

Goedbloed, J. P. : 1971, *Physica* **53**, 412.

Goedbloed, J. P. and Hagebeuk, H. J. L. : 1972, *Phys. Fluids* **15**, 1090.

Gonzalez, A. G. and Gratton, J. : 1990, *Plasma Phys. Contr. Fusion* **32**,3.

Goossens, M. : 1991, in P. Ulmschneider, E. R. Priest and R. Rosner (eds), *Mechanisms of Chromospheric and Coronal Heating*, Springer-Verlag, p.480.

Gordon, B. E. and Hollweg, J. V. : 1983, *Astrophys. J.*, **266**, 373.

Gratton, J., Gratton, F. T. and Gonzalez, A. G. : 1988, *Plasma Phys. Contr. Fusion* **30**, 435.

Grossmann, W. and Tataronis, J. : 1973, *Z. Phys.* **261**, 217.

Hasegawa, A. and Chen, L. : 1974, *Phys. Rev. Letters* **32**, 454.

Hasegawa, A. and Chen, L. : 1976, *Phys. Fluids* **19**, 1924.

Hollweg, J. V. : 1981a, in F. Orrall (ed) *Solar Active Regions*, Boulder, Colorado Associated University Press, p.277.

Hollweg, J. V. : 1981b, *Solar Phys.* **70**, 285.

Hollweg, J. V. : 1982, *J. Geophys. Res.* **87**, 8065.

Hollweg, J. V. : 1985, in B. Buti (ed) *Advances in Space Plasma Physics*, World Scientific, p.77.

Hollweg, J. V. : 1987a, *Astrophys. J.* **312**, 880.

Hollweg, J. V. : 1987b, *Astrophys. J.* **317**, 918.

Hollweg, J. V. : 1987c, *Astrophys. J.* **320**, 875.

Hollweg, J. V. : 1990a, *Comp. Phys. Reports* **12**, 205.

Hollweg, J. V. : 1990b, in C.T. Russell, E.R. Priest and L.C. Lee (eds), *Physics of Magnetic Flux Ropes,* Geophys. Mono. **58**, p23.

Hollweg, J. V. : 1991, in P. Ulmschneider, E. R. Priest and R. Rosner (eds), *Mechanisms of Chromospheric and Coronal Heating,* Springer-Verlag, p.423.

Ionson, J. A. : 1978, *Astrophys. J.* **226**, 650.

Ionson, J. A. : 1985, *Solar Phys.* **100**, 289.

Jain, R. and Roberts, B. : 1991, *Solar Phys.*, in press.

Kumar, P., Duvall Jr., T. L., Harvey, J. W., Jefferies, S. M., Pomerantz, M. A. and Thompson, M. J. : 1991, Santa Barbara conf., preprint.

Kruskal, M. and Schwarzschild, M. : 1954, *Proc. Roy. Soc.* **A223**, 348.

Lamb, H. : 1932, *Hydrodynamics,* Camb. Univ. Press, Cambridge, Art. 235.

Lee, M. A. : 1980, *Astrophys. J.* **240**, 693.

Lee, M. A. and Roberts, B. : 1986, *Astrophys. J.* **301**, 430.

Leibacher, J. W., Noyes, R. W., Toomre, J. and Ulrich, R. K. : 1985 *Scientific Amer.* **253**, 48.

Libbrecht, K G and Kaufman, J M : 1988, *Astrophys. J.* **324**, 1172.

Libbrecht, K. G.,Woodard, M. F. and Kaufman, J. M. : 1990, *Astrophys. J. suppl.*, in press.

Lighthill, J. : 1978, *Waves in Fluids*, Camb. Univ. Press, Cambridge, chap. 4.

Lites, B. W., White, O. R. and Packman, D. : 1982, *Astrophys. J.* **253**,286.

Lites, B. W. : 1988, *Astrophys. J.* **334**,1054.

Maltsev, Yu. P. and Lyatsky, W. B. : 1984, *Planet. Space Sci.* **32**, 1547.

Miles, A. J. and Roberts, B. : 1989, *Solar Phys.* **119**, 257.

Miles, A .J. and Roberts, B. : 1990, in M. Dubois, F. Bely-Dubau, D. Gresillon (eds), *Plasma Phenomena in The Solar Atmosphere.*, p.77.

Miles, A. J. and Roberts, B. : 1991a, in P. Ulmschneider, E. R. Priest and R. Rosner (eds), *Mechanisms of Chromospheric and Coronal Heating*, Springer-Verlag, p.508.

Miles, A. J. and Roberts, B. : 1991b, *Solar Phys.*, submitted.

Moisan, M., Shivarova, A. and Trivelpiece, A. W. : 1982, *Plasma Phys.* **24**, 1331.

Moore, R. L. : 1973, *Solar Phys.* **30**, 403.

Moore, R. L. : 1981a, in L. E. Cram and J. H. Thomas (eds) *The Physics of Sunspots*, Sacramento Peak Observatory, p.259.

Moore, R. L. : 1981b, *Space Sci. Rev.* **28**, 387.

Musman, S. : 1967, *Astrophys. J.* **149**, 201.

Musman, S.; Nye, A .H. and Thomas J. H. : 1976, *Astrophys. J.* **206**, L175.

Nenovski, P. I. : 1978, *Compt. Rend. Acad. Bulg. Sci.* **31**, 1297.

Nenovski, P. I. : 1985, *Planet. Space Sci.* **33**, 1313.

Nye, A. H. and Thomas, J. H. : 1974, *Solar Phys.* **38**, 399.

Nye, A. H. and Thomas, J. H. : 1976a, *Astrophys. J.* **204**, 573.

Nye, A. H. and Thomas, J. H. : 1976b, *Astrophys. J.* **204**, 582.

Press, H., Flannery, B.P., Teukolsky, S.A. and Vetterling, W.T. : 1987, *Numerical Recipes The Art of Scientific Computing*, Camb. Univ. Press, Cambridge.

Rabaey, G. F., Hill, H. A. and Barry, C. T. : 1988, *Astrophys. and Space Sci.* **143**, 81.

Rae, I. C. and Roberts, B. : 1981, *Geophys. Astrophys. Fluid Dyn.* **18**, 197.

Rae, I. C. and Roberts, B. : 1983, *Phys. Fluids* **26**, 269.

Rayleigh, Lord. : 1900, *Scientific Papers Vol (ii)*, Camb. Univ. Press,Cambridge, p.200.

Roberts, B. : 1980, *Annales de Physique* **5**, 453.

Roberts, B. : 1981a, *Solar Phys.* **69**, 27.

Roberts, B. : 1981b, *Solar Phys.* **69**, 39.

Roberts, B. : 1981c, in L. E. Cram and J. H. Thomas (eds) *The Physics of Sunspots*, Sacramento Peak Observatory, p.259.

Roberts, B. : 1984, in *The Hydromagnetics of the Sun*, ESA SP-220, p.137.

Roberts, B. : 1985, in E. R. Priest (ed), *Solar System Magnetic Fields*, Reidel, Dordrecht, chap. 3.

Roberts, B. : 1986, in W. Deinzer, M. Knölker and H. H. Voigt (eds) *Small Scale Magnetic Flux Concentrations in the Solar Photosphere*, Vandenhoeck and Ruprecht, p.169.

Roberts, B. : 1990a, in C.T. Russell, E.R. Priest and L.C. Lee (eds), *Physics of Magnetic Flux Ropes*, Geophys. Mono. **58**, p113.

Roberts, B. : 1990b, in B. Buti (ed), *Solar and Planetary Plasma Physics*, World Scientific, Singapore, p1.

Roberts, B. : 1990c, in E.R. Priest and V. Krishan (eds), *Basic Plasma Processes on the Sun*, IAU Symp. **142**, p159.

Roberts, B. : 1991, in P. Ulmschneider, E. R. Priest and R. Rosner (eds), *Mechanisms of Chromospheric and Coronal Heating*, Springer-Verlag, p.494.

Ruderman, M. S. : 1985, *Fluid Dyn.* **20**, 85.

Ruderman, M. S. : 1986, *Fluid Dyn.* **21**, 925.

Ruderman, M. S. : 1987, *Fluid Dyn.* **22**, 879.

Ruderman, M. S. : 1988, *Plasma Phys. Contr. Fusion* **30**, 1117.

Ruderman, M. S. : 1989, in S. Grzedzielski and D. E. Page (eds), *Physics of the Outer Heliosphere*, Pergamon Press, p.249.

Ruderman, M. S. : 1991, in P. Ulmschneider, E. R. Priest and R. Rosner (eds), *Mechanisms of Chromospheric and Coronal Heating*, Springer-Verlag, p.514.

Ryutova, M. P. : 1990, in J. O. Stenflo (ed) *Solar Photoshere : Structure, Convection and Magnetic Fields*, IAU Symp. **138**, p229.

Savage B. D. : 1969, *Astrophys. J.* **156**, 707.

Schmidt, H.U., Spruit, H. C. and Weiss, N. O. : 1986, *Astron. Astrophys.* **158**, 351.

Small, L. M. and Roberts, B. : 1984, in *The Hydromagnetics of the Sun*, ESA SP-220, p.257.

Somasundaram, K. and Uberoi, C. : 1982, *Solar Phys.* **81**, 19.

Southwood, D. J. : 1974, *Planet. Space Sci.* **22**, 483.

Southwood, D. J. and Hughes, W. J. : 1983, *Space Sci. Rev.* **35**, 301.

Spruit, H. C. : 1981a, in R. M. Bonnet and A. K. Dupree (eds) *Solar Phenomena in Stars and Stellar Systems*, Reidel, p.289.

Spruit, H. C. : 1981b, in S. Jordan (ed) *The Sun as a Star*, NASA SP-450, Washington, p.385.

Spruit, H. C. : 1983, in J. O. Stenflo (ed) *Solar and Stellar Magnetic Fields: Origins and Coronal Effects*, Reidel, p.41.

Spruit, H. C. : 1986, in E.H.Schröter, M. Vázquez and A.A.Wyller (eds) *The Role of Fine-Scale Magnetic Fields on the Structure of the Solar Atmosphere*, p.199.

Spruit, H. C. and Roberts, B. : 1983, *Nature* **304**, 401.

Tarbell, T., Peri, M., Frank, Z. and Title, A. : 1988, in E. J. Rolfe (ed), *Seismology of the Sun and Sun-like Stars* , ESA SP-286, p.315.

Thomas, J. H. : 1981, in L. E. Cram and J. H. Thomas (eds), *The Physics of Sunspots,* Sacramento Peak Observatory, p.345.

Thomas, J. H. : 1983, *Ann. Rev. Fluid Mech.* **15**, 321.

Thomas, J. H. : 1985, in H.U.Schmidt (ed) *Theoretical Problems in High Resolution Solar Physics* ,Max-Planck-Institut für Astrophysik, p.126.

Thomas, J. H., Cram, L. E. and Nye, A. H. : 1984, *Astrophys. J.* **285**, 368.

Uberoi, C. : 1972, *Phys. Fluids* **15**, 1673.

Uberoi, C. : 1982, *Solar Phys.* **78**, 351.

Wentzel, D. G. : 1979, *Astrophys. J.* **227**, 319.

Woodard, M. F. and Libbrecht, K. G. : 1991, *Astrophys. J. Letters.*, submitted.

Yu, C P : 1965, *Phys. Fluids* **8**, 650.

Zhugzhda, Y. D. and Dzhalilov, N. S. : 1984, *Astr. Ap.* **133**, 333.

Zirin, H. and Stein, A. : 1972, *Astrophys. J.* **178**, L85.